

**Modification of the bridging unit in luminescent Pt(II) complexes
bearing C^N*N- and C^N*N^C-ligands.**

Stefan Buss,^[a,b] M. Victoria Cappellari,^[a,b] Alexander Hepp,^[a] Jutta Kösters,^[a] and Cristian A. Strasser^{[a,b]}*

[a] Institut für Anorganische und Analytische Chemie, Westfälische Wilhelms-Universität Münster - Corrensstraße 28/30, 48149 Münster, Germany.

[b] CeNTech, CiMIC, SoN, Westfälische Wilhelms-Universität Münster - Heisenbergstraße 11, 48149 Münster,

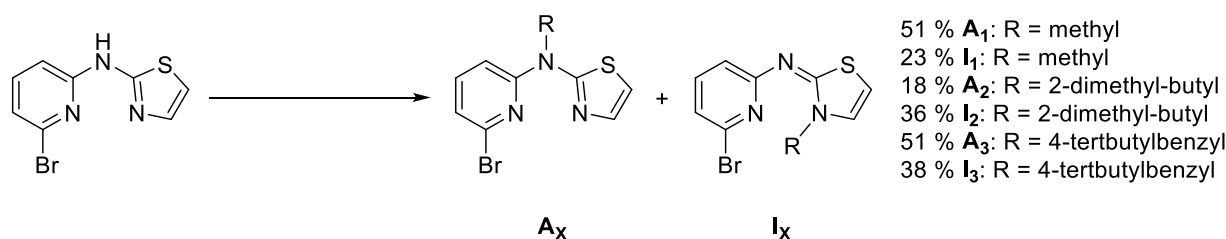
I. Synthetic procedures

Commercially available reagents were used without further purification. Silica gel 60 (0.063 – 0.200 mm) for column chromatography was purchased from Merck (mentioned as silica) was used for column chromatography if not otherwise stated. *N*-(2-bromopyridin-6-yl)-2-aminothiazole [1] and bis-(6-bromopyridin-2-yl)-amine [2] were prepared according to former published procedure.

Exact mass (EM) determination with mass spectrometry (MS) was carried out at the Organisch-Chemisches Institut Münster by Denise Defayay, using a LTQ Orbitrap LTQ XL (Thermo-Fisher Scientific, Bremen) with nanospray-injection (ESI) or Autoflex Speed MALDI-TOF with matrix assisted Laser desorption ionization (MALDI). The mass spectra of **A₂**, **I₂** and **L₆BrH** were determined using an impact II Bruker.

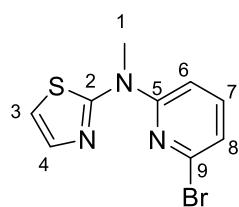
NMR-spectra for **A₁-A₆** and **L₁H** were obtained on an Agilent DD2 500/ Agilent DD2 600 or a Bruker Avance II 400 at the Organisch-Chemisches Institut Münster. The rest were obtained on a Avance (Neo)500, Avance (Neo)400, Avance (III)400 or a Avance (I)400 from Bruker. All measurements were obtained at room temperature if not otherwise mentioned. The ¹H-NMR and ¹³C-NMR chemical shifts (δ) of the signals are given in parts per million and referenced to residual protons in the deuterated solvent: CDCl₃ (7.26 ppm/ 77.0 ppm), d₂-methylene-chloride (DCM, 5.32 ppm/ 54.0 ppm (297 K), 53.8 (300 K)), d₇-dimethylformamide (DMF, 8.00 ppm/ 2.90 ppm/ 2.74 ppm/ 161.8 ppm/ 34.1 ppm/ 29.1 ppm), d₆-dimethylsulfoxide (DMSO, 2.50 ppm/ 39.5 ppm). The signal multiplicities are abbreviated as follows: s, singlet; d, doublet; t, triplet; q, quartet; m, multiplet.

Method: alkylation



N-(6-bromopyridine-2-yl)-2-aminothiazole [1] (1.0 eq) and Cs₂CO₃ (3.0 eq) were suspended in THF (25 mL). After the addition of the alkylhalide (2.0 eq), the mixture was heated for 16 h under reflux. The reaction mixture was poured on dest. H₂O (50 mL) and the aqueous phase was extracted with EtOAc (3-30 mL). The collected organic phases were washed with brine (50 mL), dried over Na₂SO₄ and the solvent was removed under reduced pressure. The residue was purified *via* column chromatography over silica to yield the desired product. [1]

Preparation of *N*-(6-bromopyridin-2-yl)-*N*-methyl-thiazol-2-amine (**A**₁)



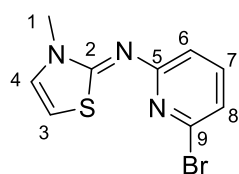
N-(2-bromopyridine-6-yl)-2-aminothiazole (503 mg; 1.96 mmol) and Cs₂CO₃ (1.98 g; 5.88 mmol) were used with methyl iodide (0.2 mL; 4.02 mmol). After column chromatography with EtOAc/Cyclohexane (1:9) the product **A**₁ (269 mg; 1.00 mmol; 51 %) as a white solid. **I**₁ (123 mg; 0.45 mmol; 23 %) eluted second and yield a white solid.

Analytical data for **A**₁:

¹H-NMR (400 MHz, DCM-*d*₂): δ (ppm) = 7.56 (dd, ³J_{HH} = 8.3 Hz, ³J_{HH} = 7.6 Hz, 1H, H₇), 7.45 (d, ³J_{HH} = 3.6 Hz, 1H, H₄), 7.09 (d, ³J_{HH} = 7.6 Hz, 1H, H₈), 7.01 (d, ³J_{HH} = 8.3 Hz, 1H, H₆), 6.92 (d, ³J_{HH} = 3.6 Hz, 1H, H₃), 3.78 (s, 3H, H₁).

¹³C{¹H}-NMR (101 MHz, DCM-*d*₂): δ (ppm) = 162.3 (C₂), 153.6 (C₅), 140.6 (C₇), 138.3 (C₉), 137.4 (C₄), 120.1 (C₈), 113.6 (C₃), 108.1 (C₆), 35.9 (C₁).

MS-ESI-EM (MeOH, M = C₉H₈N₃S₁Br₁): found 269.96961 for [M+H]⁺ (calcd. m/z = 269.96951 for [M+H]⁺).



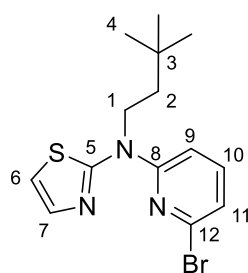
Analytical data for **I**₁:

¹H-NMR (500 MHz, DCM-*d*₂): δ (ppm) = 7.42 (dd, ³J_{HH} = 8.0 Hz, ³J_{HH} = 7.5 Hz, 1H, H₇), 6.97 (dd, ³J_{HH} = 8.0 Hz, ⁴J_{HH} = 0.8 Hz, 1H, H₆), 6.95 (dd, ³J_{HH} = 7.5 Hz, ⁴J_{HH} = 0.8 Hz, 1H, H₈), 6.85 (d, ³J_{HH} = 4.8 Hz, 1H, H₄), 6.41 (d, ³J_{HH} = 4.8 Hz, 1H, H₃), 3.62 (s, 3H, H₁).

¹³C{¹H}-NMR (101 MHz, DCM-*d*₂): δ (ppm) = 160.7 (C₂), 159.1 (C₅), 139.4 (C₇), 138.1 (C₉), 127.1 (C₄), 118.9 (C₆), 117.7 (C₆), 105.2 (C₃), 35.2 (C₁).

MS-ESI-EM (MeOH, M = C₉H₈N₃S₁Br₁): found 269.96977 for [M+H]⁺ (calcd. m/z = 269.96951 for [M+H]⁺), found 291.95133 for [M+Na]⁺ (calcd. m/z = 291.95145 [M+Na]⁺).

Preparation of *N*-(6-bromopyridin-2-yl)-*N*-(3,3-dimethyl-butyl)-thiazol-2-amine (**A₂**)



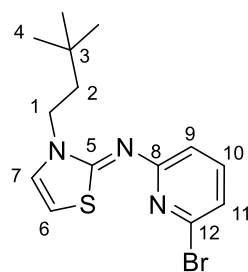
N-(2-bromopyridine-6-yl)-2-aminothiazole (500 mg; 1.95 mmol) and Cs₂CO₃ (2.00 g; 6.14 mmol) were used with 1-bromo-3,3-dimethyl-butane (0.55 mL; 3.90 mmol). After column chromatography with THF/n-hexane (1:39) the product **A₂** (117 mg; 0.34 mmol; 18 %) as a white solid. **I₂** (241 mg; 0.71 mmol; 36 %) eluated second and yield a white solid.

Analytical data for **A₂**:

¹H-NMR (500 MHz, DCM-*d*₂): δ (ppm) = 7.53 (dd, ³*J*_{HH} = 8.4 Hz, ³*J*_{HH} = 7.5 Hz, 1H, H₁₀), 7.47 (d, ³*J*_{HH} = 3.6 Hz, 1H, H₇), 7.06 (dd, ³*J*_{HH} = 7.6 Hz, ³*J*_{HH} = 0.5 Hz, 1H, H₁₁), 6.98 (dd, ³*J*_{HH} = 8.4 Hz, ³*J*_{HH} = 0.5 Hz, 1H, H₉), 6.92 (d, ³*J*_{HH} = 3.6 Hz, 1H, H₆), 4.57 – 4.14 (m, 2H, H₁), 1.71 – 1.62 (m, 2H, H₂), 1.07 (s, 9H, H₄).

¹³C{¹H}-NMR (126 MHz, DCM-*d*₂): δ (ppm) = 161.4 (C₅), 152.8 (C₈), 140.5 (C₁₀), 138.4 (C₁₂), 137.7 (C₇), 119.7 (C₁₁), 113.5 (C₆), 107.9 (C₉), 45.5 (C₁), 39.8 (C₂), 30.5 (C₃), 29.6 (C₄).

MS-ESI-EM (MeOH, M = C₁₄H₁₈N₃S₁Br₁): found 340.0472 for [M+H]⁺ (calcd. m/z = 340.0478 for [M+H]⁺), found 362.0292 for [M+Na]⁺ (calcd. m/z = 340.0297 for [M+Na]⁺).



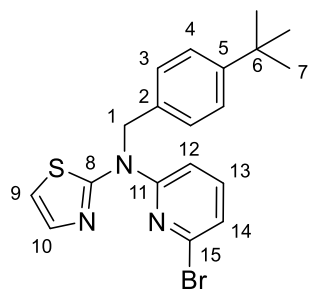
Analytical data for **I₂**:

¹H-NMR (400 MHz, DCM-*d*₂): δ (ppm) = 7.41 (dd, ³*J*_{HH} = 8.1 Hz, ³*J*_{HH} = 7.5 Hz, 1H, H₁₀), 6.97 (dd, ³*J*_{HH} = 8.0 Hz, ⁴*J*_{HH} = 0.8 Hz, 1H, H₉), 6.94 (dd, ³*J*_{HH} = 7.5 Hz, ⁴*J*_{HH} = 0.8 Hz, 1H, H₁₁), 6.88 (d, ³*J*_{HH} = 4.8 Hz, 1H, H₇), 6.41 (d, ³*J*_{HH} = 4.9 Hz, 1H, H₆), 4.24 – 3.98 (m, 2H, H₁), 1.77 – 1.60 (m, 2H, H₂), 1.03 (s, 9H, H₄).

¹³C{¹H}-NMR (101 MHz, DCM-*d*₂): δ (ppm) = 160.0 (C₅), 159.2 (C₈), 139.2 (C₁₀), 138.1 (C₁₂), 126.1 (C₇), 118.7 (C₁₁), 117.9 (C₉), 105.4 (C₆), 45.0 (C₁), 42.7 (C₂), 30.3 (C₃), 29.4 (C₄).

MS-ESI-EM (MeOH, M = C₁₄H₁₈N₃S₁Br₁): found 340.0450 for [M+H]⁺ (calcd. m/z = 340.0478 for [M+H]⁺), found 362.0270 for [M+Na]⁺ (calcd. m/z = 340.0297 for [M+Na]⁺).

Preparation of *N*-(6-bromopyridin-2-yl)-*N*-(4-*tert*-butylbenzyl)-thiazol-2-amine (**A₃**)



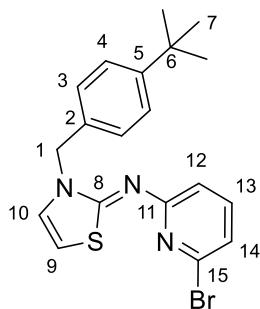
N-(2-bromopyridine-6-yl)-2-aminothiazole (501 mg; 1.96 mmol) and Cs₂CO₃ (2.06 g; 6.32 mmol) were used with Methyl iodid (0.7 mL; 3.90 mmol). After column chromatography with THF/Cyclohexane (0 → 5 % THF; for complete separation two runs were necessary) the product **A₃** (401 mg; 1.00 mmol; 51 %) as a white solid. **I₃** (275 mg; 0.68 mmol; 35 %) eluated second and yield a white solid.

Analytical data for **A₃**:

¹H-NMR (400 MHz, DCM-*d*₂): δ (ppm) = 7.45 (dd, ³*J*_{HH} = 8.4 Hz, ³*J*_{HH} = 7.5 Hz, 1H, H₁₃), 7.44 (d, ³*J*_{HH} = 3.6 Hz, 1H, H₁₀), 7.35 – 7.29 (m, 2H, H₄), 7.17 – 7.11 (m, 2H, H₃), 7.09 (dd, ³*J*_{HH} = 7.6 Hz, ⁴*J*_{HH} = 0.5 Hz, 1H, H₁₄), 6.98 (d, ³*J*_{HH} = 3.6 Hz, 1H, H₉), 6.87 (dd, ³*J*_{HH} = 8.4 Hz, ⁴*J*_{HH} = 0.5 Hz, 1H, H₁₂), 5.61 (s, 2H, H₁), 1.28 (s, 9H, H₇).

¹³C{¹H}-NMR (101 MHz, DCM-*d*₂): δ (ppm) = 162.0 (C₈), 153.2 (C₁₁), 150.8 (C₅), 140.6 (C₁₃), 138.3 (C₁₅), 137.5 (C₁₀), 133.9 (C₂), 126.4 (C₃), 126.2 (C₄), 120.3 (C₁₄), 114.1 (C₉), 108.7 (C₁₂), 51.7 (C₁), 34.9 (C₆), 31.6 (C₇).

MS-ESI-EM (MeOH, M = C₁₉H₂₀N₃S₁Br₁): found 402.06340 for [M+H]⁺ (calcd. m/z = 402.06341 for [M+H]⁺), found 424.04532 for [M+Na]⁺ (calcd. m/z = 424.04535 for [M+Na]⁺).



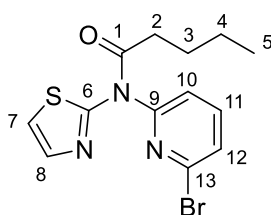
Analytical data for **I3**:

¹H-NMR (400 MHz, DCM-*d*₂): δ (ppm) = 7.43 (dd, ³*J*_{HH} = 8.0 Hz, ³*J*_{HH} = 7.5 Hz, 1H, H₁₃), 7.40 – 7.35 (m, 2H, H₄), 7.28 – 7.21 (m, 2H, H₃), 6.99 (dd, ³*J*_{HH} = 8.0 Hz, ⁴*J*_{HH} = 0.8 Hz, 1H, H₁₂), 6.96 (dd, ³*J*_{HH} = 7.5 Hz, ⁴*J*_{HH} = 0.8 Hz, 1H, H₁₄), 6.87 (d, ³*J*_{HH} = 4.9 Hz, 1H, H₁₀), 6.43 (d, ³*J*_{HH} = 4.9 Hz, 1H, H₉), 5.29 (s, 2H, H₁), 1.30 (s, 9H, H₇).

¹³C{¹H}-NMR (101 MHz, DCM-*d*₂): δ (ppm) = 160.6 (C₈), 159.1 (C₁₁), 151.4 (C₅), 139.4 (C₁₃), 138.1 (C₁₅), 134.0 (C₂), 128.0 (C₃), 126.1 (C₄), 126.1 (C₁₀), 119.1 (C₁₄), 117.9 (C₁₂), 105.8 (C₉), 50.7 (C₁), 34.8 (C₆), 31.4 (C₇).

MS-ESI-EM (CHCl₃/MeOH, M = C₁₉H₂₀N₃S₁Br₁): found 402.06371 for [M+H]⁺ (calcd. m/z = 402.06341 for [M+H]⁺), found 424.04548 for [M+Na]⁺ (calcd. m/z = 424.04535 for [M+Na]⁺).

Preparation of *N*-(6-bromopyridin-2-yl)-*N*-thiazol-2-yl-pentanamide (**A4**)



N-(2-bromopyridin-6-yl)-2-aminothiazole (535 mg; 2.09 mmol) was suspended in valeric anhydride (3 mL). The mixture was heated to 170 °C (till everything was dissolved) and heated for 2 h. The solvent was removed under reduced pressure at 80 °C. After column chromatography (SiO₂, EtOAc/Cyclohexane: 1/4) the product **A4** (340 mg; 1.00 mmol; 48 %) was obtained as a white crystalline solid.

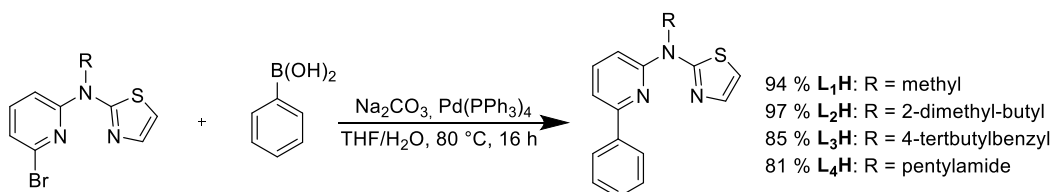
Analytical data for **A4**:

¹H-NMR (400 MHz, DCM-*d*₂): δ (ppm) = 7.82 (t, ³*J*_{HH} = 7.8 Hz, 1H, H₁₁), 7.66 (dd, ³*J*_{HH} = 7.9 Hz, ⁴*J*_{HH} = 0.8 Hz, 1H, H₁₀), 7.41 (dd, ³*J*_{HH} = 7.7 Hz, ⁴*J*_{HH} = 0.8 Hz, 1H, H₁₂), 7.34 (d, ³*J*_{HH} = 3.6 Hz, 1H, H₈), 7.06 (d, ³*J*_{HH} = 3.6 Hz, 1H, H₇), 2.26 – 2.18 (m, 2H, H₂), 1.71 – 1.59 (m, 2H, H₃), 1.35 – 1.22 (m, 2H, H₄), 0.86 (t, ³*J*_{HH} = 7.4 Hz, 3H, H₅).

¹³C{¹H}-NMR (101 MHz, DCM-*d*₂): δ (ppm) = 172.0 (C₁), 160.6 (C₆), 152.9 (C₉), 141.6 (C₁₃), 141.6 (C₁₁), 137.8(C₈), 129.4 (C₁₀), 124.1 (C₁₂), 115.2 (C₇), 35.7 (C₂), 27.1 (C₃), 22.7 (C₄), 14.1 (C₅).

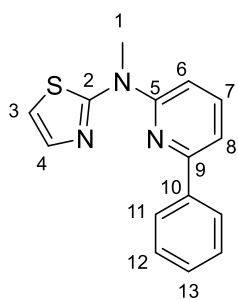
MS-ESI-EM (MeOH, M = C₁₃H₁₄N₃S₁O₁Br₁): found 340.01138 for [M+H]⁺ (calcd. m/z = 340.01137 for [M+H]⁺), found 363.99105 for [M+Na]⁺ (calcd. m/z = 363.99127 for [M+Na]⁺).

Method: Suzuki-Miyaura cross-coupling



Arylbromide (1.0 eq), arylboronic acid (1.5 eq) and [Pd(PPh₃)₄] (0.1 eq) were dissolved in THF and deoxygenated for 10 min. Afterwards a 2M solution of aqueous K₂CO₃ was added and the mixture was again deoxygenated for 5 min. The reaction was heated to reflux for 16 h and after reaching room, the mixture was poured on dest. H₂O (10 mL) and EtOAc (10 mL). The H₂O-phase was extracted with EtOAc (3·30 mL). The combined organic phases were dried over Na₂SO₄ and the solvent was removed under reduced pressure. After purification *via* column chromatography over silica the product was obtained.

Preparation of *N*-(6-phenyl-pyridin-2-yl)-*N*-methyl-thiazol-2-amine (**L₁H**)



A₁ (405 mg; 1.5 mmol) and phenylboronic acid (272 mg; 2.25 mmol) were used with [Pd(PPh₃)₄] (150 mg; 0.13 mmol) in 30 mL THF with 5 mL aqueous K₂CO₃ (2 M). After column chromatography (EtOAc:cyclohexane 3:17) to yield **L₁H** as orange oil (376 mg; 1.4 mmol; 94 %).

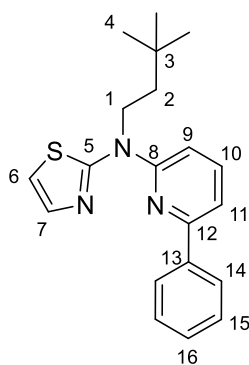
Analytical data for **L₁H**:

¹H-NMR (500 MHz, DCM-*d*₂): δ (ppm) = 8.20 – 8.13 (m, 2H, H₁₁), 7.81 (dd, ³J_{HH} = 8.4 Hz, ³J_{HH} = 7.6 Hz, 1H, H₇), 7.56 – 7.50 (m, 2H, H₁₂), 7.48 – 7.43 (m, 2H, H₄₊₁₃), 7.41 (dd, ³J_{HH} = 7.6 Hz, ⁴J_{HH} = 0.6 Hz, 1H, H₈), 7.06 (dd, ³J_{HH} = 8.4 Hz, ⁴J_{HH} = 0.6 Hz, 1H, H₆), 6.86 (d, ³J_{HH} = 3.6 Hz, 1H, H₃), 3.87 (s, 3H, H₁).

¹³C{¹H}-NMR (126 MHz, DCM-*d*₂): δ (ppm) = 162.7 (C₂), 156.1 (C₉), 154.2 (C₅), 139.6 (C₁₀), 139.3 (C₇), 137.3 (C₄), 129.6 (C₁₃), 129.2 (C₁₂), 128.1 (C₁₁), 114.0 (C₈), 112.6 (C₃), 108.4 (C₆), 36.4 (C₁).

MS-ESI-EM (MeOH, M = C₁₅H₁₃N₃S₁): found 268.09038 for [M+H]⁺ (calcd. m/z = 268.09029 for [M+H]⁺), found 290.07210 for [M+Na]⁺ (calcd. m/z = 290.07224 for [M+Na]⁺).

Preparation of *N*-(6-phenyl-pyridin-2-yl)-*N*-(3,3-dimethyl-butyl)-thiazol-2-amine (**L₂H**)



A₂ (137 mg; 0.4 mmol) and phenylboronic acid (73 mg; 0.6 mmol) were used with [Pd(PPh₃)₄] (46 mg; 0.04 mmol) in 20 mL THF with 3 mL aqueous K₂CO₃ (2 M). After column chromatography (EtOAc:cyclohexane 1:99) to yield **L₂H** as colorless oil (131 mg; 0.39 mmol; 97 %).

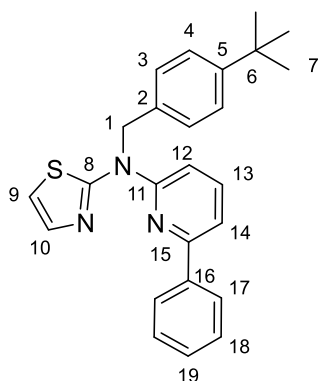
Analytical data for **L₂H**:

¹H-NMR (500 MHz, DCM-*d*₂): δ (ppm) = 8.24 – 8.12 (m, 2H, H₁₄), 7.78 (dd, ³J_{HH} = 8.5 Hz, ³J_{HH} = 7.5 Hz, 1H, H₁₀), 7.56 – 7.51 (m, 2H, H₁₅), 7.49 (d, ³J_{HH} = 3.6 Hz, 1H, H₇), 7.49 – 7.45 (m, 1H, H₁₆), 7.37 (d, ³J_{HH} = 7.5 Hz, 1H, H₁₁), 7.06 (d, ³J_{HH} = 8.4 Hz, 1H, H₉), 6.88 (d, ³J_{HH} = 3.6 Hz, 1H, H₆), 4.71 – 4.18 (m, 2H, H₁), 1.99 – 1.66 (m, 2H, H₂), 1.12 (s, 9H, H₄).

¹³C{¹H}-NMR (101 MHz, DCM-*d*₂): δ (ppm) = 161.7 (C₅), 156.1 (C₁₂), 153.2 (C₈), 139.6 (C₁₃), 139.1 (C₁₀), 137.4 (C₇), 129.4 (C₁₆), 129.0 (C₁₅), 128.0 (C₁₄), 113.6 (C₁₁), 112.4 (C₆), 108.2 (C₉), 45.6 (C₁), 39.8 (C₂), 30.4 (C₃), 29.5 (C₄).

MS-ESI-EM (MeOH, M = C₂₀H₂₃N₃S₁): found 338.16844 for [M+H]⁺ (calcd. m/z = 338.16855 for [M+H]⁺).

Preparation of *N*-(6-phenyl-pyridin-2-yl)-*N*-(4-*tert*-butylbenzyl)-thiazol-2-amine (**L₃H**)



A₃ (196 mg; 0.49 mmol) and phenylboronic acid (92 mg; 0.73 mmol) were used with [Pd(PPh₃)₄] (66 mg; 0.06 mmol) in 25 mL THF with 3 mL aqueous K₂CO₃ (2 M). After column chromatography (EtOAc:n-hexane 1:19) to yield **L₃H** as colorless solid (166 mg; 0.415 mmol; 85 %).

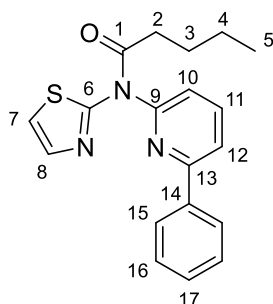
Analytical data for **L₃H**:

¹H-NMR (400 MHz, DCM-*d*₂): δ (ppm) = 8.25 – 8.16 (m, 2H, H₁₇), 7.66 (dd, ³J_{HH} = 8.5 Hz, ³J_{HH} = 7.6 Hz, 1H, H₁₃), 7.60 – 7.53 (m, 2H, H₁₈), 7.53 – 7.48 (m, 1H, H₁₉), 7.47 (d, ³J_{HH} = 3.6 Hz, 1H, H₁₀), 7.40 – 7.34 (m, 3H, H₄₊₁₄), 7.22 (dt, ³J_{HH} = 7.2 Hz, ⁴J_{HH} = 0.9 Hz, 2H, H₃), 6.95 (d, ³J_{HH} = 3.6 Hz, 1H, H₉), 6.91 (dd, ³J_{HH} = 8.4 Hz, ⁴J_{HH} = 0.6 Hz, 1H, H₁₂), 5.71 (s, 2H, H₁), 1.33 (s, 9H, H₇).

¹³C{¹H}-NMR (101 MHz, DCM-*d*₂): δ (ppm) = 162.1 (C₈), 156.1 (C₁₅), 153.5 (C₁₁), 150.4 (C₅), 139.5 (C₁₆), 139.1 (C₁₃), 137.3 (C₁₀), 134.5 (C₂), 129.5 (C₁₉), 129.1 (C₁₈), 128.0 (C₁₇), 126.3 (C₃), 126.0 (C₄), 114.1 (C₁₄), 113.0 (C₉), 108.9 (C₁₂), 51.9 (C₁), 34.8 (C₆), 31.5 (C₇).

MS-ESI-EM (MeOH, M = C₂₅H₂₅N₃S₁): found. 400.18401 for [M+H]⁺ (calcd. m/z = 400.18420 for [M+H]⁺), found 422.16580 for [M+Na]⁺ (calcd. m/z = 422.16614 for [M+Na]⁺).

Preparation of *N*-(6-phenyl-pyridin-2-yl)-*N*-thiazol-2-yl-pentanamide (**L₄H**)



A₂ (510 mg; 1.5 mmol) and phenylboronic acid (272 mg; 2.3 mmol) were used with [Pd(PPh₃)₄] (173 mg; 0.15 mmol) in 40 mL THF with 3 mL aqueous K₂CO₃ (2 M). After column chromatography (EtOAc:cyclohexane 1:3) to yield **L₄H** as colorless oil (411 mg; 1.22 mmol; 81 %).

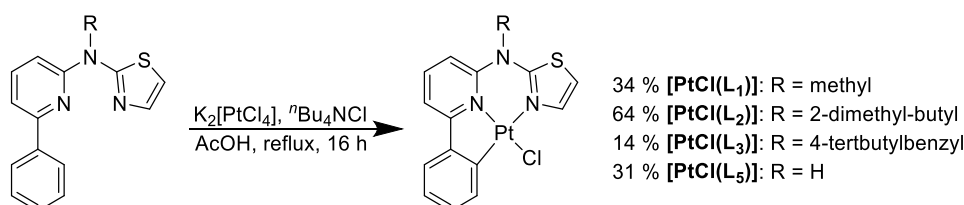
Analytical data for **L₄H**:

¹H-NMR (500 MHz, CDCl₃): δ (ppm) = 8.05 – 8.00 (m, 2H, H₁₅), 7.97 (t, ³J_{HH} = 7.8 Hz, 1H, H₁₁), 7.87 (dd, ³J_{HH} = 7.9 Hz, ⁴J_{HH} = 0.9 Hz, 1H, H₁₂), 7.48 – 7.43 (m, 2H, H₁₆), 7.44 – 7.41 (m, 1H, H₁₇), 7.40 (d, ³J_{HH} = 3.5 Hz, 1H, H₈), 7.34 (dd, ³J_{HH} = 7.7 Hz, ³J_{HH} = 0.9 Hz, 1H, H₁₀), 7.01 (d, ³J_{HH} = 3.5 Hz, 1H, H₇), 2.31 (t, ³J_{HH} = 7.4 Hz, 2H, H₂), 1.71 (p, ³J_{HH} = 7.5 Hz, 2H, H₃), 1.37 – 1.19 (m, 2H, H₄), 0.83 (t, ³J_{HH} = 7.4 Hz, 3H, H₅).

¹³C{¹H}-NMR (126 MHz, CDCl₃): δ (ppm) = 171.9 (C₁), 160.3 (C₆), 157.9 (C₁₃), 152.2 (C₉), 139.6 (C₁₁), 137.7 (C₁₄), 137.3 (C₈), 129.4 (C₁₇), 128.7 (C₁₆), 126.8 (C₁₅), 122.2 (C₁₀), 120.5 (C₁₂), 114.2 (C₇), 35.0 (C₂), 26.6 (C₃), 22.0 (C₄), 13.6 (C₅).

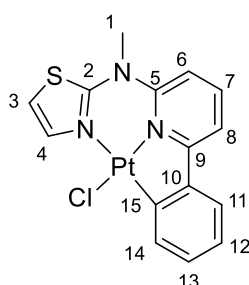
MS-ESI-EM (MeOH, M = C₁₉H₁₉N₃S₁O₁): found 360.11445 for [M+Na]⁺ (calcd. m/z = 360.11410 for [M+Na]⁺), found 697.24068 for [2M+Na]⁺ (calcd. m/z = 697.23899 for [2M+Na]⁺).

Method: Cyclometalation (acetic acid route)



The ligand-precursor (1.0 eq), K₂[PtCl₄] (1.0 eq) and ^tBu₄NCl (catalytic amounts) were dissolved in glacial acetic acid and the mixture was deoxygenated with Argon for 10 min. The reaction was refluxed for 16 h. After reaching room temperature the solvent was removed under reduced pressure and after purification *via* column chromatography over silica, with an eluent of DCM, the product was obtained.

Preparation of Chlorido-(κ³_{CNN}-*N*-(6-phenylpyridin-2-yl)-*N*-methyl-thiazole-2-amino)-platinum(II) ([PtCl(L₁)])



L₁H (170 mg; 0.64 mmol) and K₂[PtCl₄] (264 mg; 0.64 mmol) was refluxed in 20 mL glacial acetic acid. After column chromatography the product was obtained as a yellow solid (108 mg; 0.22 mmol; 34 %).

Analytical data for [PtCl(L₁)]:

¹H-NMR (500 MHz, DMSO-*d*₆): δ (ppm) = 8.32 (d, ³J_{HH} = 4.1 Hz, 1H, H₄), 8.24 (dd, ³J_{HH} = 8.5 Hz, ³J_{HH} = 7.8 Hz, 1H, H₇), 7.90 (dd, ³J_{HH} = 7.9 Hz, ³J_{HH} = 1.0 Hz, 1H, H₈), 7.89 (dd, ³J_{HH} = 7.6 Hz, ⁴J_{HH} = 1.4 Hz, 1H, H₁₄), 7.73 (dd, ³J_{HH} = 7.8 Hz, ⁴J_{HH} = 1.4 Hz, 1H, H₁₁), 7.53 (d, ³J_{HH} = 4.0 Hz, 1H, H₃), 7.48 (dd, ³J_{HH} = 8.5 Hz, ⁴J_{HH} = 1.0 Hz, 1H,

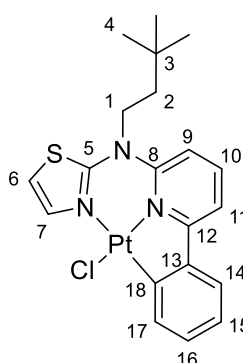
H₆), 7.15 (td, ³J_{HH} = 7.4 Hz, ³J_{HH} = 1.4 Hz, 1H, H₁₃), 7.08 (td, ³J_{HH} = 7.4 Hz, ³J_{HH} = 1.4 Hz, 1H, H₁₂), 3.90 (s, 3H, H₁).

¹³C{¹H}-NMR (126 MHz, DMSO-*d*₆): δ (ppm) = 165.1 (C₉), 161.3 (C₂), 148.6 (C₅), 144.7 (C₁₀), 143.3 (C₁₅), 138.9 (C₇), 137.2 (C₄), 134.1 (C₁₄), 128.5 (C₁₃), 123.6 (C₁₁), 123.3 (C₁₂), 113.8 (C₈), 113.2 (C₃), 113.1 (C₆), 43.5 (C₁).

¹⁹⁵Pt-NMR (107 MHz, DMSO-*d*₆): δ (ppm) = -3279.

MS-ESI-EM (MeOH, M = C₁₅H₁₂N₃S₁PtCl₁): found 460.03638 for [M-Cl]⁺ (calcd. m/z = 460.03730 for [M-Cl]⁺), found 497.01634 for [M+H]⁺ (calcd. m/z = 497.01609 for [M+H]⁺).

Preparation of Chlorido-(κ³_{CNN}-*N*-(6-phenylpyridin-2-yl)-*N*-(3,3-dimethyl-butyl)-thiazole-2-amino)-platinum(II) ([PtCl(L₂)])



L₂H (120 mg; 0.35 mmol) and K₂[PtCl₄] (141 mg; 0.34 mmol) was refluxed in 15 mL glacial acetic acid. After column chromatography the product was obtained as a yellow solid (127 mg; 0.22 mmol; 64 %).

Analytical data for [PtCl(L₂)]:

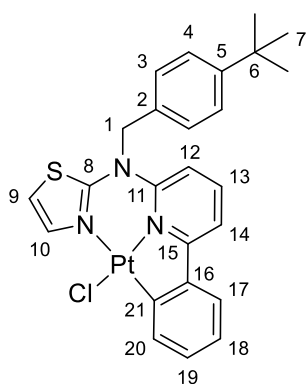
¹H-NMR (400 MHz, DCM-*d*₂/MeOD-*d*₄): δ (ppm) = 8.48 (d, ³J_{HH} = 4.2 Hz, 1H, H₇), 8.02 (dd, ³J_{HH} = 7.7 Hz, ⁴J_{HH} = 1.3 Hz, 1H, H₁₇), 7.96 (dd, ³J_{HH} = 8.6 Hz, ³J_{HH} = 7.8 Hz, 1H, H₁₀), 7.50 (m, 2H, H₁₁₊₁₄), 7.21 (td, ³J_{HH} = 7.4 Hz, ³J_{HH} = 1.4 Hz, 1H, H₁₆), 7.13 – 7.07 (m, 2H, H₉₊₁₅), 6.99 (d, ³J_{HH} = 4.1 Hz, 1H, H₆), 4.33 – 4.03 (m, 2H, H₁), 1.97 – 1.72 (m, 2H, H₂), 1.05 (s, 9H, H₄).

¹³C{¹H}-NMR (101 MHz, DCM-*d*₂/MeOD-*d*₄): δ (ppm) = 167.2 (C₁₂), 160.4 (C₇), 148.4 (C₈), 145.2 (C₁₃), 143.6 (C₁₈), 139.0 (C₇), 138.6 (C₁₀), 134.9 (C₁₇), 129.7 (C₁₆), 124.1 (C₁₅), 123.9 (C₁₄), 114.0 (C₁₁), 112.1 (C₉), 111.1 (C₆), 55.2 (C₁), 39.3 (C₂), 30.6 (C₃), 29.2 (C₄).

¹⁹⁵Pt-NMR (107 MHz, DCM-*d*₂/MeOD-*d*₄): δ (ppm) = -3257.

MS-ESI-EM (CHCl₃/MeOH, M = C₂₀H₂₂N₃S₂PtCl₁): found 567.09468 for [M+H]⁺ (calcd. m/z = 567.09435 for [M+H]⁺), found 589.07678 for [M+Na]⁺ (calcd. m/z = 589.07629 for [M+Na]⁺).

Preparation of Chlorido-(κ³_{CNN}-*N*-(6-phenylpyridin-2-yl)-*N*-(4-*tert*-butylbenzyl)-thiazole-2-amino)-platinum(II) ([PtCl(L₃)])



L₃H (155 mg; 0.388 mmol) and K₂[PtCl₄] (161 mg; 0.388 mmol) was refluxed in 25 mL glacial acetic acid. After column chromatography the product was obtained as a yellow solid (35 mg; 0.056 mmol; 14 %).

Analytical data for [PtCl(L₃)]:

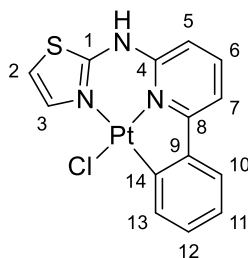
¹H-NMR (500 MHz, DCM-*d*₂): δ (ppm) = 8.56 (d, ³J_{HH} = 4.1 Hz, 1H, H₁₀), 8.06 (dd, ³J_{HH} = 7.8 Hz, ⁴J_{HH} = 1.3 Hz, 1H, H₂₀), 7.85 (dd, ³J_{HH} = 8.5 Hz, ³J_{HH} = 7.8 Hz, 1H, H₁₃), 7.53 (ddd, ³J_{HH} = 7.9 Hz, ³J_{HH} = 5.0 Hz, ⁴J_{HH} = 1.2 Hz, 2H, H₁₄₊₁₇), 7.48 – 7.41 (m, 2H, H₄), 7.27 – 7.16 (m, 3H, H₃₊₁₉), 7.15 – 7.09 (m, 1H, H₁₈), 7.02 (dd, ³J_{HH} = 8.6 Hz, ⁴J_{HH} = 1.0 Hz, 1H, H₁₂), 6.93 (d, ³J_{HH} = 4.1 Hz, 1H, H₉), 5.45 (s, 2H, H₁), 1.32 (s, 9H, H₇).

¹³C{¹H}-NMR (101 MHz, DCM-*d*₂): δ (ppm) = 167.1 (C₁₅), 160.8 (C₈), 152.1 (C₅), 149.4 (C₁₁), 145.1 (C₁₆), 143.8 (C₂₁), 138.8 (C₁₀), 138.5 (C₁₃), 135.1 (C₂₀), 129.9 (C₂), 129.7 (C₁₉), 126.8 (C₄), 126.1 (C₃), 124.0 (C₁₈), 123.9 (C₁₇), 114.3 (C₁₄), 112.6 (C₁₂), 111.6 (C₉), 61.3 (C₁), 35.0 (C₆), 31.4 (C₇).

¹⁹⁵Pt-NMR (107 MHz, DCM-*d*₂): δ (ppm) = -3269.

MS-ESI-EM (CHCl₃/MeOH, M = C₂₅H₂₄N₃S₁Pt₁Cl₁): found 629.11052 for [M+H]⁺ (calcd. m/z = 629.11019 for [M+H]⁺), found 651.09248 for [M+Na]⁺ (calcd. m/z = 651.09214 for [M+Na]⁺).

Preparation of Chlorido-(κ³CNN-N-(6-phenylpyridin-2-yl)-thiazole-2-amino)-platinum(II) ([PtCl(L₅)])



L₄H (92 mg; 0.27 mmol) and K₂[PtCl₄] (113 mg; 0.27 mmol) was refluxed in 25 mL glacial acetic acid. After column chromatography (Al₂O₃; EtOAc:MeOH 5%) the product was obtained as the second fraction. After washing with DCM (3·3 mL) and diethylether (1·10 mL) the residue was filtrated over silica (DCM:MeOH; 39:1). The product was obtained as a yellow solid (40.5 mg; 0.084 mmol; 31 %).

Analytical data for [PtCl(L₅)]:

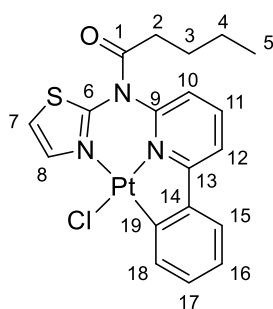
¹H-NMR (400 MHz, DMSO-*d*₆): δ (ppm) = 12.59 (s, 1H, NH), 8.30 (d, ³J_{HH} = 4.1 Hz, 1H, H₃), 8.18 (t, ³J_{HH} = 8.0 Hz, 1H, H₆), 7.98 (dd, ³J_{HH} = 7.6 Hz, ⁴J_{HH} = 1.4 Hz, 1H, H₁₃), 7.80 (dd, ³J_{HH} = 7.9 Hz, ⁴J_{HH} = 1.2 Hz, 1H, H₇), 7.74 (dd, ³J_{HH} = 7.8 Hz, ⁴J_{HH} = 1.5 Hz, 1H, H₁₀), 7.32 (d, ³J_{HH} = 4.0 Hz, 1H, H₂), 7.19 – 7.11 (m, 2H, H₅₊₁₂), 7.08 (td, ³J_{HH} = 7.4 Hz, ⁴J_{HH} = 1.4 Hz, 1H, H₁₁).

¹³C{¹H}-NMR (101 MHz, DMSO-*d*₆): δ (ppm) = 164.0 (C₈), 155.1 (C₁), 144.7 (C₄), 144.1 (C₉), 142.2 (C₁₄), 138.3 (C₆), 135.9 (C₃), 134.3 (C₁₃), 128.3 (C₁₂), 123.1 (C₁₀₊₁₁), 112.6 (C_{5/7}), 112.6 (C_{5/7}), 111.9 (C₂).

¹⁹⁵Pt-NMR (86 MHz, DMSO-*d*₆): δ (ppm) = -3229.

MS-ESI-EM (MeOH, M = C₁₄H₁₀N₃S₁Pt₁Cl₁): found 483.00094 for [M+H]⁺ (calcd. m/z = 483.00044 for [M+H]⁺), found 504.98284 for [M+Na]⁺ (calcd. m/z = 504.98239 for [M+Na]⁺).

Preparation of Chlorido-(κ³CNN-N-(6-phenyl-pyridin-2-yl)-N-thiazol-2-yl-pentanamide)-platinum(II) ([PtCl(L₄)])



L₄H (103 mg; 0.31 mmol) and K₂[PtCl₄] (127 mg; 0.31 mmol) were dissolved in a mixture of MeCN:H₂O (40 mL; v/v = 1/1), deoxygenated for 10 min with argon and heated to reflux for 16 h. After reaching room temperature the mixture was poured on DCM (30 mL) and H₂O (30 mL). The H₂O-phase was extracted with DCM (3·30 mL) and the solvent of the combined organic phases were removed under reduced pressure. The product (9.3 mg; 0.016 mmol; 5 %) was obtained as a yellow semi-solid after column chromatography (SiO₂; DCM).

Analytical data for [PtCl(L₄)]:

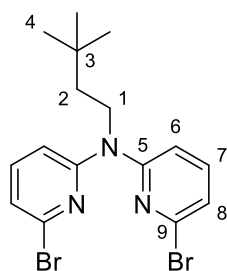
¹H-NMR (400 MHz, DCM-*d*₂): δ (ppm) = 8.43 (d, ³J_{HH} = 3.9 Hz, 1H, H₈), 8.00 (t, ³J_{HH} = 7.9 Hz, 1H, H₁₁), 7.89 (dd, ³J_{HH} = 7.7 Hz, ⁴J_{HH} = 1.3 Hz, 1H, H₁₈), 7.74 (dd, ³J_{HH} = 8.1 Hz, ⁴J_{HH} = 1.2 Hz, 1H, H₁₂), 7.56 (d, ³J_{HH} = 3.9 Hz, 1H, H₇), 7.52 (dd, ³J_{HH} = 7.7 Hz, ⁴J_{HH} = 1.4 Hz, 1H, H₁₅), 7.31 – 7.18 (m, 2H, H₁₀₊₁₇), 7.14 (td, ³J_{HH} = 7.5 Hz, ⁴J_{HH} = 1.3 Hz, 1H, H₁₆), 2.49 – 2.36 (m, 2H, H₂), 1.60 (p, ³J_{HH} = 7.5 Hz, 2H, H₃), 1.42 – 1.15 (m, 2H, H₄), 0.83 (t, ³J_{HH} = 7.4 Hz, 3H, H₅).

¹³C{¹H}-NMR (101 MHz, DCM-*d*₂): δ (ppm) = 173.2 (C₁), 169.5 (C₁₃), 157.2 (C₆), 148.7 (C₉), 145.0 (C₁₄), 142.8 (C₁₉), 139.3 (C₁₁), 138.8 (C₈), 135.2 (C₁₈), 130.6 (C₁₇), 124.6 (C₁₅), 124.6 (C₁₆), 120.6 (C₁₀), 120.4 (C₇), 118.4 (C₁₂), 36.2 (C₂), 27.7 (C₃), 22.4 (C₄), 13.8 (C₅).

¹⁹⁵Pt-NMR (86 MHz, DCM-*d*₂): δ (ppm) = -3397.

MS-ESI-EM (MeOH, M = C₁₉H₁₈N₃S₁O₁Pt₁Cl₁): found 567.05842 for [M+H]⁺ (calcd. m/z = 567.05796 for [M+H]⁺), found 589.04034 for [M+Na]⁺ (calcd. m/z = 589.03990 for [M+Na]⁺).

Preparation of 6-bromo-*N*-(6-bromopyridin-2-yl)-*N*-(3,3-dimethylbutyl)pyridin-2-amine (**A₆**)



Bis-(6-bromopyridine-2-yl)-amine (432 mg; 1.3 mmol) was dissolved in DMF (10 mL) and cooled to 0 °C. NaH (94.5 mg; 3.9 mmol) was added and the mixture was stirred for 15 min at room temperature before 1-bromo-3,3-dimethyl-butane (0.37 mL; 2.6 mmol) was added. The mixture was stirred at this temperature for 18 h before the reaction was quenched with dest. H₂O (40 mL). EtOAc (15 mL) was added and the mixture was extracted with EtOAc (3·50 mL). The solvent of the combined organic phases was removed under reduced pressure and the after column chromatography (SiO₂; EtOAc:n-hexane 1:19) the product (327 mg; 0.79 mmol; 61 %) was obtained as a white solid/colorless oil.

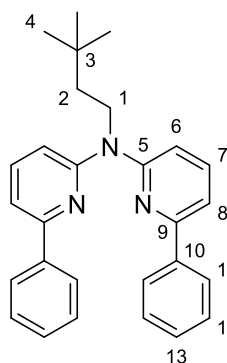
Analytical data for **A₆**:

¹H-NMR (400 MHz, DCM-*d*₂): δ (ppm) = 7.41 (dd, ³J_{HH} = 8.2 Hz, ³J_{HH} = 7.6 Hz, 2H, H₇), 7.12 (dd, ³J_{HH} = 8.2 Hz, ⁴J_{HH} = 0.6 Hz, 2H, H₆), 7.05 (dd, ³J_{HH} = 7.6 Hz, ⁴J_{HH} = 0.6 Hz, 2H, H₈), 4.24 – 4.09 (m, 2H, H₁), 1.68 – 1.53 (m, 2H, H₂), 0.99 (s, 9H, H₄).

¹³C{¹H}-NMR (101 MHz, DCM-*d*₂): δ (ppm) = 156.9 (C₅), 140.1 (C₉), 140.0 (C₇), 121.3 (C₈), 113.3 (C₆), 46.0 (C₁), 41.2 (C₂), 30.4 (C₃), 29.6 (C₄).

MS-ESI-EM (MeOH, M = C₁₆H₁₉N₃Br₂): found 380.12031 for [M+H]⁺ (calcd. m/z = 380.12497 for [M+H]⁺), found 413.99981 for [M+Na]⁺ (calcd. m/z = 413.99987 for [M+Na]⁺).

Preparation of *N*-(3,3-dimethylbutyl)-6-phenyl-*N*-(6-phenylpyridin-2-yl)-pyridin-2-amine (**L₆H**)



A₆ (150 mg; 0.35 mmol, 1.0 eq.), phenylboronic acid (126 mg; 1.04 mmol; 3.0 eq.) and [Pd(PPh₃)₄] (40 mg; 0.03 mmol; 0.1 eq.) were dissolved in THF (20 mL) and deoxygenated for 10 min. Afterwards a 2M solution of aqueous K₂CO₃ (3 mL) was added and the mixture was deoxygenated again for 5 min. The reaction was heated to reflux for 16 h and after reaching room, the mixture was poored on dest. H₂O (10 mL) and EtOAc (10 mL). The H₂O-phase was extracted with EtOAc (3·30 mL). The combined organic phases were dried over Na₂SO₄ and the solvent was removed under reduced pressure. After purification *via* column chromatography over silica (*n*-hexane/DCM: 70/30) the mono-substituted product **L₆BrH** (62 mg; 0.15 mmol; 43 %) was obtained first as a colorless oil and second as white crystalline solid the product **L₆H₂** (48 mg;

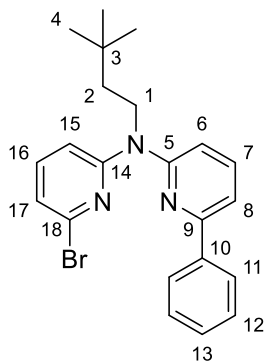
0.12 mmol; 34 %).

Analytical data for **L₆H₂**:

¹H-NMR (500 MHz, CDCl₃): δ (ppm) = 8.20 – 8.10 (m, 4H, H₁₁), 7.62 (dd, ³J_{HH} = 8.3 Hz, ³J_{HH} = 7.5 Hz, 2H, H₇), 7.56 – 7.49 (m, 4H, H₁₂), 7.48 – 7.42 (m, 2H, H₁₃), 7.40 – 7.36 (m, 2H, H₈), 7.22 (dd, ³J_{HH} = 8.3 Hz, ⁴J_{HH} = 0.7 Hz, 2H, H₆), 4.70 – 4.47 (m, 2H, H₁), 2.16 – 1.69 (m, 2H, H₂), 1.14 (s, 9H, H₄).

¹³C{¹H}-NMR (126 MHz, CDCl₃): δ (ppm) = 156.8 (C₅), 155.4 (C₉), 139.4 (C₁₀), 137.6 (C₇), 128.7 (C₁₃), 128.5 (C₁₂), 126.6 (C₁₁), 112.9 (C₆), 112.7 (C₈), 44.8 (C₁), 41.2 (C₂), 30.0 (C₃), 29.6 (C₄).

MS-ESI-EM (MeOH, M = C₂₈H₂₉N₃): found 408.24316 for [M+H]⁺ (calcd. m/z = 408.24342 for [M+H]⁺).



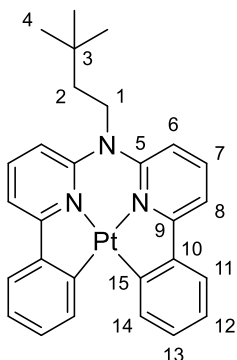
Analytical data for **L₆BrH**:

¹H-NMR (400 MHz, DCM-*d*₂): δ (ppm) = 8.11 – 8.00 (m, 2H, H₁₁), 7.67 (dd, ³*J*_{HH} = 8.2 Hz, ³*J*_{HH} = 7.6 Hz, 1H, H₇), 7.51 – 7.42 (m, 3H, H₈₊₁₂), 7.43 – 7.39 (m, 1H, H₁₃), 7.36 (dd, ³*J*_{HH} = 8.3 Hz, ³*J*_{HH} = 7.5 Hz, 1H, H₁₆), 7.16 (dd, ³*J*_{HH} = 8.2 Hz, ⁴*J*_{HH} = 0.7 Hz, 1H, H₆), 7.12 (dd, ³*J*_{HH} = 8.3 Hz, ⁴*J*_{HH} = 0.6 Hz, 1H, H₁₅), 6.99 (dd, ³*J*_{HH} = 7.5 Hz, ⁴*J*_{HH} = 0.6 Hz, 1H, H₁₇), 4.39 – 4.21 (m, 2H, H₁), 1.81 – 1.59 (m, 2H, H₂), 1.04 (s, 9H, H₄).

¹³C{¹H}-NMR (101 MHz, DCM-*d*₂): δ (ppm) = 157.5 (C₁₄), 156.6 (C₅), 156.0 (C₉), 140.0 (C₁₈), 139.5 (C₁₀), 139.4 (C₁₆), 138.5 (C₇), 129.3 (C₁₃), 129.0 (C₁₂), 127.0 (C₁₁), 119.6 (C₁₇), 114.5 (C₈), 114.3 (C₆), 112.1 (C₁₅), 45.6 (C₁), 41.3 (C₂), 30.3 (C₃), 29.6 (C₄).

MS-ESI-EM (MeOH, M = C₂₂H₂₄N₃Br₁): found 412.1197 for [M+H]⁺ (calcd. m/z = 412.1206 for [M+H]⁺).

Preparation of (*κ*⁴_{CNNC}-*N*-(3,3-dimethylbutyl)-6-phenyl-*N*-(6-phenylpyridin-2-yl)-pyridin-2-amine)-platinum(II) ([Pt(L₆)])



L₆H₂ (120 mg; 0.29 mmol), K₂[PtCl₄] (122 mg; 0.29 mmol) and a catalytically amount of ⁿBu₄NCl were suspended in glacial acetic acid (25 mL). The mixture was deoxygenated with argon for 10 min and afterwards heated to reflux for 48 h. The solvent was evaporated under reduced pressure and the residue was purified *via* column chromatography (SiO₂; DCM). The yellow spot was collected and the resulting solid was washed with diethylether (2·10 mL), suspended in DCM (10 mL) before diethylether (10 mL) was added. The solvent mixture was discarded and the remaining solid was dried under reduced pressure. The product (117.5 mg; 0.196 mmol; 67 %) was obtained as yellow solid.

Analytical data for [Pt(L₆)]:

¹H-NMR (500 MHz, DCM-*d*₂): δ (ppm) = 8.23 (dd, ³*J*_{HH} = 7.6 Hz, ⁴*J*_{HH} = 1.2 Hz, 2H, H₁₄), 7.96 (dd, ³*J*_{HH} = 8.4 Hz, ³*J*_{HH} = 7.7 Hz, 2H, H₇), 7.75 (dd, ³*J*_{HH} = 7.8 Hz, ⁴*J*_{HH} = 1.4 Hz, 2H, H₁₁), 7.61 (dd, ³*J*_{HH} = 7.9 Hz, ⁴*J*_{HH} = 0.9 Hz, 2H, H₈), 7.35 (td, ³*J*_{HH} = 7.4 Hz, ⁴*J*_{HH} = 1.4 Hz, 2H, H₁₃), 7.28 (dd, ³*J*_{HH} = 8.4 Hz, ⁴*J*_{HH} = 0.9 Hz, 2H, H₆), 7.17 (td, ³*J*_{HH} = 7.4 Hz, ⁴*J*_{HH} = 1.2 Hz, 2H, H₁₂), 4.51 – 4.07 (m, 2H, H₁), 1.81 – 1.57 (m, 2H, H₂), 0.92 (s, 9H, H₄).

¹³C{¹H}-NMR (101 MHz, DCM-*d*₂): δ (ppm) = 164.4 (C₉), 151.4 (C₅), 149.7 (C₁₅), 148.0 (C₁₀), 138.2 (C₇), 135.8 (C₁₄), 129.5 (C₁₃), 124.3 (C₁₁), 123.5 (C₁₂), 114.3 (C₆), 112.9 (C₈), 52.6 (C₁), 41.9 (C₂), 30.4 (C₃), 29.4 (C₄).

¹⁹⁵Pt-NMR (86 MHz, DCM-*d*₂): δ (ppm) = -3543.

MS-ESI-EM (MeOH, M = C₂₈H₂₇N₃Pt₁): found 601.19318 for [M+H]⁺ (calcd. m/z = 601.19044 for [M+H]⁺).

II. NMR spectroscopy

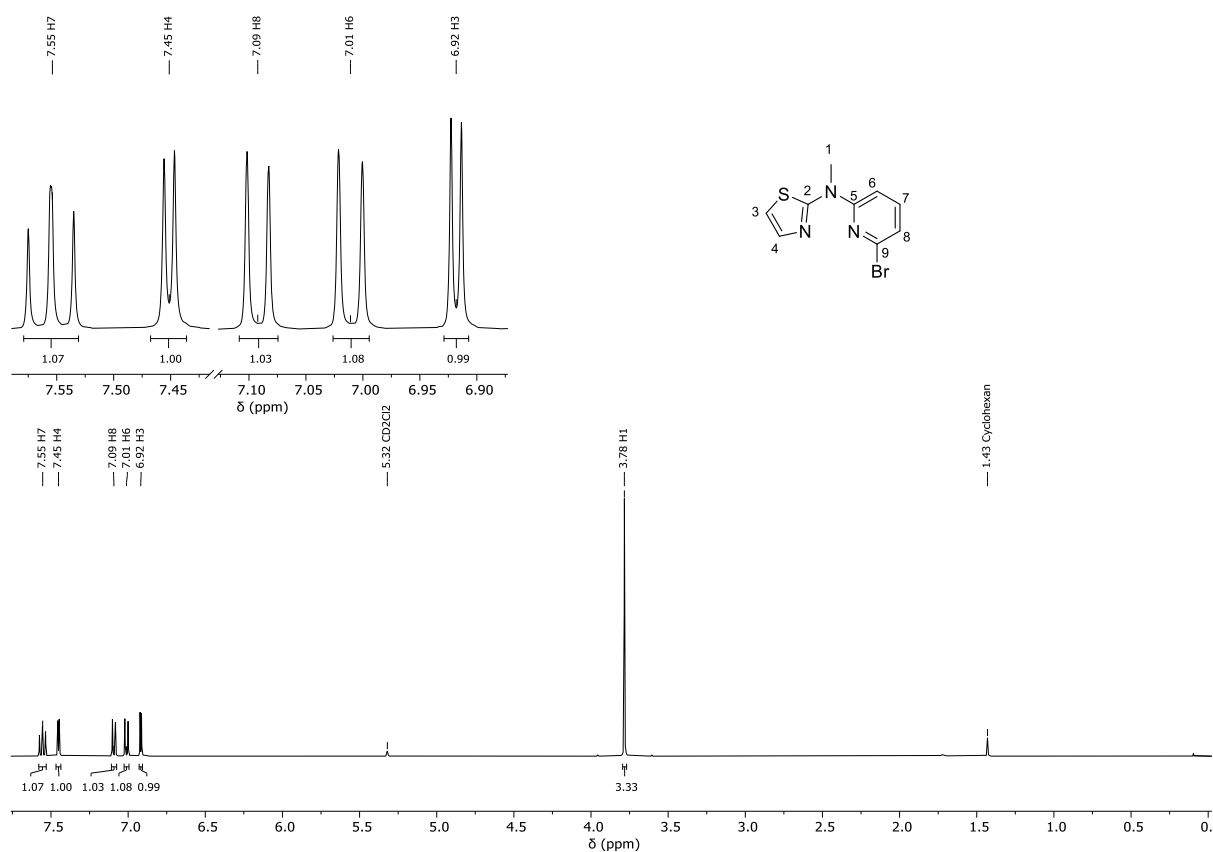


Figure S1: ¹H-NMR spectrum (400 MHz, DCM-d₂) of A₁.

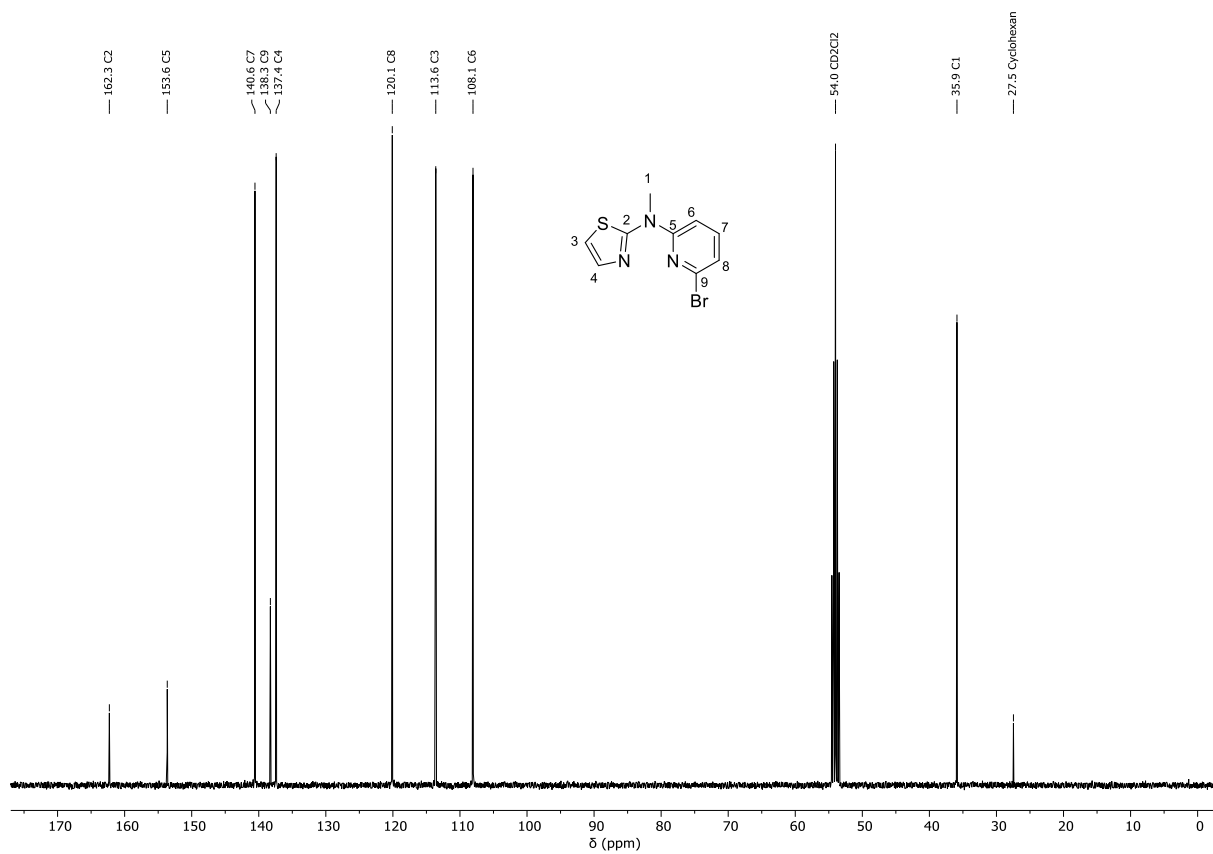


Figure S2: ¹³C-¹H-NMR spectrum (101 MHz, DCM-d₂) of A₁.

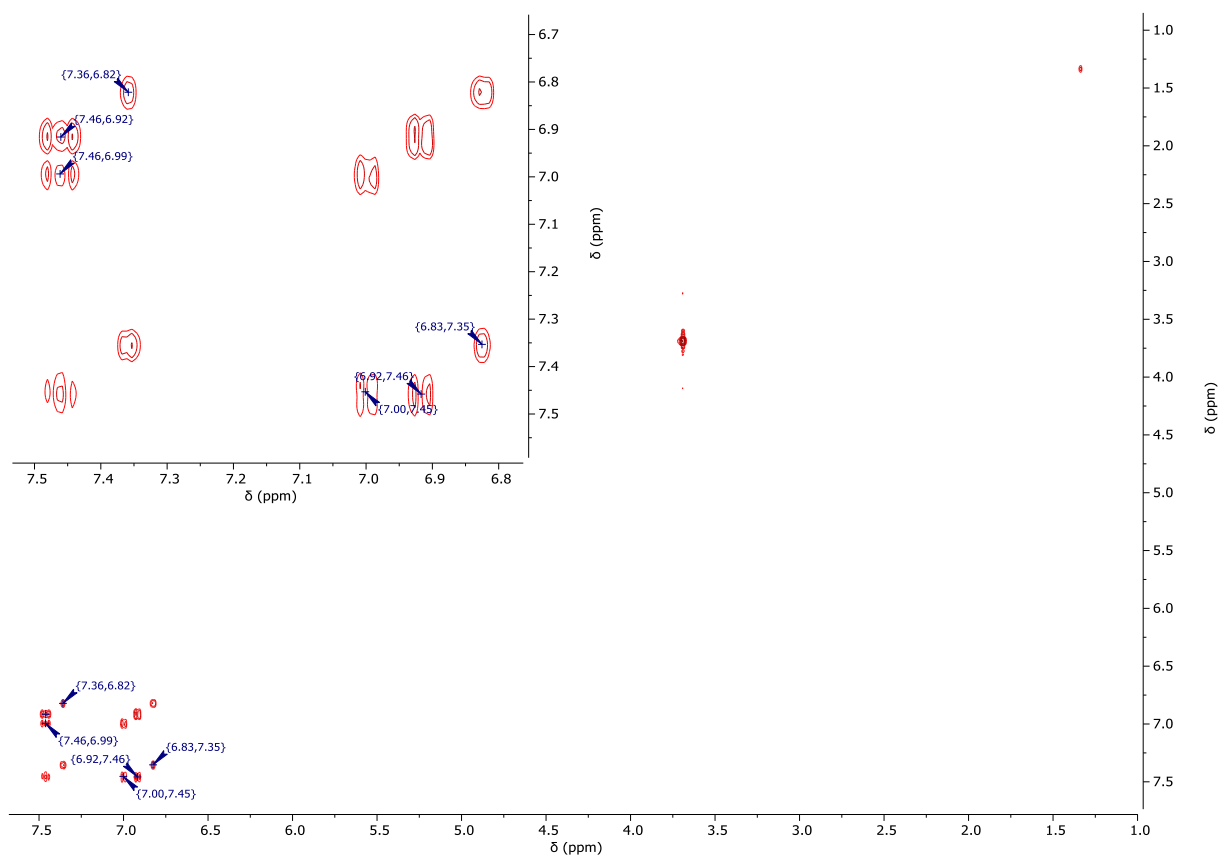


Figure S3: $^1\text{H}/^1\text{H}$ -COSY-NMR spectrum (400 MHz/400 MHz, $\text{DCM-}d_2$) of **A1**.

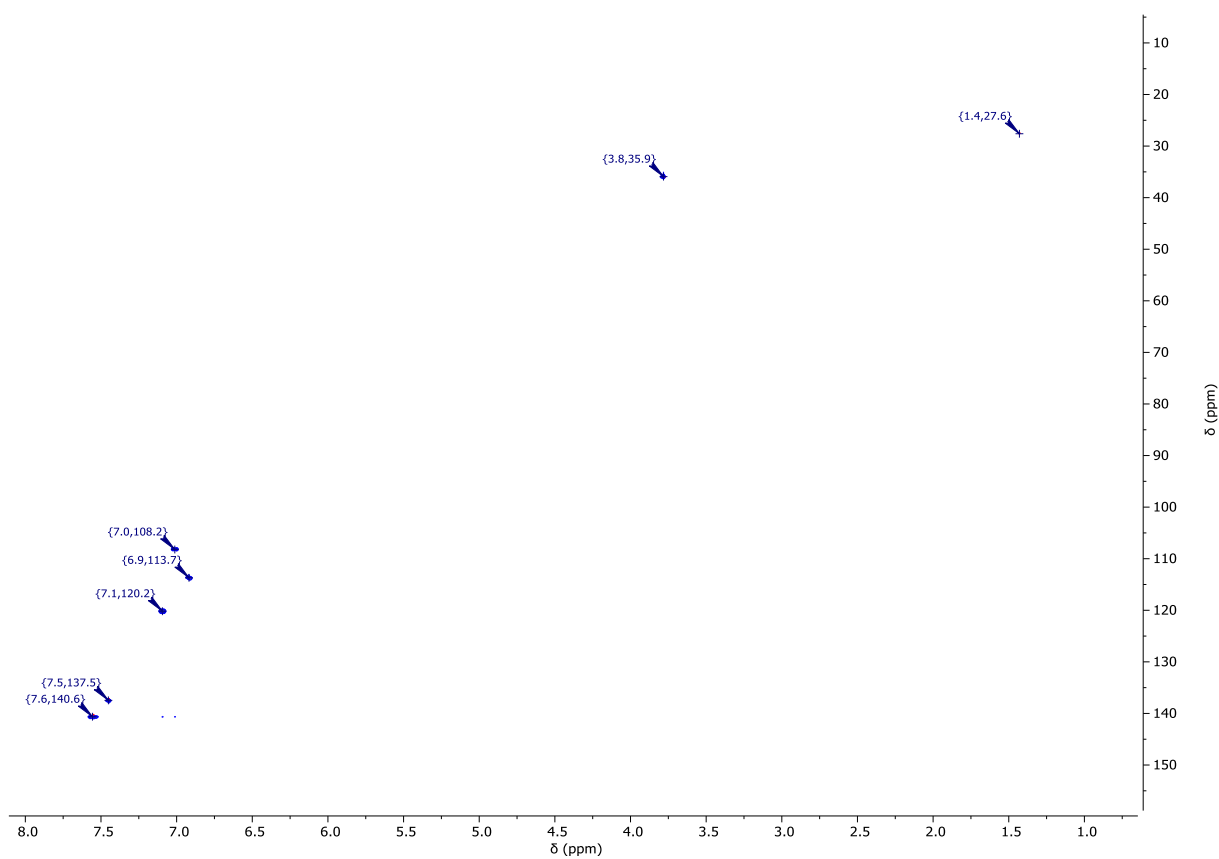


Figure S4: $^1\text{H}/^{13}\text{C}$ -gHSQC-NMR spectrum (400 MHz/101 MHz, $\text{DCM-}d_2$) of **A1**.

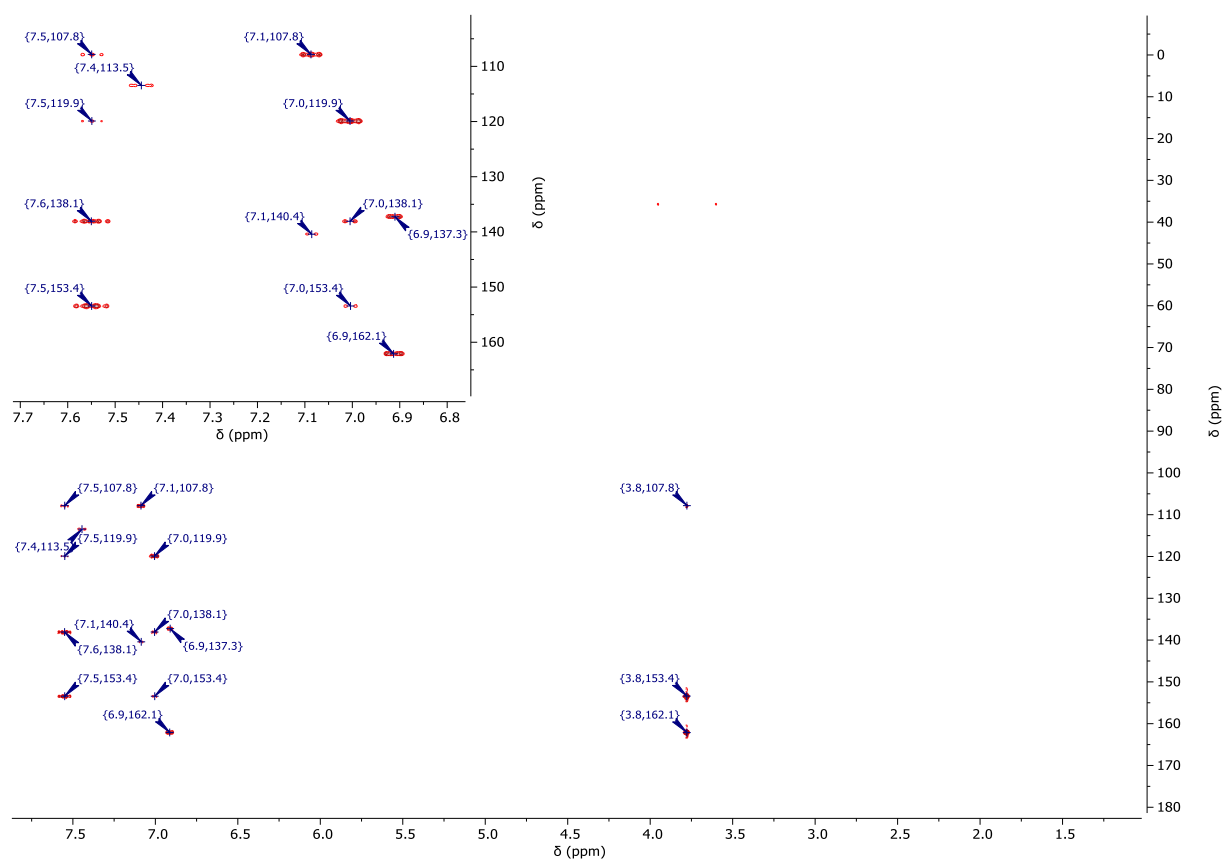


Figure S5: $^1\text{H}/^{13}\text{C}$ -gHMBC-NMR spectrum (400 MHz/101 MHz, $\text{DCM}-d_2$) of **A1**.

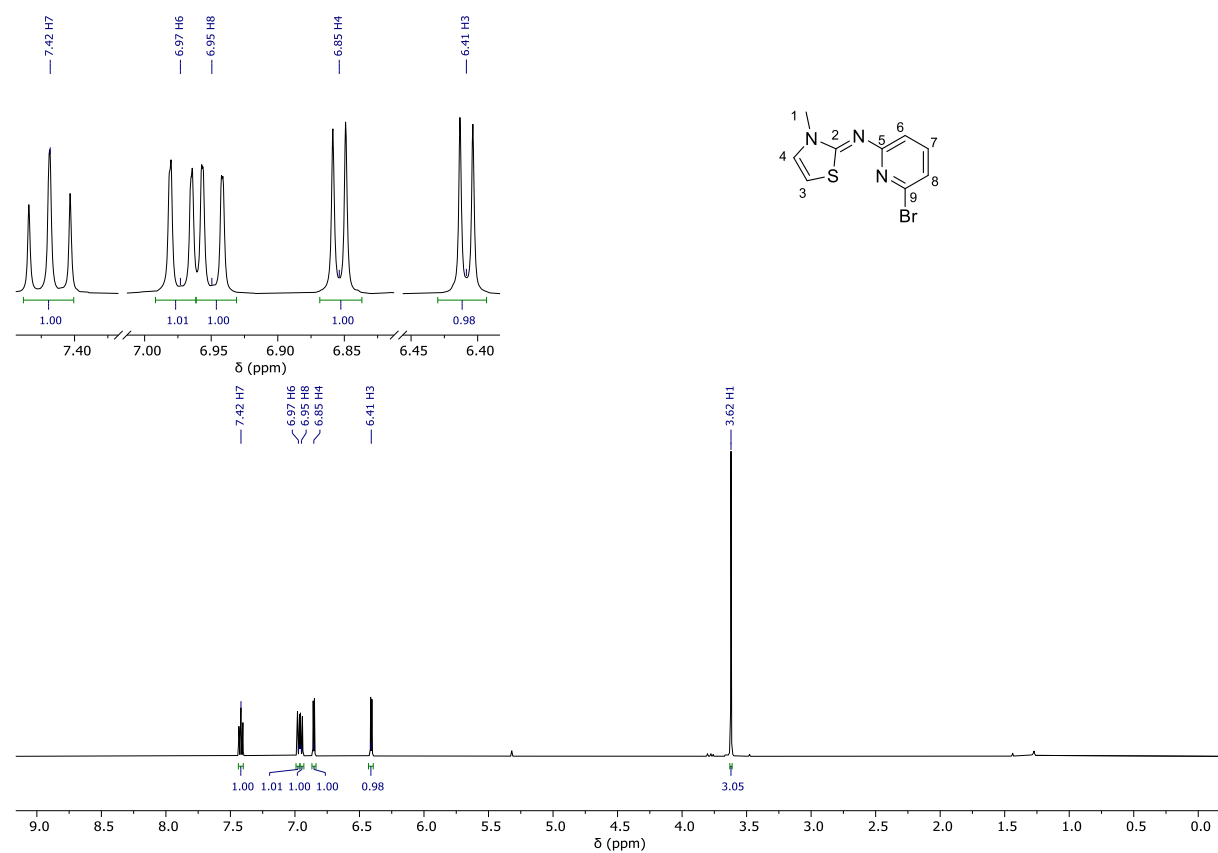


Figure S6: ^1H -NMR spectrum (500 MHz, $\text{DCM}-d_2$) of **I1**.

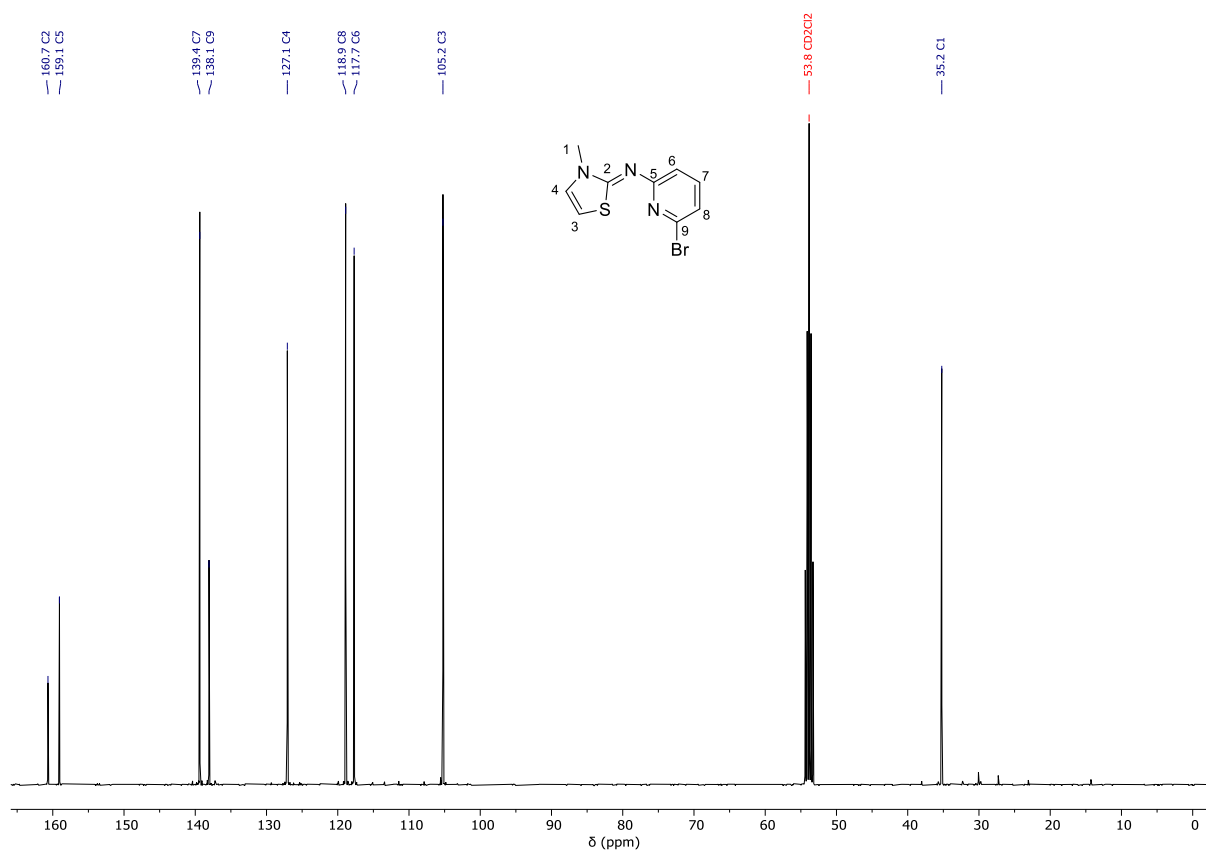


Figure S7: ^{13}C - ^1H -NMR spectrum (101 MHz, DCM-d_2) of **I1**.

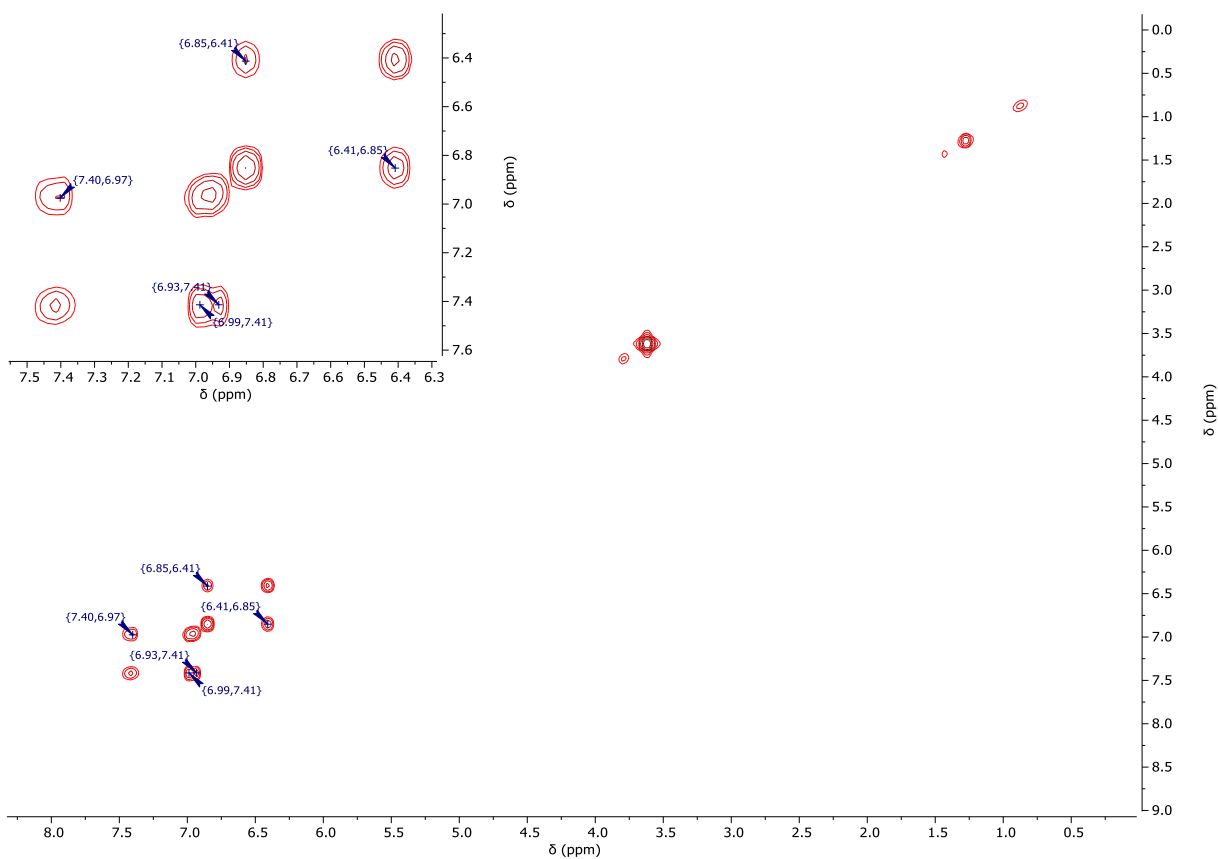


Figure S8: ^1H - ^1H -COSY-NMR spectrum (400 MHz/400 MHz, DCM-d_2) of **I1**.

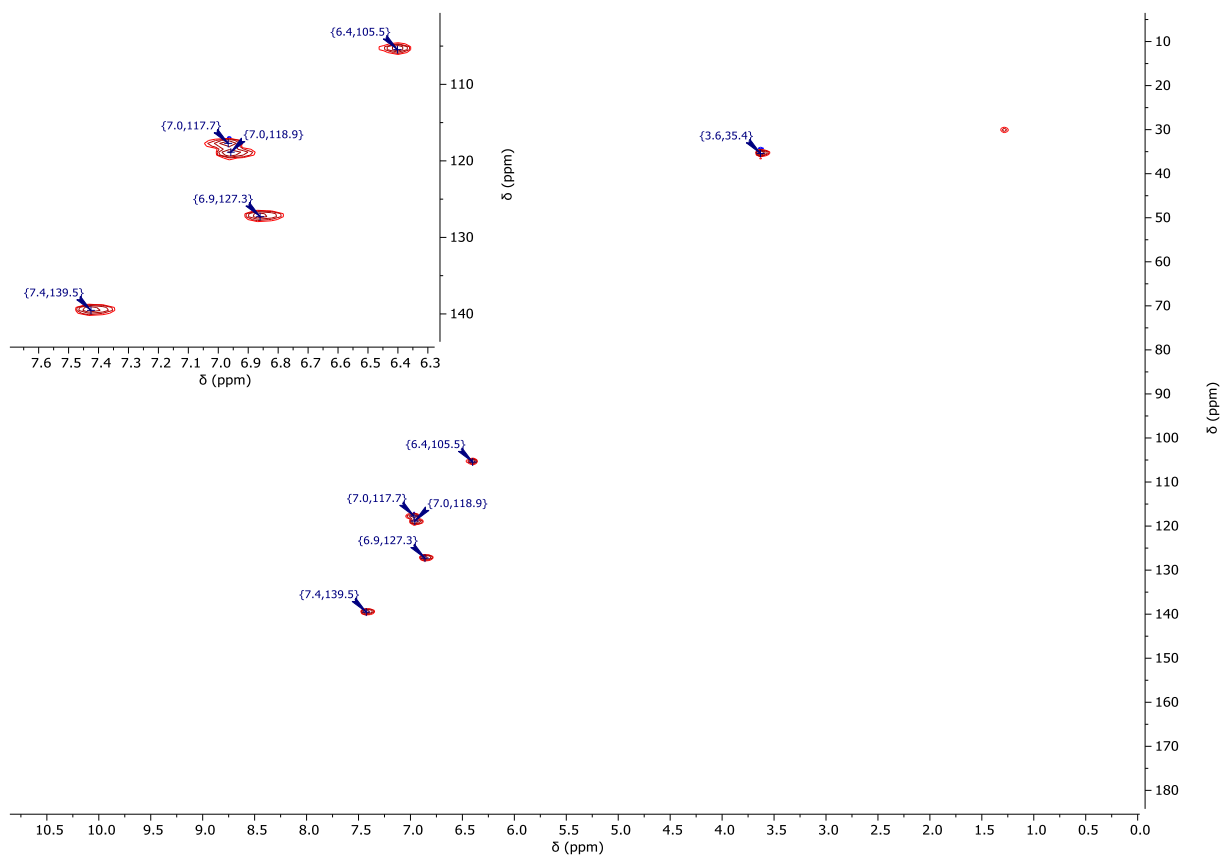


Figure S9: $^1\text{H}/^{13}\text{C}$ -gHSQC-NMR spectrum (400 MHz/101 MHz, $\text{DCM-}d_2$) of **I₁**.

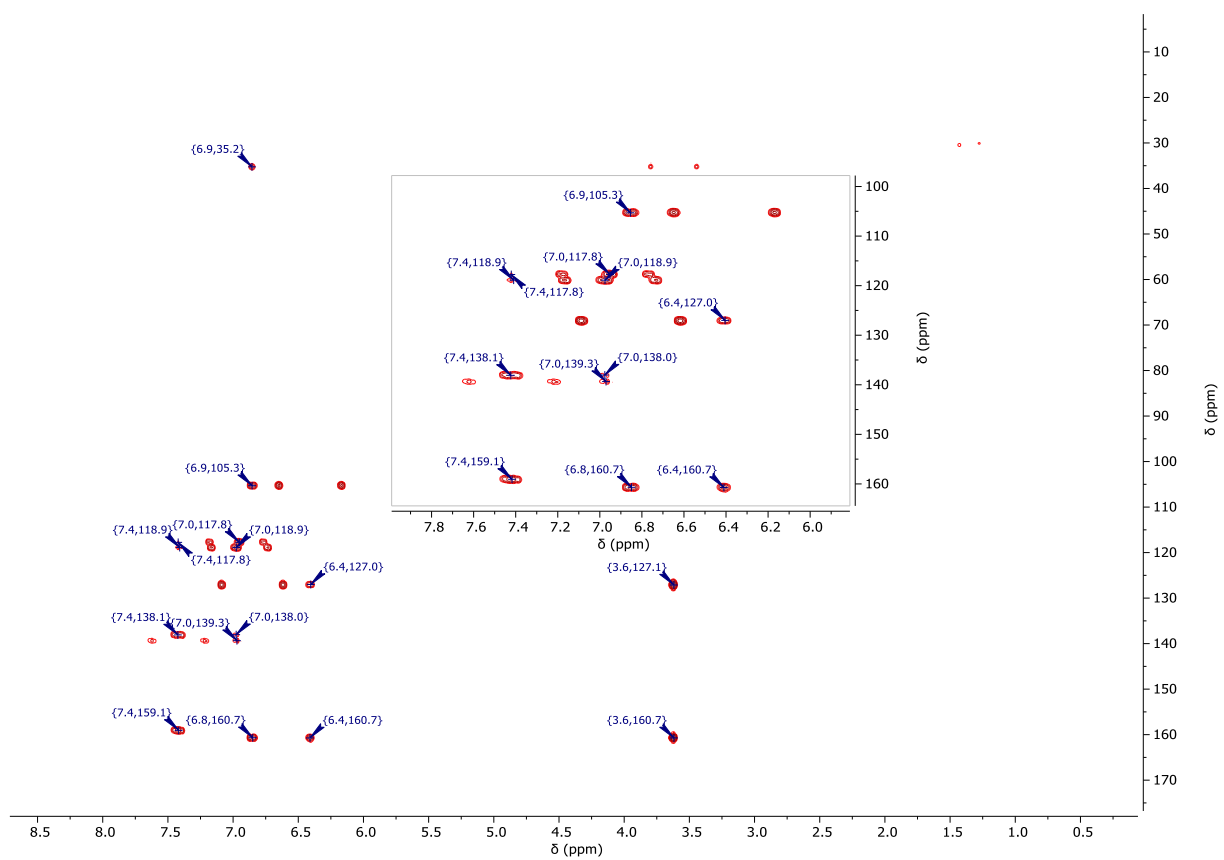


Figure S10: $^1\text{H}/^{13}\text{C}$ -gHMBC-NMR spectrum (400 MHz/101 MHz, $\text{DCM-}d_2$) of **I₁**.

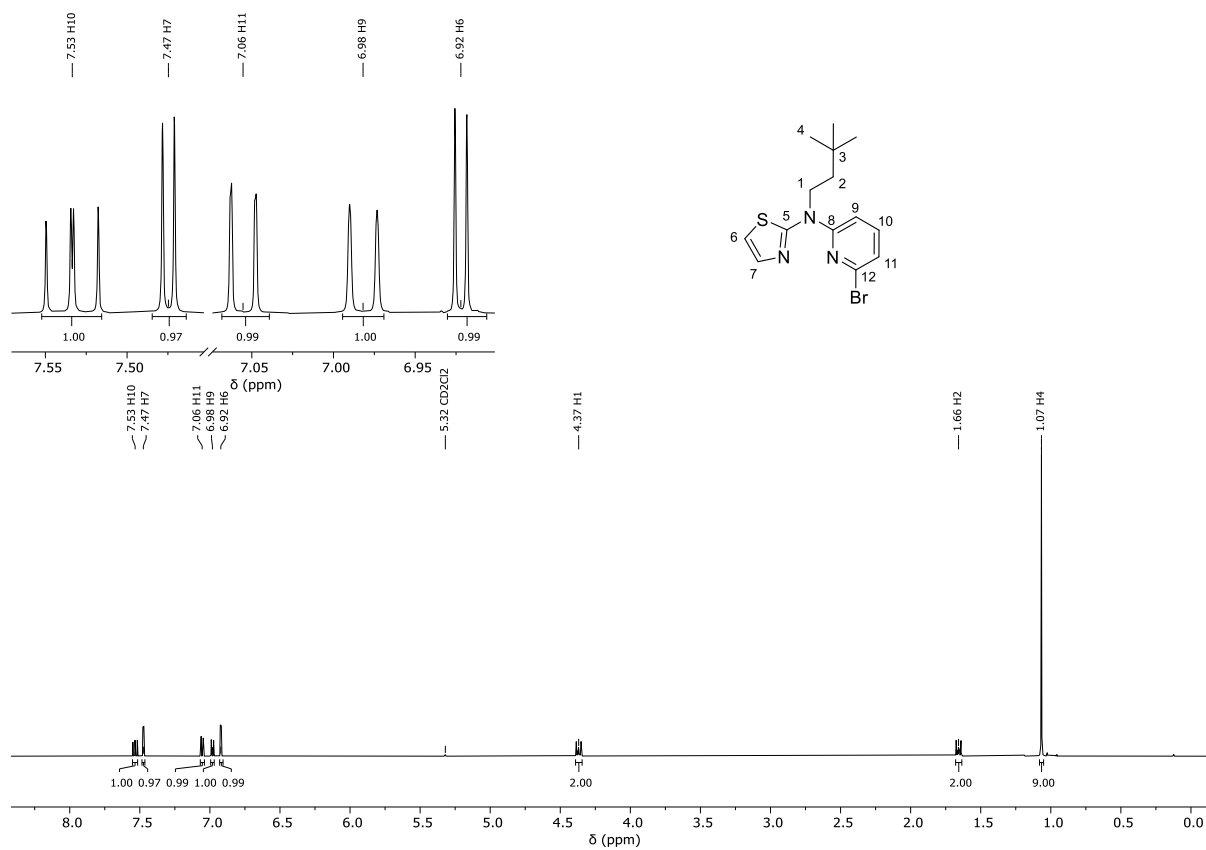


Figure S11: ¹H-NMR spectrum (500 MHz, DCM-*d*₂) of **A₂**.

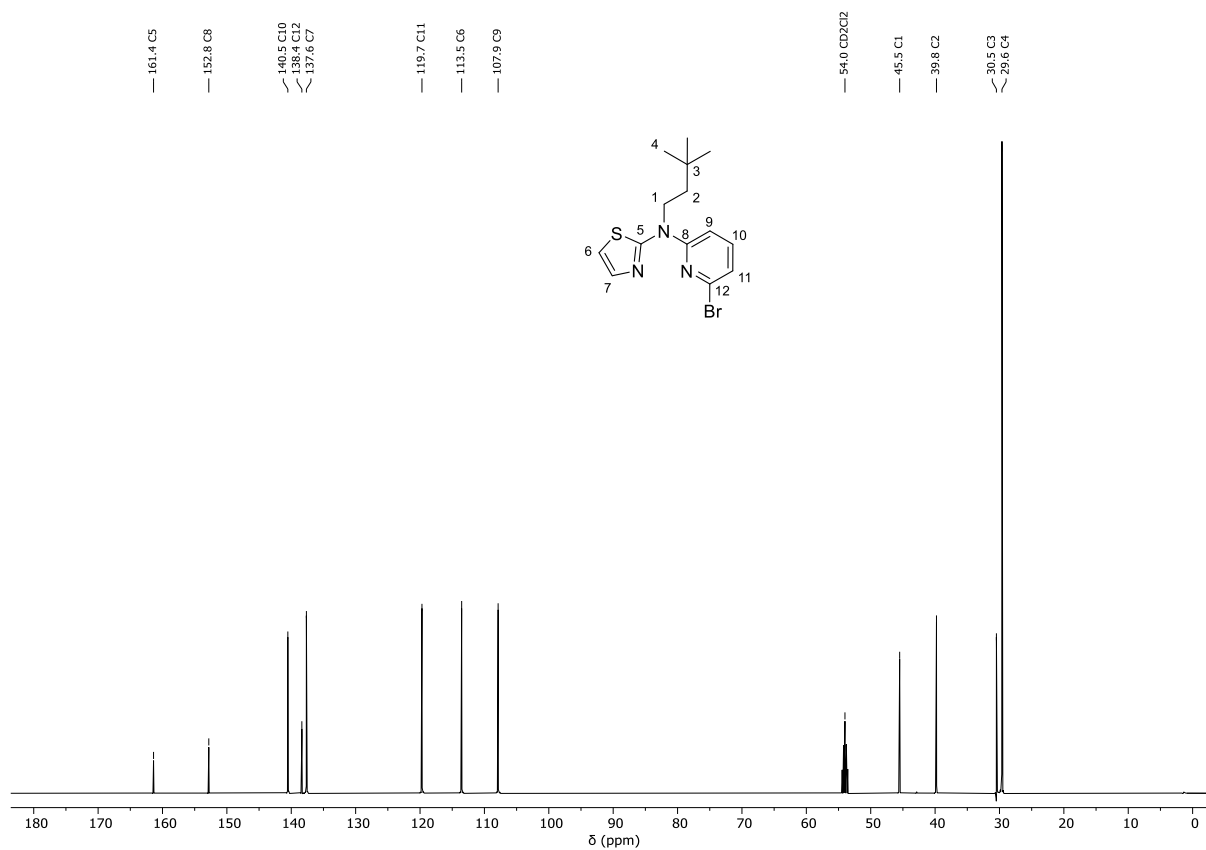


Figure S12: ¹³C-¹H-NMR spectrum (126 MHz, DCM-*d*₂) of **A₂**.

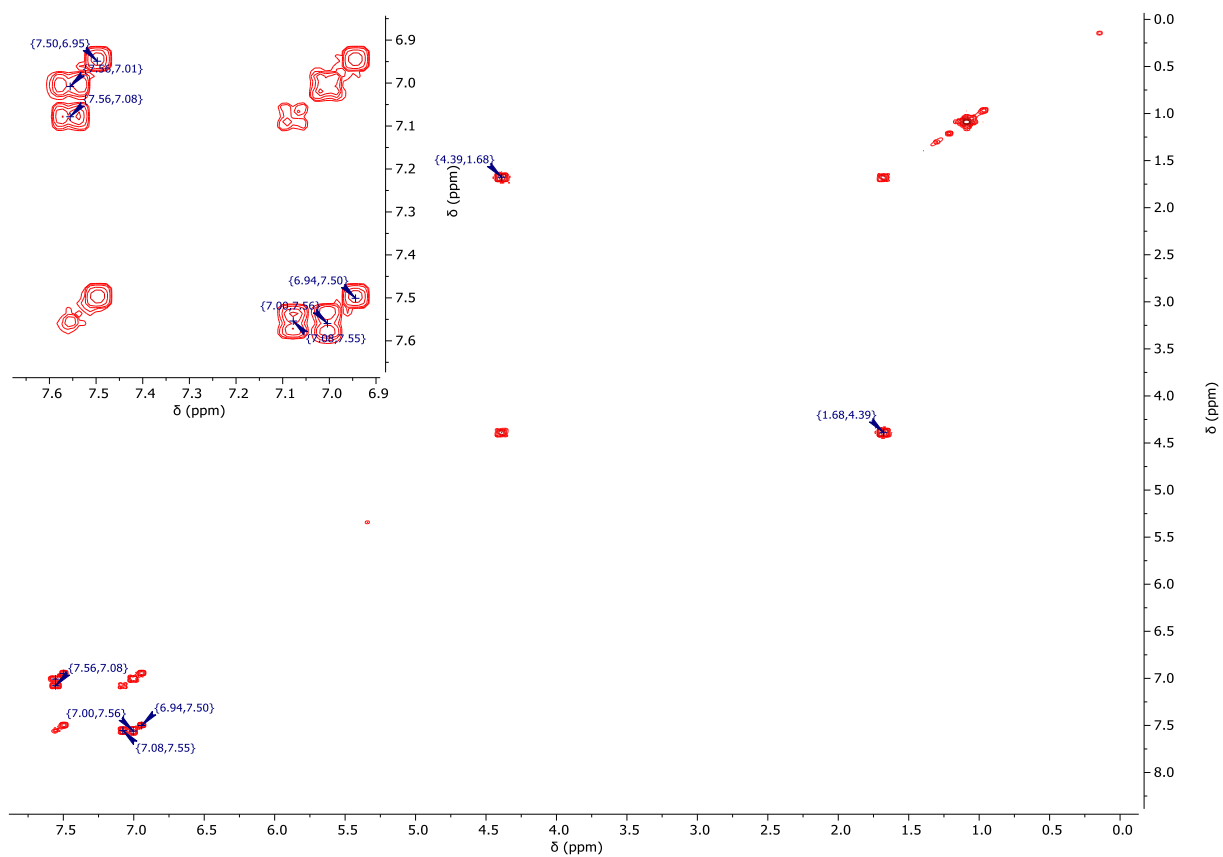


Figure S13: $^1\text{H}/^1\text{H}$ -COSY-NMR spectrum (500 MHz/500 MHz, $\text{DCM-}d_2$) of **A₂**.

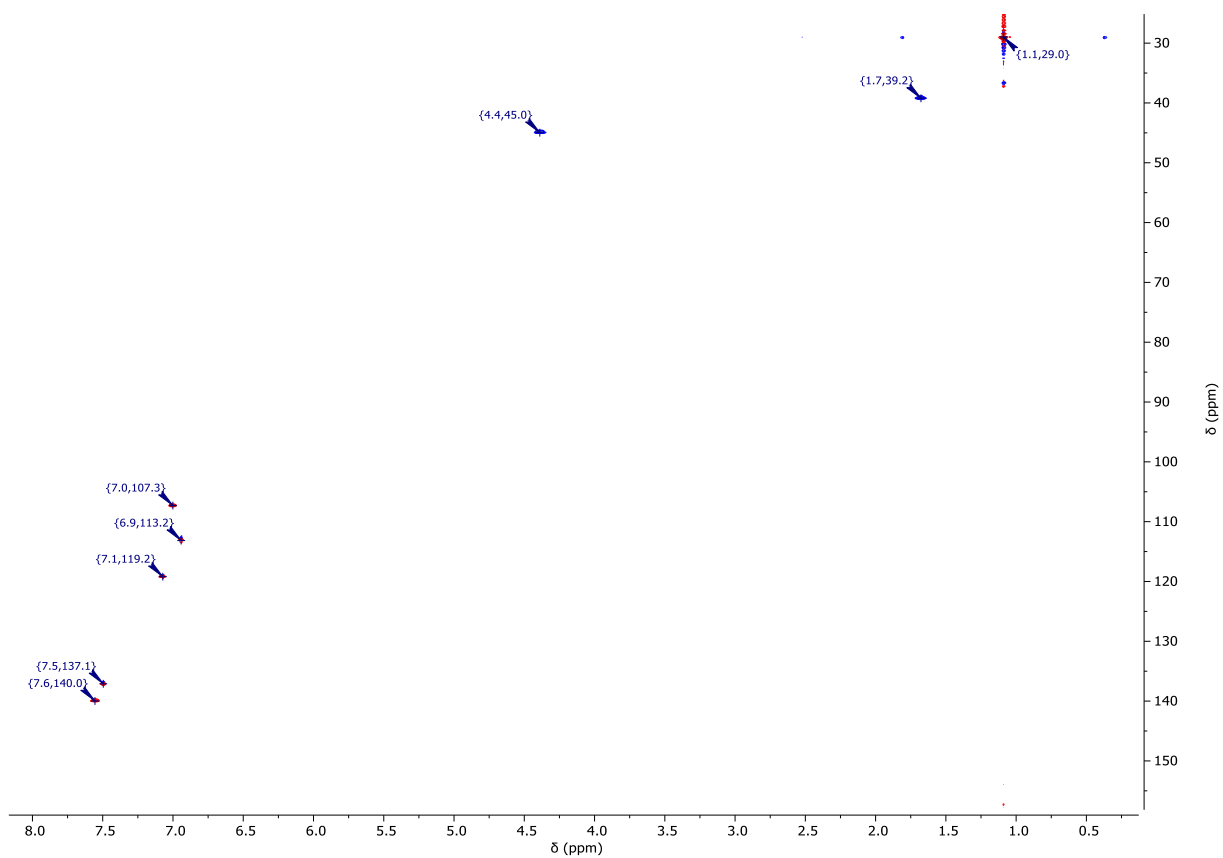


Figure S14: $^1\text{H}/^{13}\text{C}$ -gHSQC-NMR spectrum (500 MHz/126 MHz, $\text{DCM-}d_2$) of **A₂**.

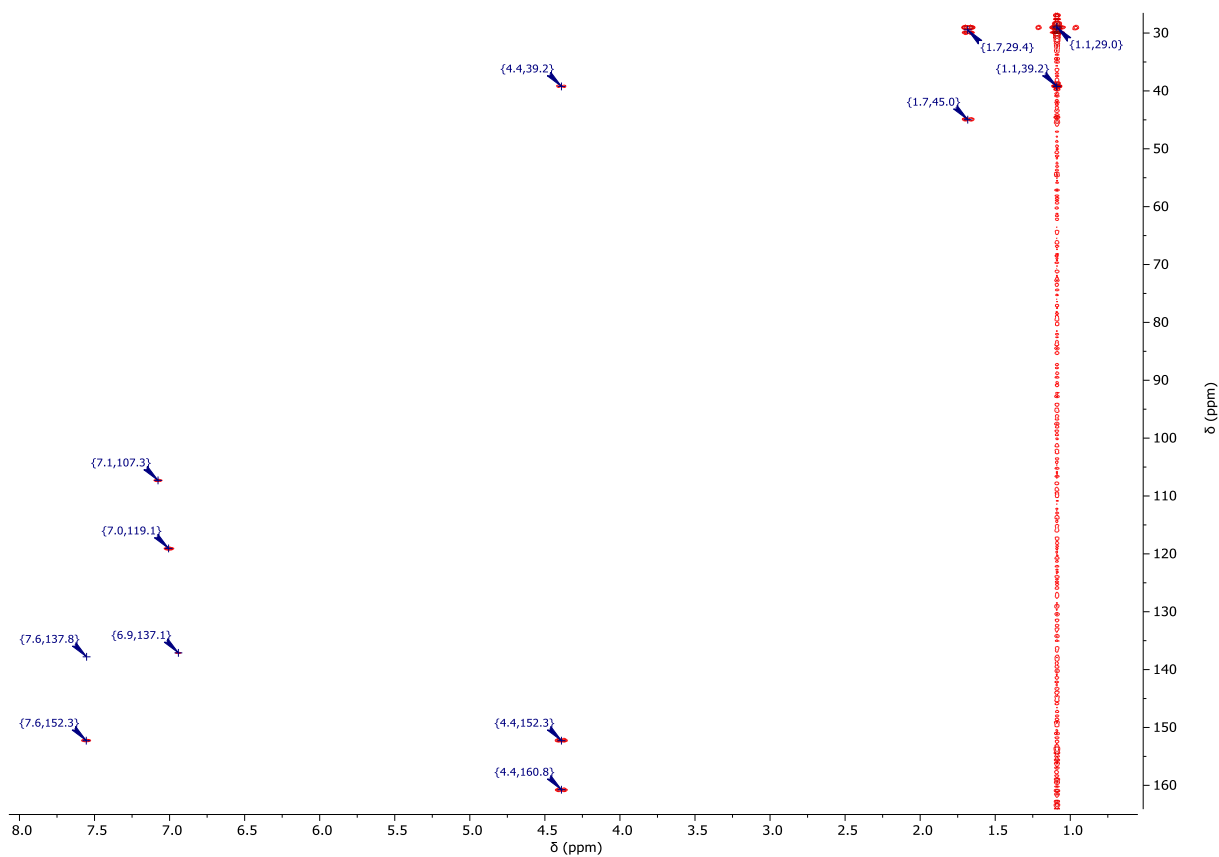


Figure S15: $^1\text{H}/^{13}\text{C}$ -gHMBC-NMR spectrum (500 MHz/126 MHz, DCM-d_2) of **A2**.

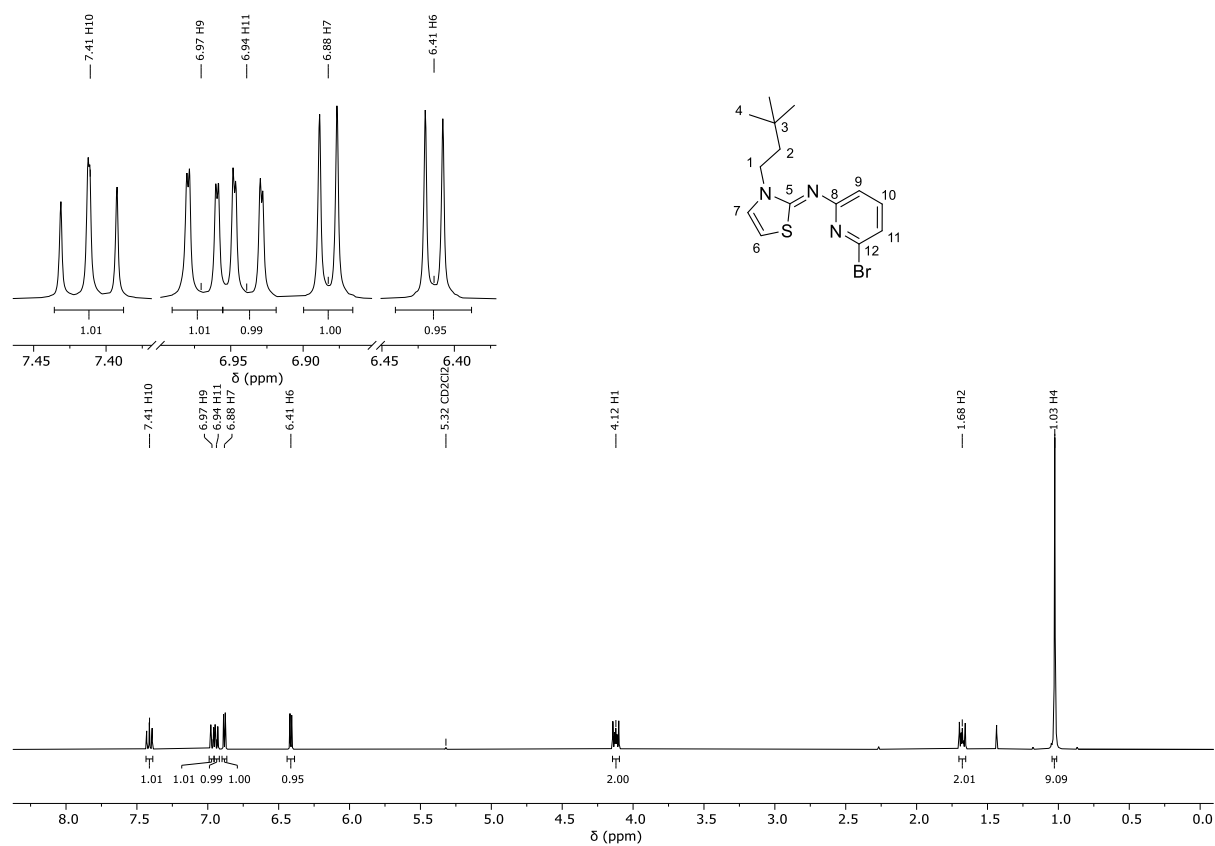


Figure S16: ^1H -NMR spectrum (400 MHz, DCM-d_2) of **I2**.

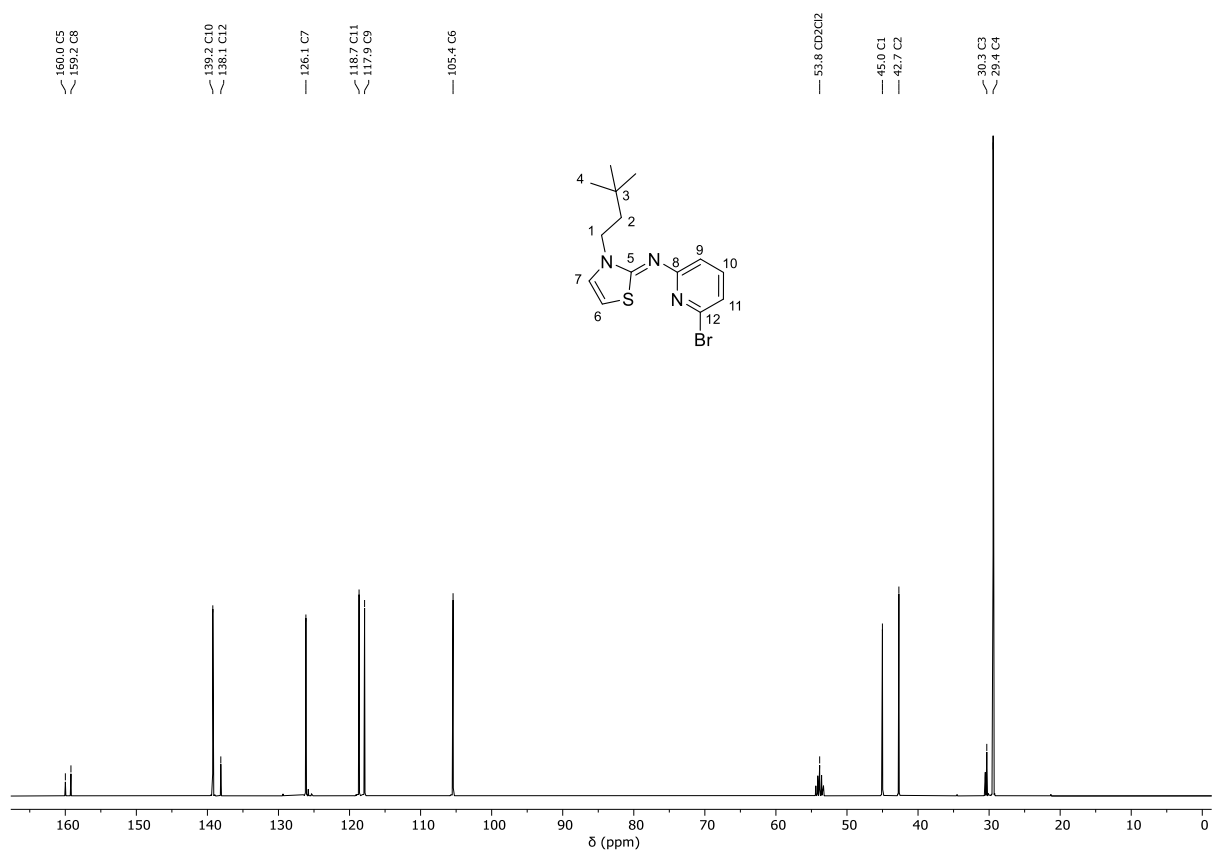


Figure S17: ¹³C-¹H-NMR spectrum (101 MHz, DCM-d₂) of **I₂**.

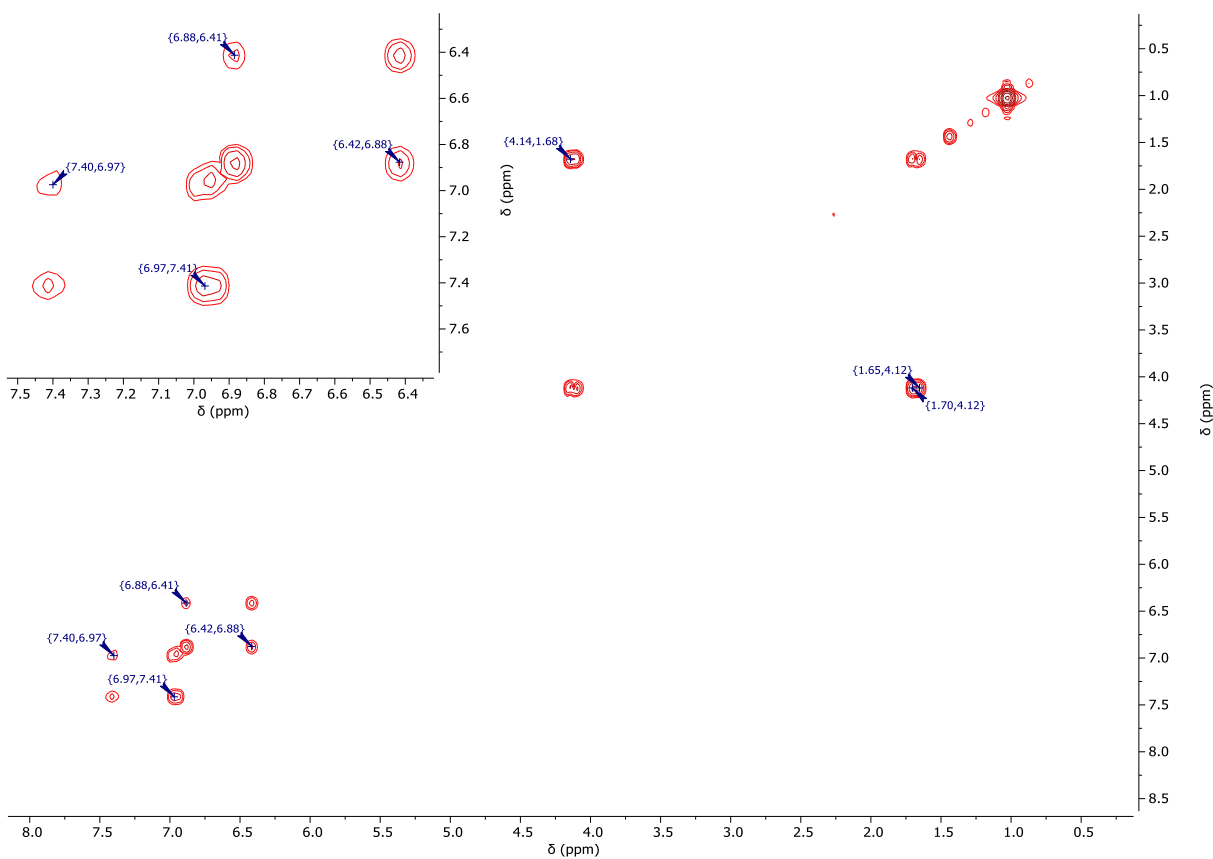


Figure S18: ¹H/¹H-COSY-NMR spectrum (400 MHz/400 MHz, DCM-d₂) of **I₂**.

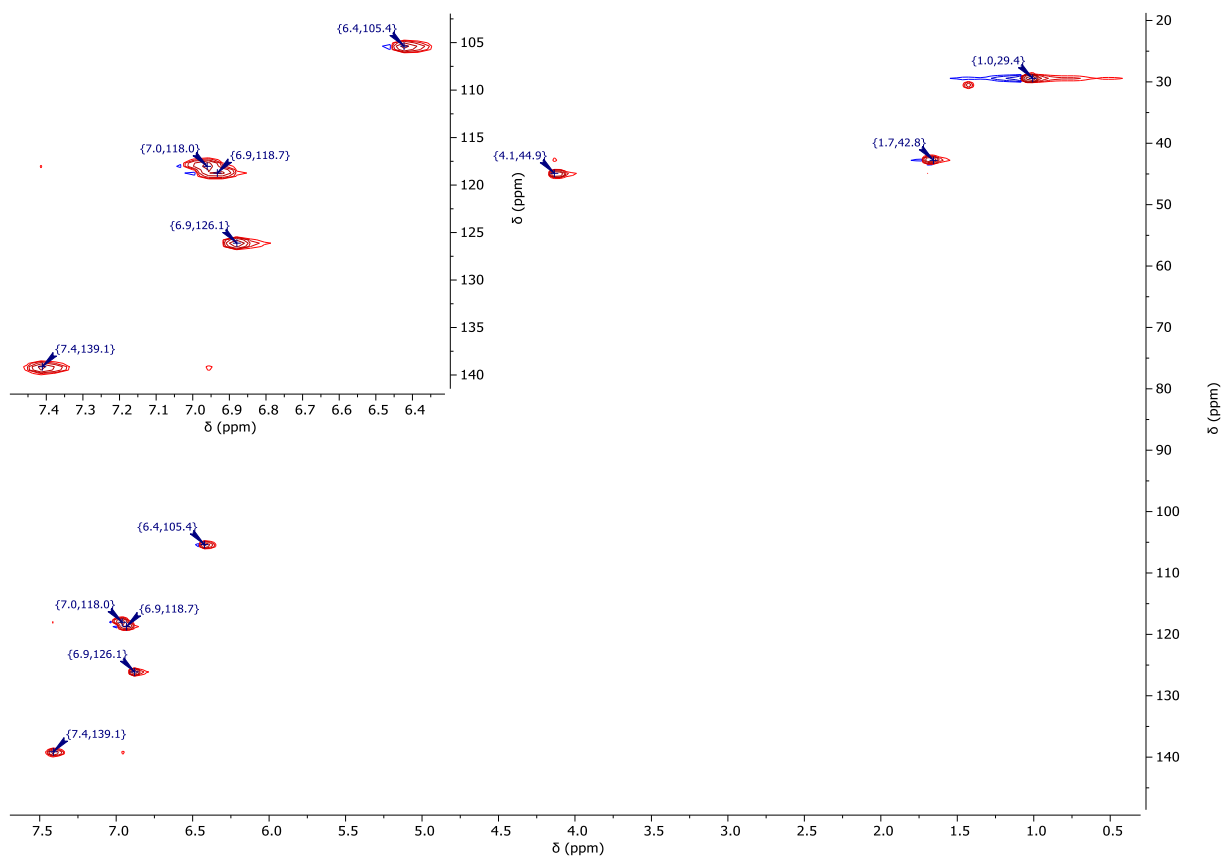


Figure S19: $^1\text{H}/^{13}\text{C}$ -gHSQC-NMR spectrum (400 MHz/101 MHz, $\text{DCM}-d_2$) of **12**.

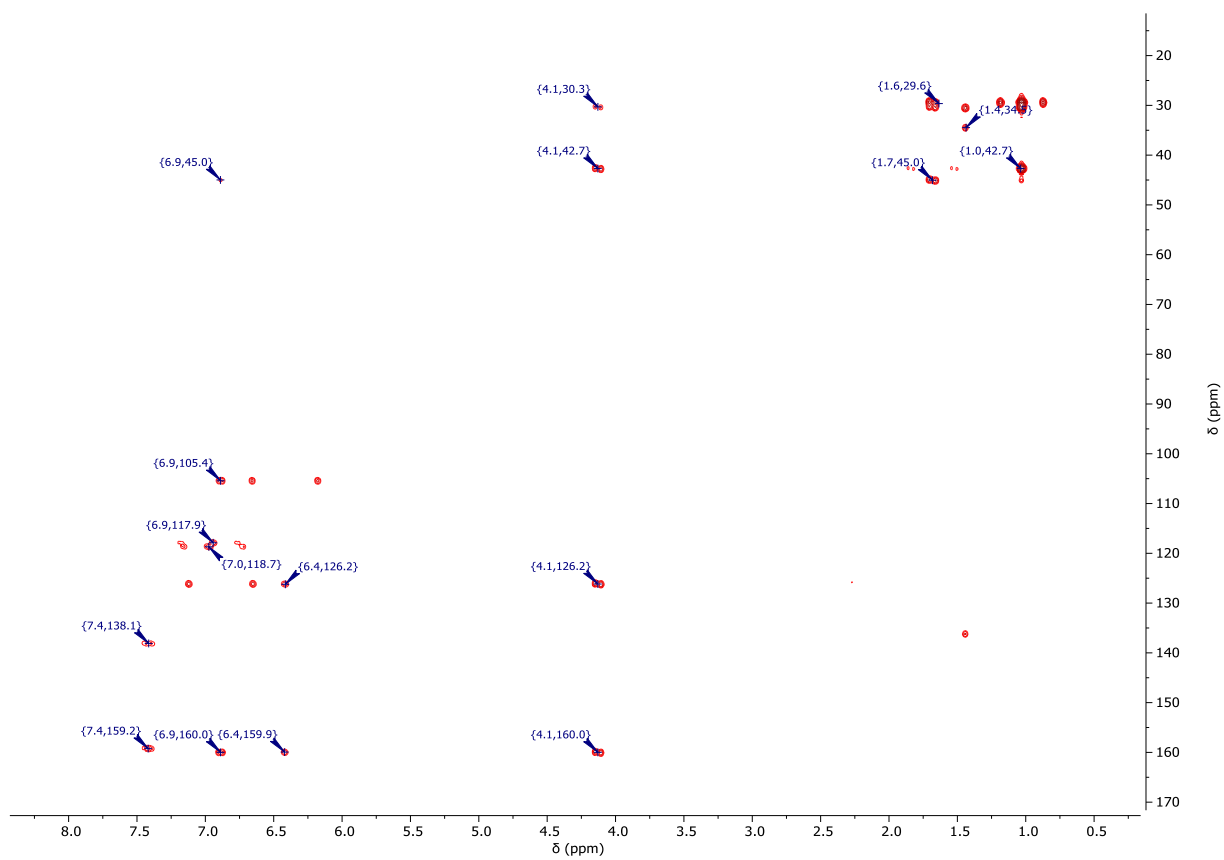


Figure S20: $^1\text{H}/^{13}\text{C}$ -gHMBC-NMR spectrum (400 MHz/101 MHz, $\text{DCM}-d_2$) of **12**.

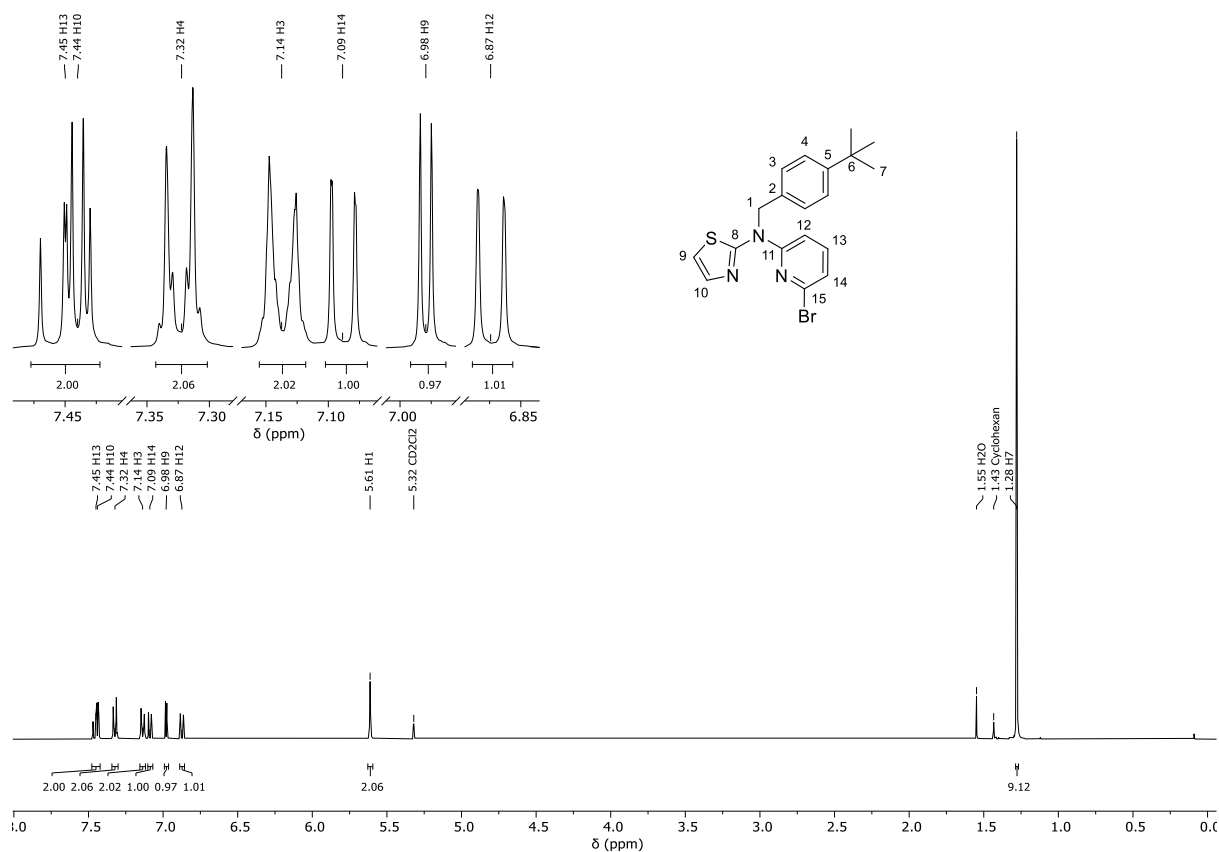


Figure S21: $^1\text{H-NMR}$ spectrum (400 MHz, DCM-d_2) of A_3 .

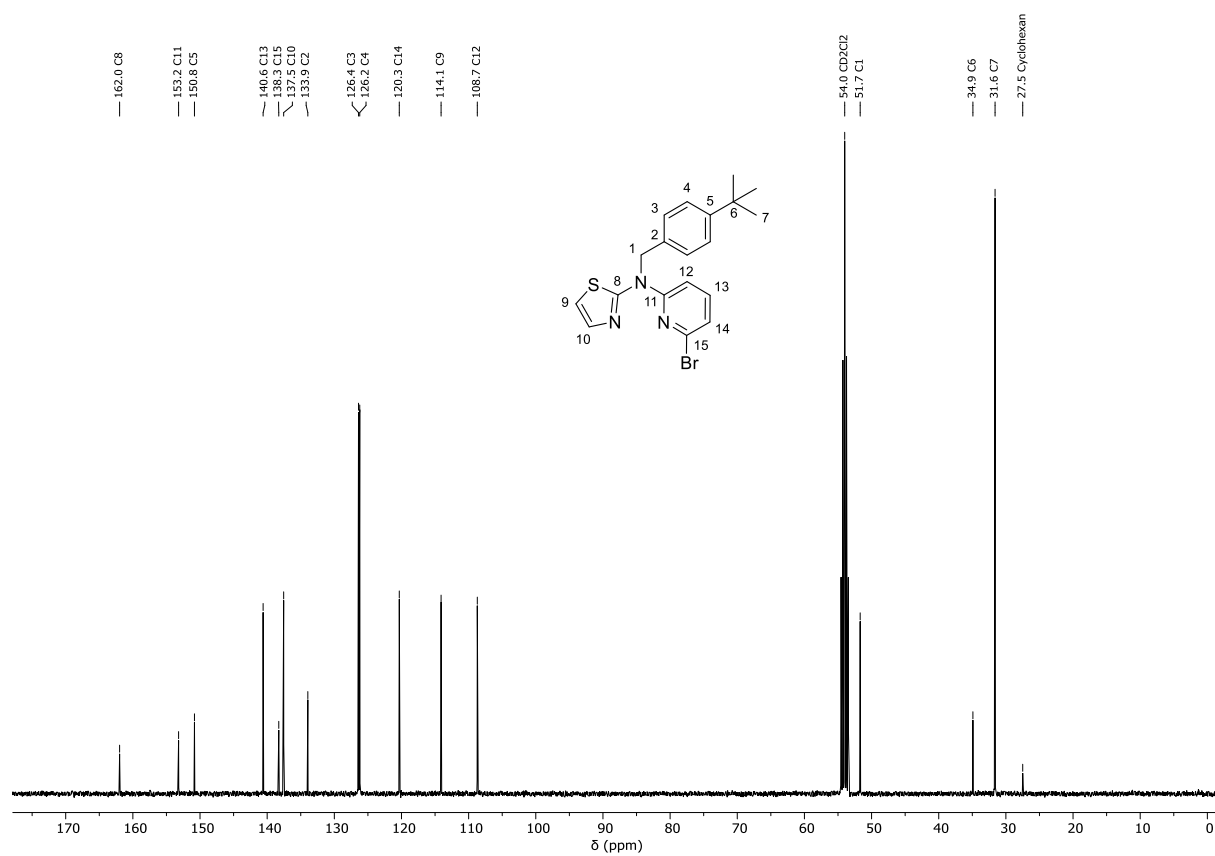


Figure S22: $^{13}\text{C-}\{^1\text{H}\}$ -NMR spectrum (101 MHz, DCM-d_2) of A_3 .

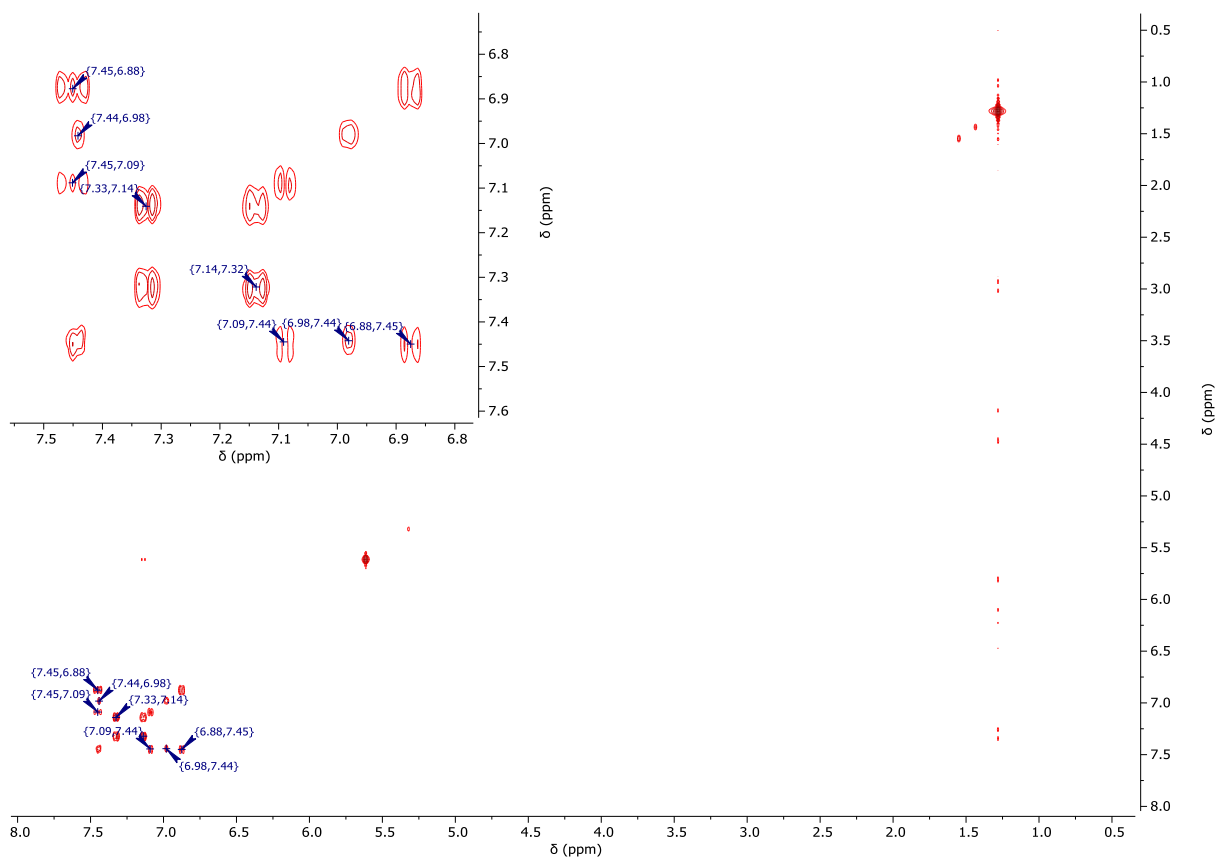


Figure S23: $^1\text{H}/^1\text{H}$ -COSY-NMR spectrum (400 MHz/400 MHz, DCM-d_2) of A_3 .

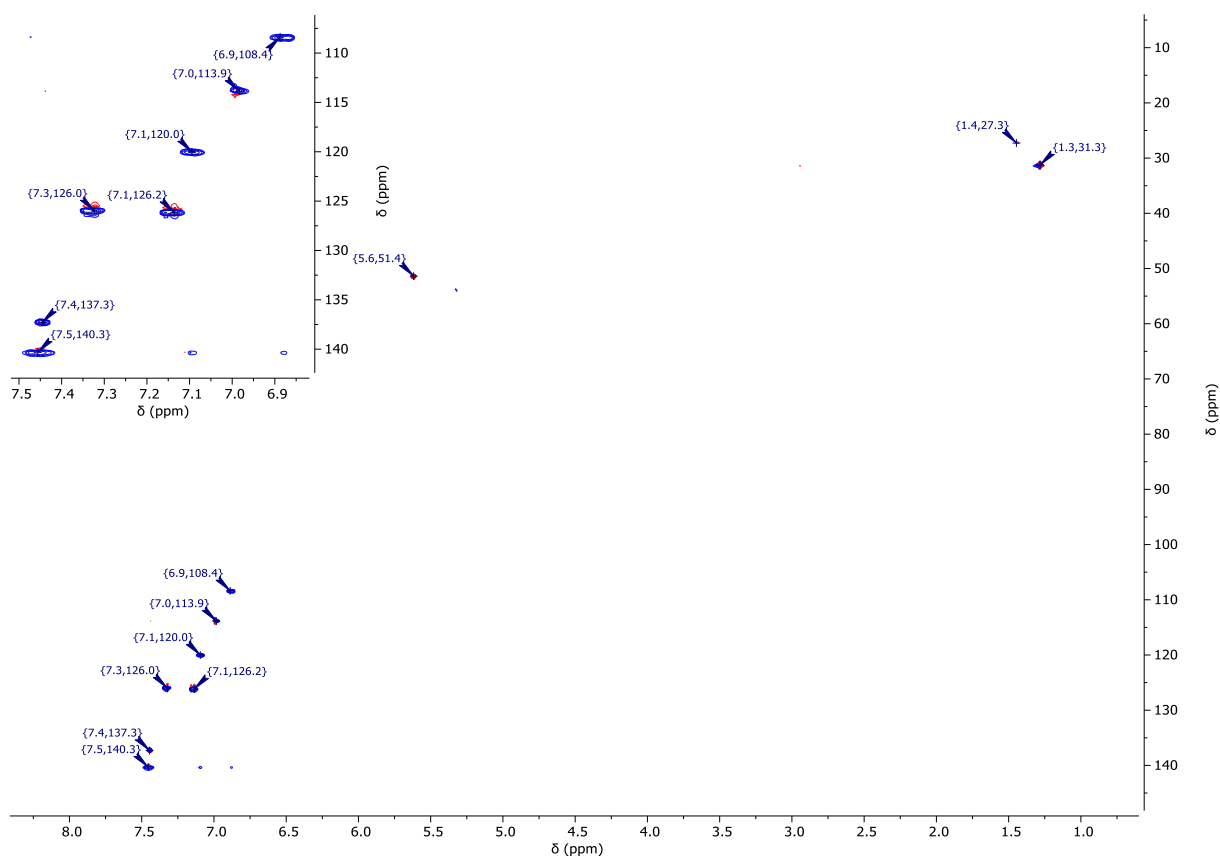


Figure S24: $^1\text{H}/^{13}\text{C}$ -gHSQC-NMR spectrum (400 MHz/101 MHz, DCM-d_2) of A_3 .

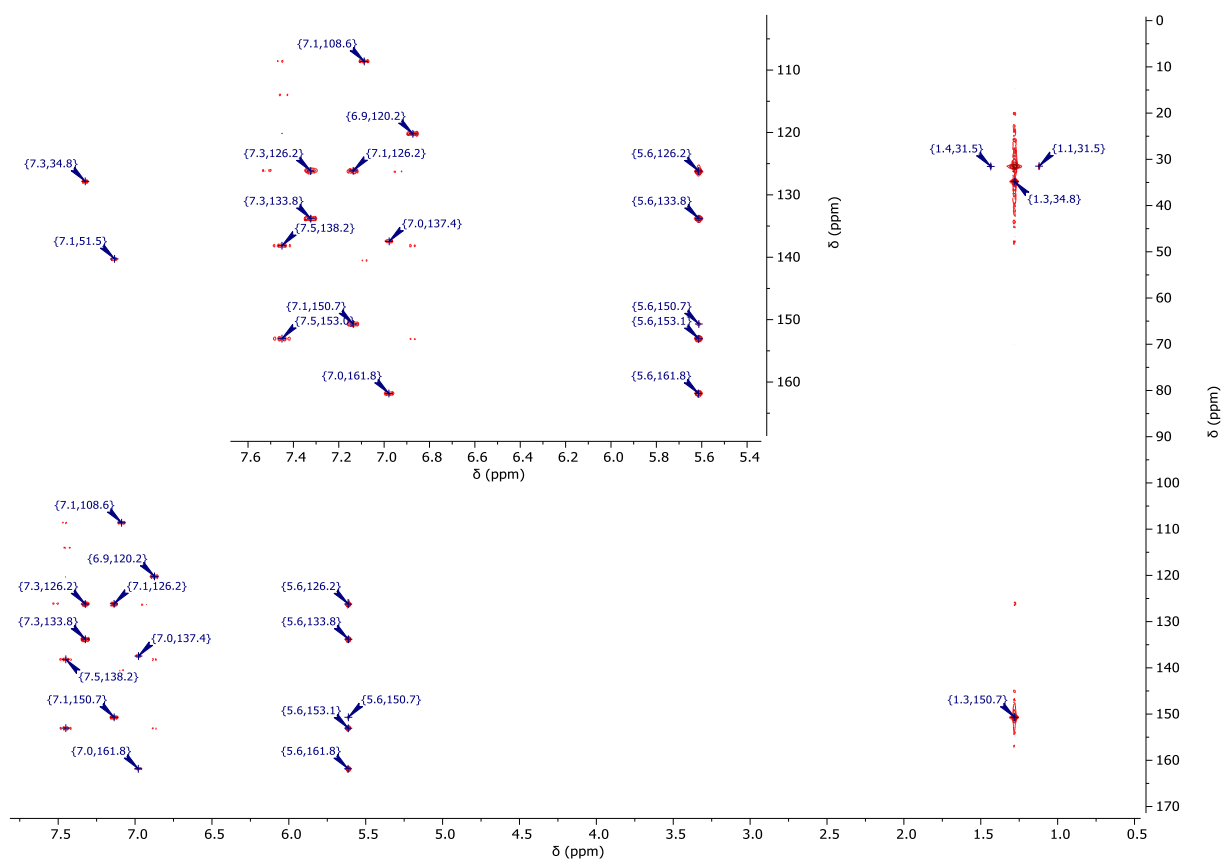


Figure S25: $^1\text{H}/^{13}\text{C}$ -gHMBC-NMR spectrum (400 MHz/101 MHz, $\text{DCM-}d_2$) of **A₃**.

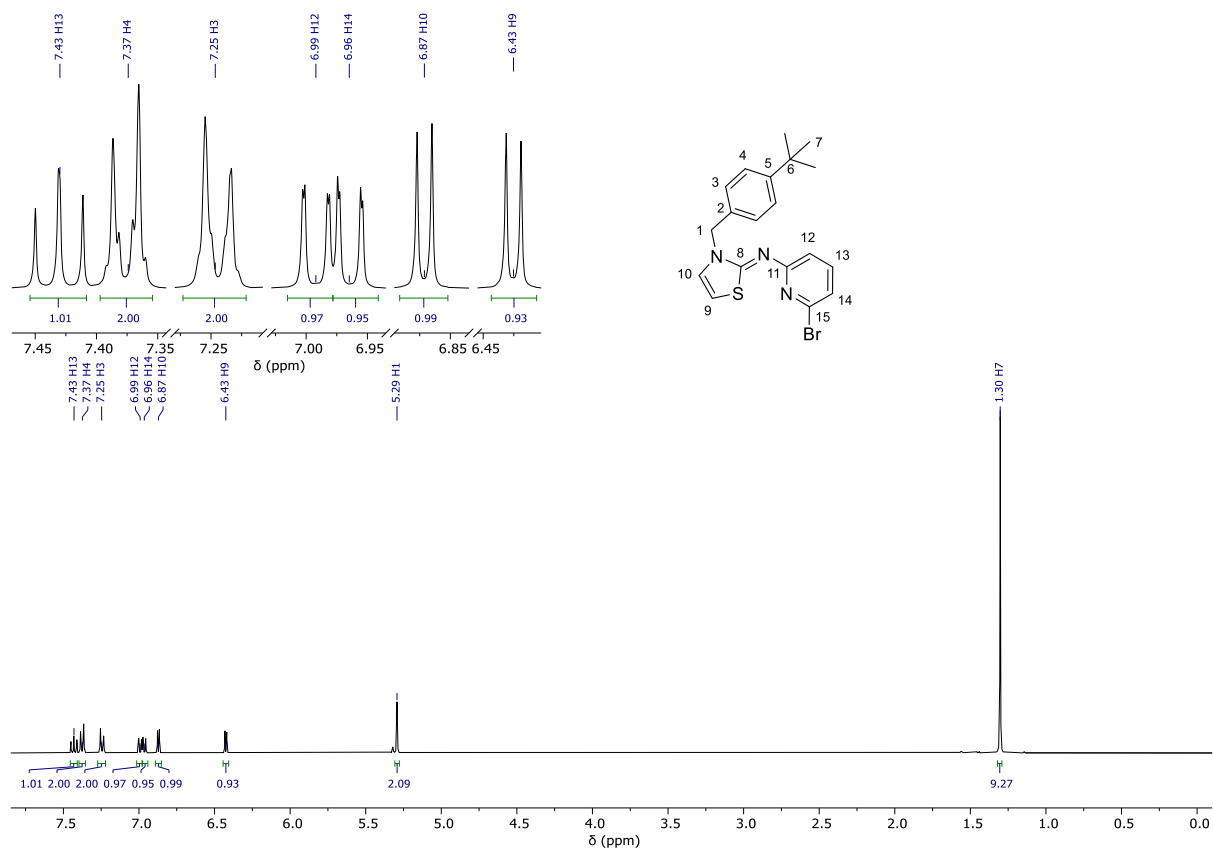


Figure S26: ^1H -NMR spectrum (400 MHz, $\text{DCM-}d_2$) of **I₃**.

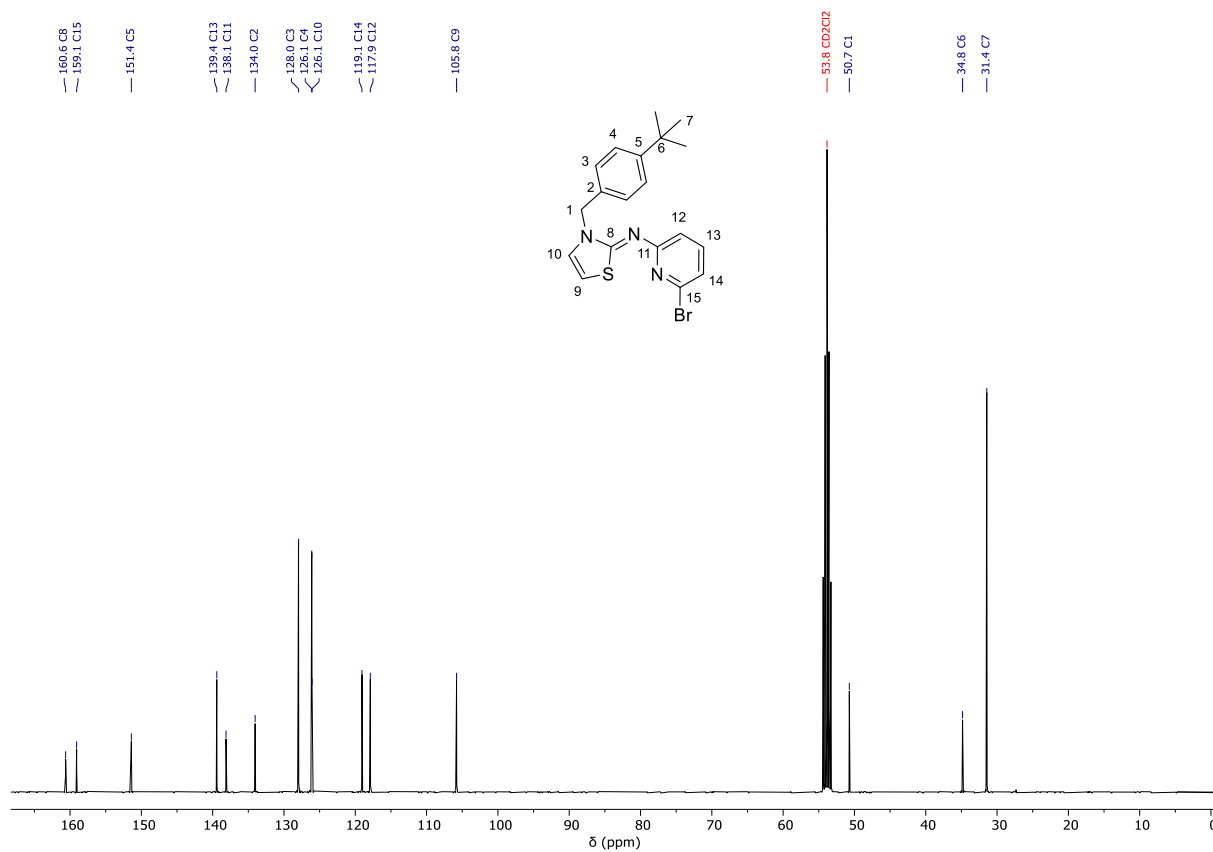


Figure S27: ^{13}C - $\{^1\text{H}\}$ -NMR spectrum (101 MHz, DCM-d_2) of **I**₃.

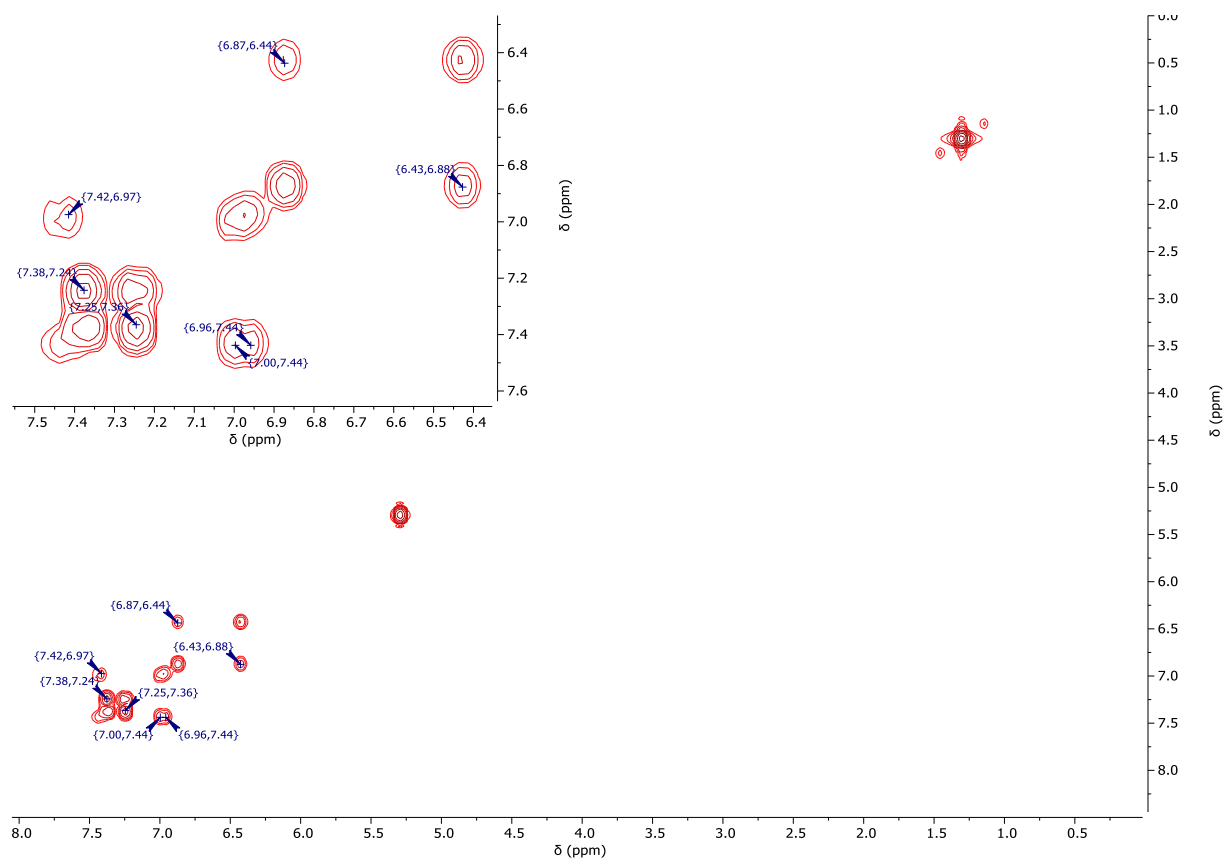


Figure S28: H^1H -COSY-NMR spectrum (400 MHz/400 MHz, DCM-d_2) of **I**₃.

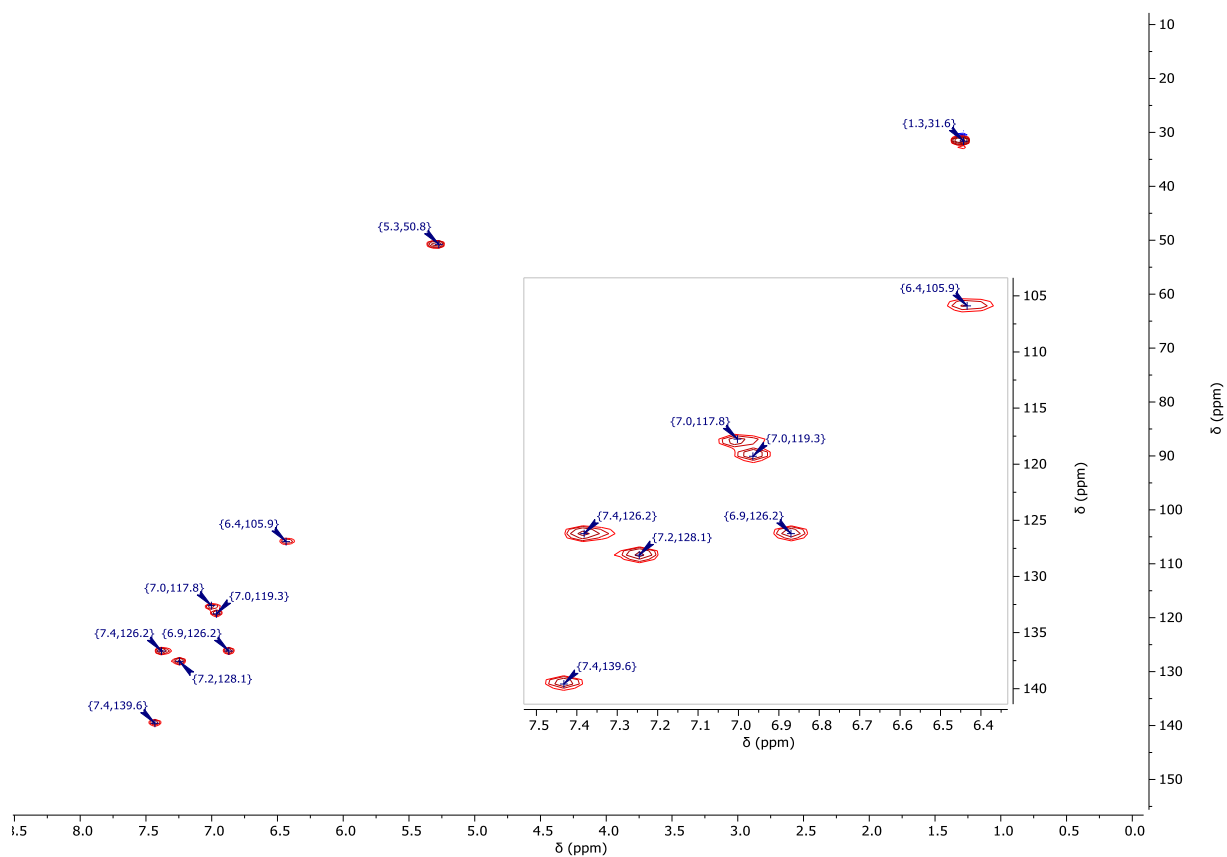


Figure S29: $^1\text{H}/^{13}\text{C}$ -gHSQC-NMR spectrum (400 MHz/101 MHz, $\text{DCM}-d_2$) of **I3**.

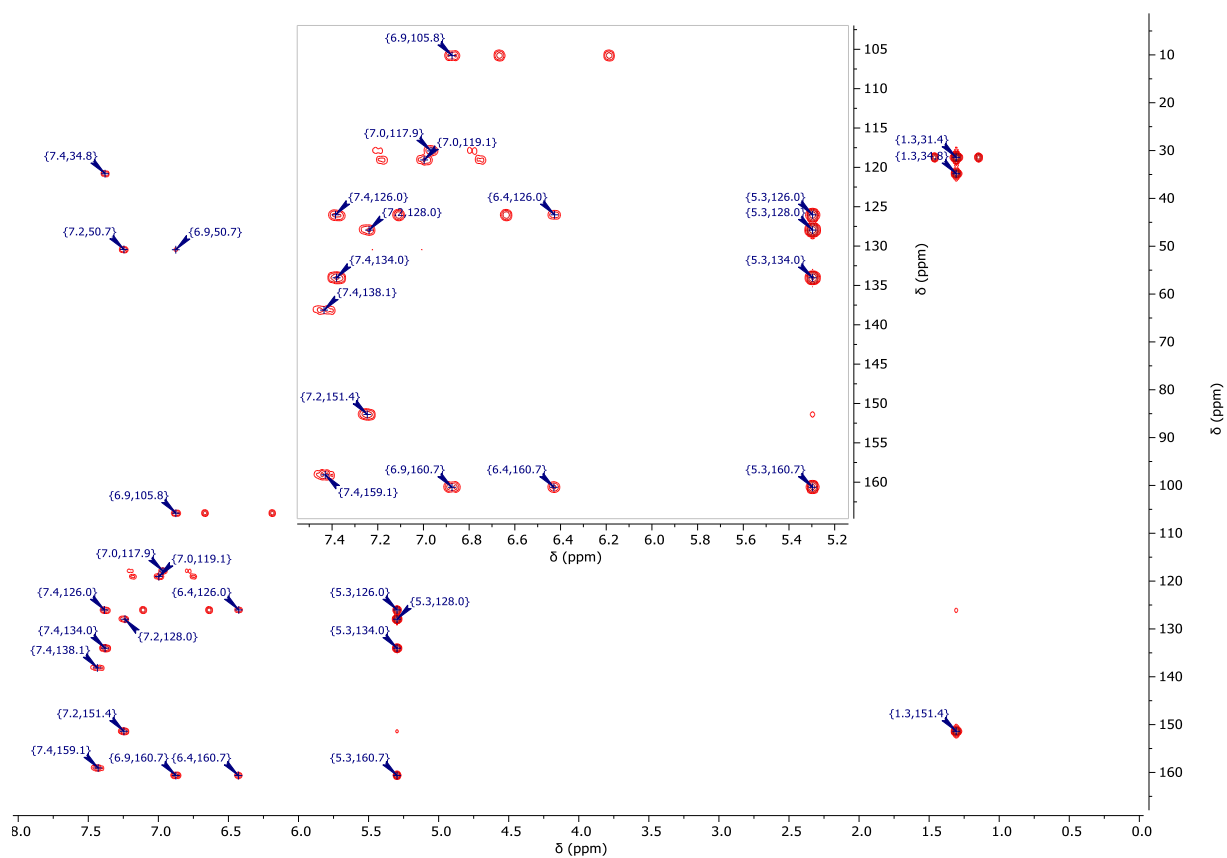


Figure S30: $^1\text{H}/^{13}\text{C}$ -gHMBC-NMR spectrum (400 MHz/101 MHz, $\text{DCM}-d_2$) of **I3**.

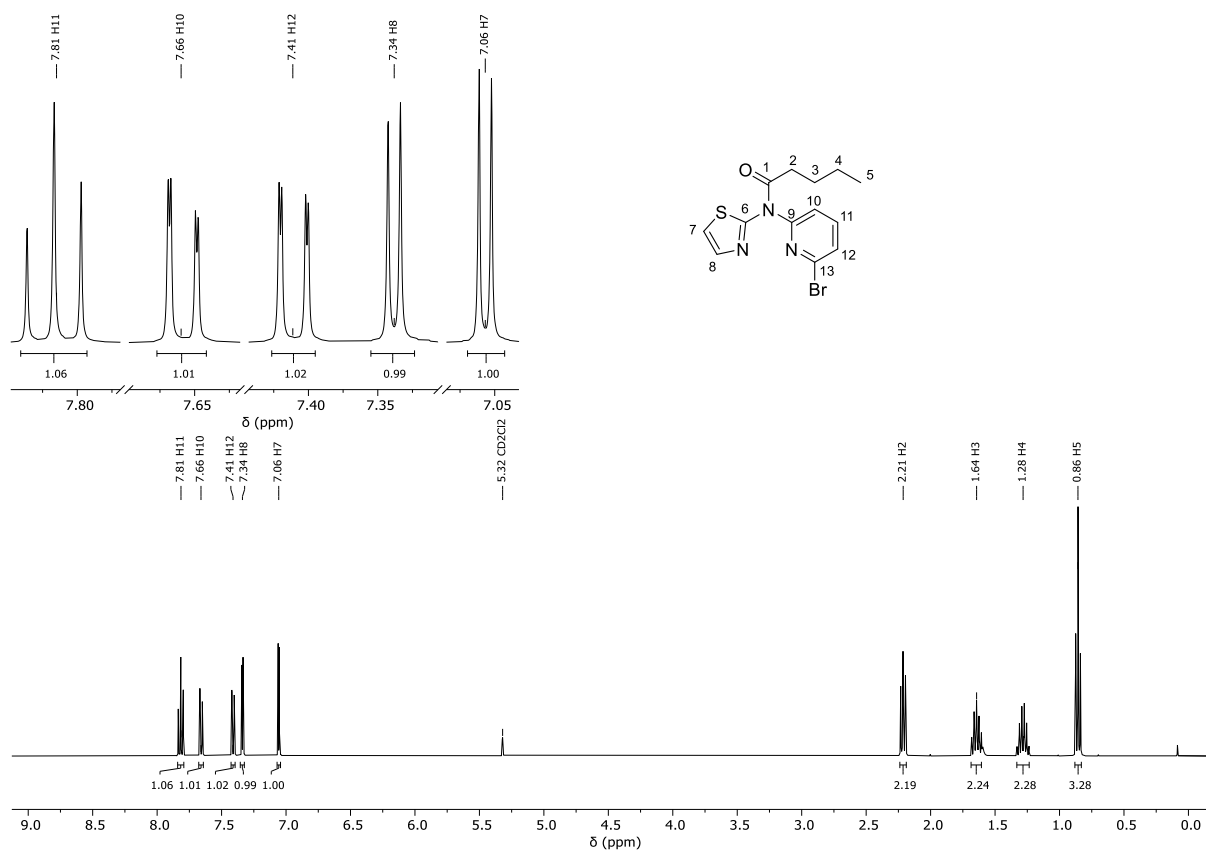


Figure S31: ¹H-NMR spectrum (400 MHz, DCM-*d*₂) of **A4**.

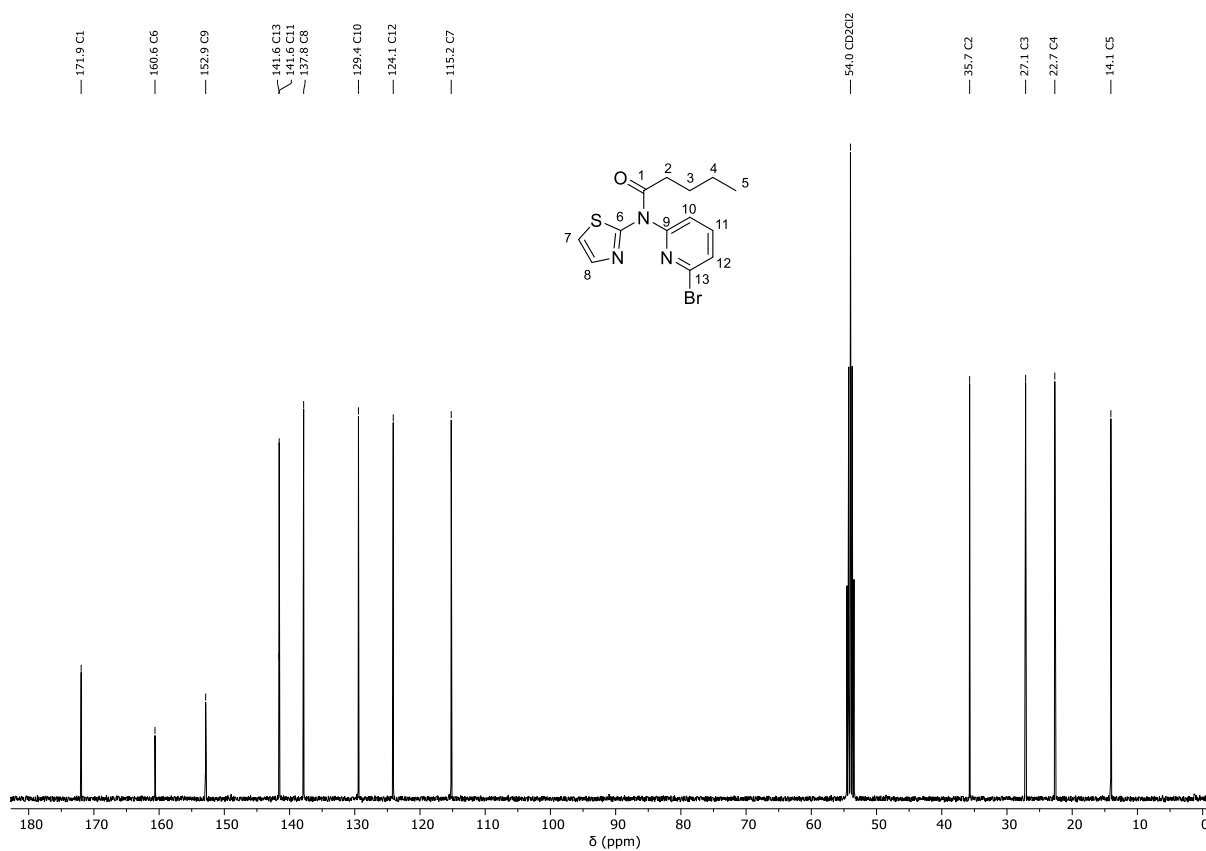


Figure S32: ¹³C-¹H-NMR spectrum (101 MHz, DCM-*d*₂) of **A4**.

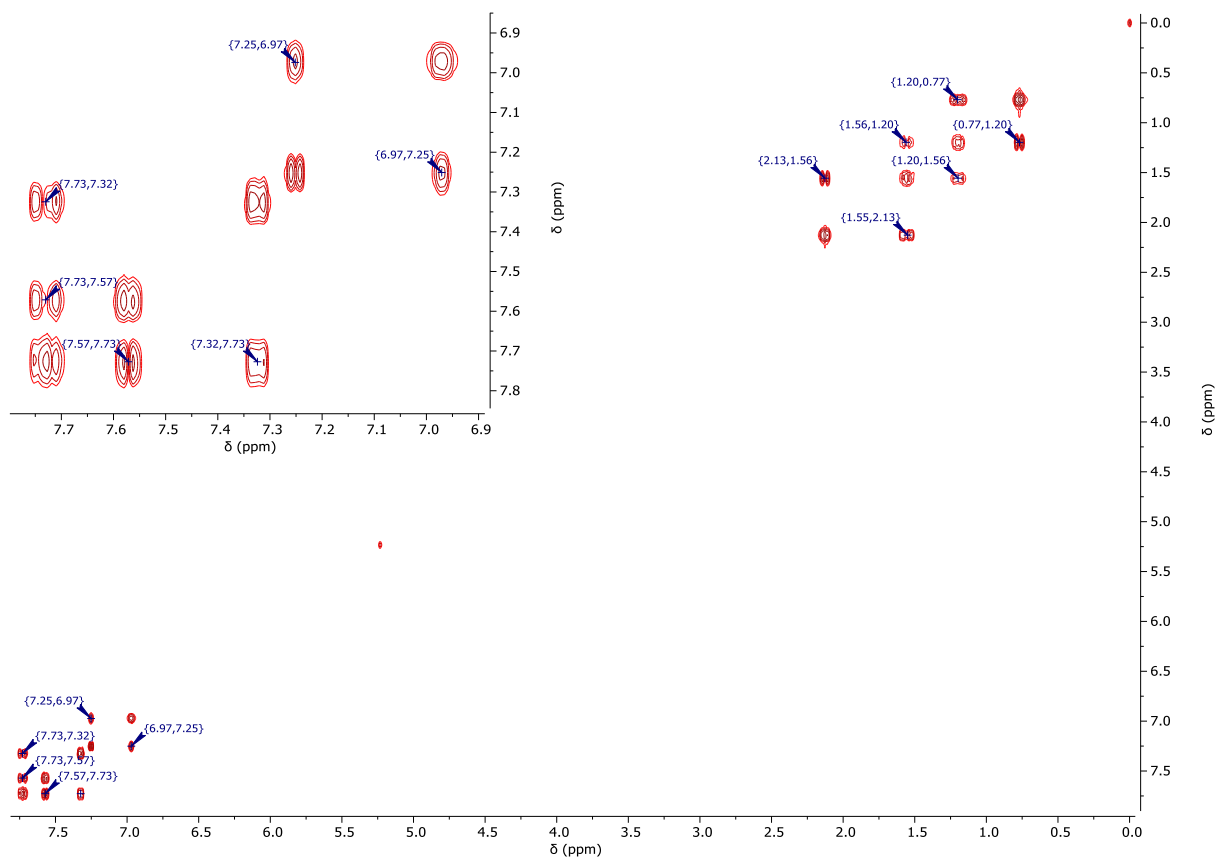


Figure S33: $^1\text{H}/^1\text{H}$ -COSY-NMR spectrum (400 MHz/400 MHz, $\text{DCM}-d_2$) of **A4**.

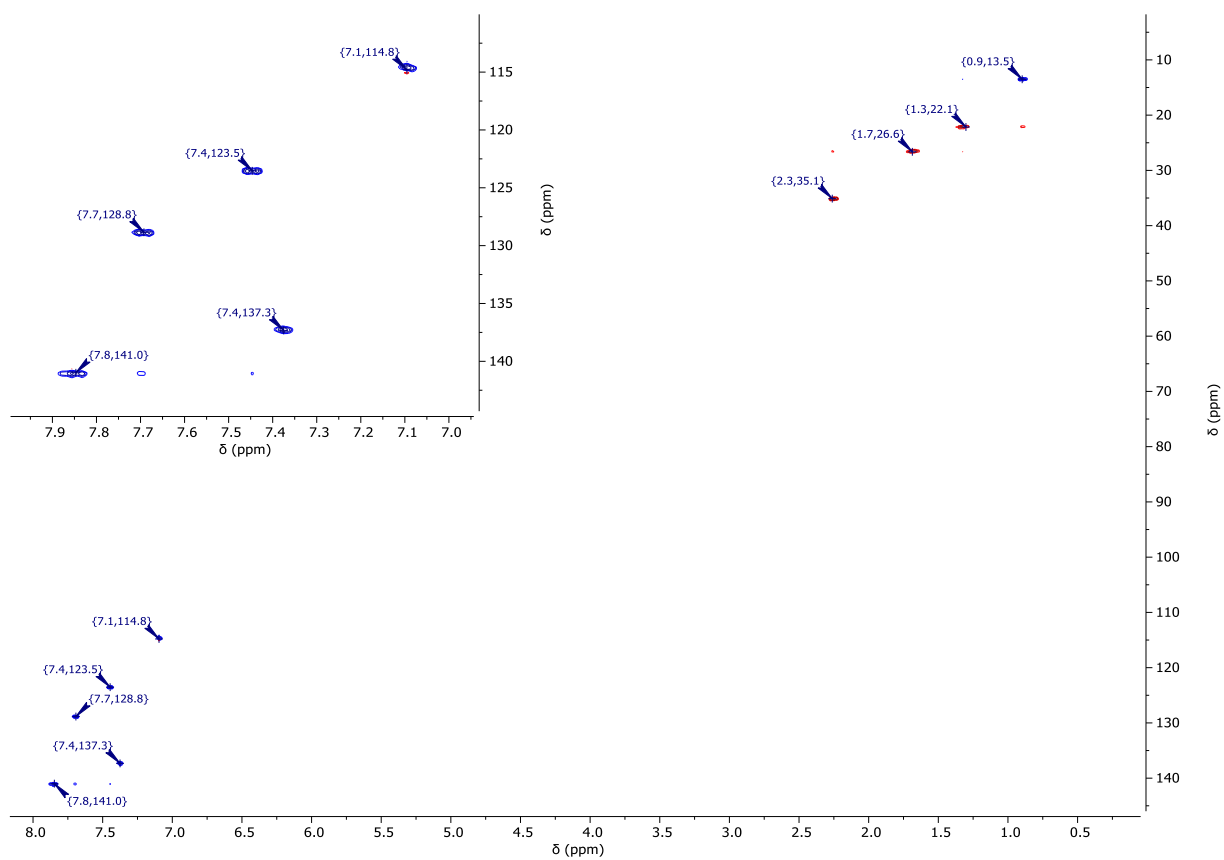


Figure S34: $^1\text{H}/^{13}\text{C}$ -gHSQC-NMR spectrum (400 MHz/101 MHz, $\text{DCM}-d_2$) of **A4**.

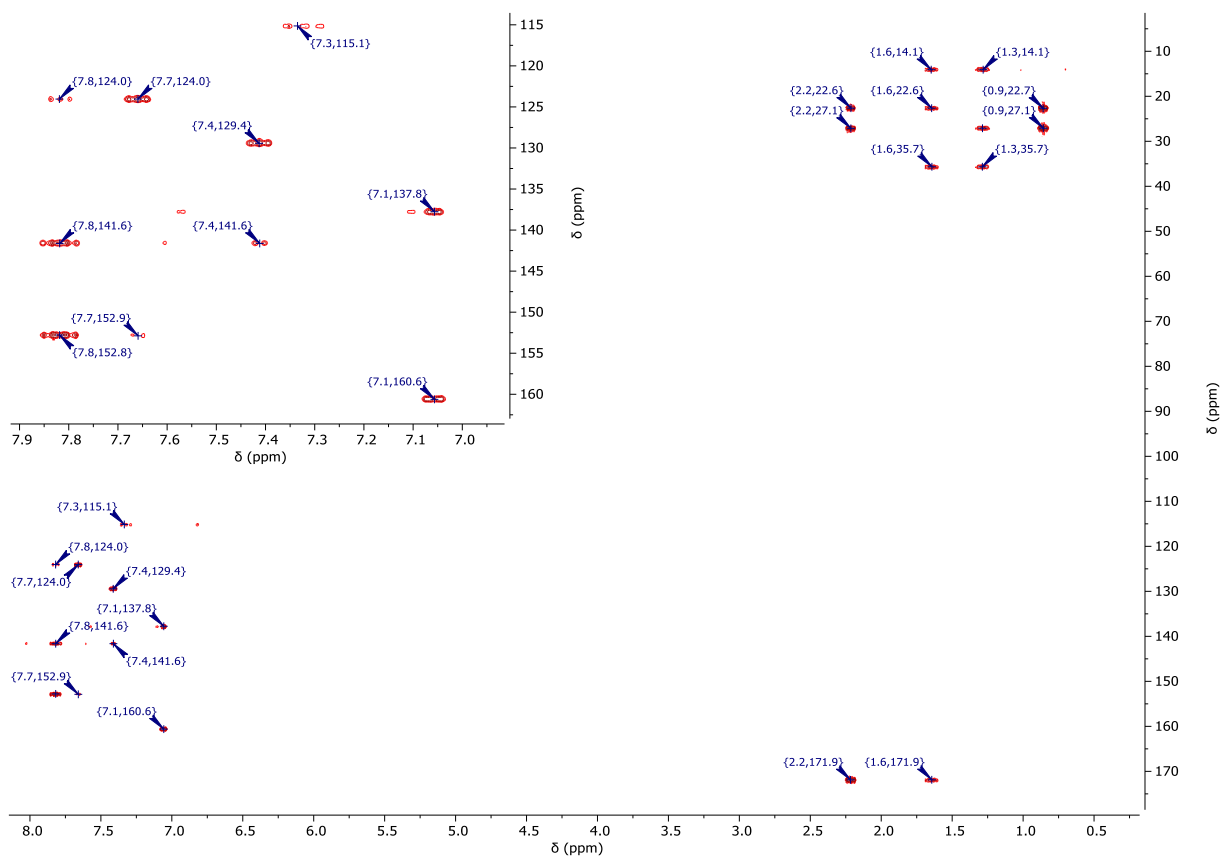


Figure S35: $^1\text{H}/^{13}\text{C}$ -gHMBC-NMR spectrum (400 MHz/101 MHz, $\text{DCM}-d_2$) of **A4**.

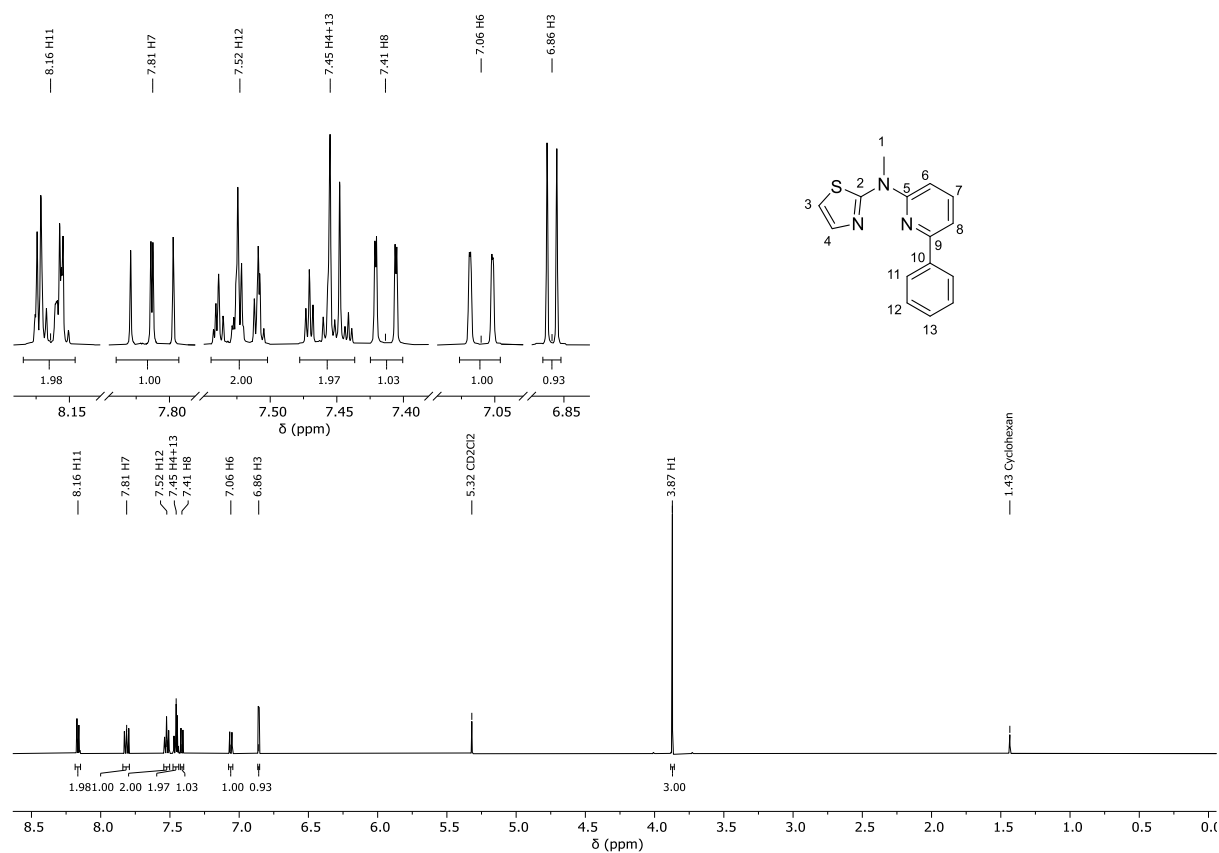


Figure S36: ^1H -NMR spectrum (500 MHz, $\text{DCM}-d_2$) of **L1H**.

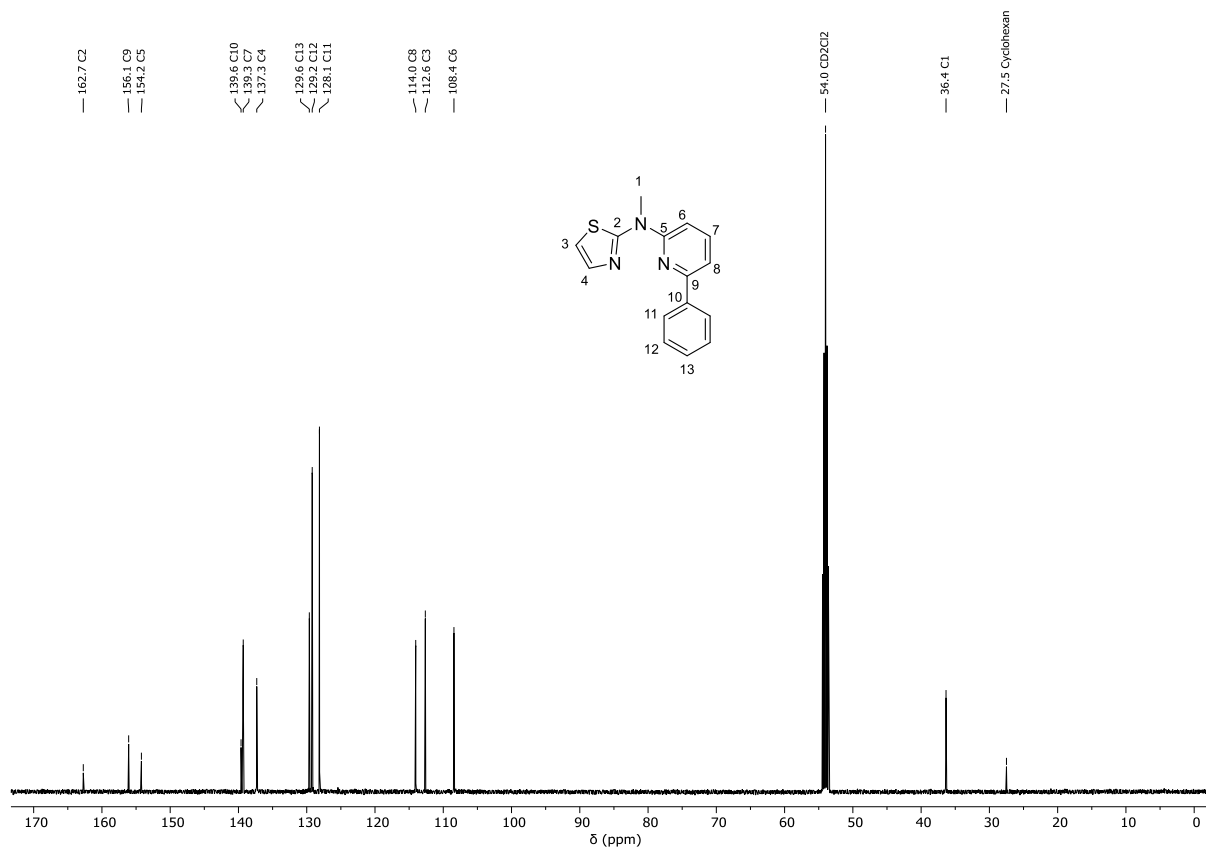


Figure S37: ^{13}C - $\{^1\text{H}\}$ -NMR spectrum (126 MHz, DCM-d_2) of L_1H .

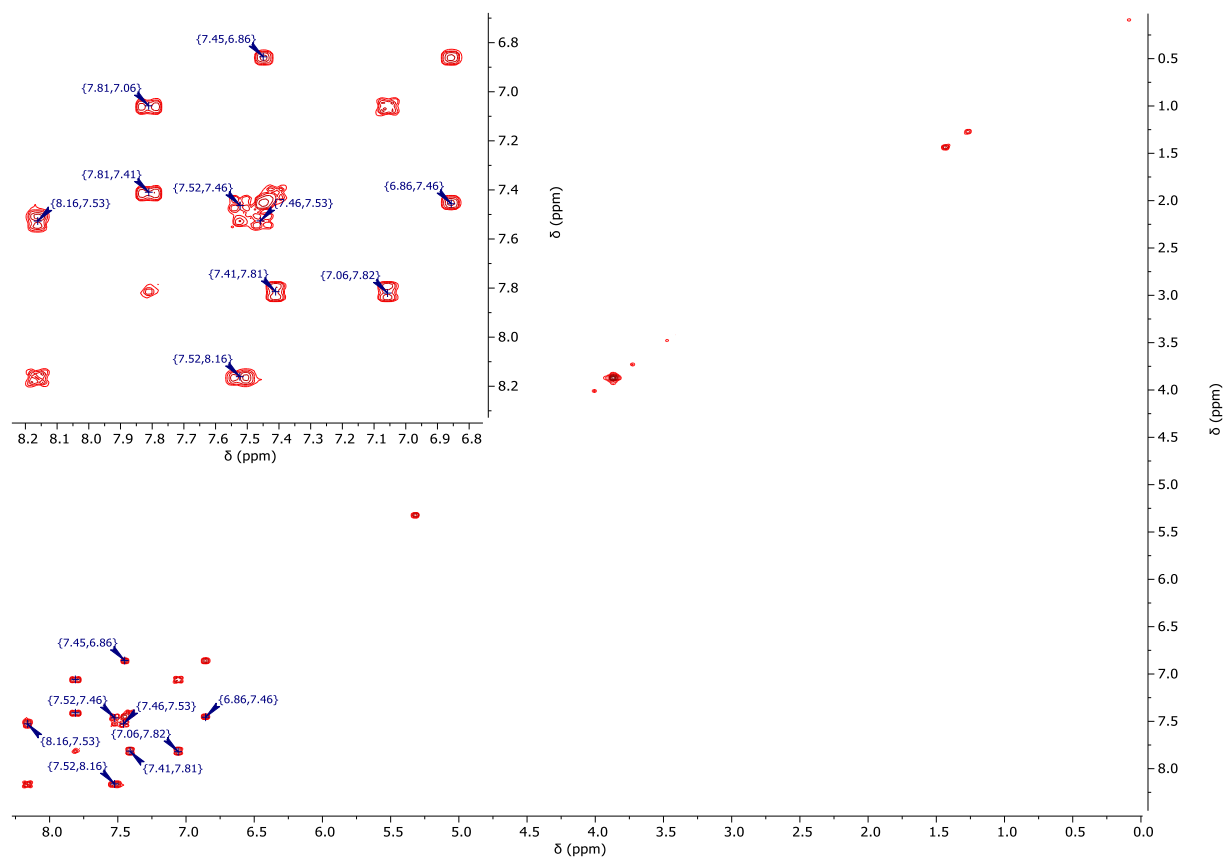


Figure S38: $^1\text{H}/^1\text{H}$ -COSY-NMR spectrum (500 MHz/500 MHz, DCM-d_2) of L_1H .

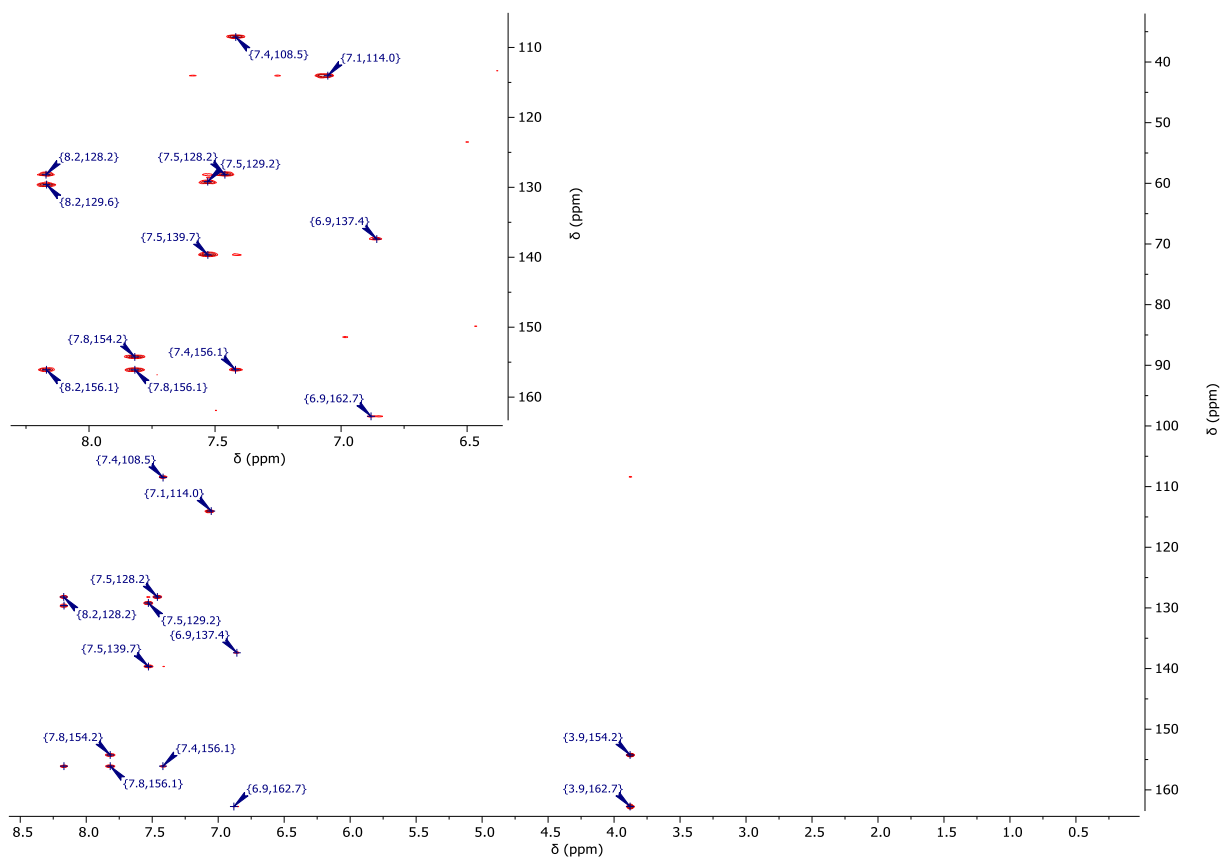


Figure S39: $^1\text{H}/^{13}\text{C}$ -gHSQC-NMR spectrum (500 MHz/126 MHz, $\text{DCM}-d_2$) of L_1H .

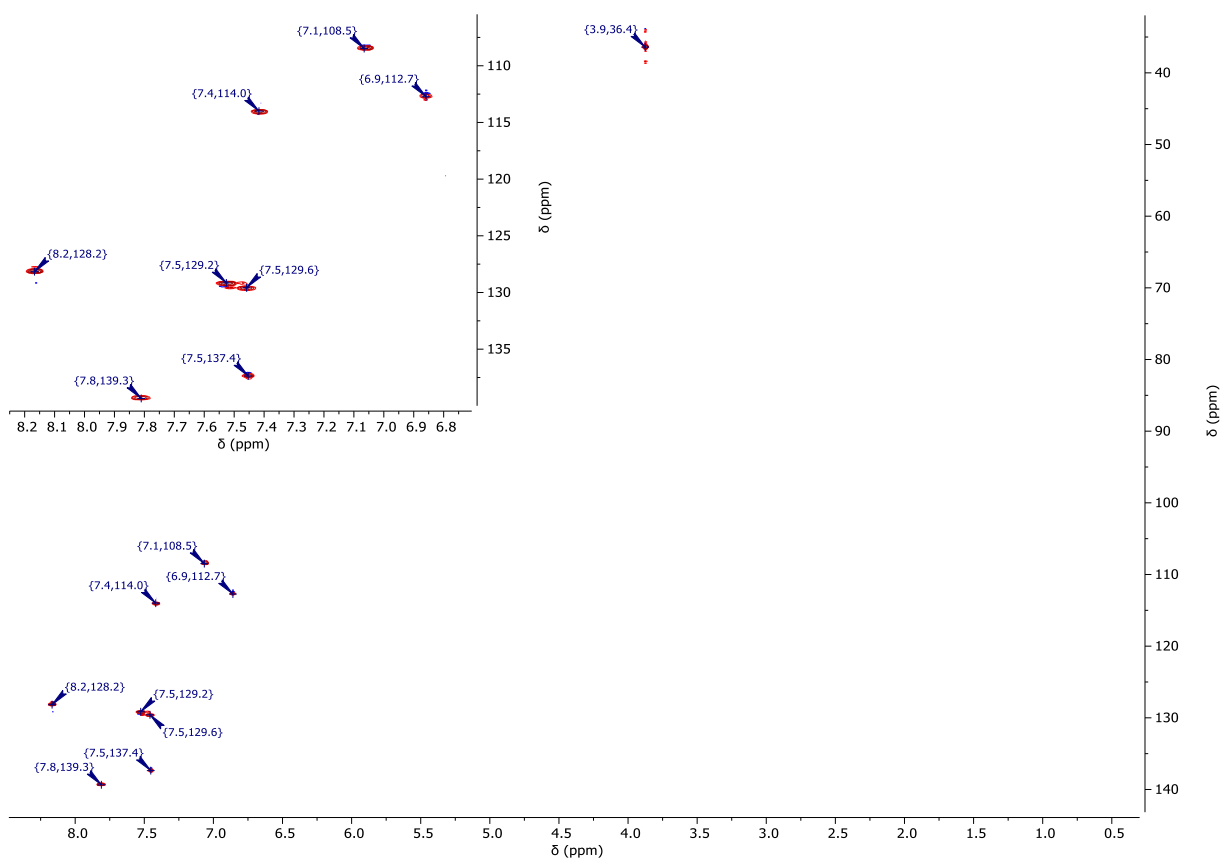


Figure S40: $^1\text{H}/^{13}\text{C}$ -gHMBC-NMR spectrum (500 MHz/126 MHz, $\text{DCM}-d_2$) of L_1H .

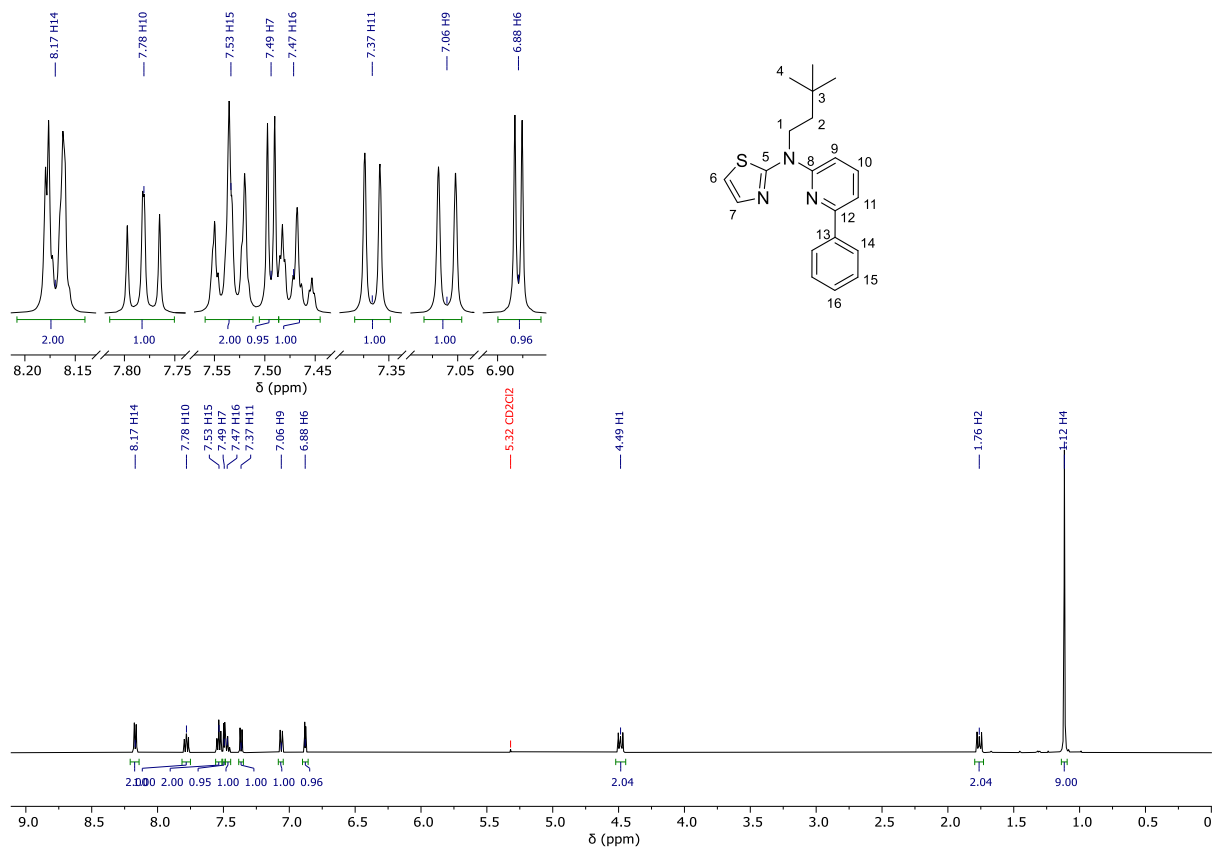


Figure S41: $^1\text{H-NMR}$ spectrum (500 MHz, DCM-d_2) of L_2H .

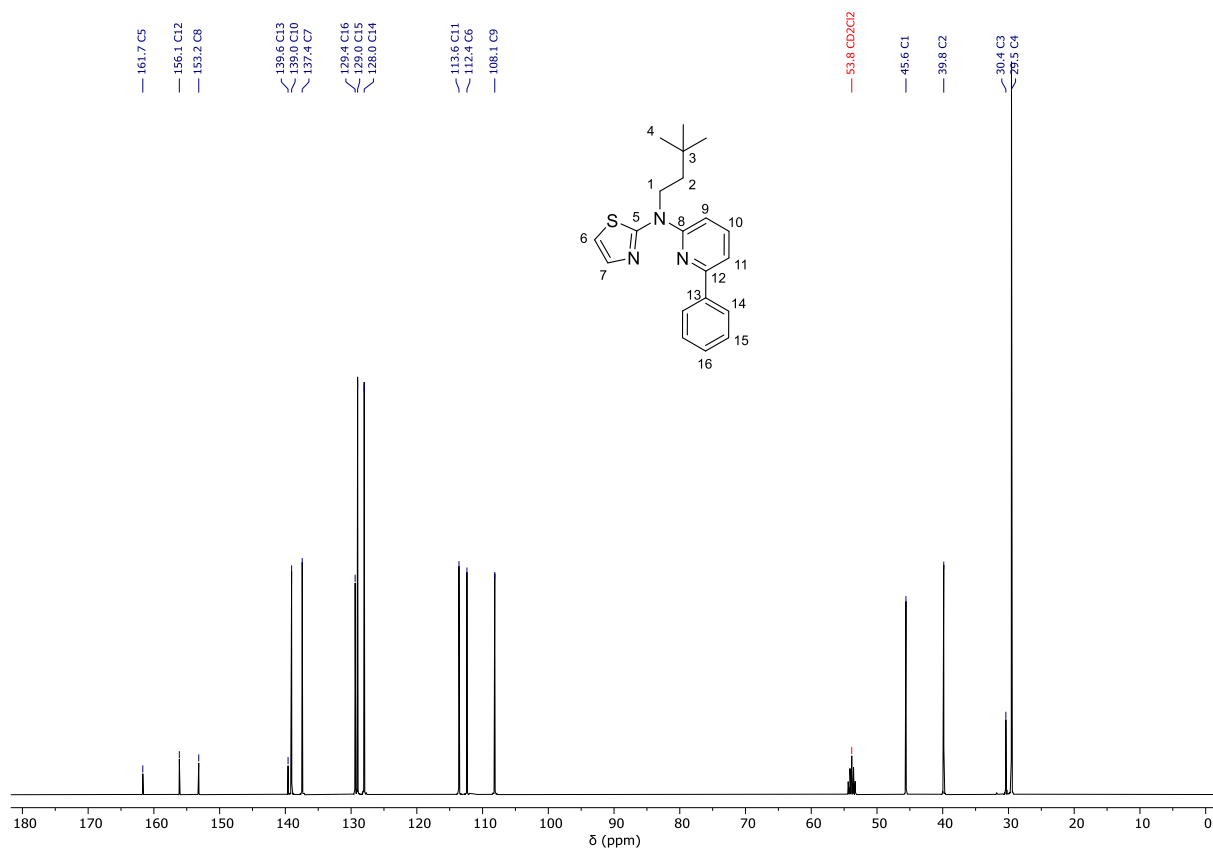


Figure S42: $^{13}\text{C-}\{^1\text{H}\}$ -NMR spectrum (101 MHz, DCM-d_2) of L_2H .

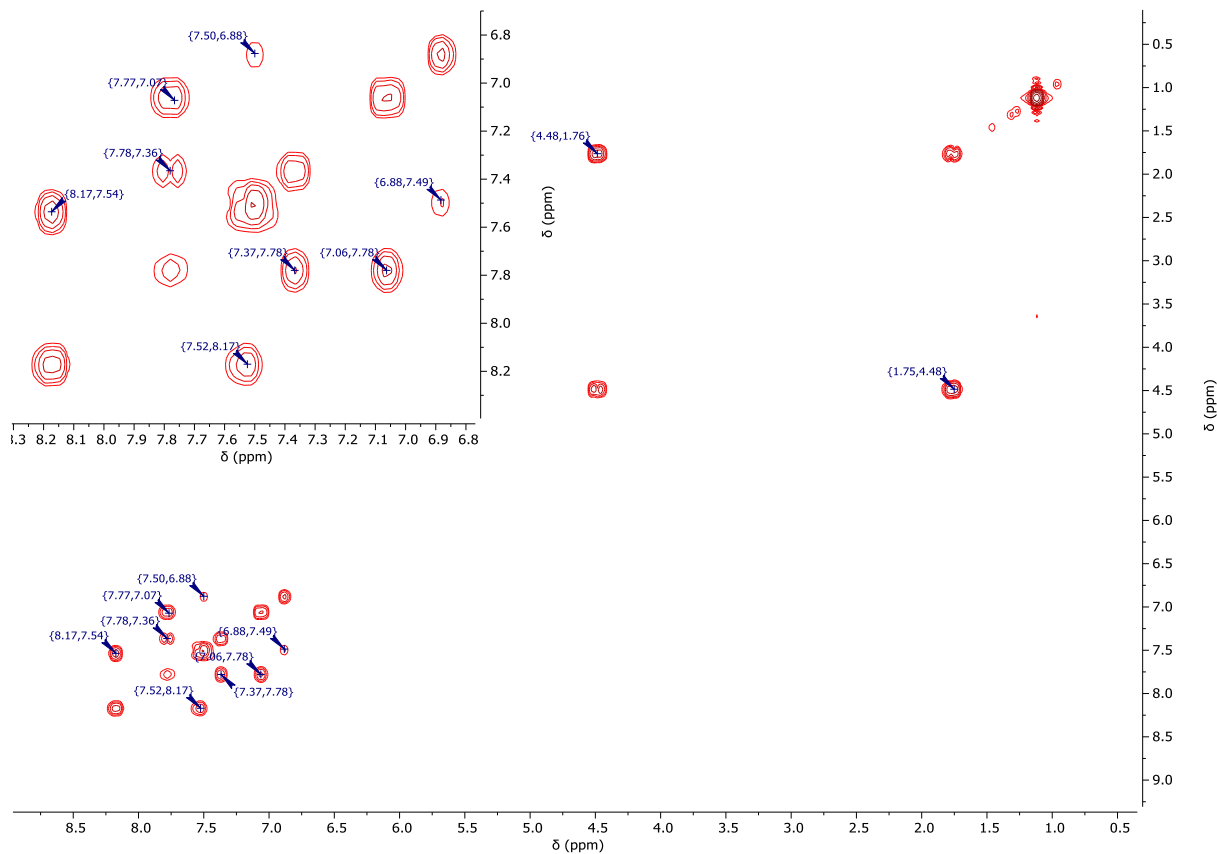


Figure S43: $^1\text{H}/^1\text{H}$ -COSY-NMR spectrum (400 MHz/400 MHz, DCM-d_2) of L_2H .

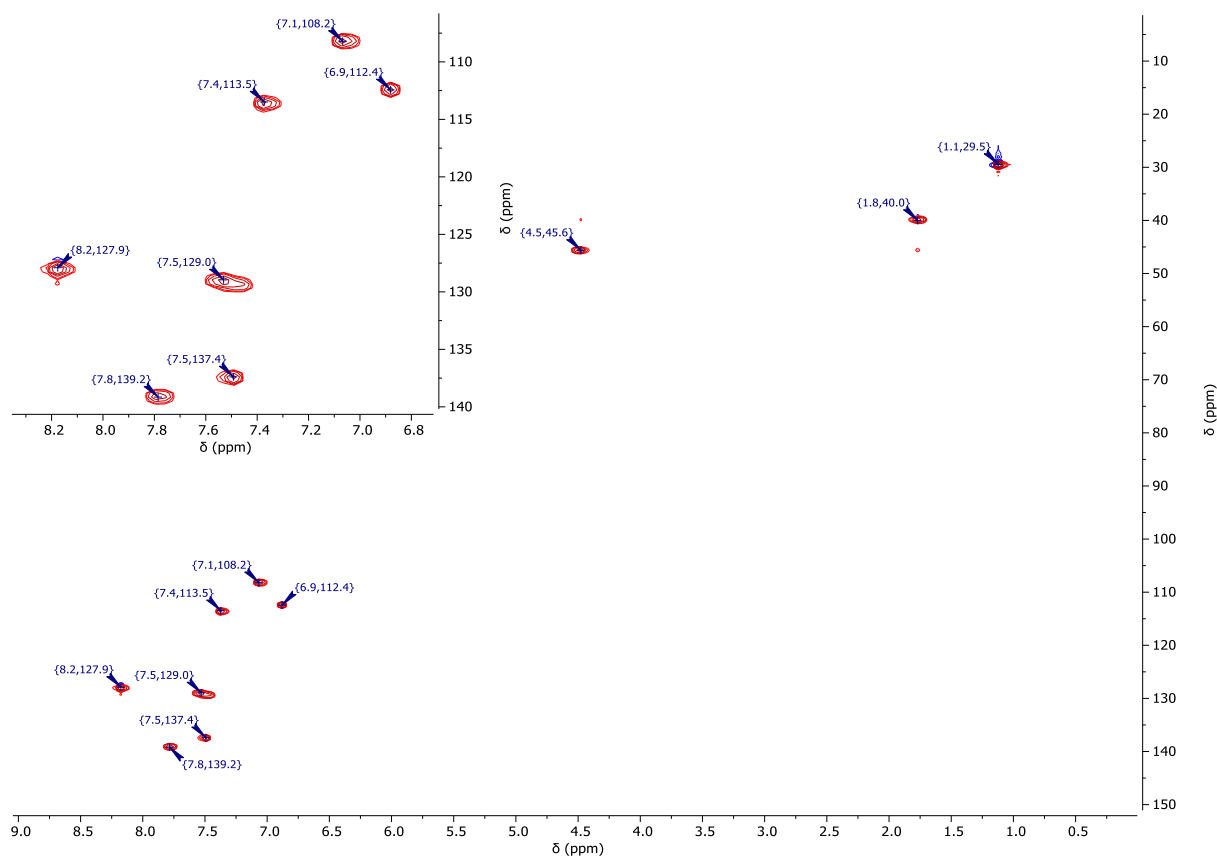


Figure S44: $^1\text{H}/^{13}\text{C}$ -gHSQC-NMR spectrum (400 MHz/101 MHz, DCM-d_2) of L_2H .

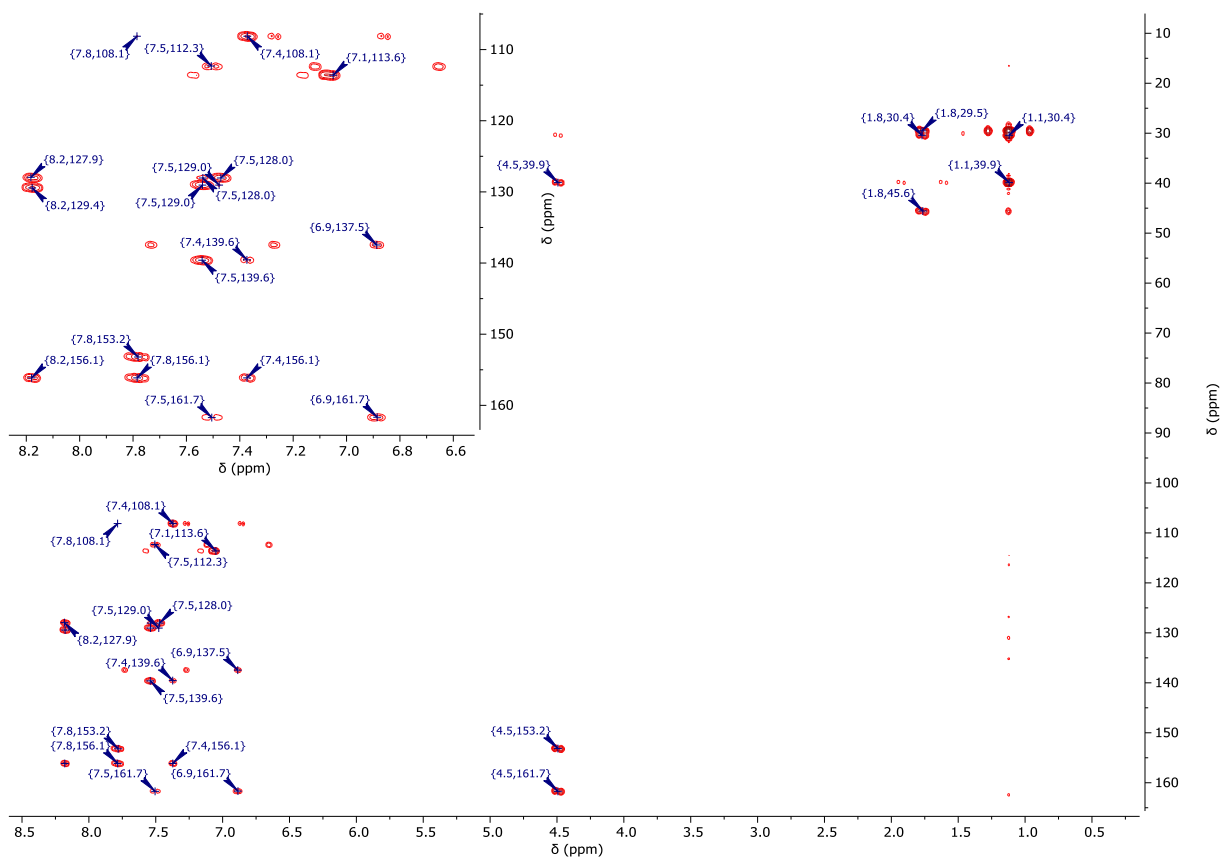


Figure S45: $^1\text{H}/^{13}\text{C}$ -gHMBC-NMR spectrum (400 MHz/101 MHz, DCM-d_2) of L_2H .

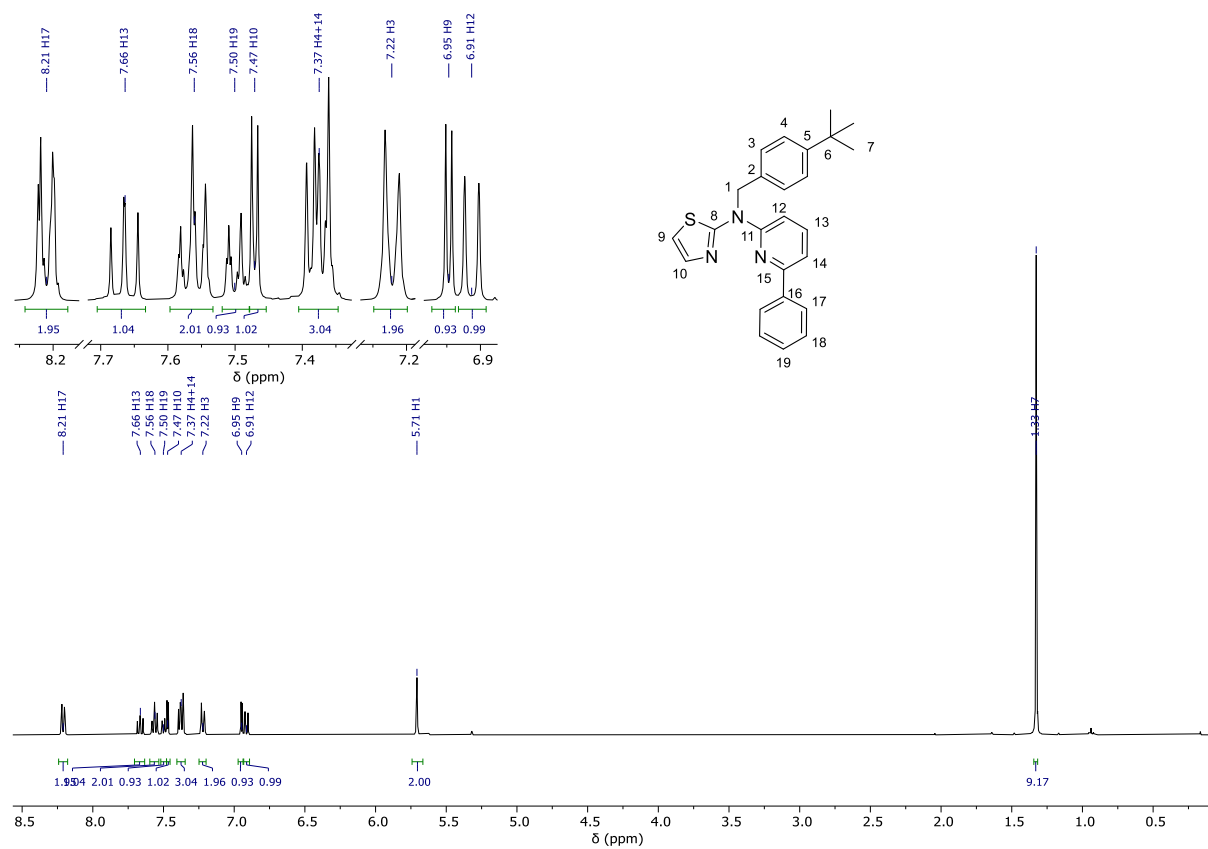


Figure S46: ^1H -NMR spectrum (400 MHz, DCM-d_2) of L_3H .

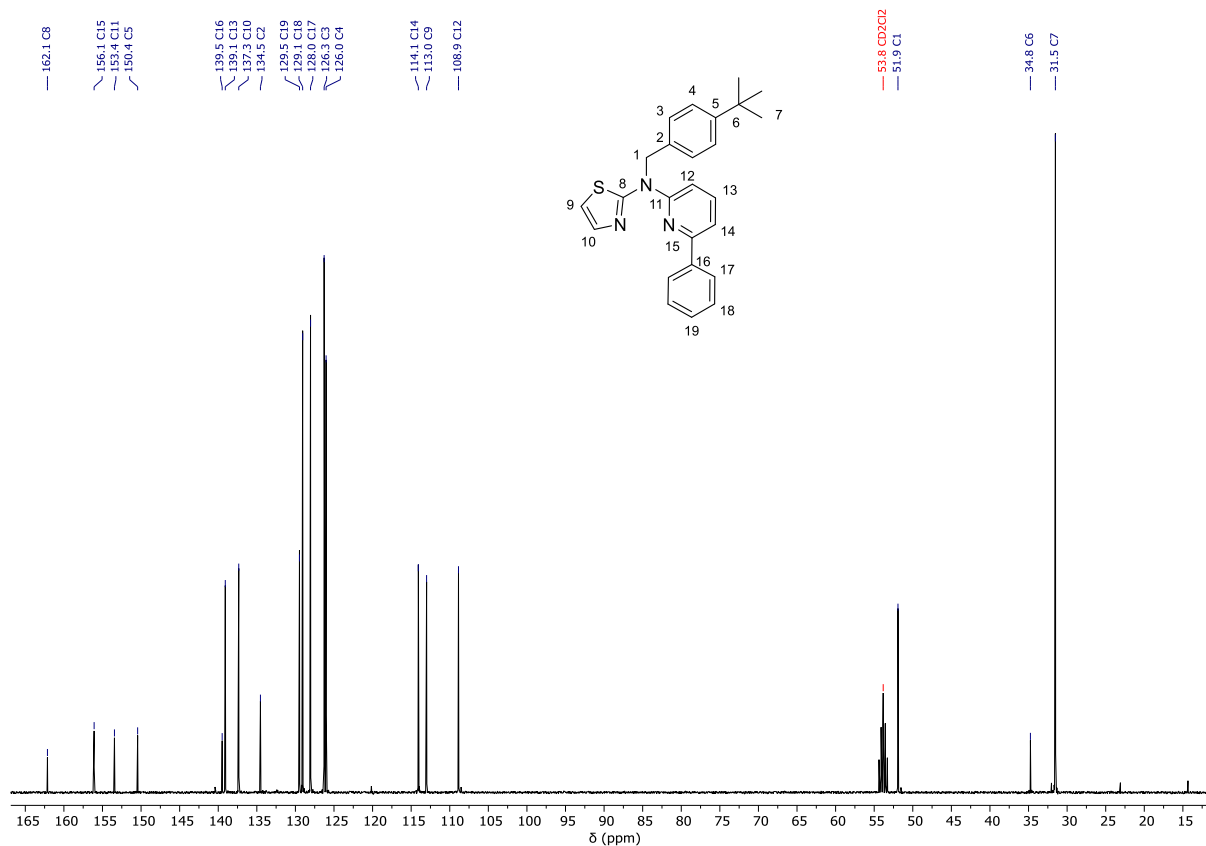


Figure S47: ^{13}C - $\{^1\text{H}\}$ -NMR spectrum (101 MHz, DCM-d_2) of **L3H**.

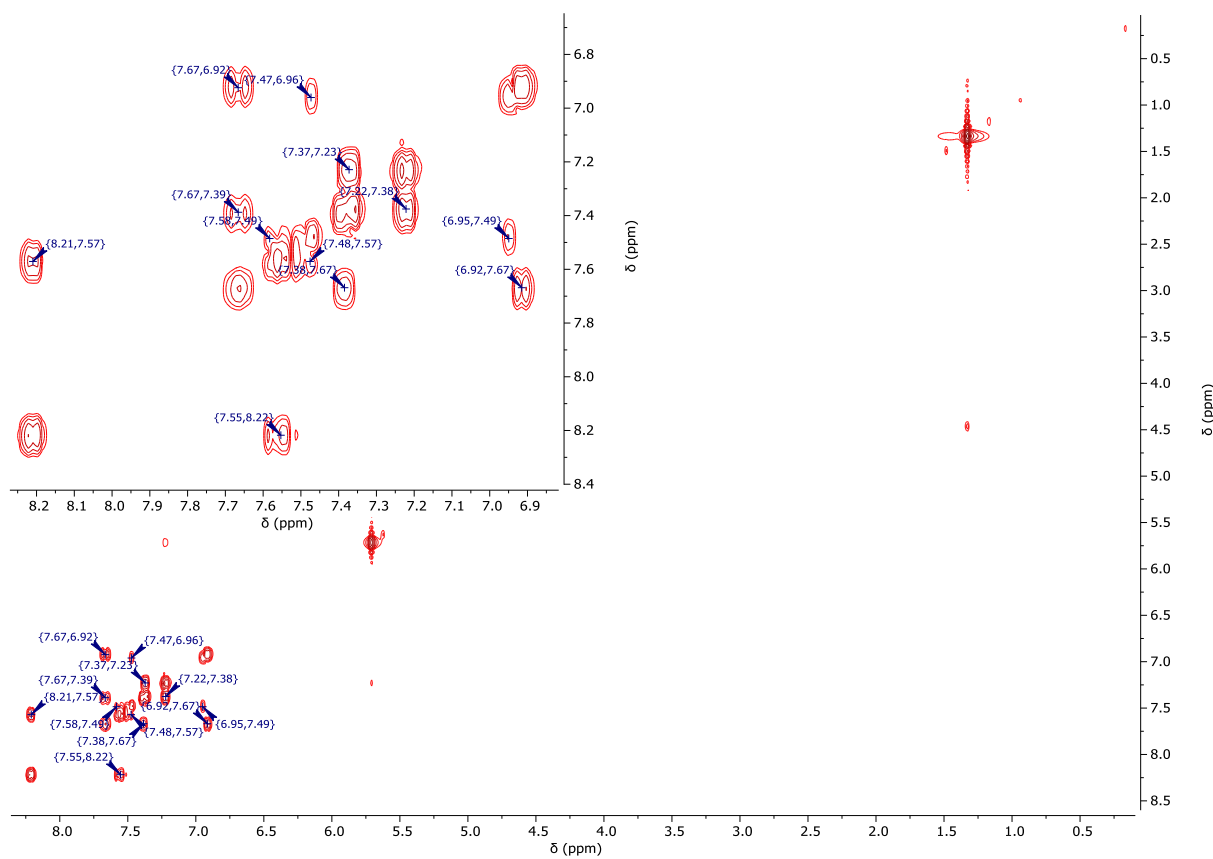


Figure S48: $^1\text{H}/^1\text{H}$ -COSY-NMR spectrum (400 MHz/400 MHz, DCM-d_2) of **L3H**.

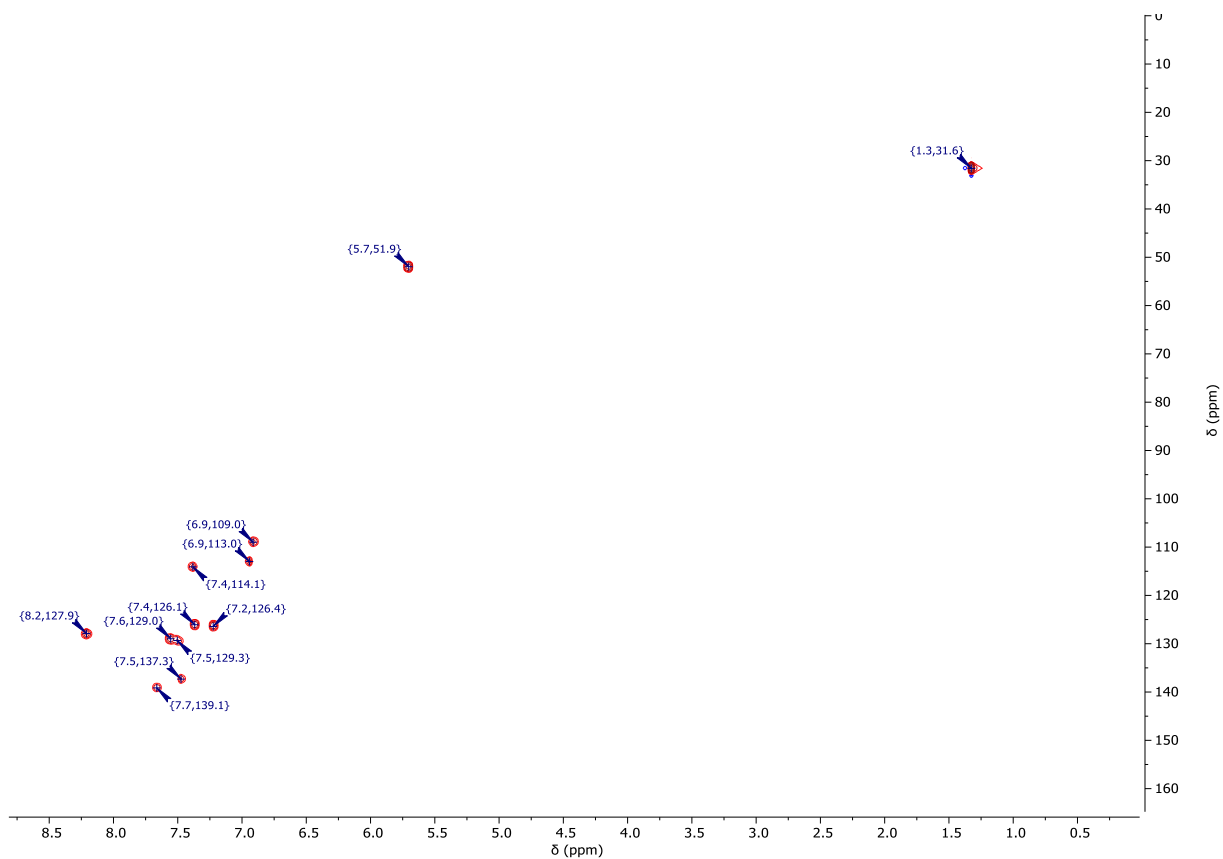


Figure S49: $^1\text{H}/^{13}\text{C}$ -gHSQC-NMR spectrum (400 MHz/101 MHz, DCM-d_2) of L_3H .

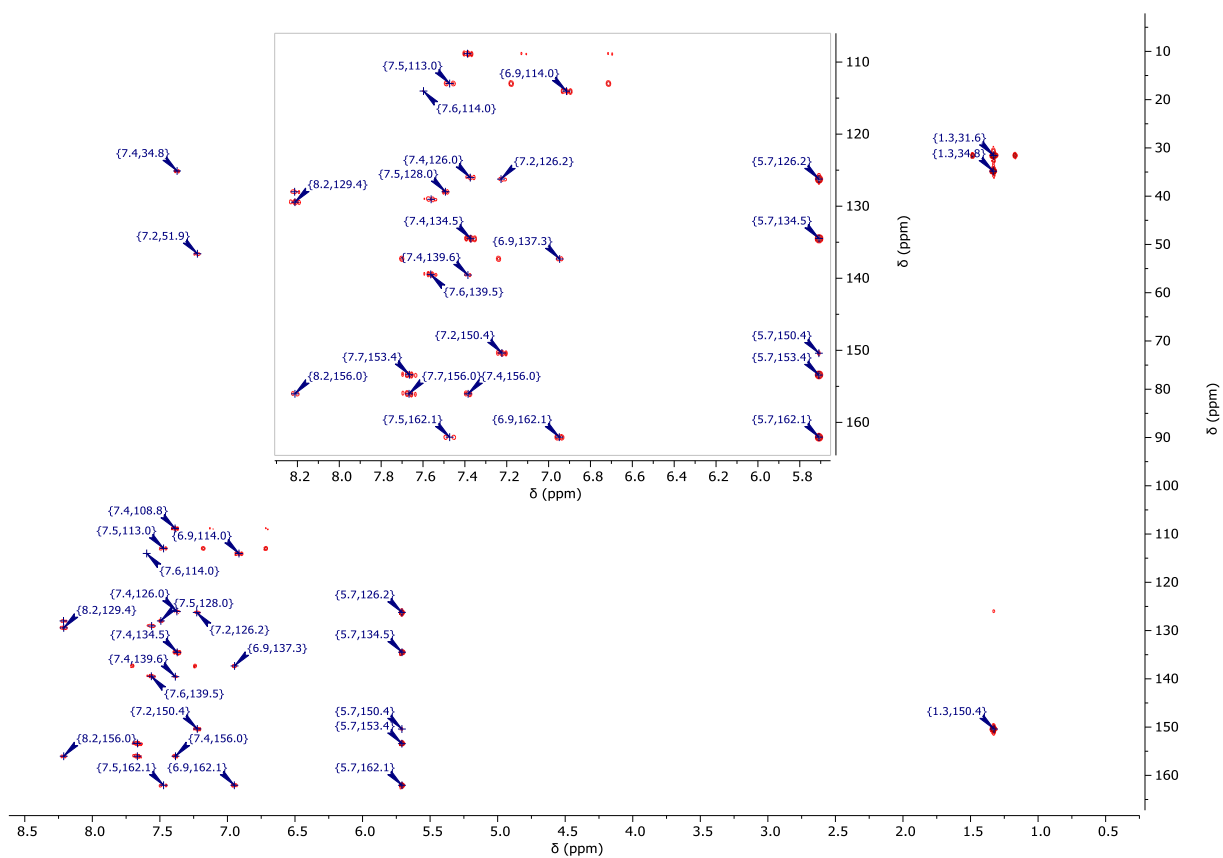


Figure S50: $^1\text{H}/^{13}\text{C}$ -gHMBC-NMR spectrum (400 MHz/101 MHz, DCM-d_2) of L_3H .

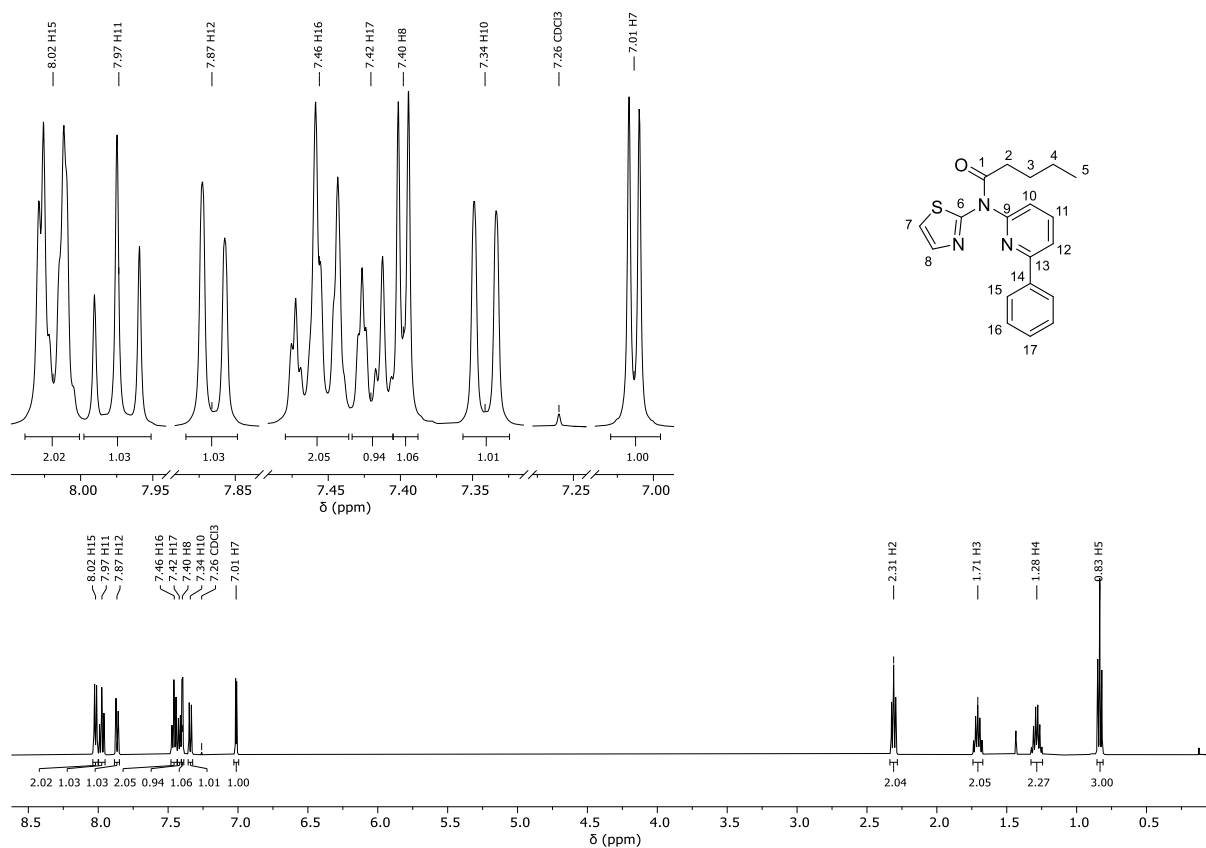


Figure S51: $^1\text{H-NMR}$ spectrum (500 MHz, CDCl_3) of **L4H.**

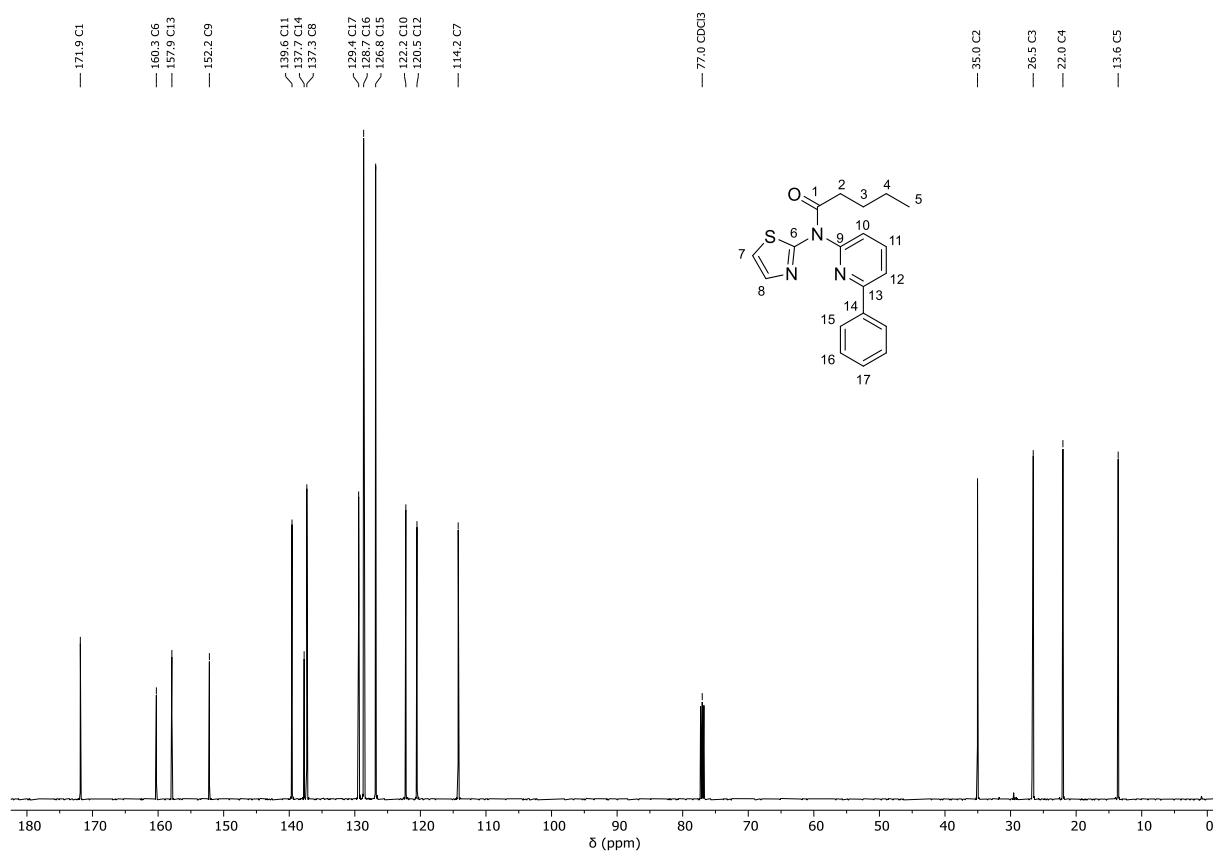


Figure S52: $^{13}\text{C-}\{^1\text{H}\}$ -NMR spectrum (126 MHz, CDCl_3) of **L4H.**

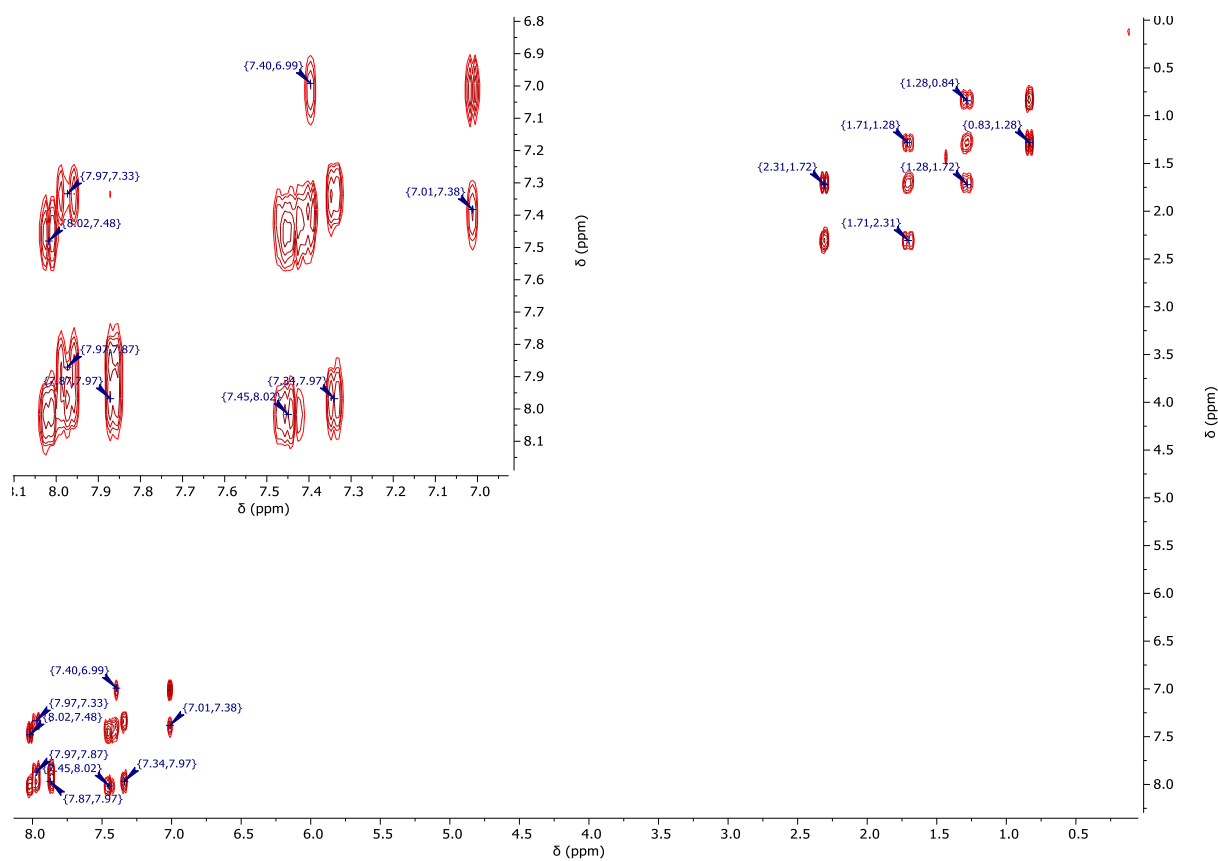


Figure S53: $^1\text{H}/^1\text{H}$ -COSY-NMR spectrum (500 MHz/500 MHz, CDCl_3) of **L4H**.

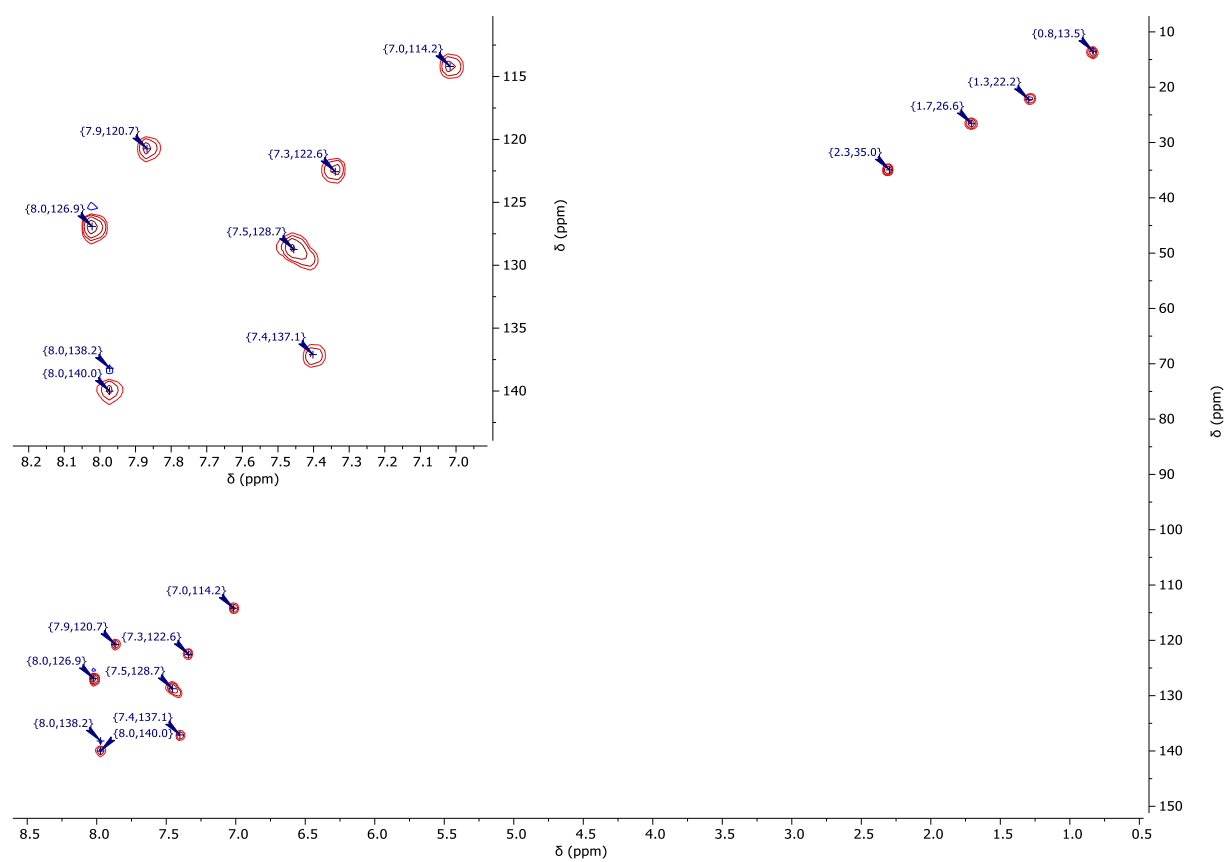


Figure S54: $^1\text{H}/^{13}\text{C}$ -gHSQC-NMR spectrum (500 MHz/126 MHz, CDCl_3) of **L4H**.

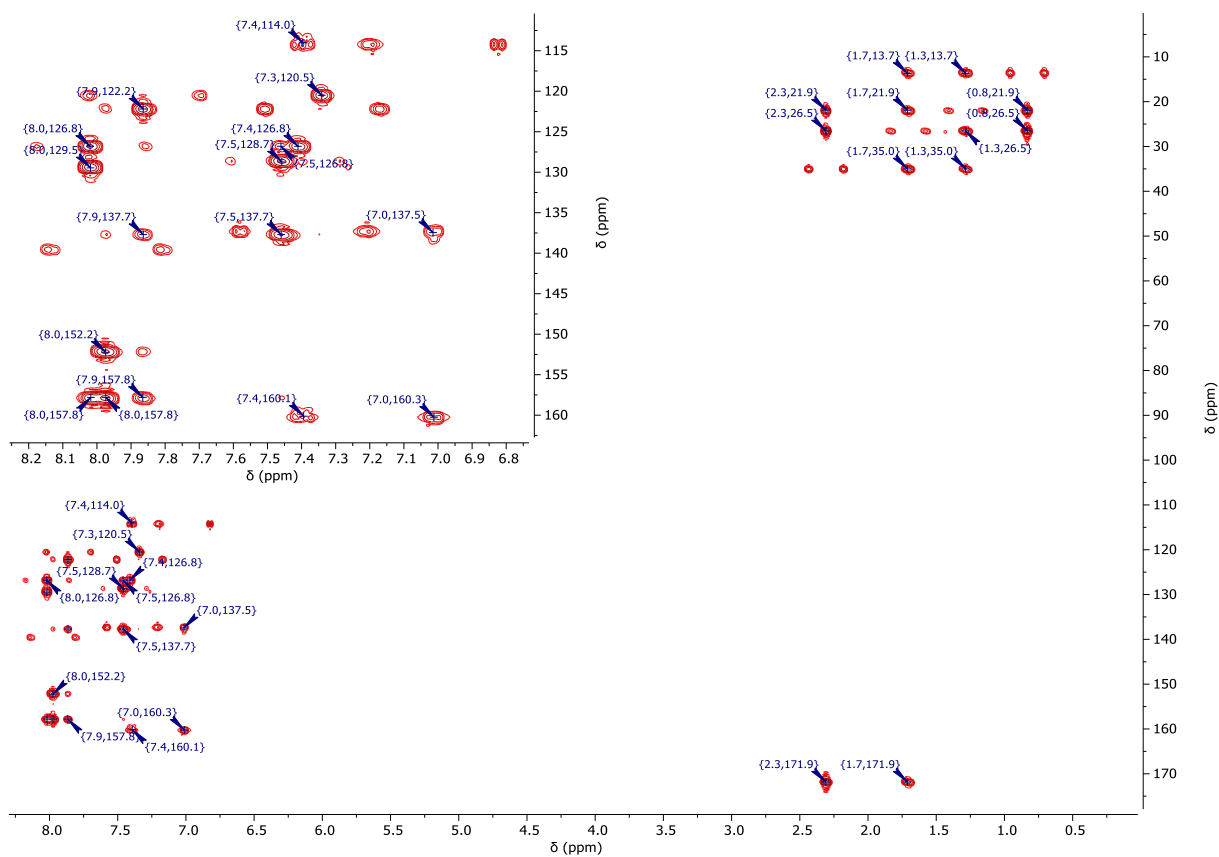


Figure S55: $^1\text{H}/^{13}\text{C}$ -gHMBC-NMR spectrum (500 MHz/126 MHz, CDCl_3) of **L4H**.

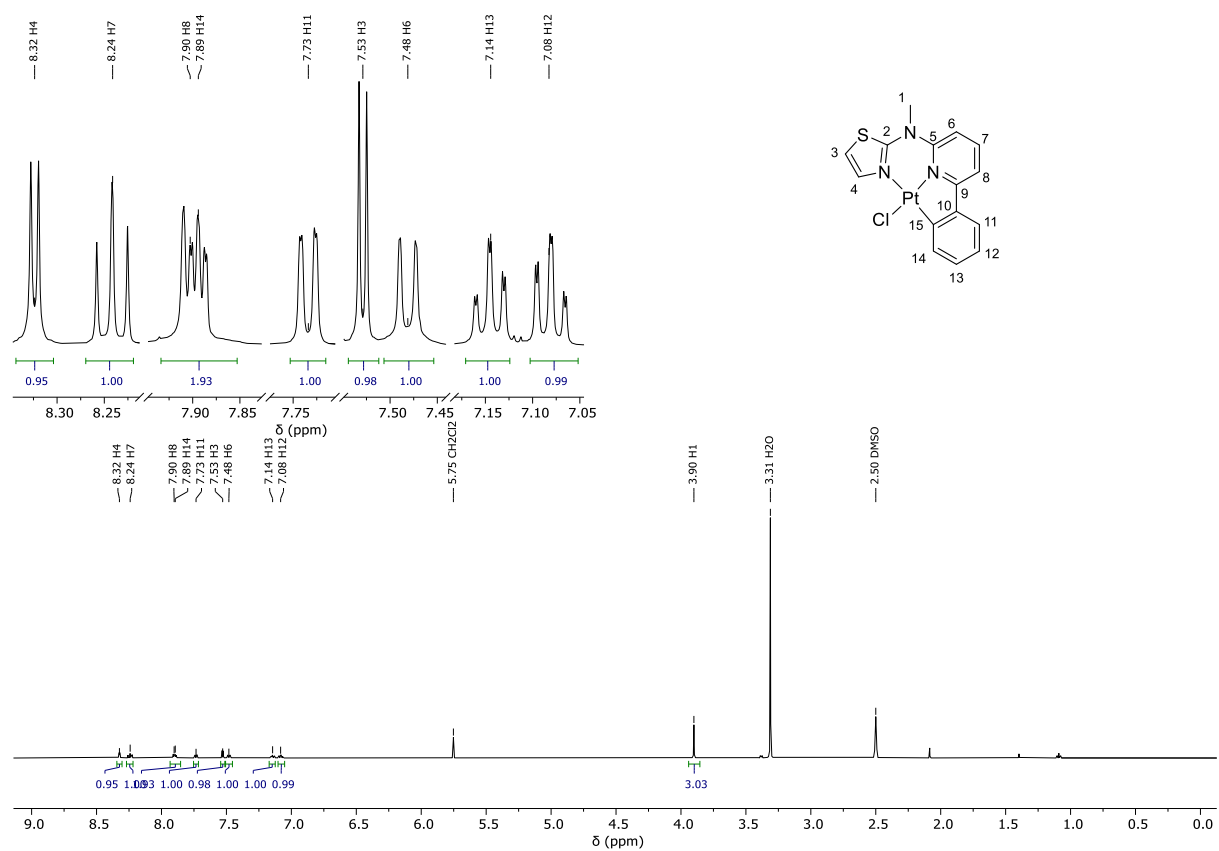


Figure S56: ^1H -NMR spectrum (500 MHz, $\text{DMSO}-d_6$) of $[\text{PtCl}(\text{L}_1)]$.

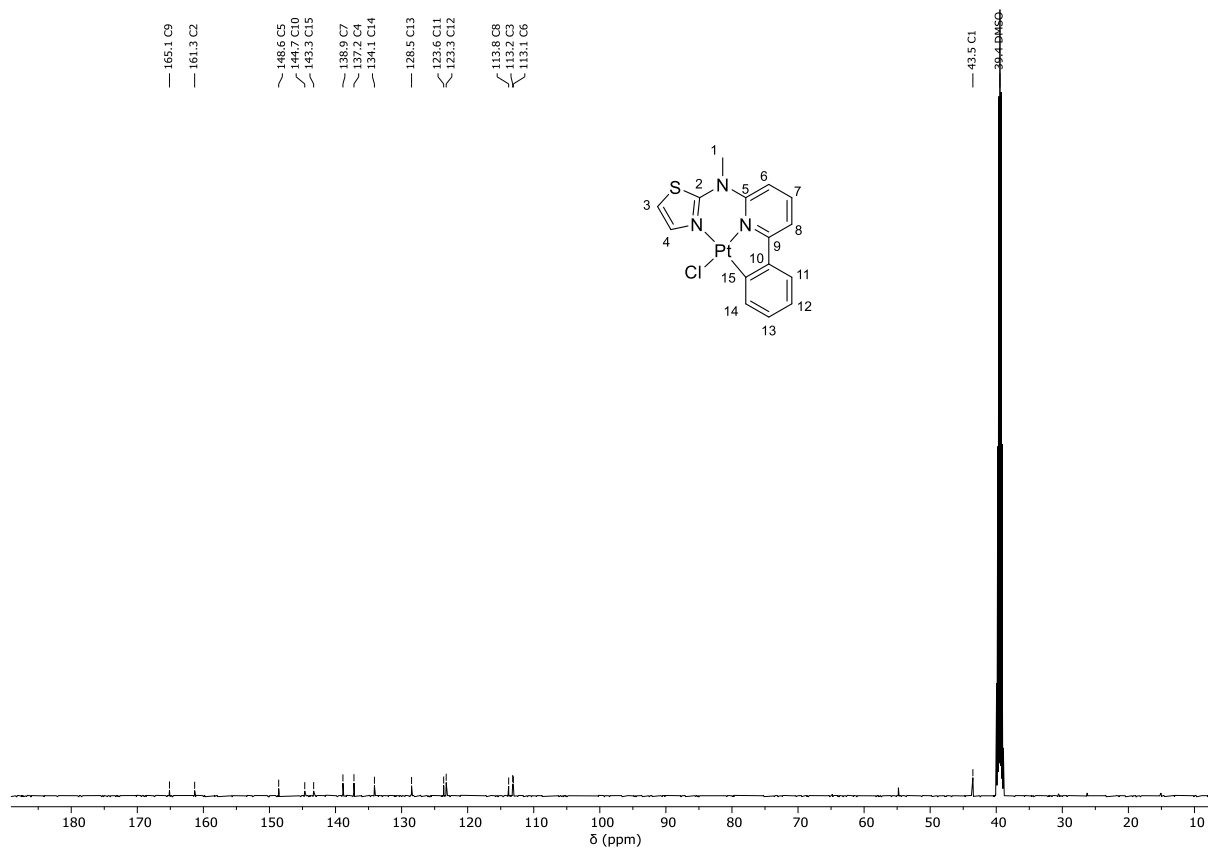


Figure S57: ^{13}C - $\{^1\text{H}\}$ -NMR spectrum (126 MHz, $\text{DMSO-}d_6$) of $[\text{PtCl}(\text{L}_1)]$.

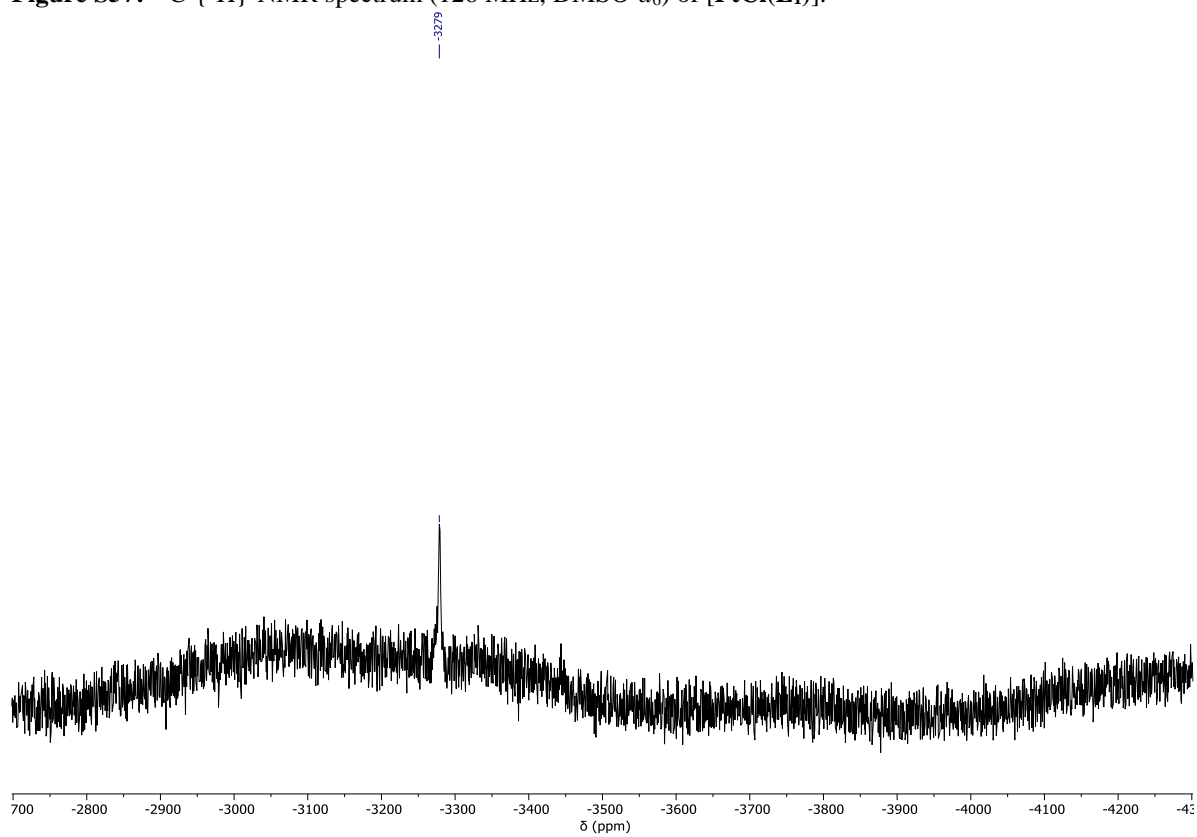


Figure S58: ^{195}Pt -NMR spectrum (107 MHz, $\text{DMSO-}d_6$) of $[\text{PtCl}(\text{L}_1)]$.

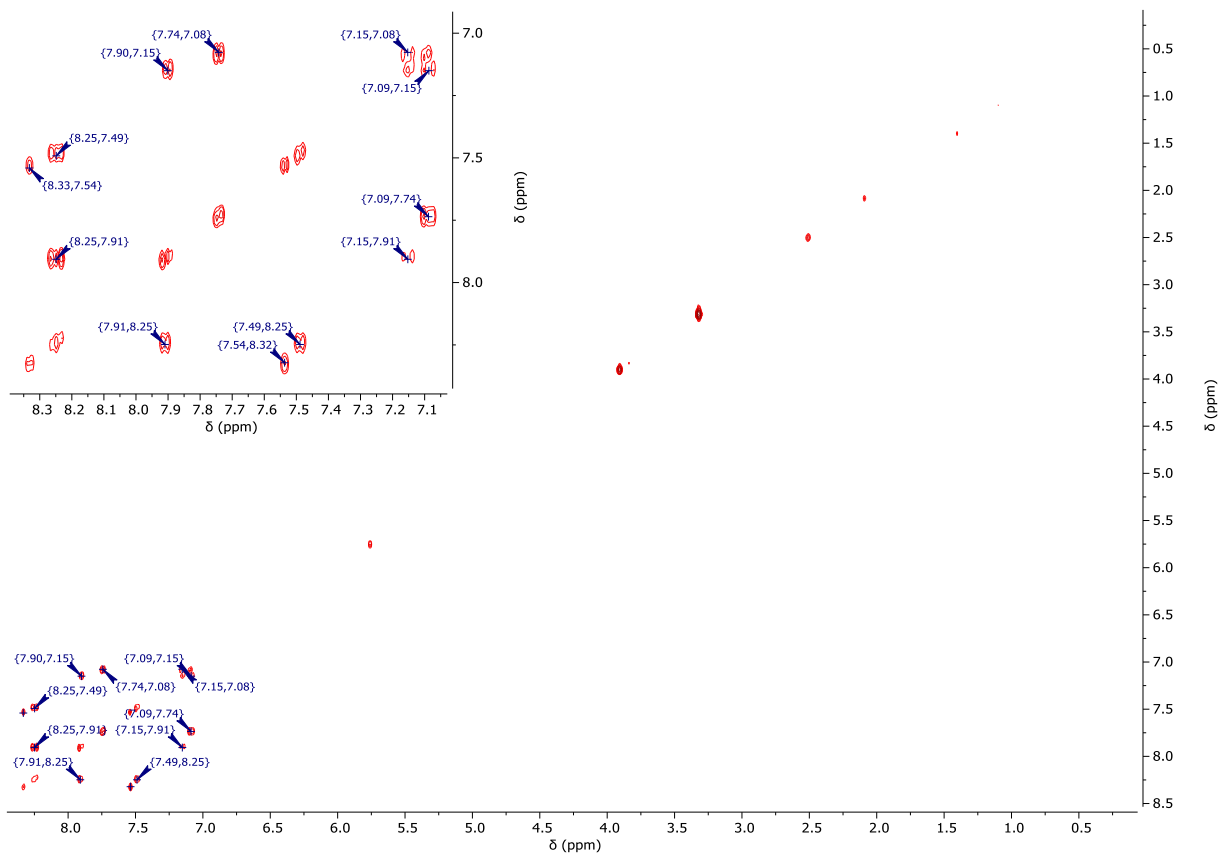


Figure S59: $^1\text{H}/^1\text{H}$ -COSY-NMR spectrum (500 MHz/500 MHz, $\text{DMSO}-d_6$) of $[\text{PtCl}(\text{L}_1)]$.

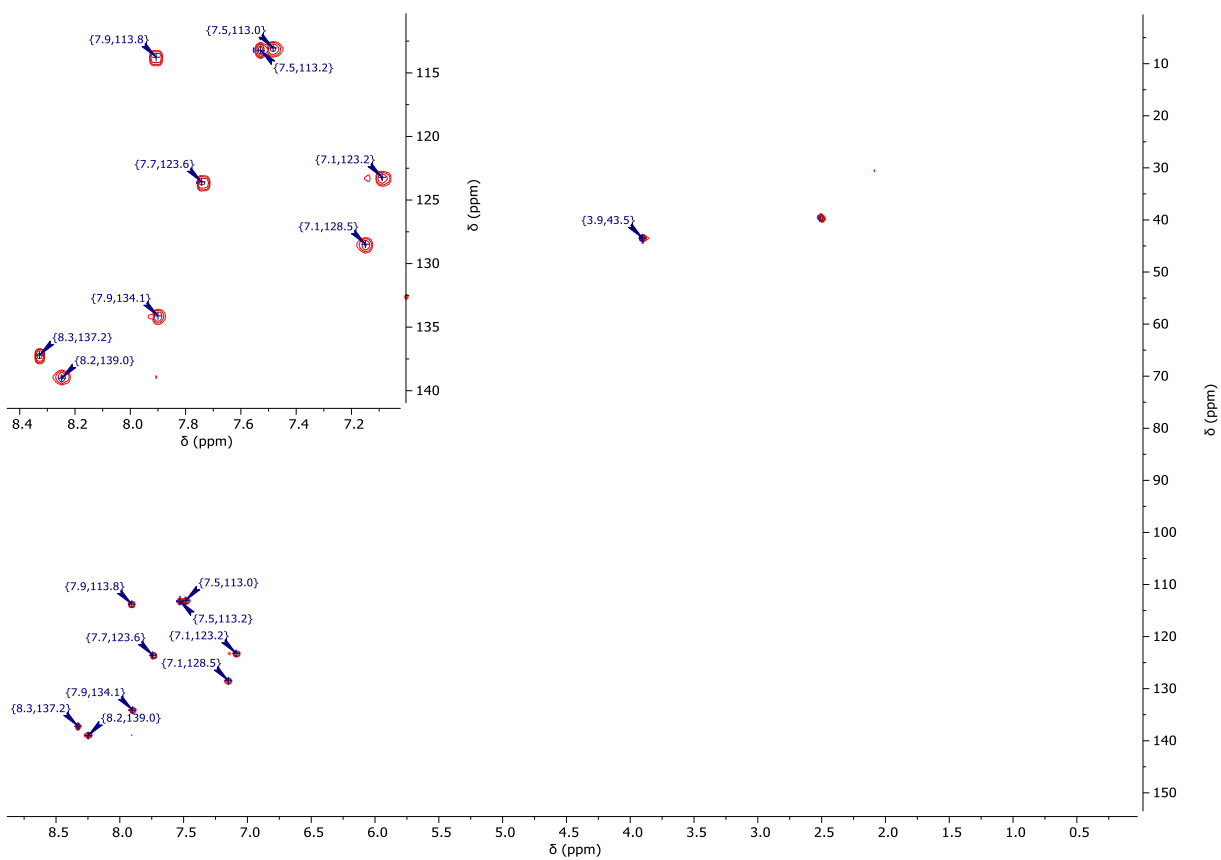


Figure S60: $^1\text{H}/^{13}\text{C}$ -gHSQC-NMR spectrum (500 MHz/126 MHz, $\text{DMSO}-d_6$) of $[\text{PtCl}(\text{L}_1)]$.

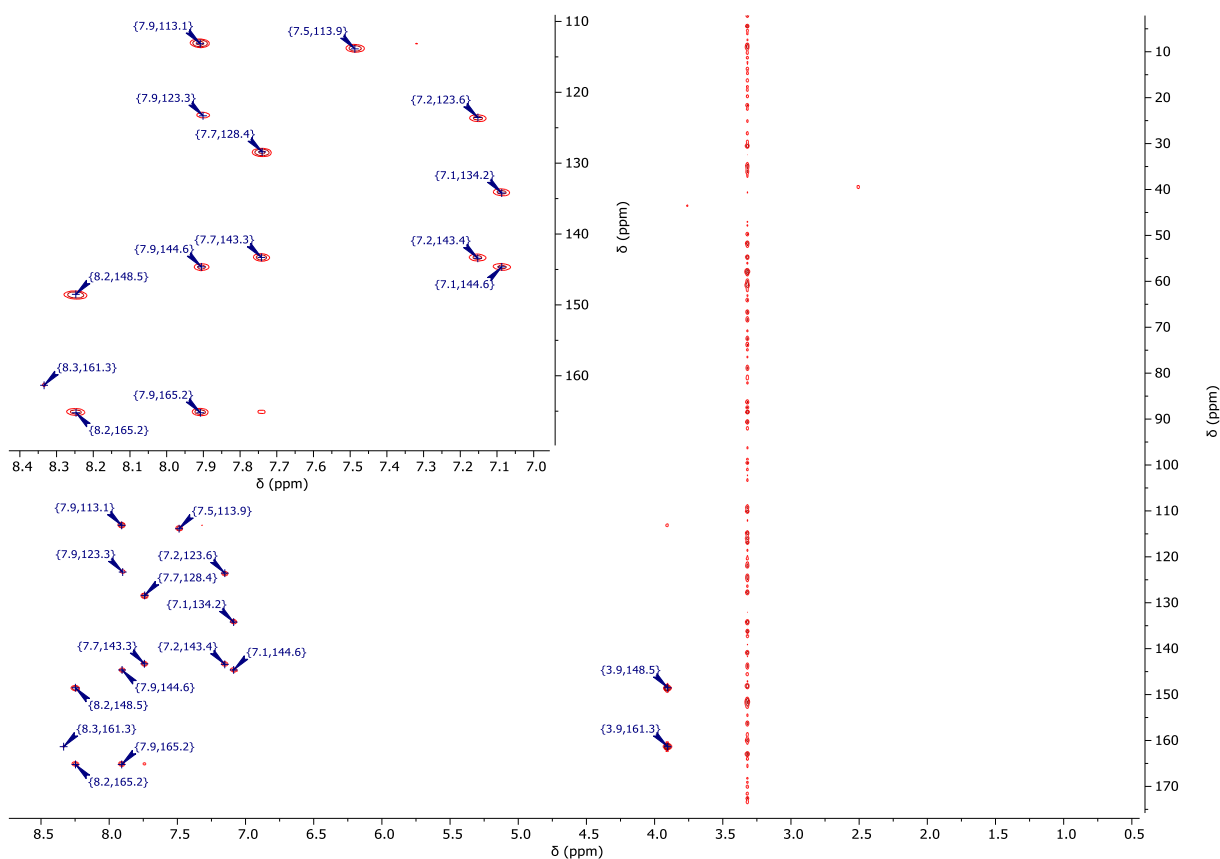


Figure S61: $^1\text{H}/^{13}\text{C}$ -gHMBC-NMR spectrum (500 MHz/126 MHz, $\text{DMSO}-d_6$) of $[\text{PtCl}(\text{L}_1)]$.

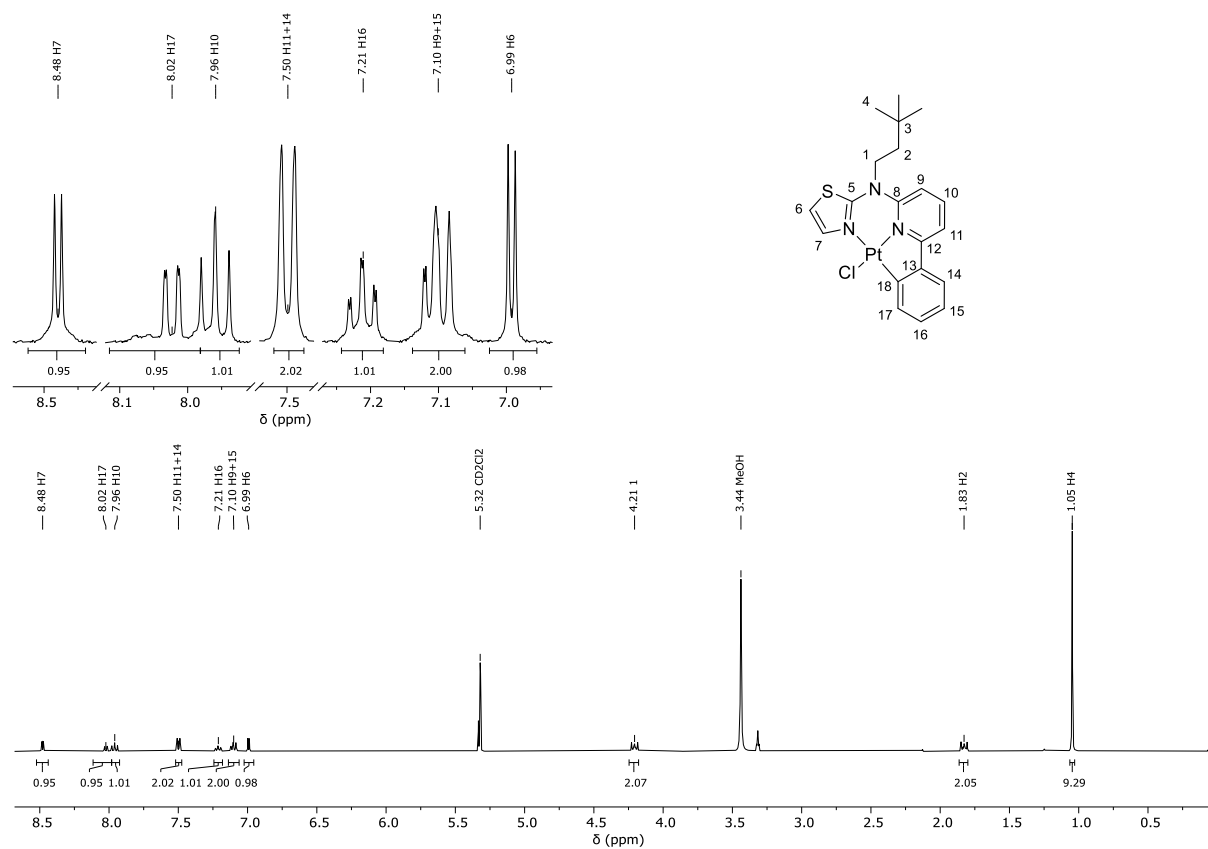


Figure S62: ^1H -NMR spectrum (400 MHz, $\text{DCM}-d_2/\text{MeOD}-d_4$) of $[\text{PtCl}(\text{L}_2)]$.

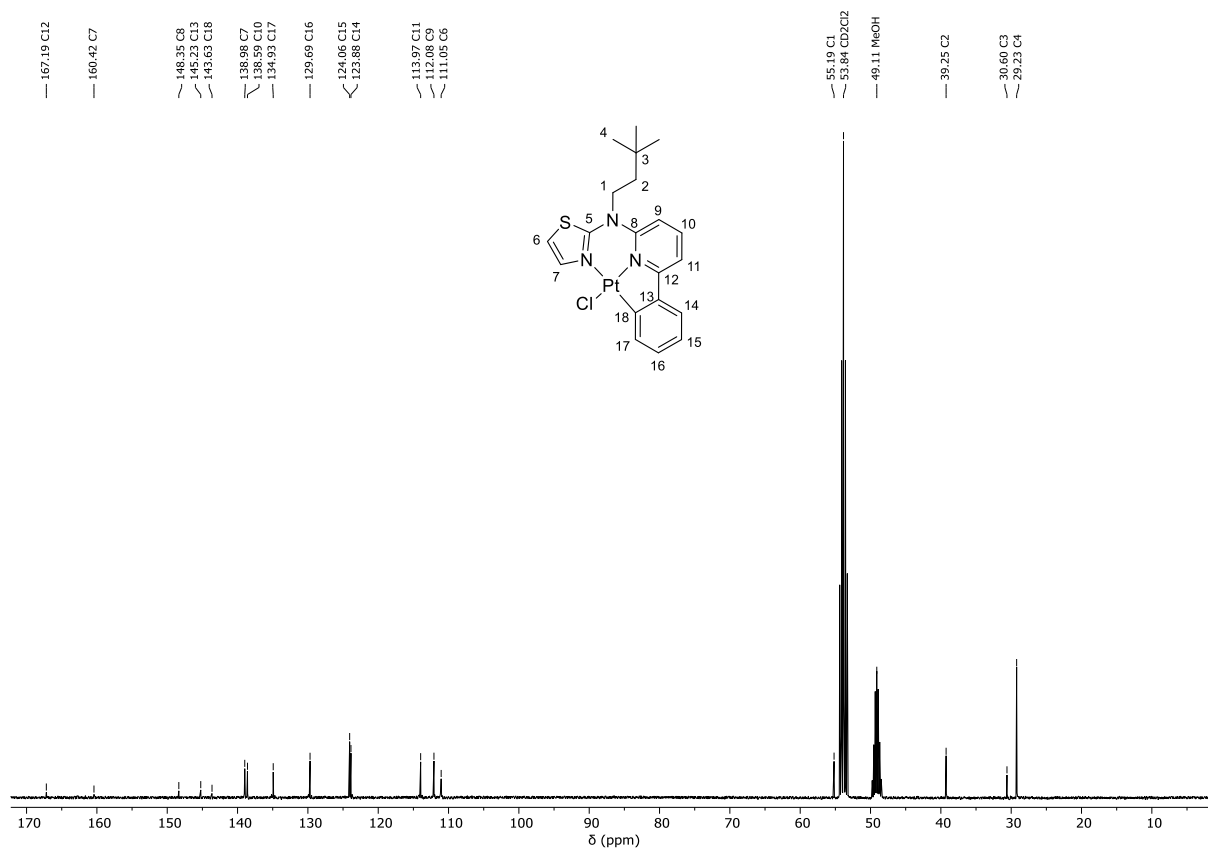


Figure S63: ^{13}C - $\{^1\text{H}\}$ -NMR spectrum (101 MHz, $\text{DCM-d}_2/\text{MeOD-d}_4$) of $[\text{PtCl}(\text{L}_2)]$.

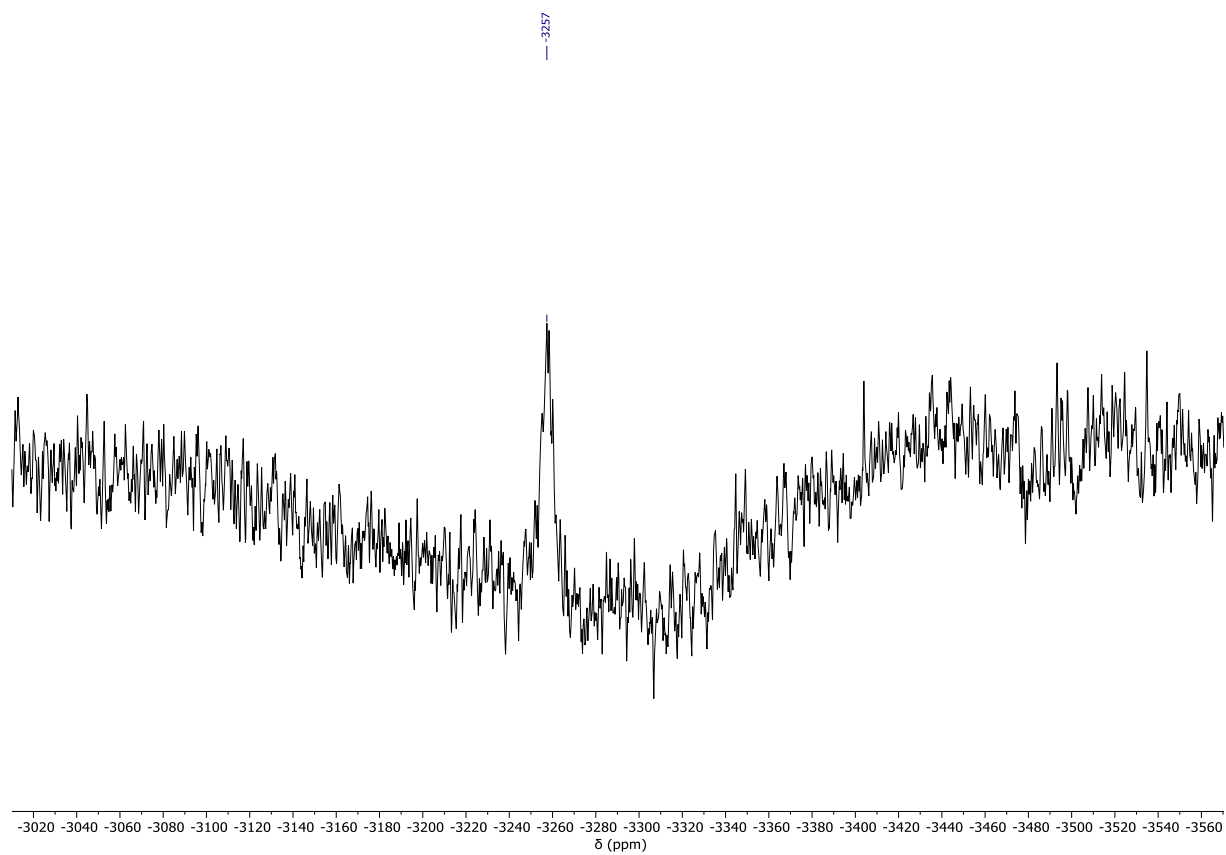


Figure S64: ^{195}Pt -NMR spectrum (107 MHz, $\text{DCM-d}_2/\text{MeOD-d}_4$) of $[\text{PtCl}(\text{L}_2)]$.

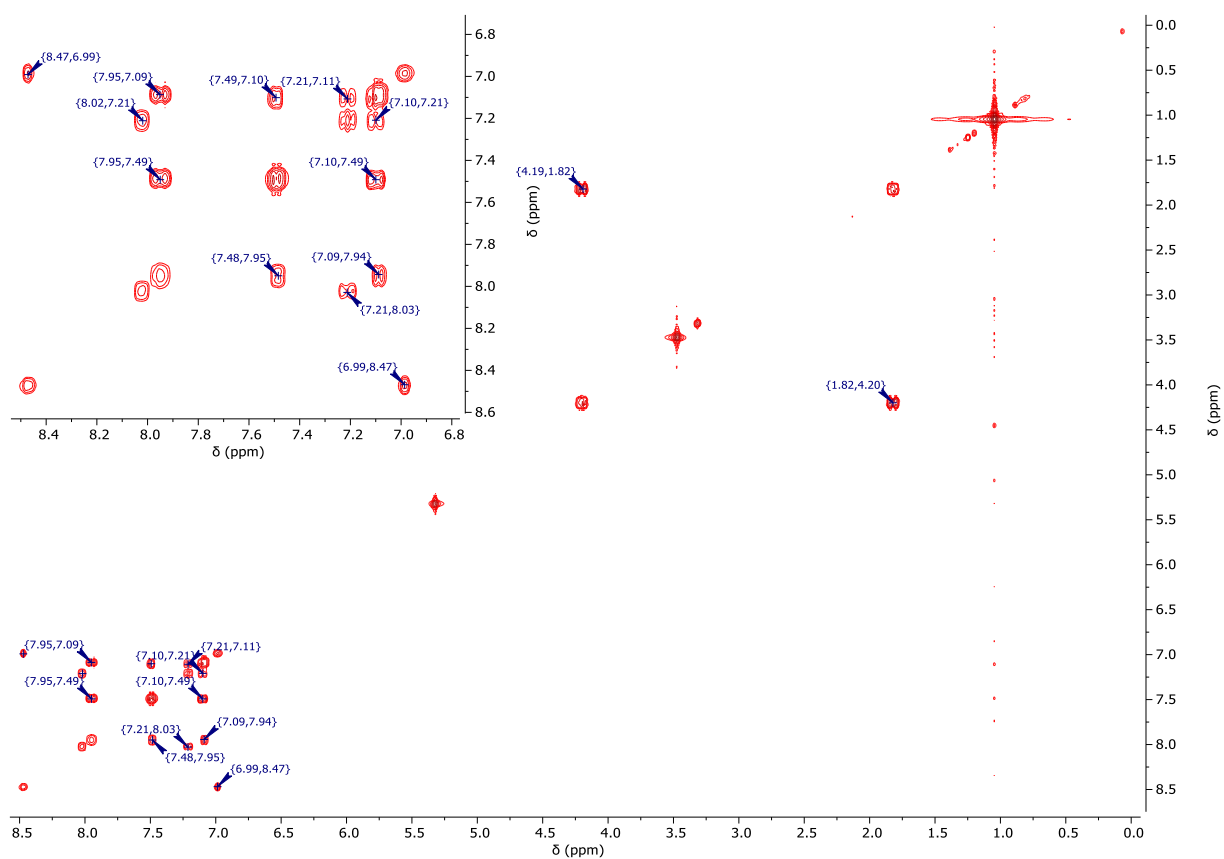


Figure S65: $^1\text{H}/^1\text{H}$ -COSY-NMR spectrum (400 MHz/400 MHz, $\text{DCM-}d_2/\text{MeOD-}d_4$) of $[\text{PtCl}(\text{L}_2)]$.

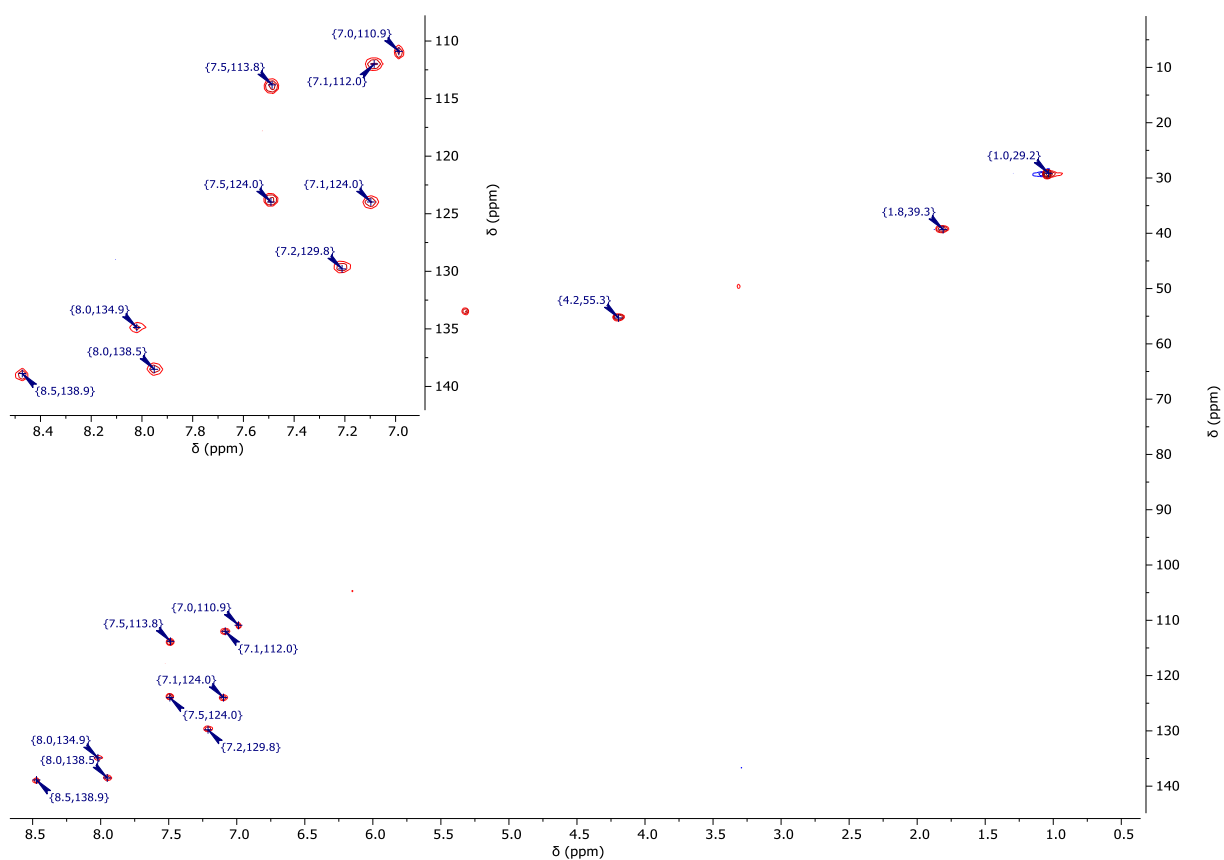


Figure S66: $^1\text{H}/^{13}\text{C}$ -gHSQC-NMR spectrum (400 MHz/101 MHz, $\text{DCM-}d_2/\text{MeOD-}d_4$) of $[\text{PtCl}(\text{L}_2)]$.

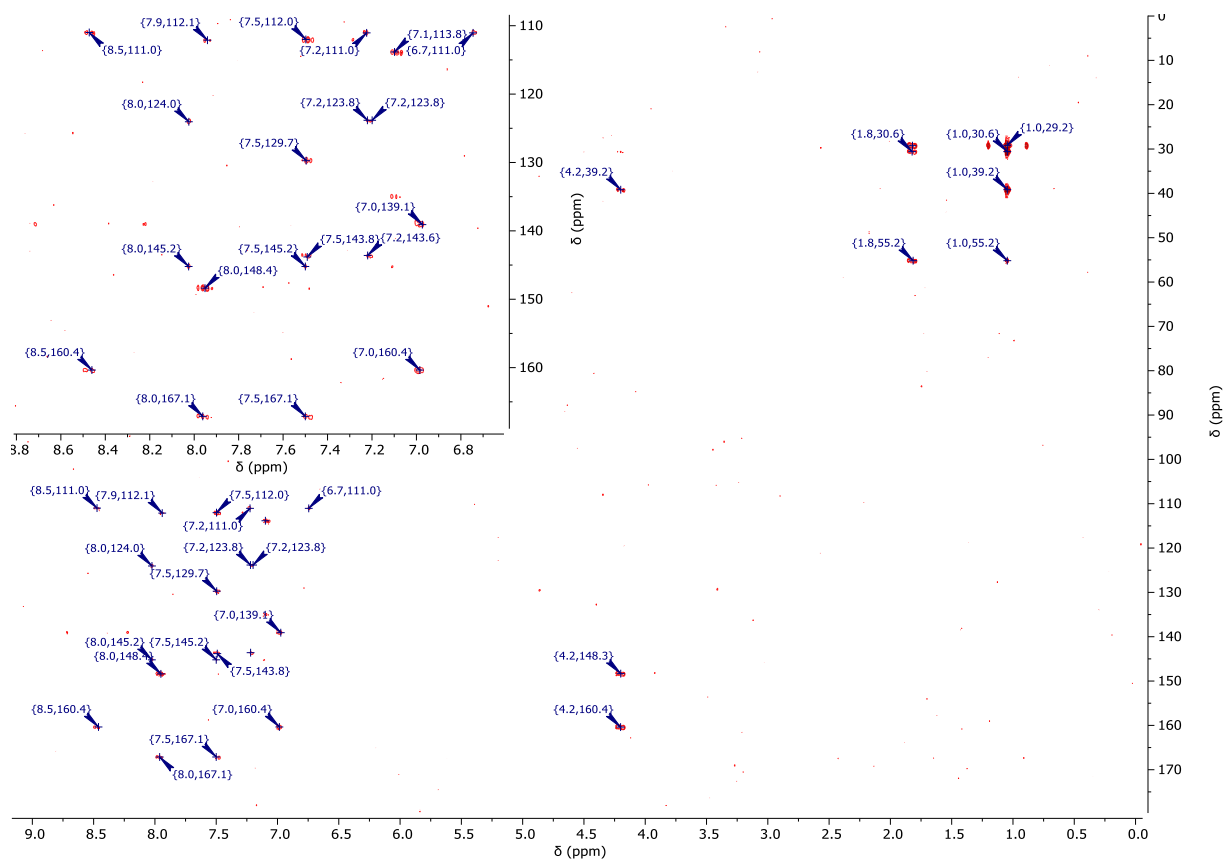


Figure S67: $^1\text{H}/^{13}\text{C}$ -gHMBC-NMR spectrum (400 MHz/ ^{13}C 101 MHz, $\text{DCM}-d_2/\text{MeOD}-d_4$) of $[\text{PtCl}(\text{L}_2)]$.

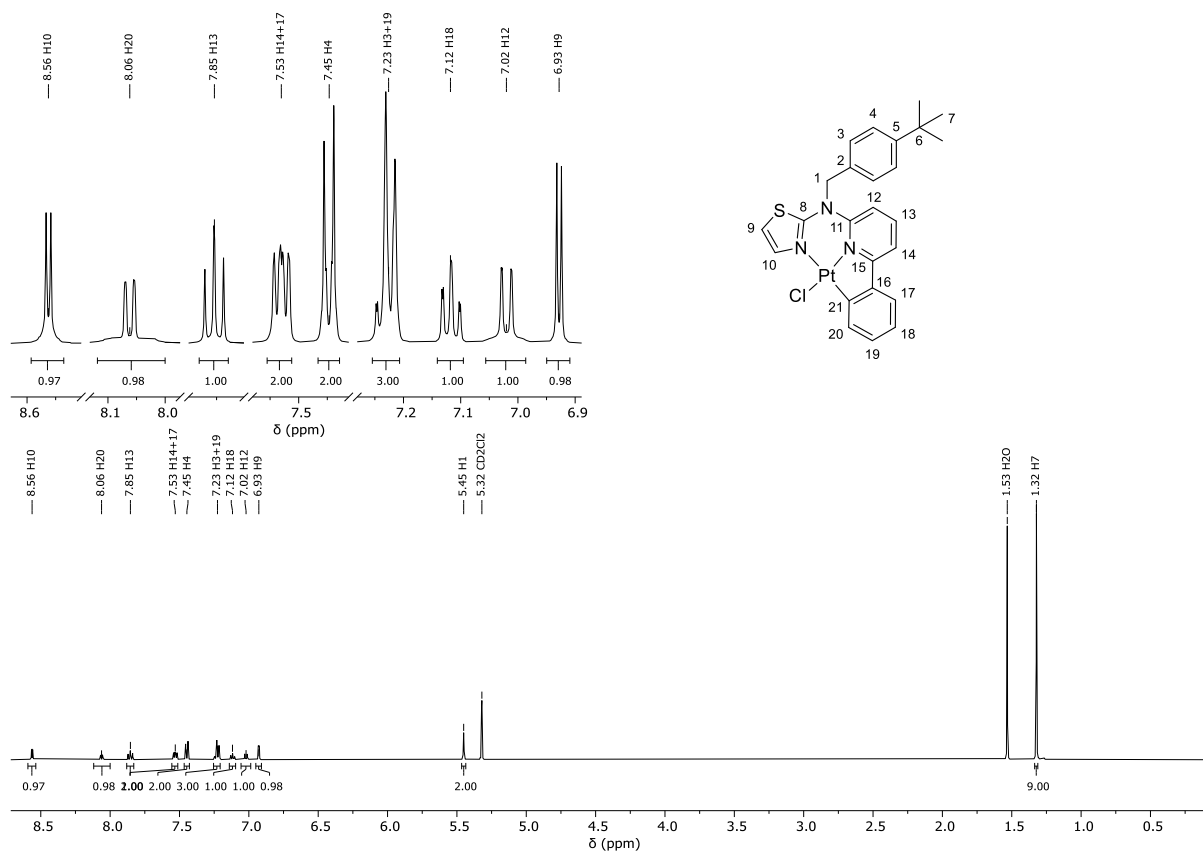


Figure S68: ^1H -NMR spectrum (500 MHz, $\text{DCM}-d_2$) of $[\text{PtCl}(\text{L}_3)]$.

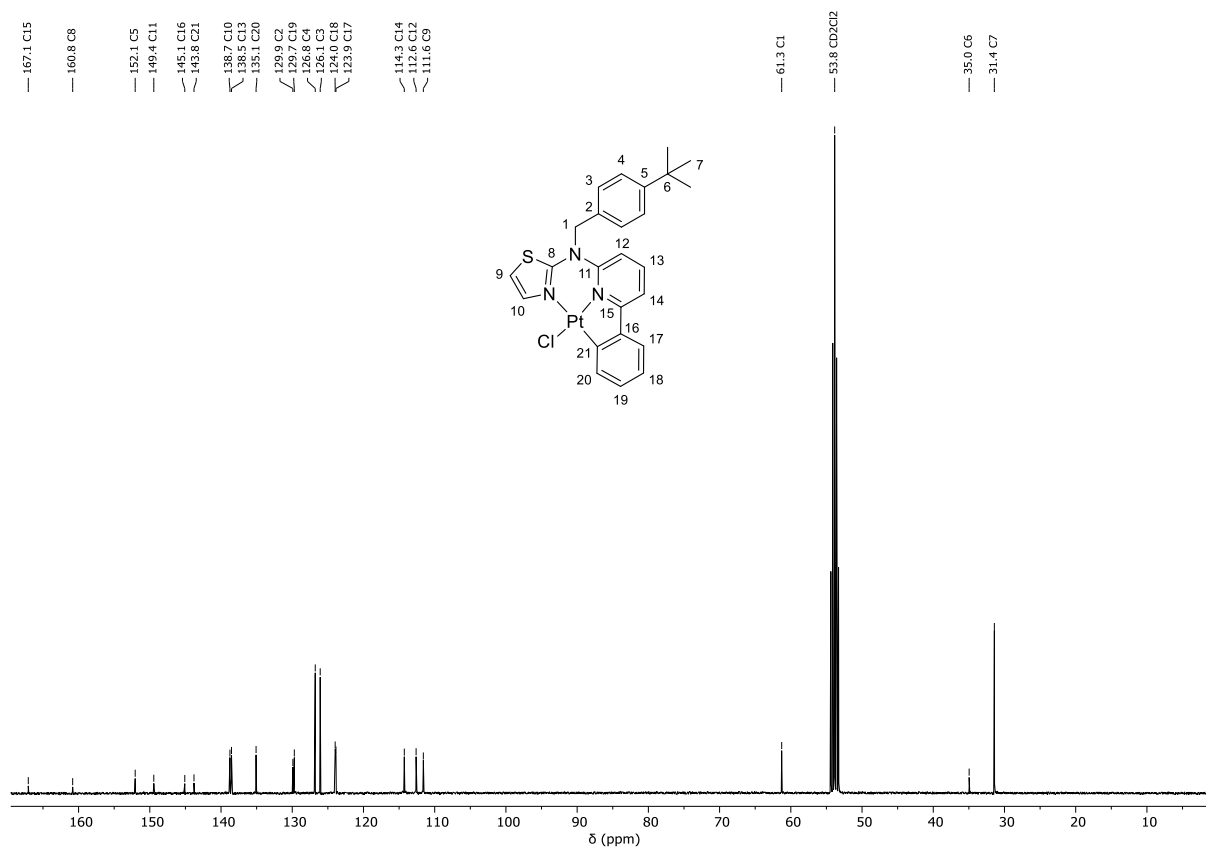


Figure S69: ^{13}C - $\{^1\text{H}\}$ -NMR spectrum (101 MHz, DCM-d_2) of $[\text{PtCl}(\text{L}_3)]$.

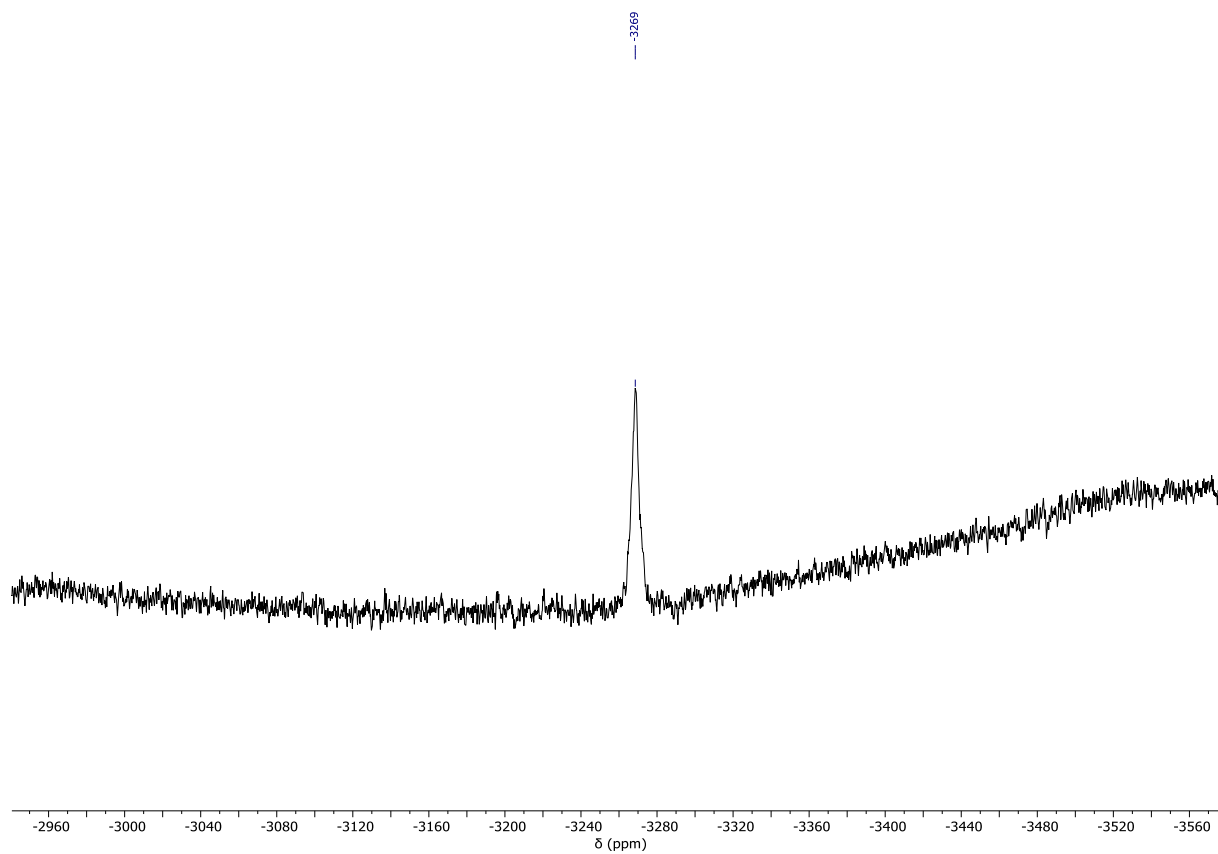


Figure S70: ^{195}Pt -NMR spectrum (107 MHz, DCM-d_2) of $[\text{PtCl}(\text{L}_3)]$.

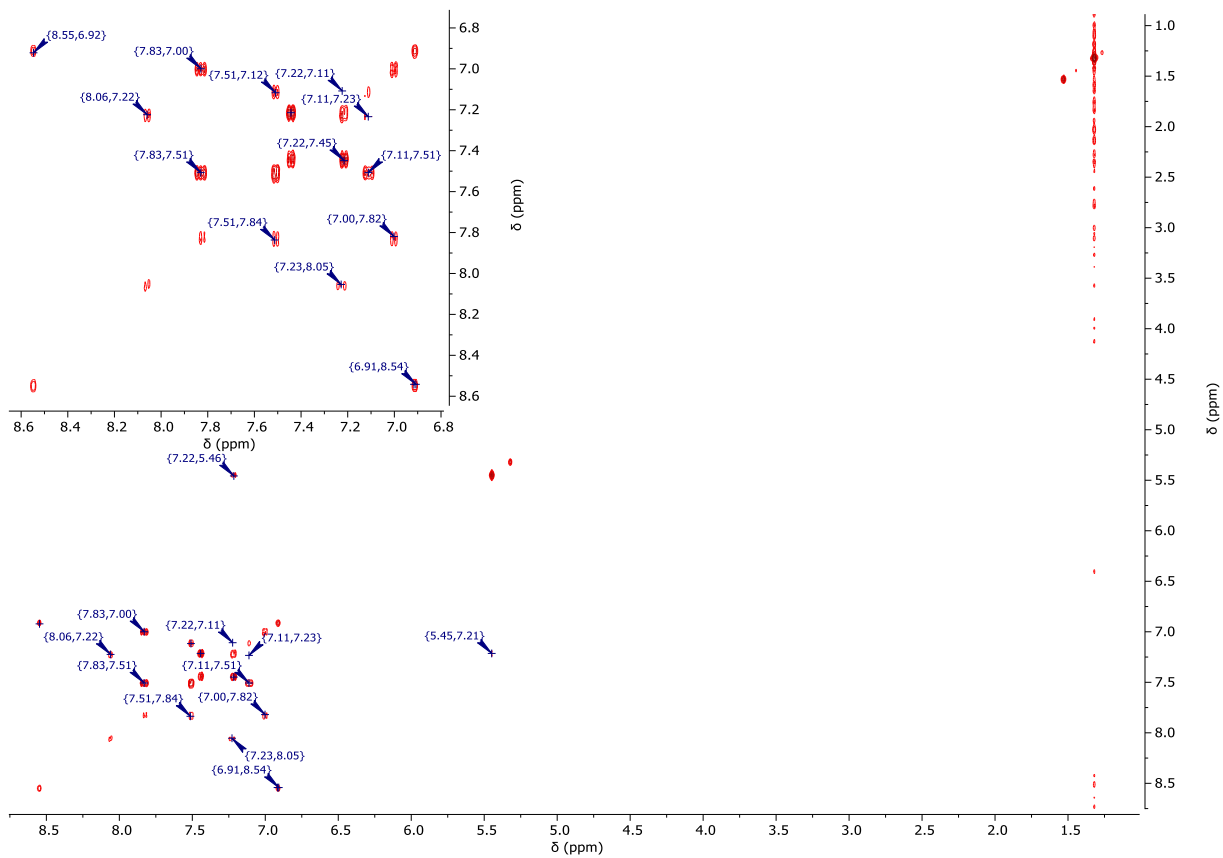


Figure S71: $^1\text{H}/^1\text{H}$ -COSY-NMR spectrum (400 MHz/400 MHz, DCM-d_2) of $[\text{PtCl}(\text{L}_3)]$.

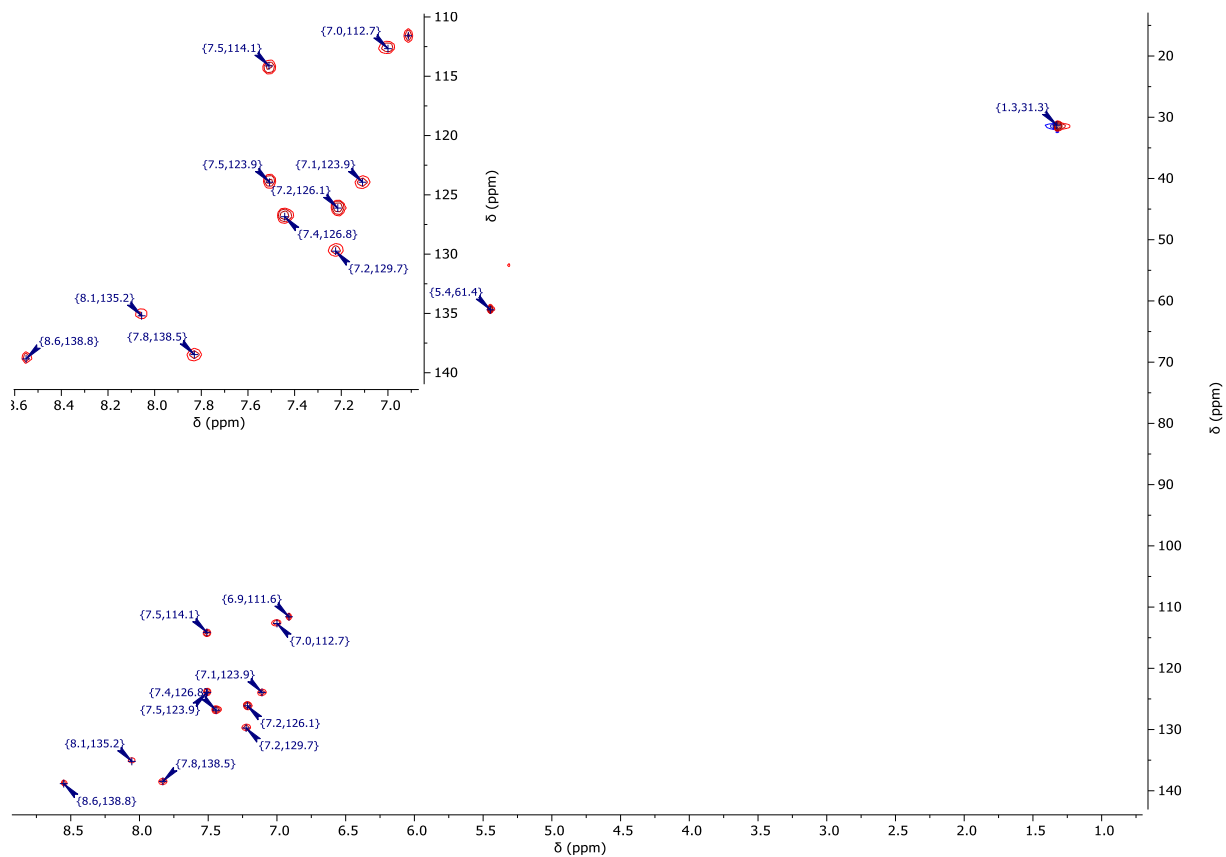


Figure S72: $^1\text{H}/^{13}\text{C}$ -gHSQC-NMR spectrum (400 MHz/101 MHz, DCM-d_2) of $[\text{PtCl}(\text{L}_3)]$.

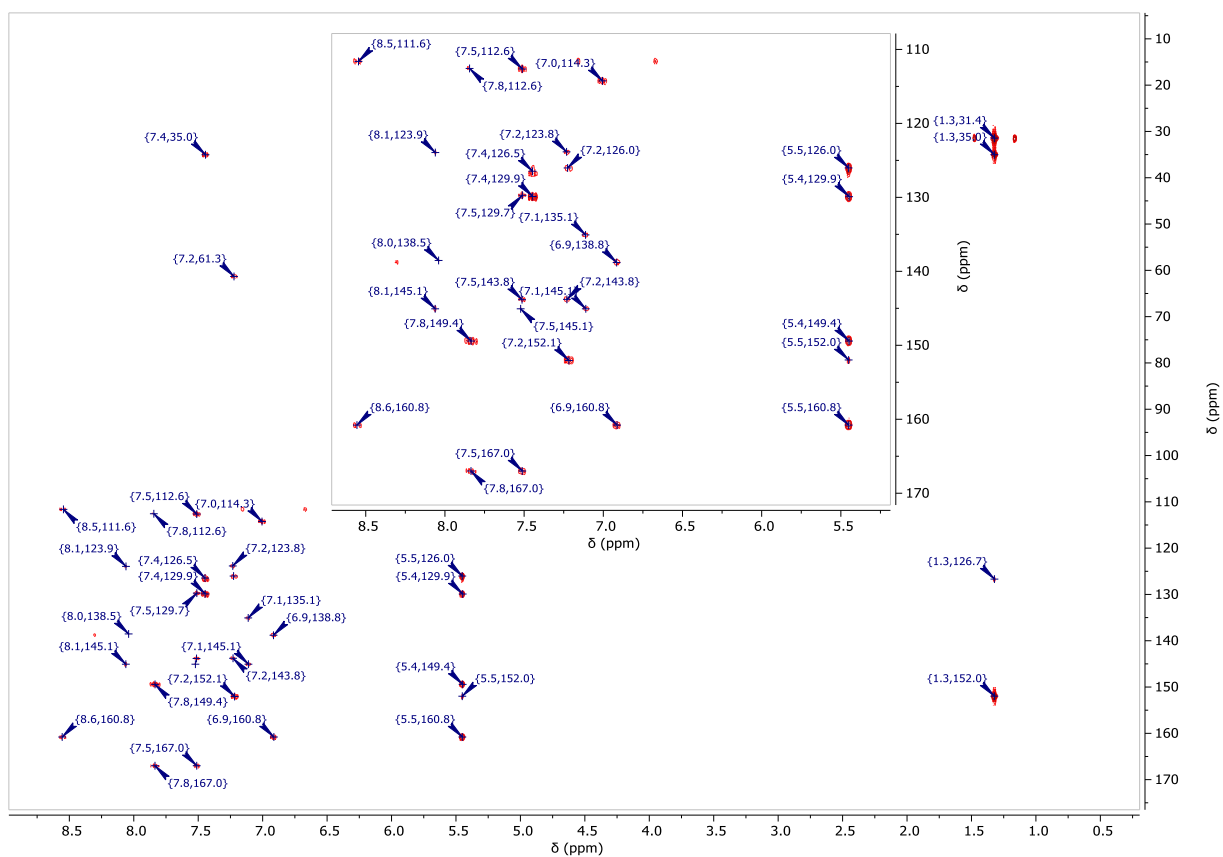


Figure S73: $^1\text{H}/^{13}\text{C}$ -gHMBC-NMR spectrum (400 MHz/ ^{13}C 101 MHz, $\text{DCM}-d_2$) of $[\text{PtCl}(\text{L}_3)]$.

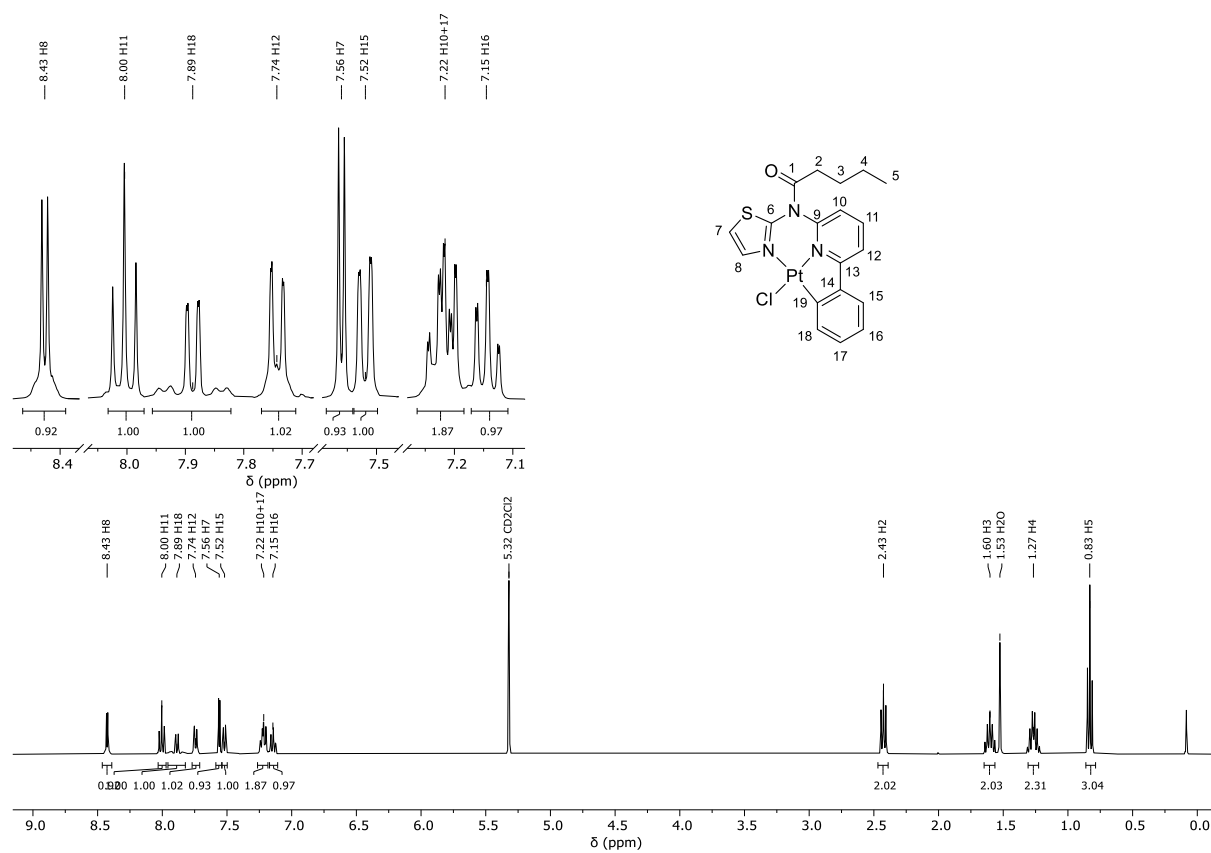


Figure S74: ^1H -NMR spectrum (400 MHz, $\text{DCM}-d_2$) of $[\text{PtCl}(\text{L}_4)]$.

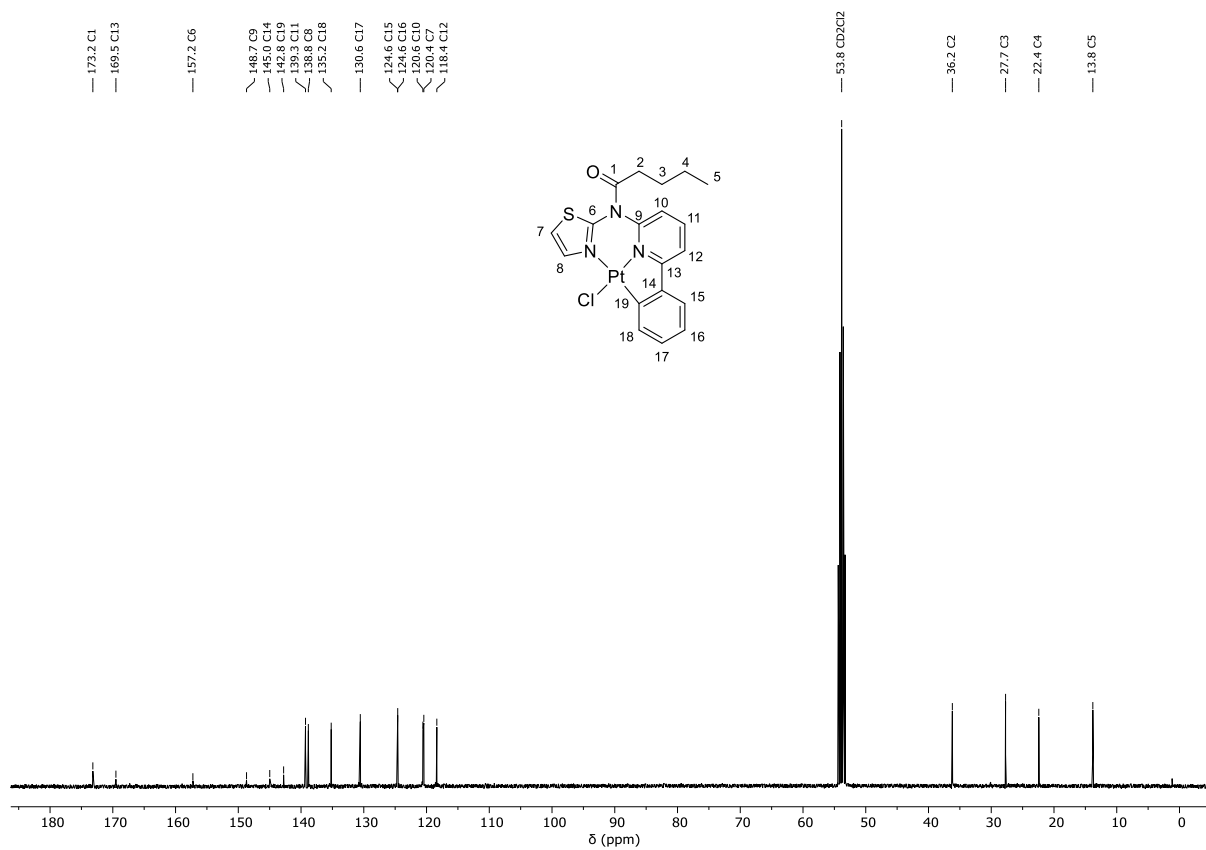


Figure S75: $^{13}\text{C}\{-^1\text{H}\}$ -NMR spectrum (101 MHz, $\text{DCM}-d_2$) of $[\text{PtCl}(\text{L}_4)]$.

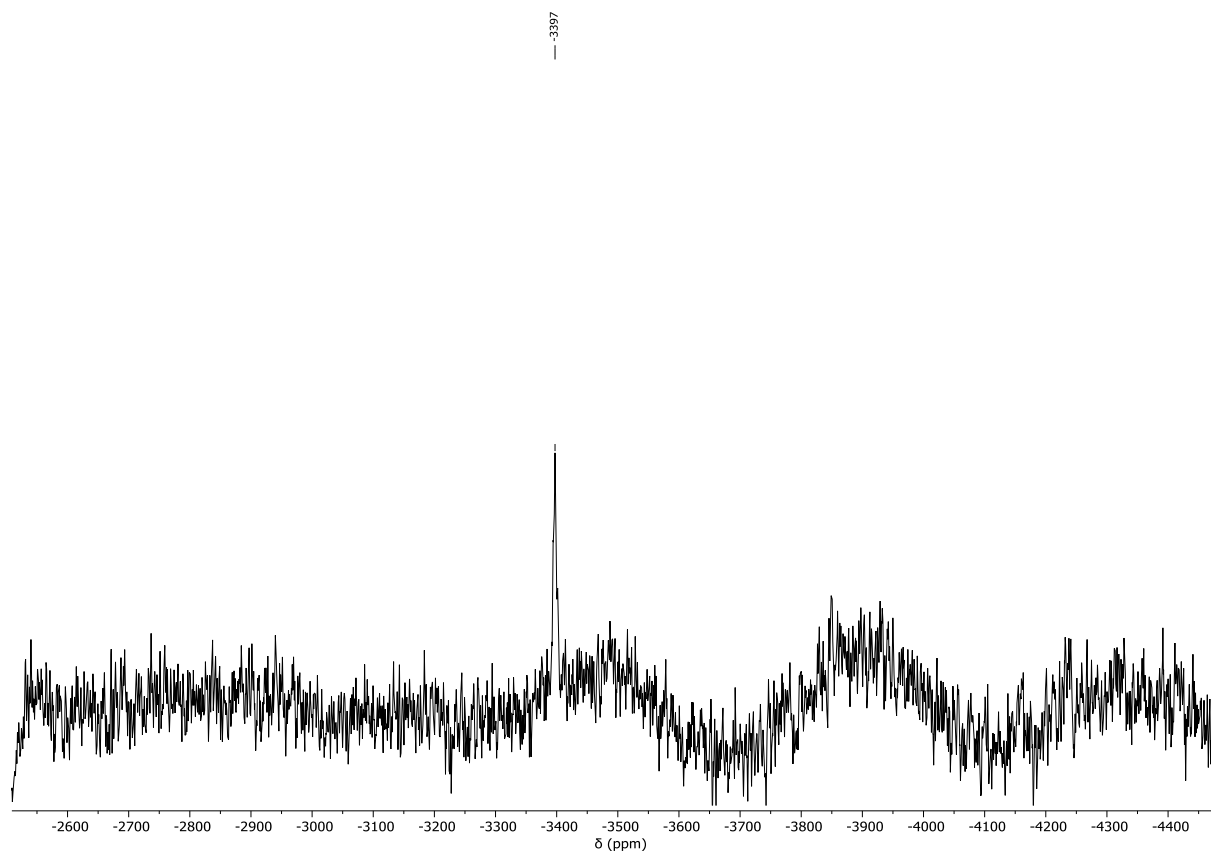


Figure S76: ^{195}Pt -NMR spectrum (86 MHz, $\text{DCM}-d_2$) of $[\text{PtCl}(\text{L}_4)]$.

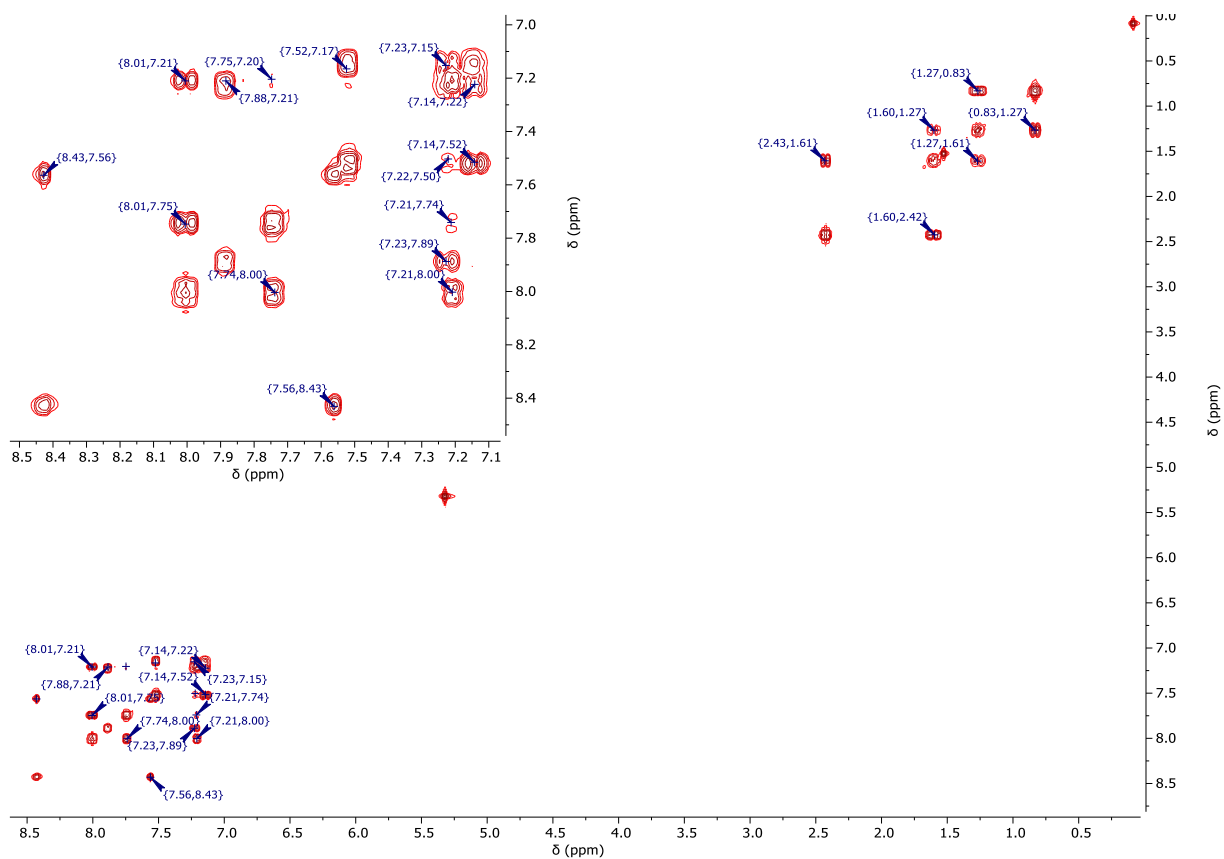


Figure S77: $^1\text{H}/^1\text{H}$ -COSY-NMR spectrum (400 MHz/400 MHz, $\text{DCM-}d_2$) of $[\text{PtCl}(\text{L}_4)]$.

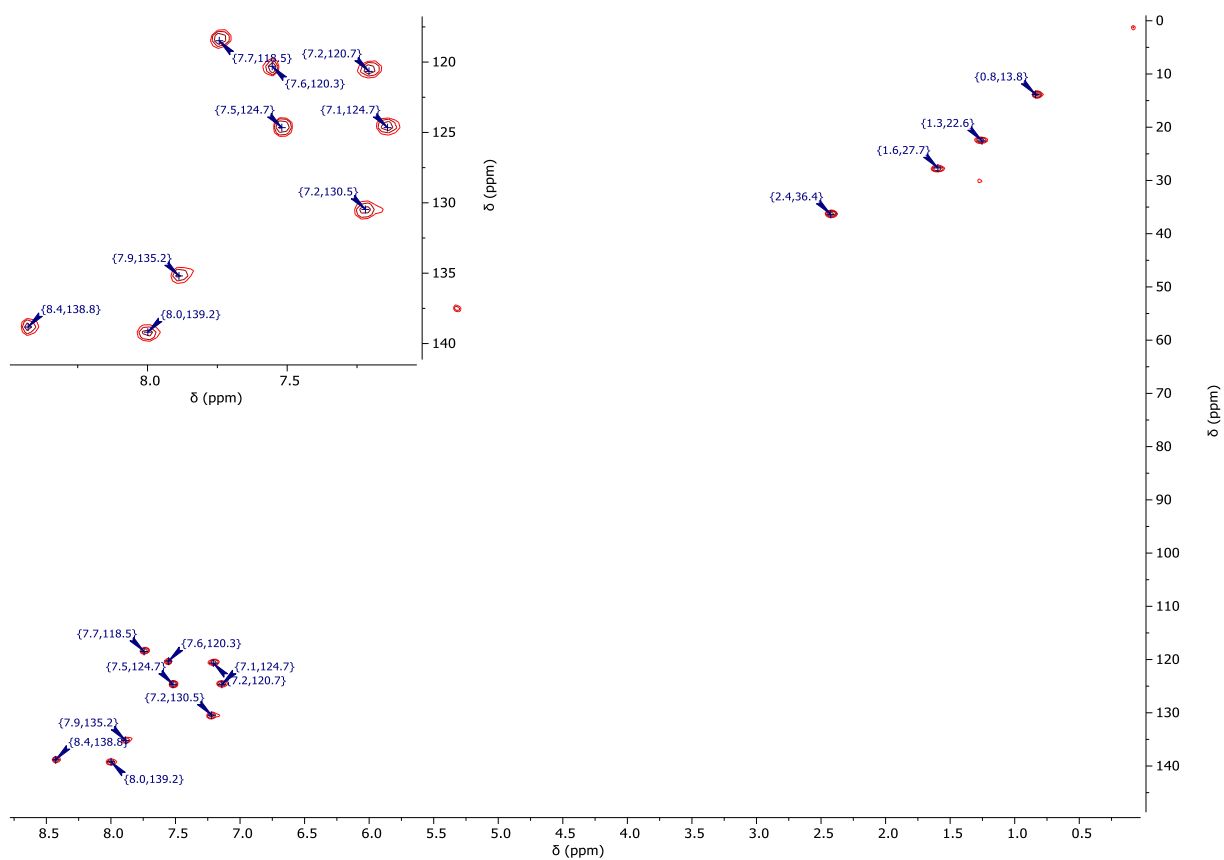


Figure S78: $^1\text{H}/^{13}\text{C}$ -gHSQC-NMR spectrum (400 MHz/101 MHz, $\text{DCM-}d_2$) of $[\text{PtCl}(\text{L}_4)]$.

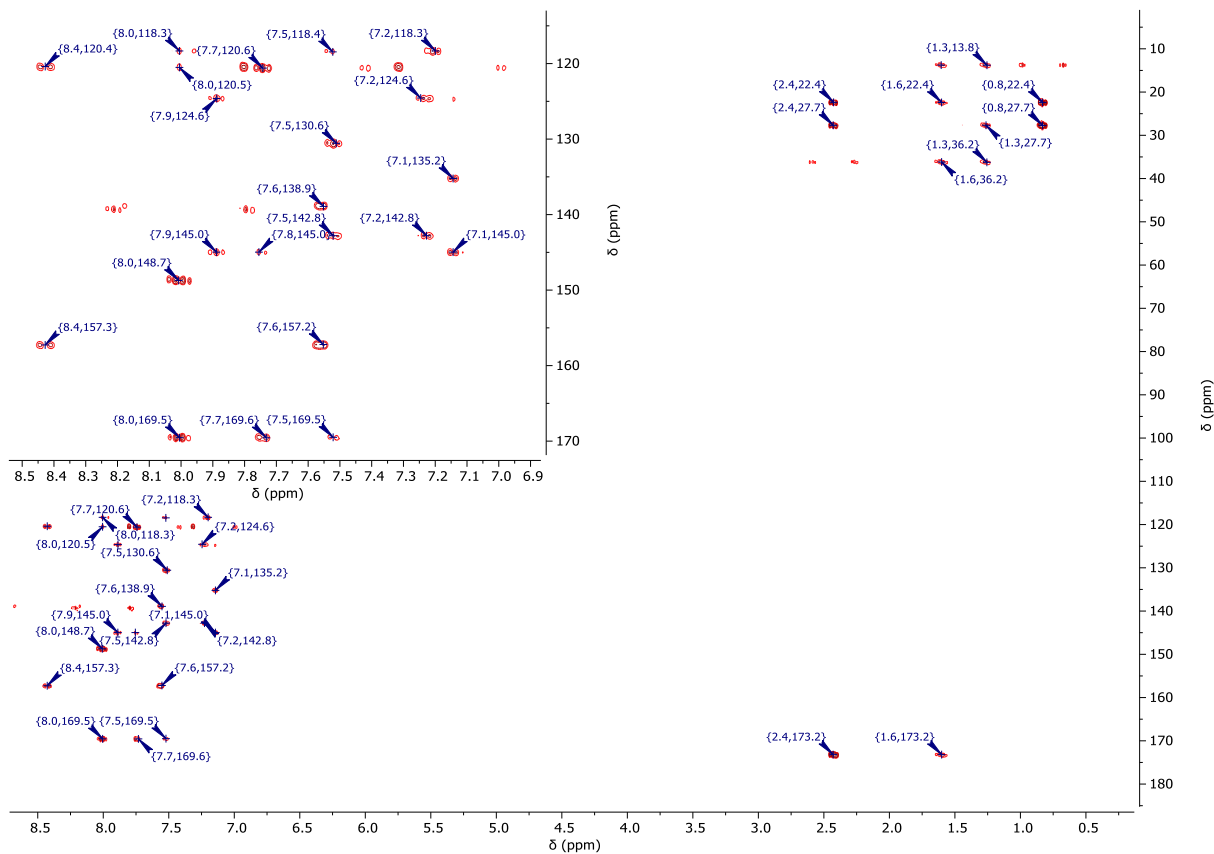


Figure S79: $^1\text{H}/^{13}\text{C}$ -gHMBC-NMR spectrum (400 MHz/101 MHz, $\text{DCM}-d_2$) of $[\text{PtCl}(\text{L}_4)]$.

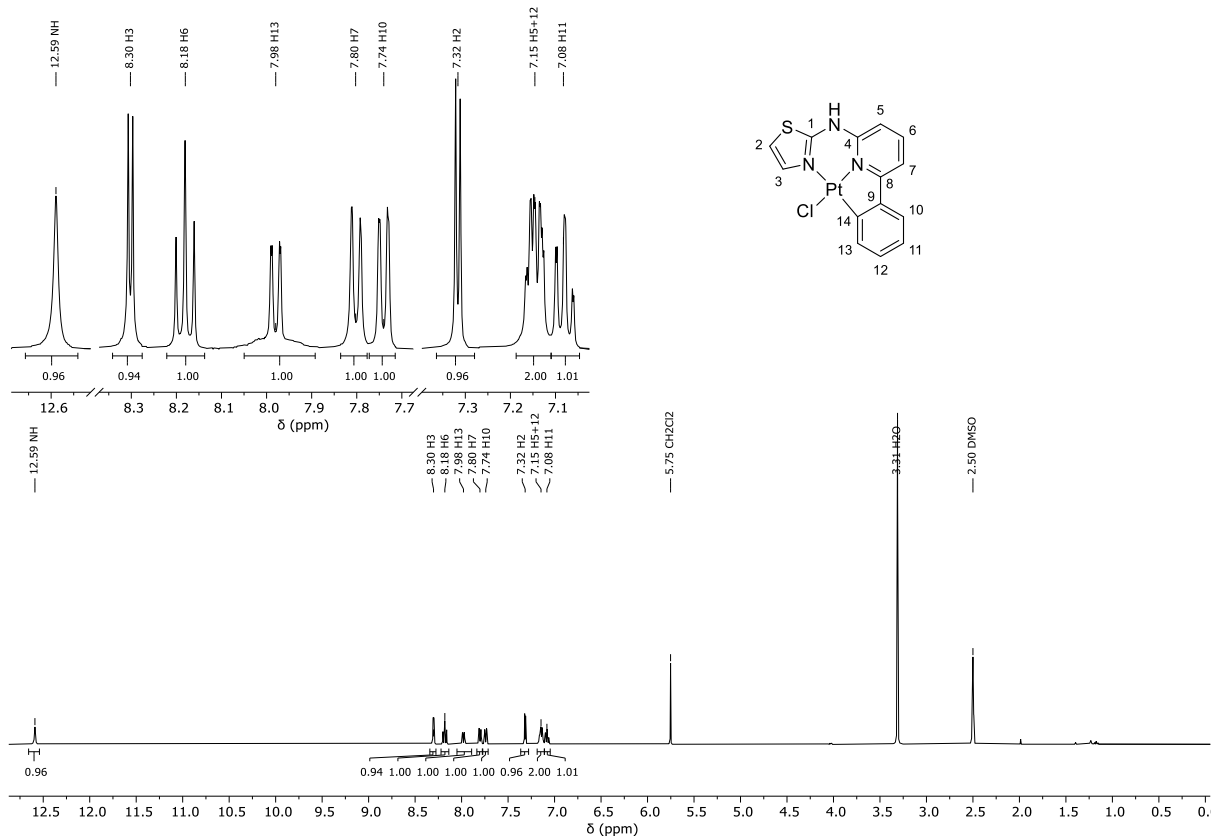


Figure S80: ^1H -NMR spectrum (400 MHz, $\text{DMSO}-d_6$) of $[\text{PtCl}(\text{L}_5)]$.

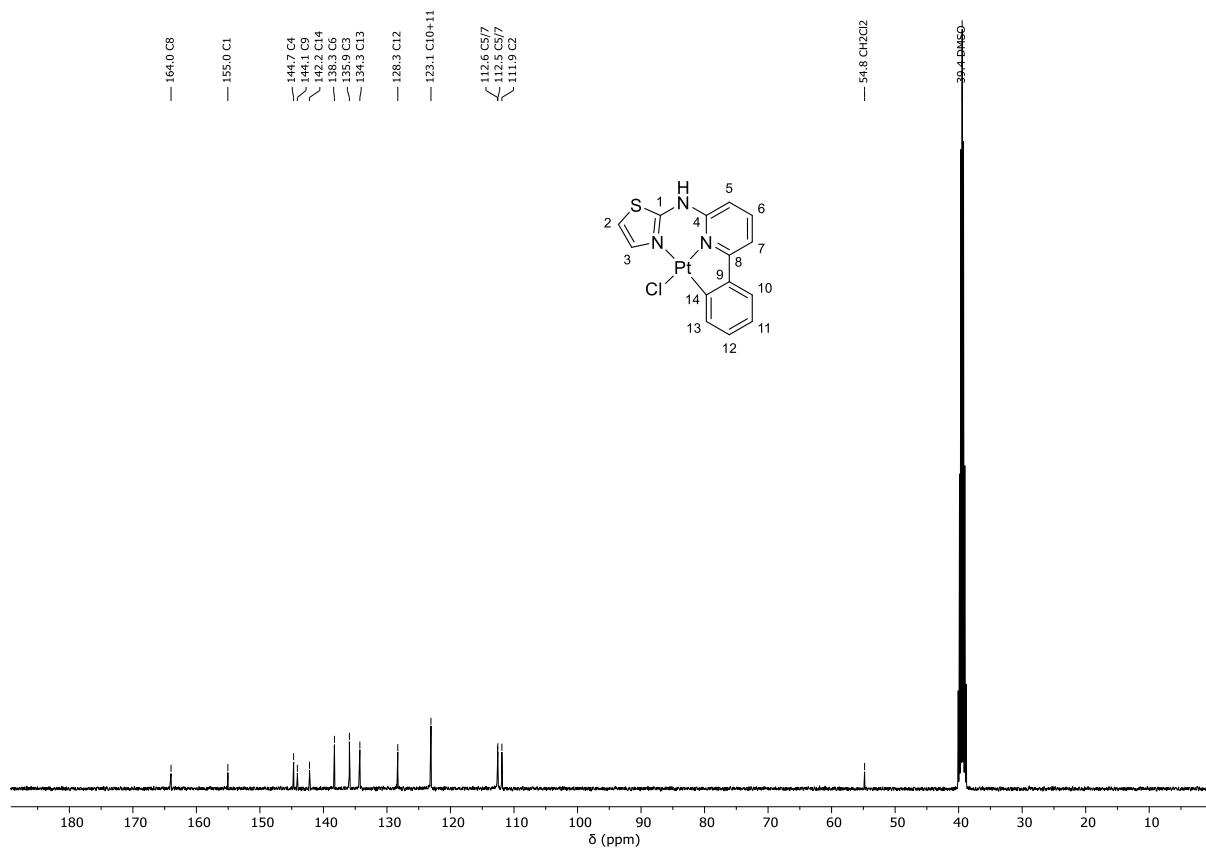


Figure S81: ^{13}C - $\{^1\text{H}\}$ -NMR spectrum (101 MHz, $\text{DMSO-}d_6$) of $[\text{PtCl}(\text{L}_5)]$.

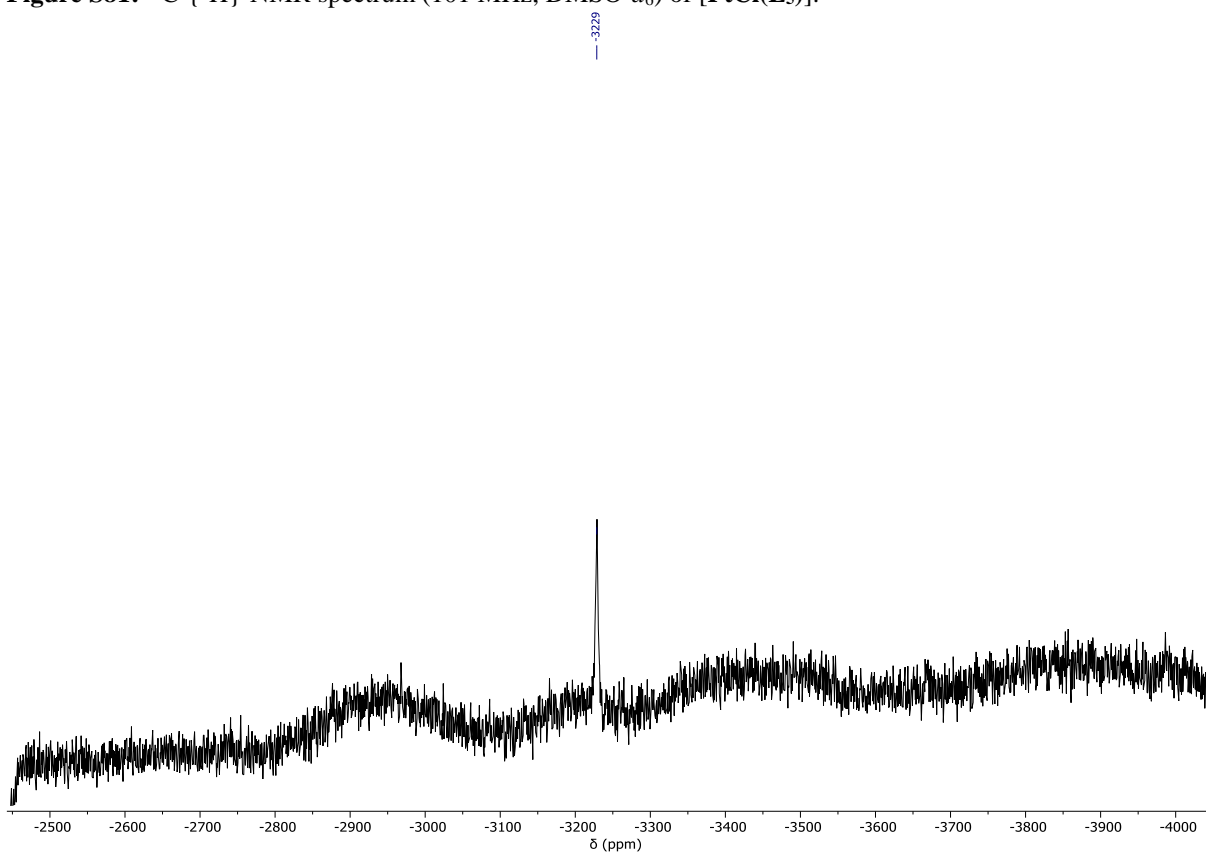


Figure S82: ^{195}Pt -NMR spectrum (86 MHz, $\text{DMSO-}d_6$) of $[\text{PtCl}(\text{L}_5)]$.

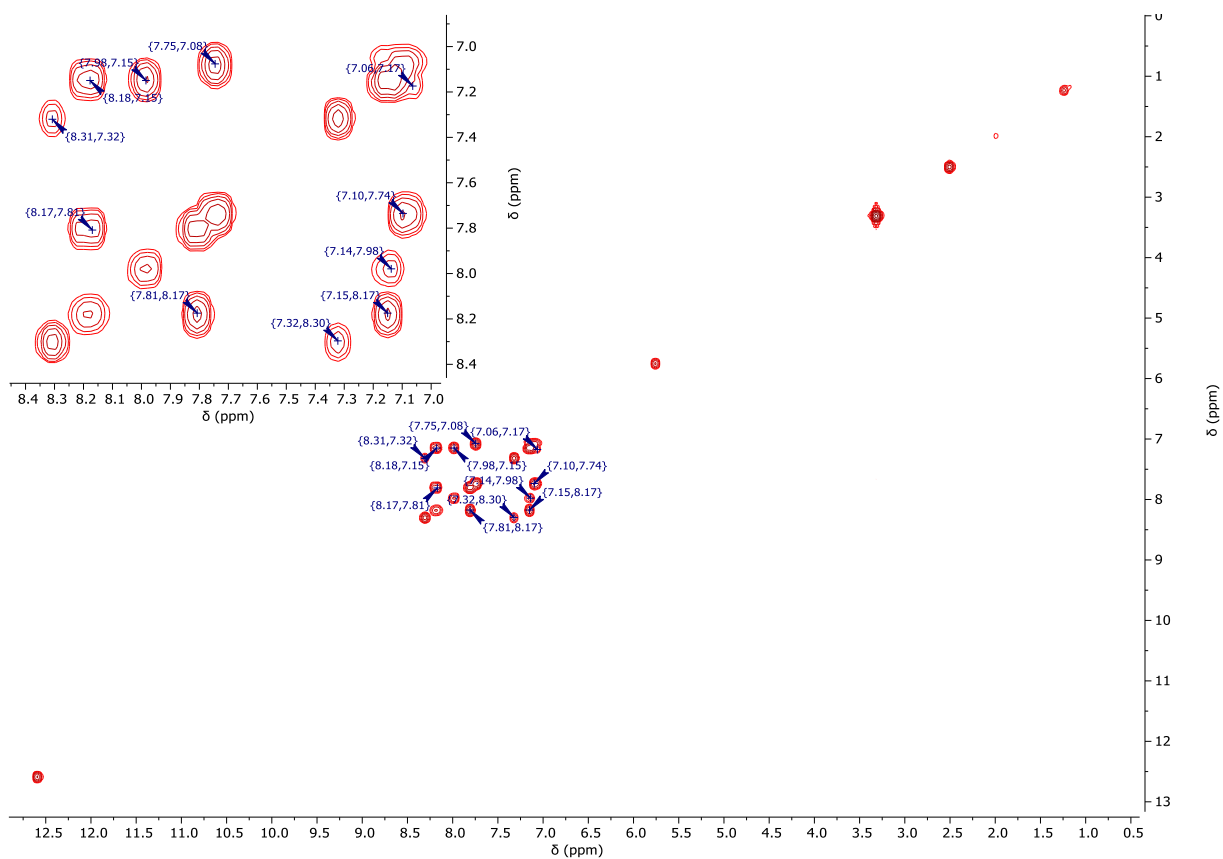


Figure S83: $^1\text{H}/^1\text{H}$ -COSY-NMR spectrum (400 MHz/400 MHz, $\text{DMSO-}d_6$) of $[\text{PtCl}(\text{L}_5)]$.

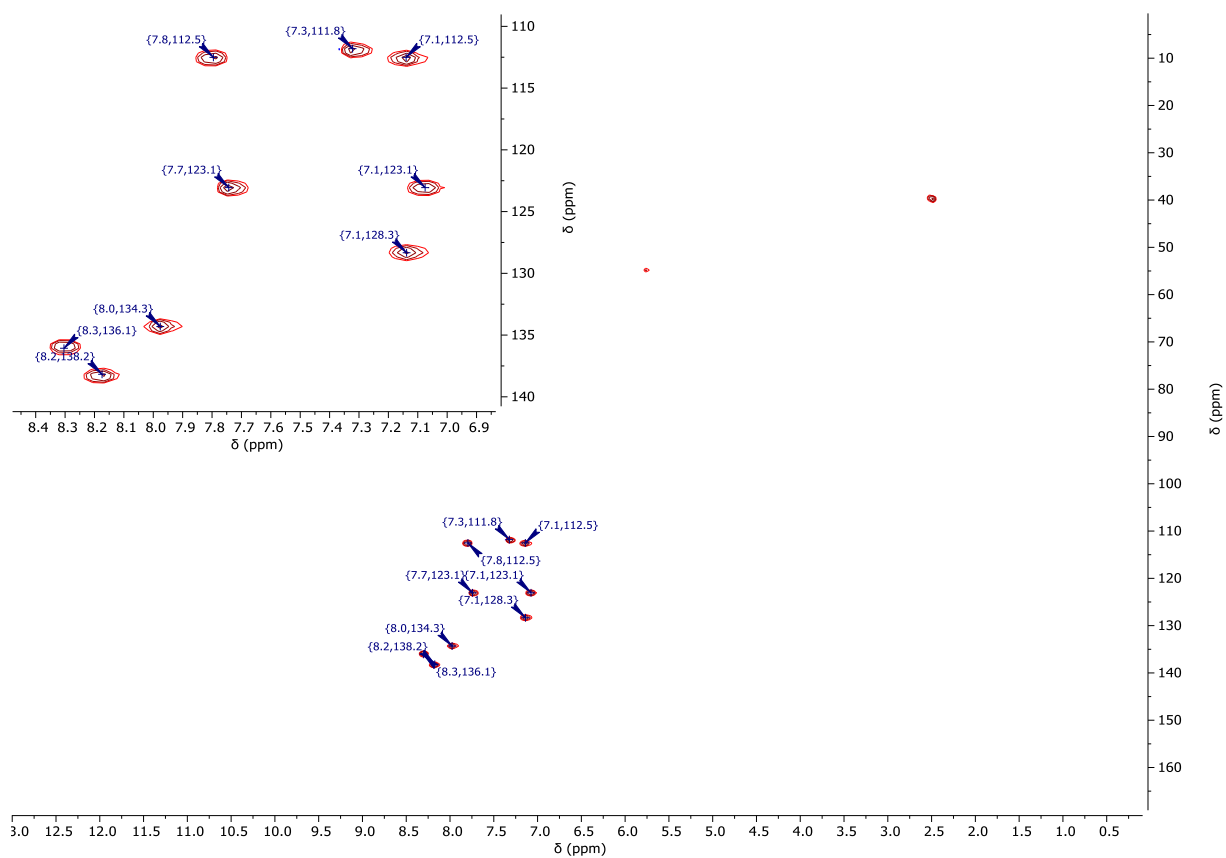


Figure S84: $^1\text{H}/^{13}\text{C}$ -gHSQC-NMR spectrum (400 MHz/101 MHz, $\text{DMSO-}d_6$) of $[\text{PtCl}(\text{L}_5)]$.

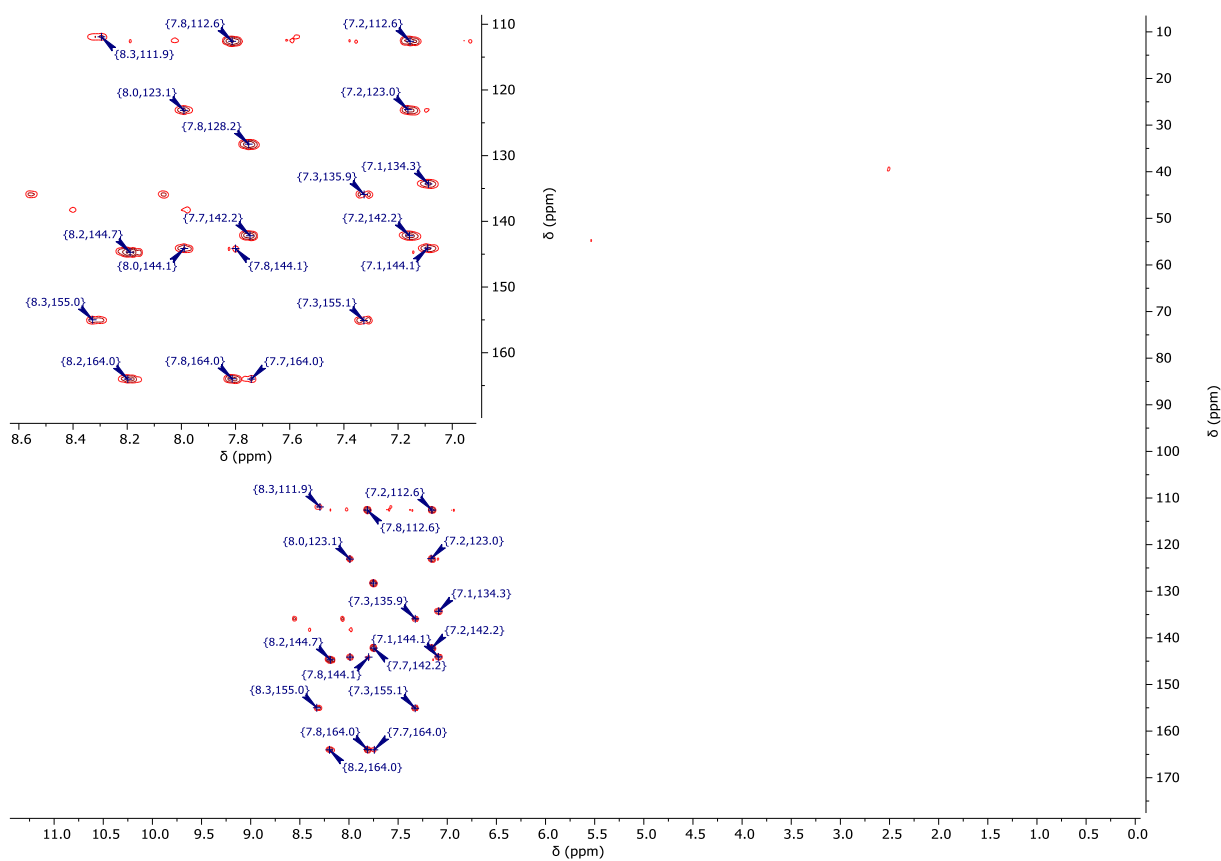


Figure S85: $^1\text{H}/^{13}\text{C}$ -gHMBC-NMR spectrum (400 MHz/101 MHz, $\text{DMSO}-d_6$) of $[\text{PtCl}(\text{L}_5)]$.

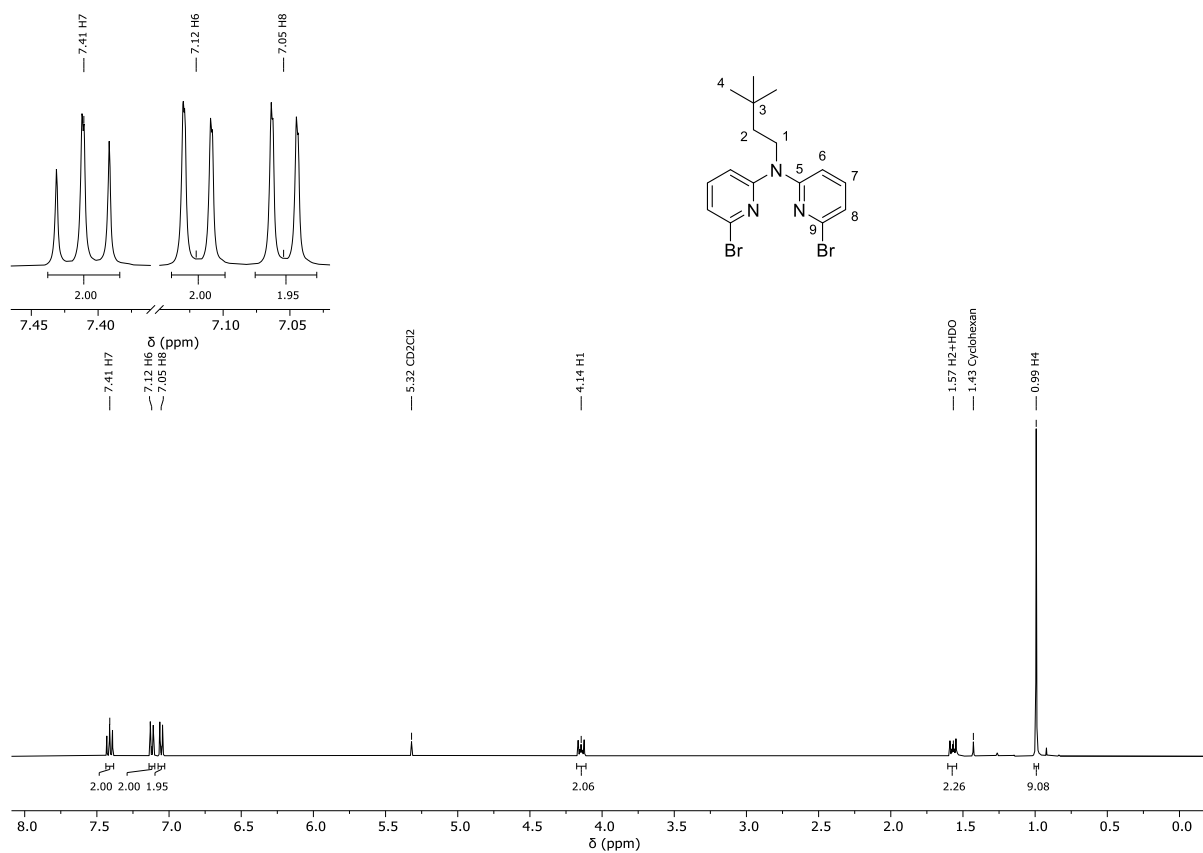


Figure S86: ^1H -NMR spectrum (400 MHz, $\text{DCM}-d_2$) of A_6 .

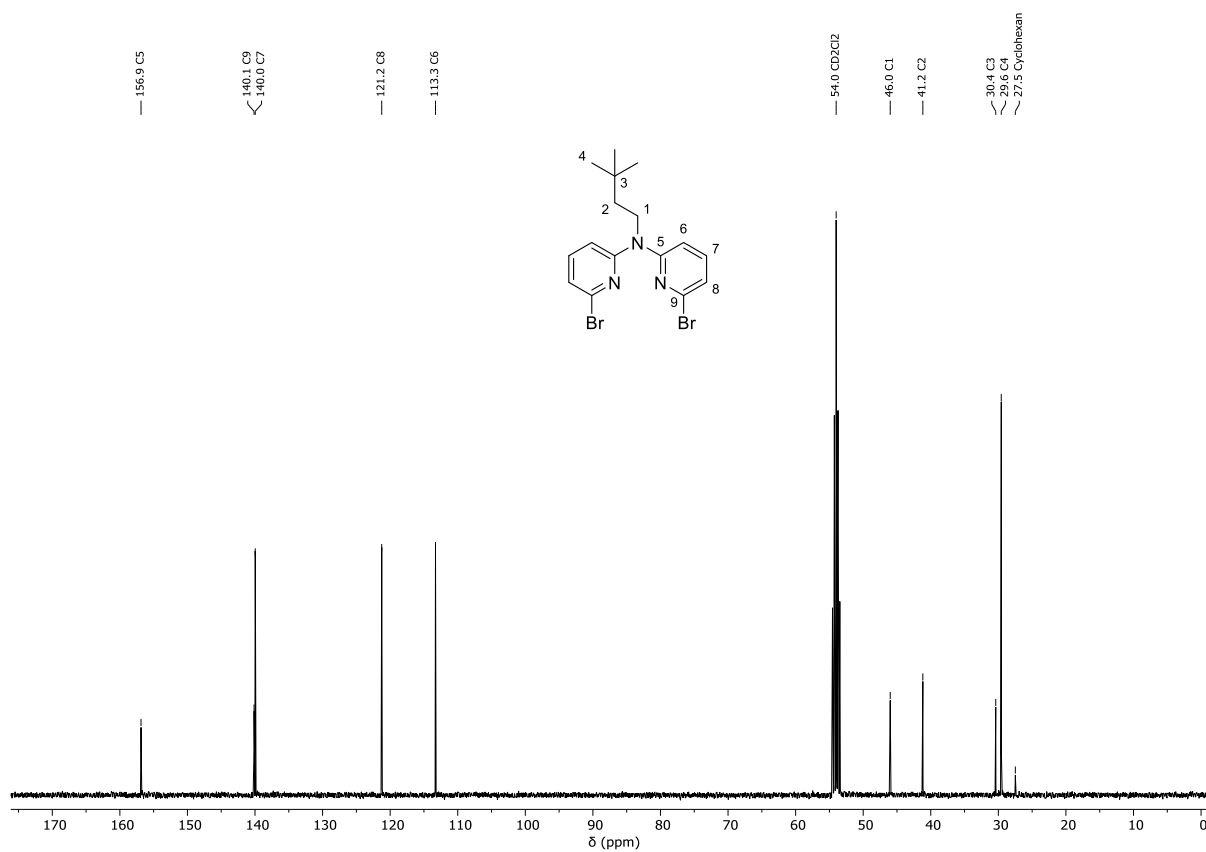


Figure S87: ¹³C-¹H-NMR spectrum (101 MHz, DCM-d₂) of **A6**.

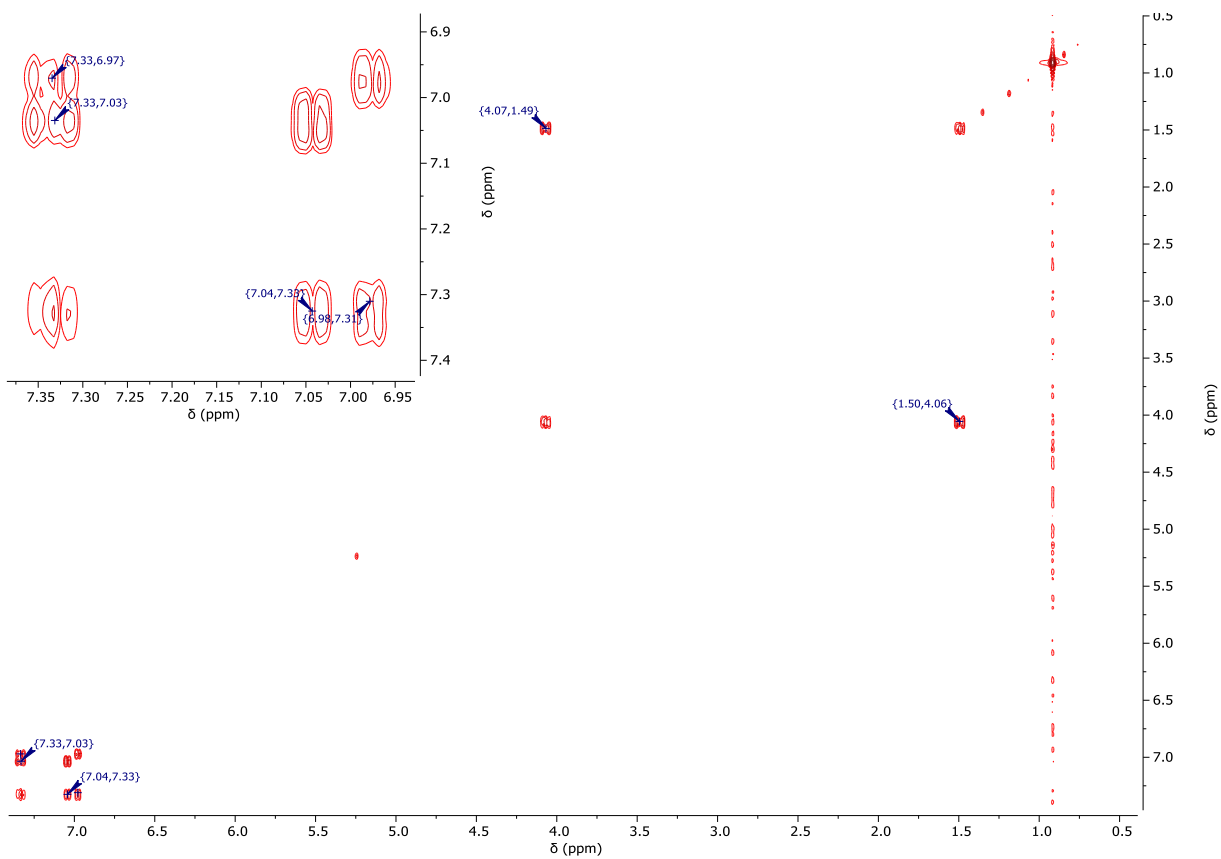


Figure S88: ¹H/¹H-COSY-NMR spectrum (400 MHz/400 MHz, DCM-d₂) of **A6**.

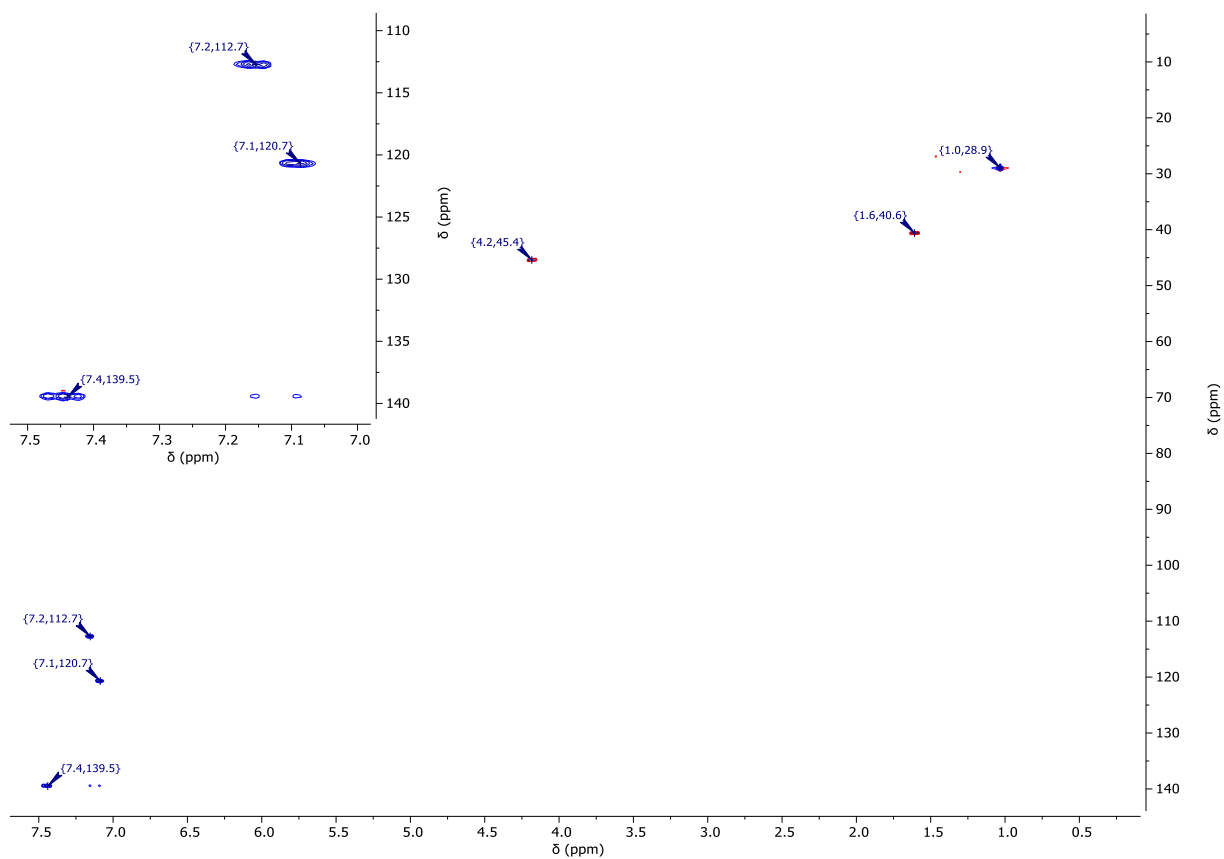


Figure S89: $^1\text{H}/^{13}\text{C}$ -gHSQC-NMR spectrum (400 MHz/101 MHz, DCM-d_2) of **A6**.

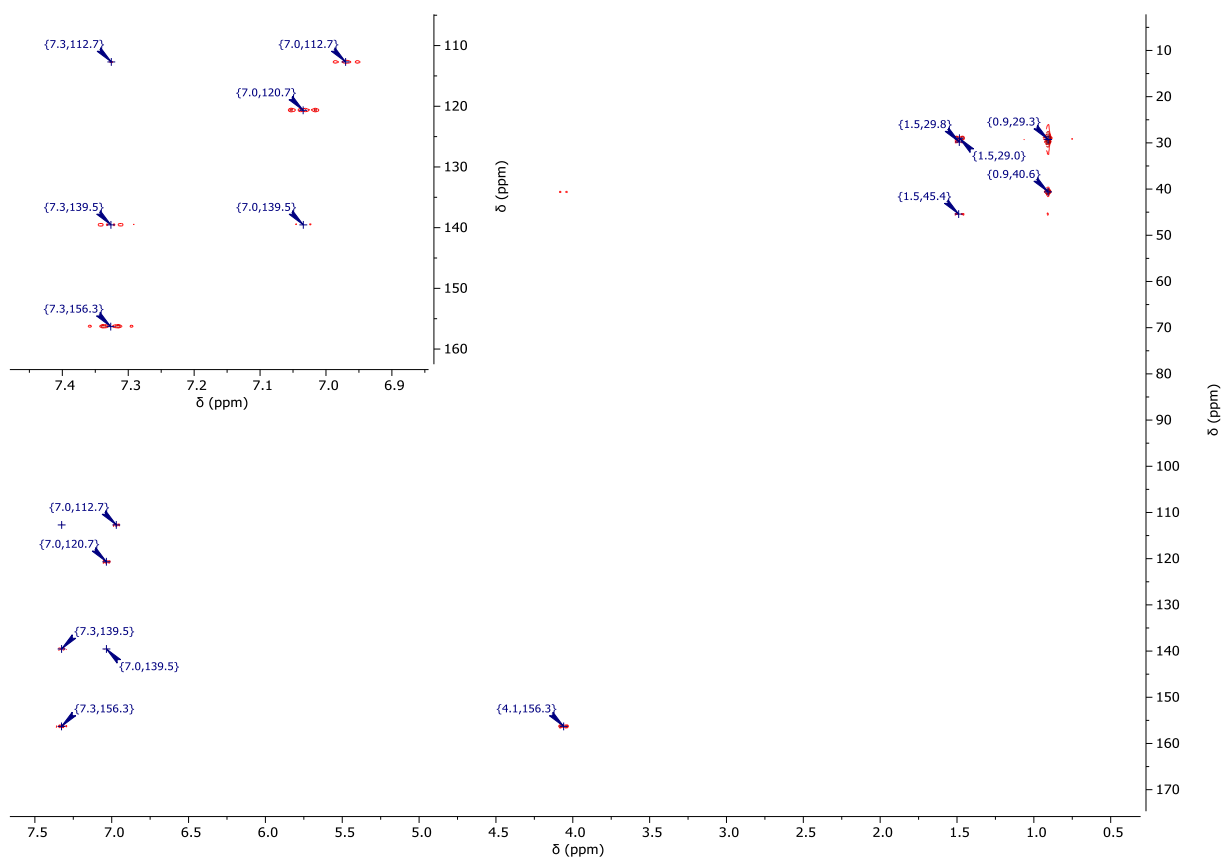


Figure S90: $^1\text{H}/^{13}\text{C}$ -gHMBC-NMR spectrum (400 MHz/101 MHz, DCM-d_2) of **A6**.

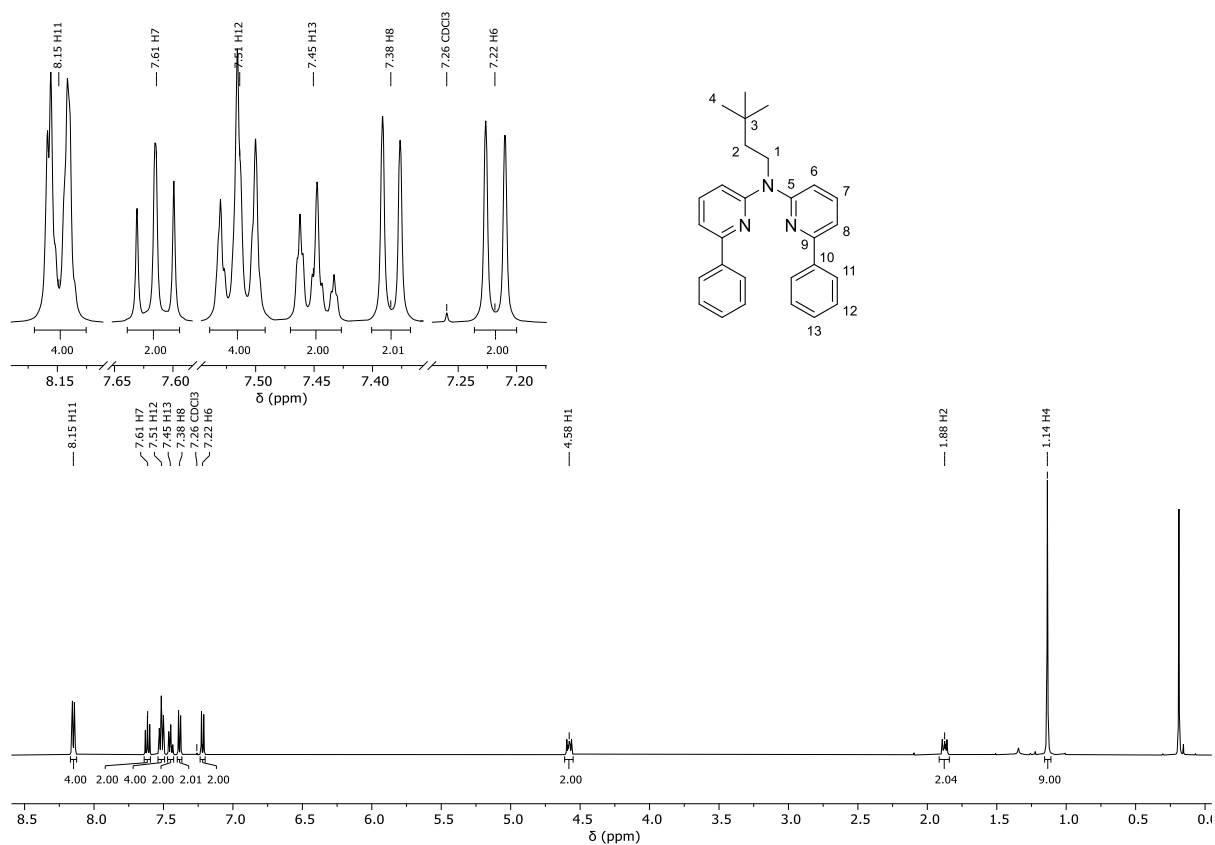


Figure S91: ^1H -NMR spectrum (500 MHz, CDCl_3) of L_6H_2 .

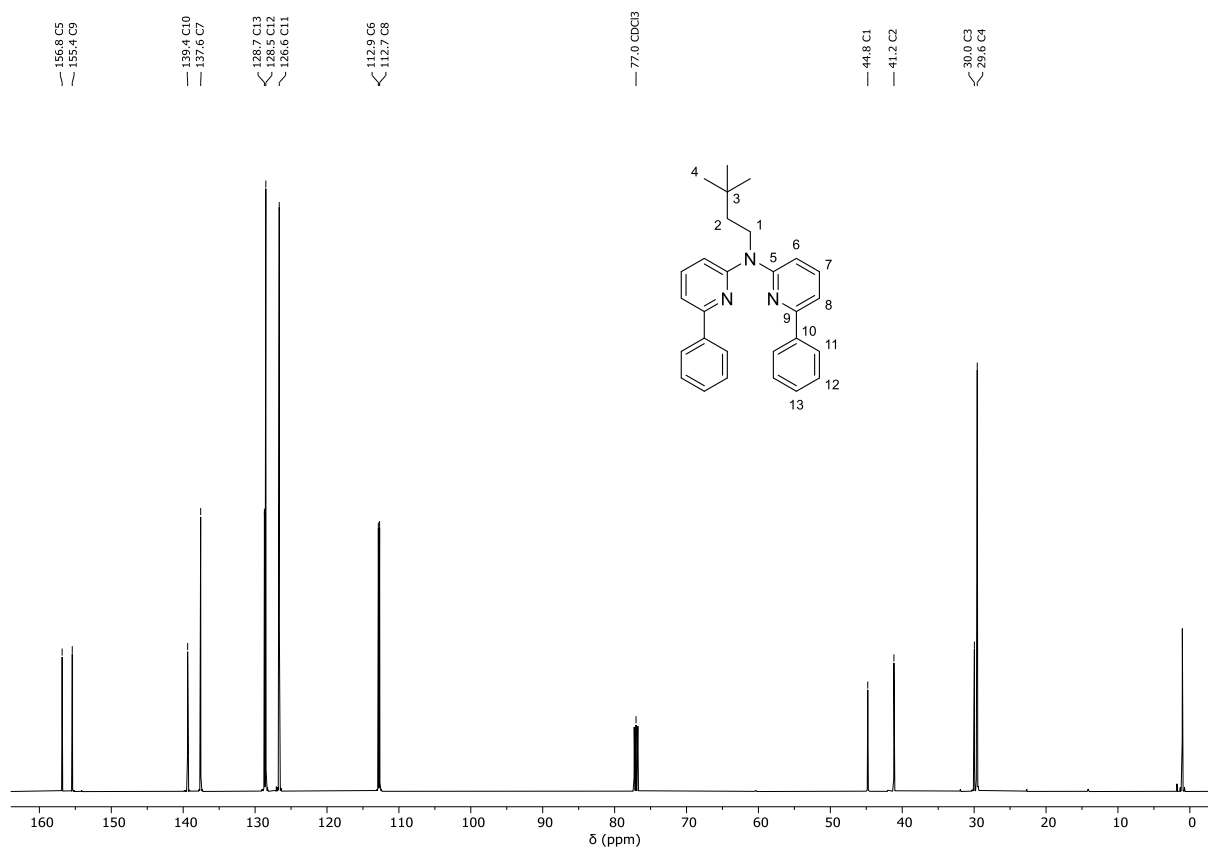


Figure S92: ^{13}C - $\{^1\text{H}\}$ -NMR spectrum (126 MHz, CDCl_3) of L_6H_2 .

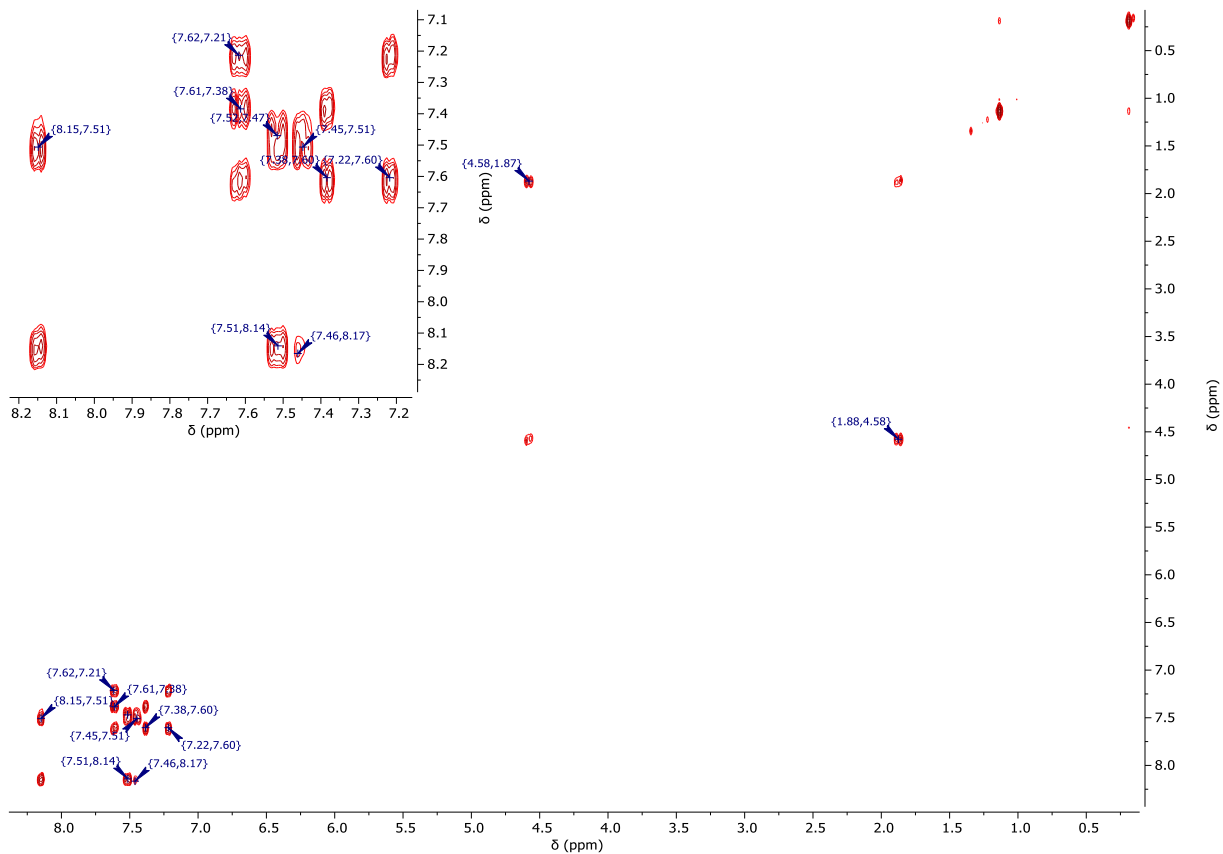


Figure S93: $^1\text{H}/^1\text{H}$ -COSY-NMR spectrum (500 MHz/500 MHz, CDCl_3) of L_6H_2 .

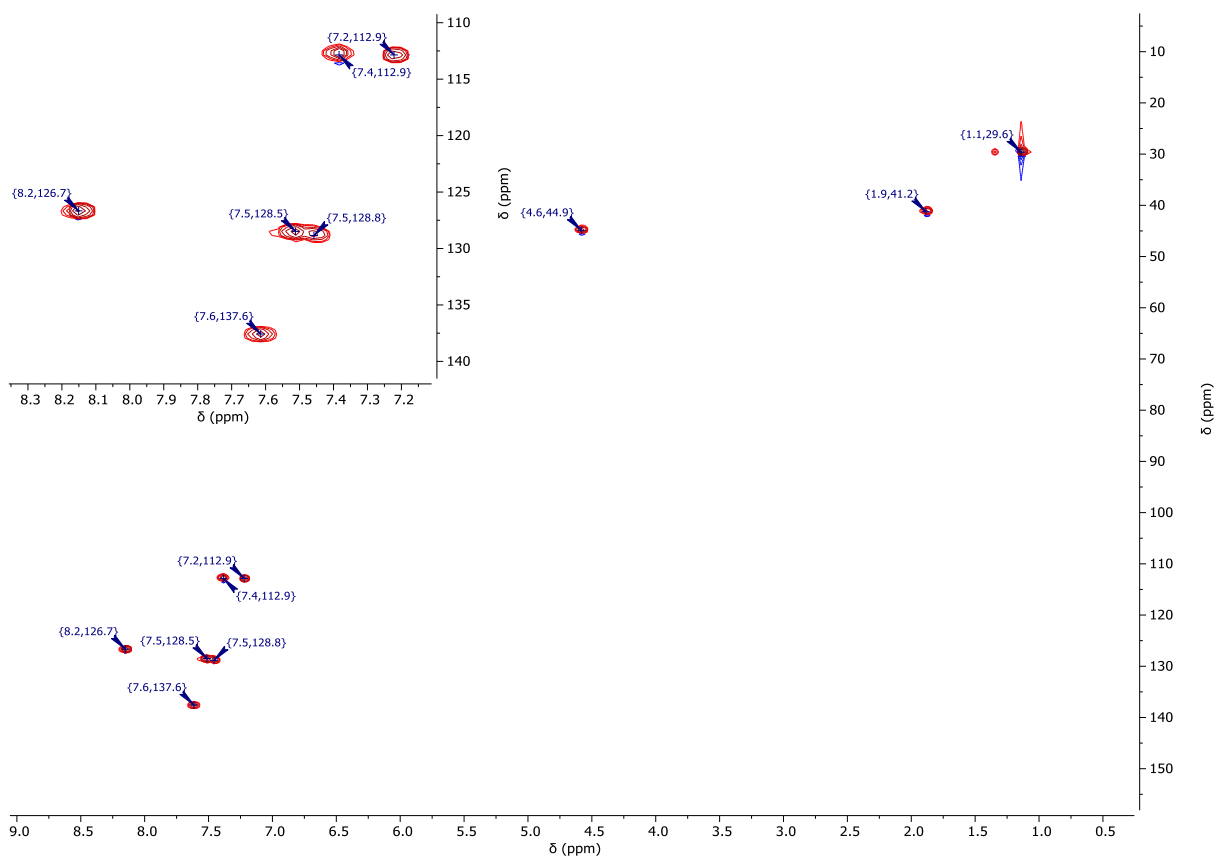


Figure S94: $^1\text{H}/^{13}\text{C}$ -gHSQC-NMR spectrum (500 MHz/126 MHz, CDCl_3) of L_6H_2 .

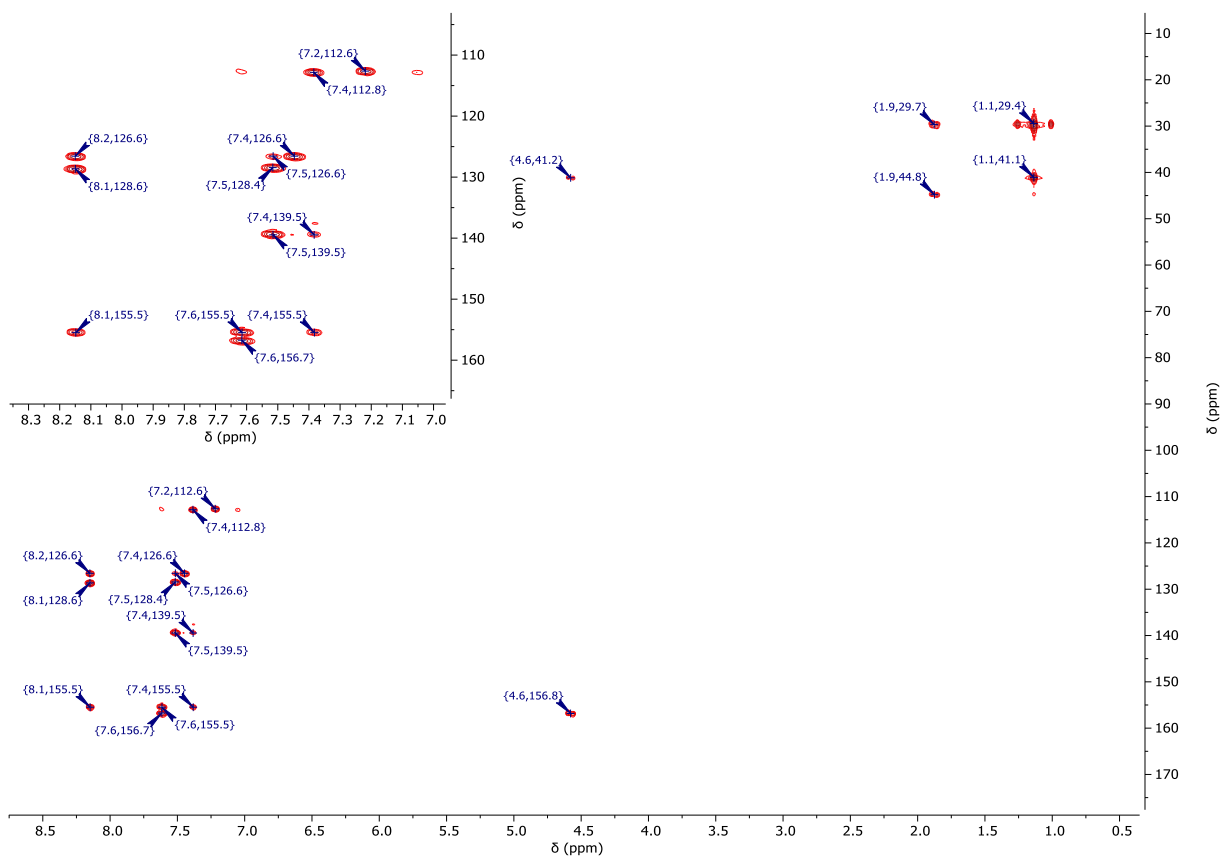


Figure S95: $^1\text{H}/^{13}\text{C}$ -gHMBC-NMR spectrum (500 MHz/126 MHz, CDCl_3) of L_6H_2 .

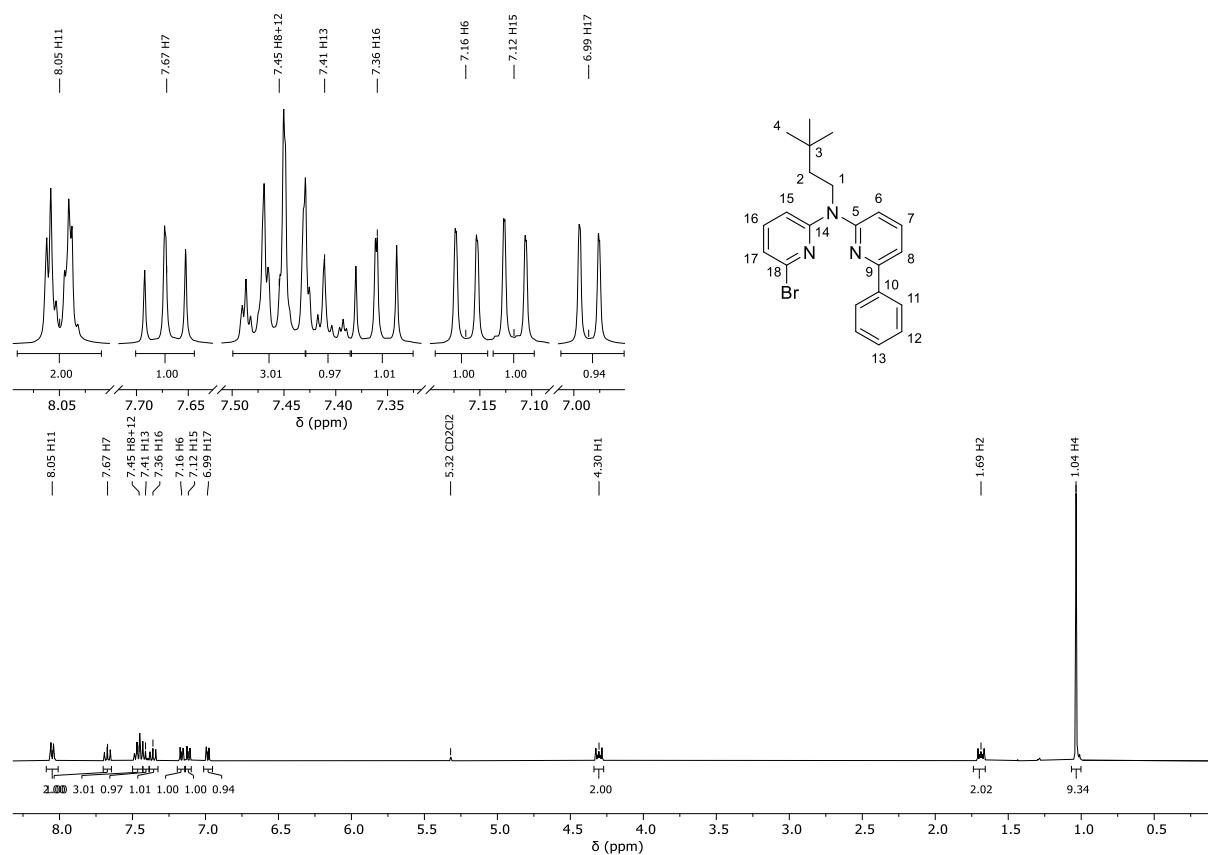


Figure S96: ^1H -NMR spectrum (400 MHz, $\text{DCM}-d_2$) of L_6BrH .

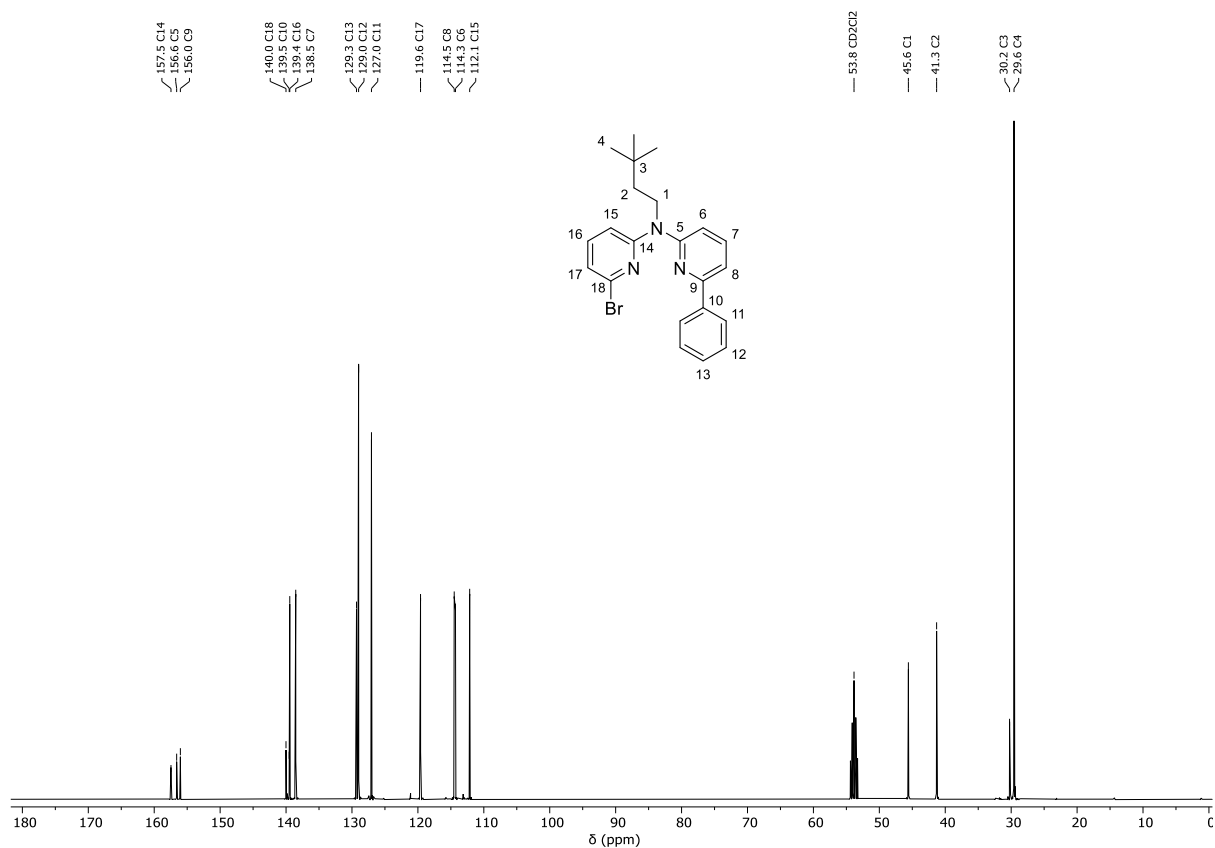


Figure S97: ¹³C-¹H-NMR spectrum (101 MHz, DCM-d₂) of **L₆BrH**.

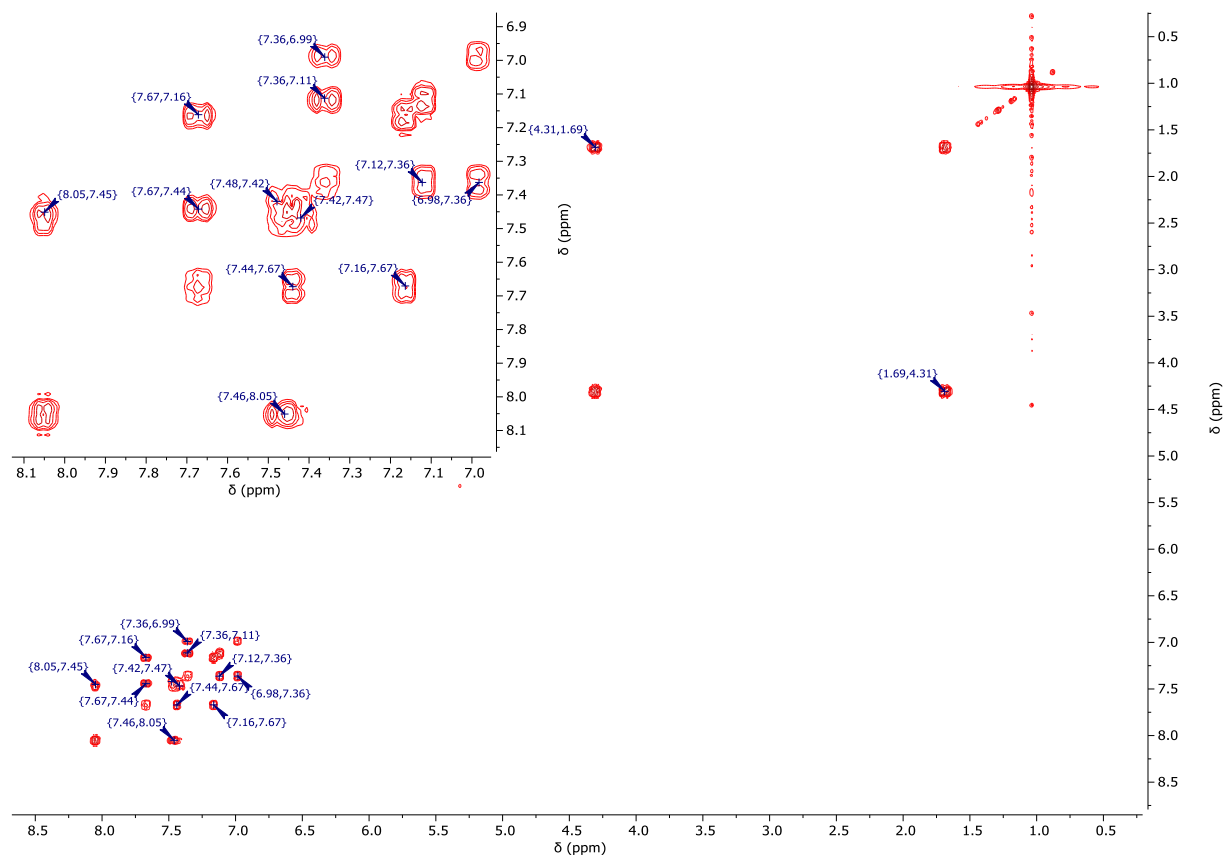


Figure S98: ¹H/¹H-COSY-NMR spectrum (400 MHz/400 MHz, DCM-d₂) of **L₆BrH**.

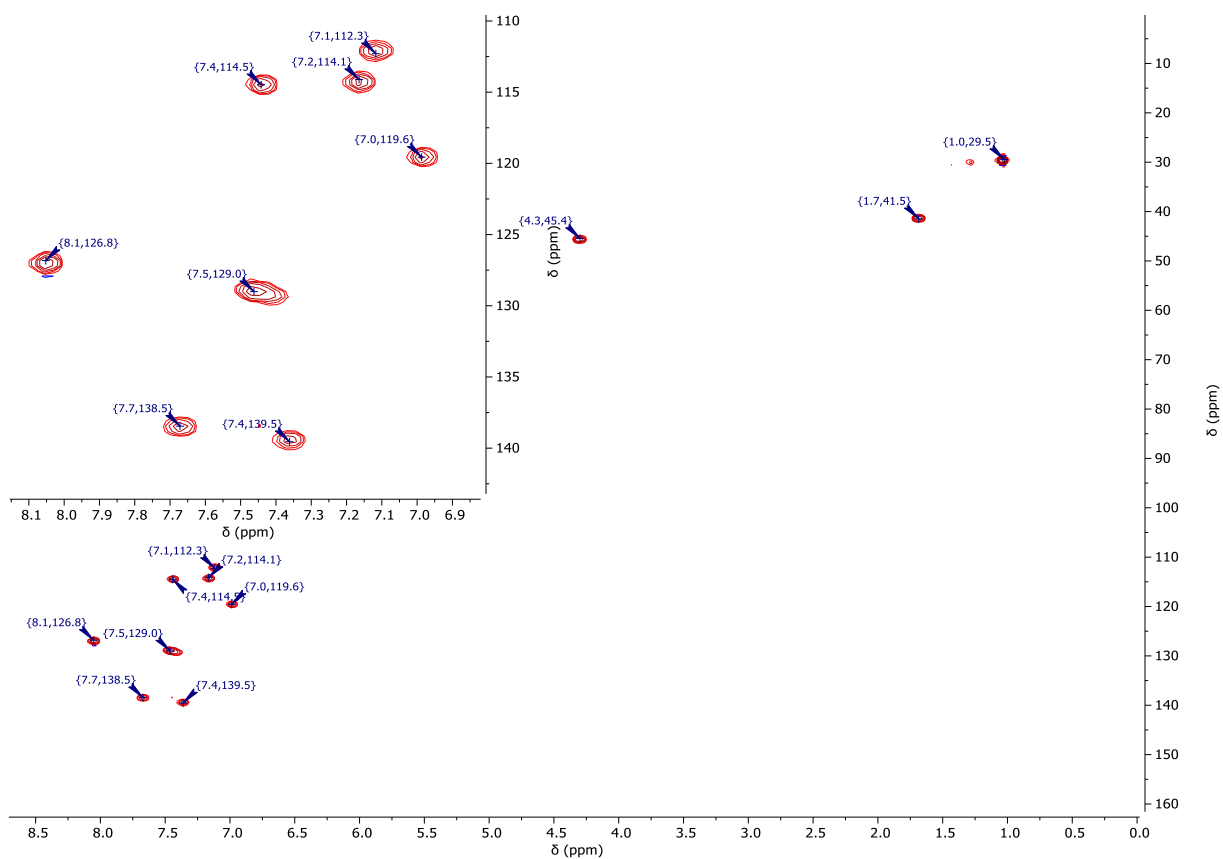


Figure S99: $^1\text{H}/^{13}\text{C}$ -gHSQC-NMR spectrum (400 MHz/101 MHz, DCM-d_2) of L_6BrH .

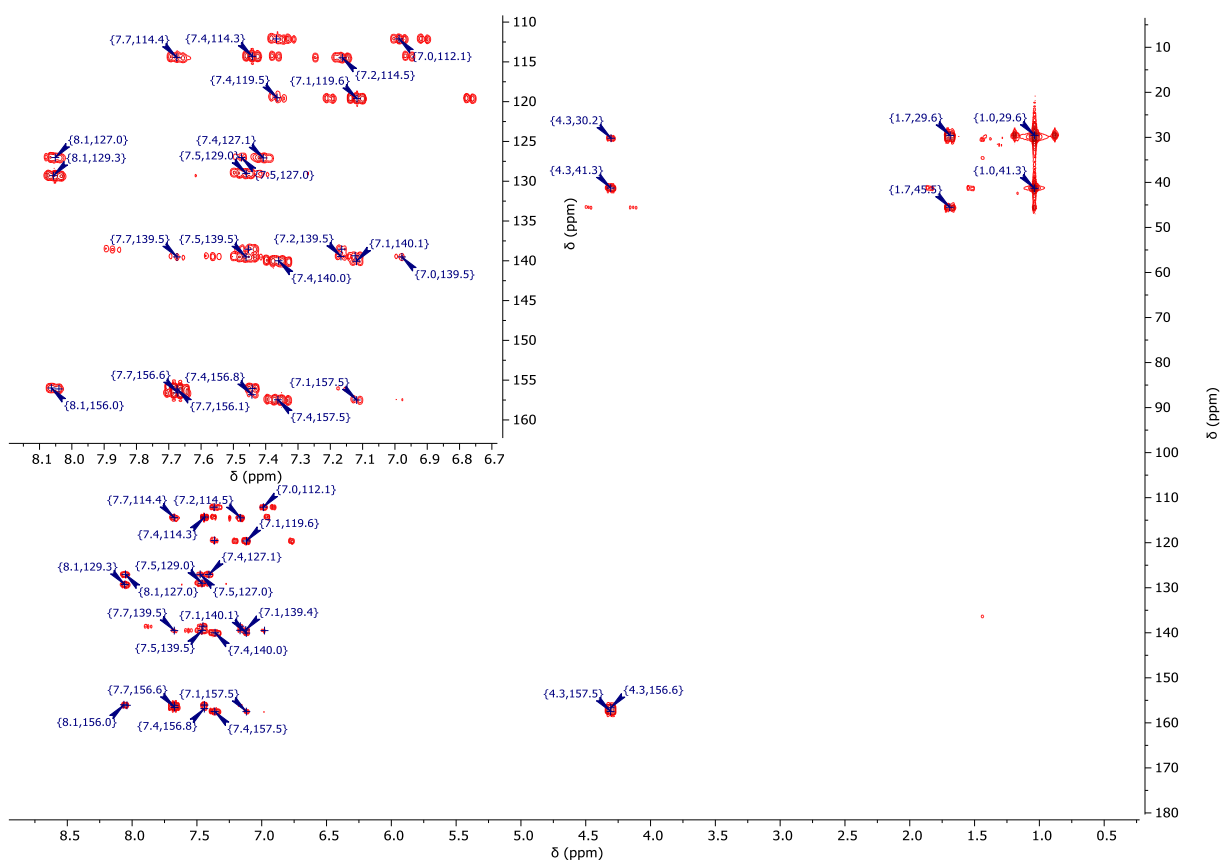


Figure S100: $^1\text{H}/^{13}\text{C}$ -gHMBC-NMR spectrum (400 MHz/101 MHz, DCM-d_2) of L_6BrH .

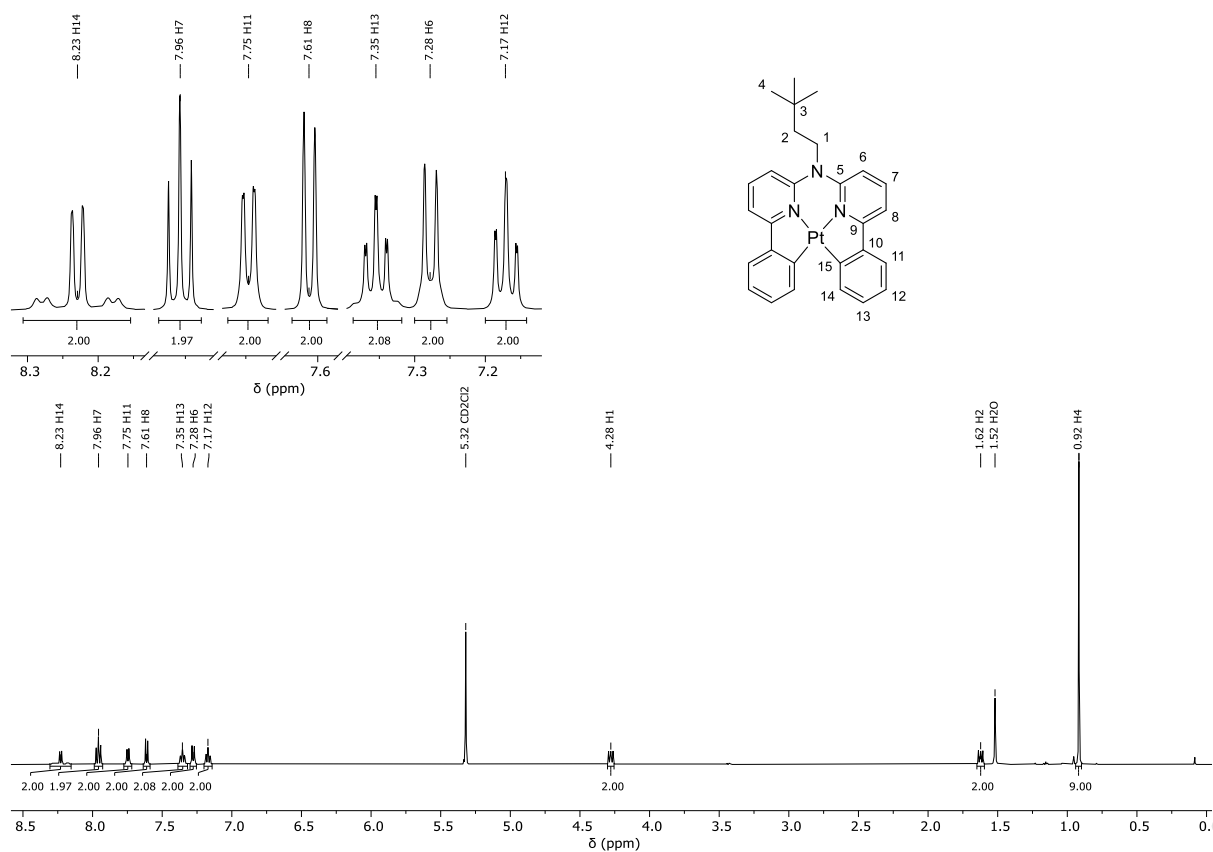


Figure S101: $^1\text{H-NMR}$ spectrum (500 MHz, DCM-d_2) of $[\text{PtL}_6]$.

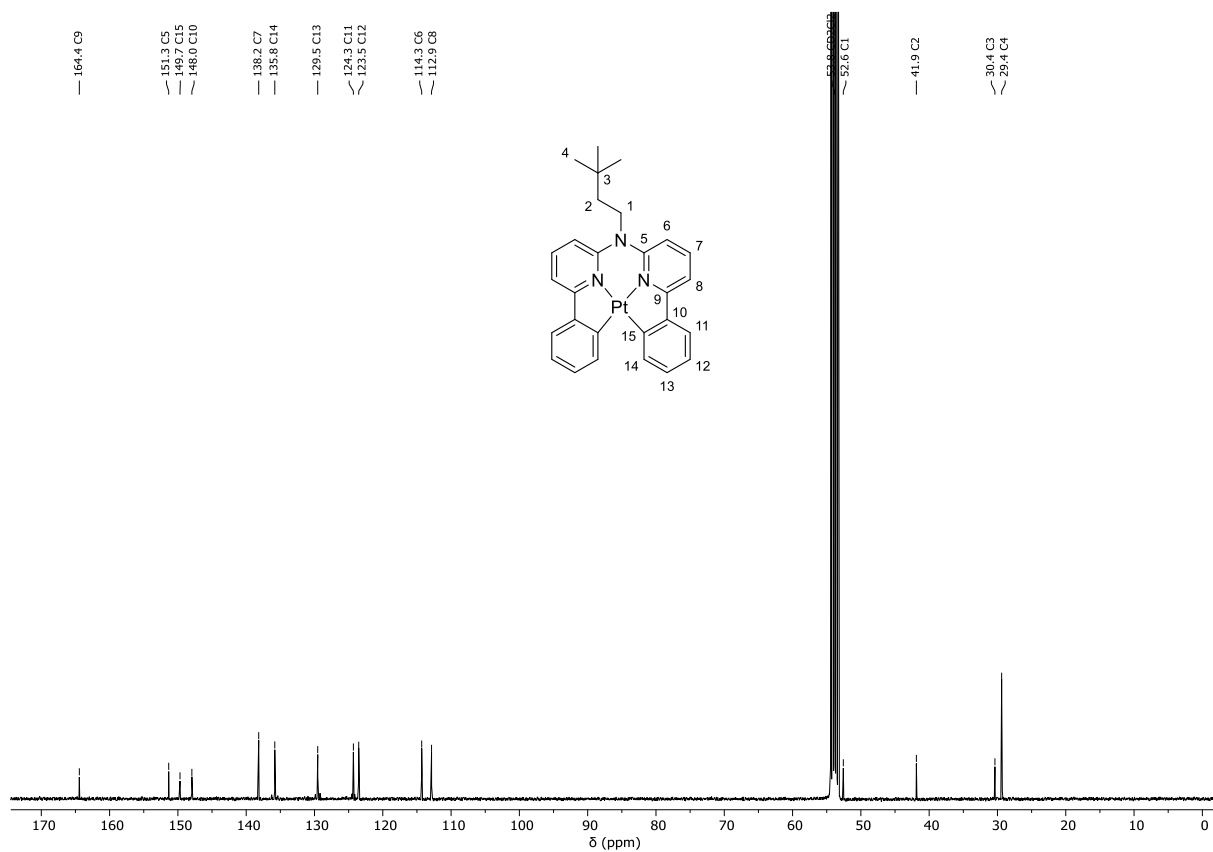


Figure S102: $^{13}\text{C}\{-^1\text{H}\}$ -NMR spectrum (101 MHz, DCM-d_2) of $[\text{PtL}_6]$.

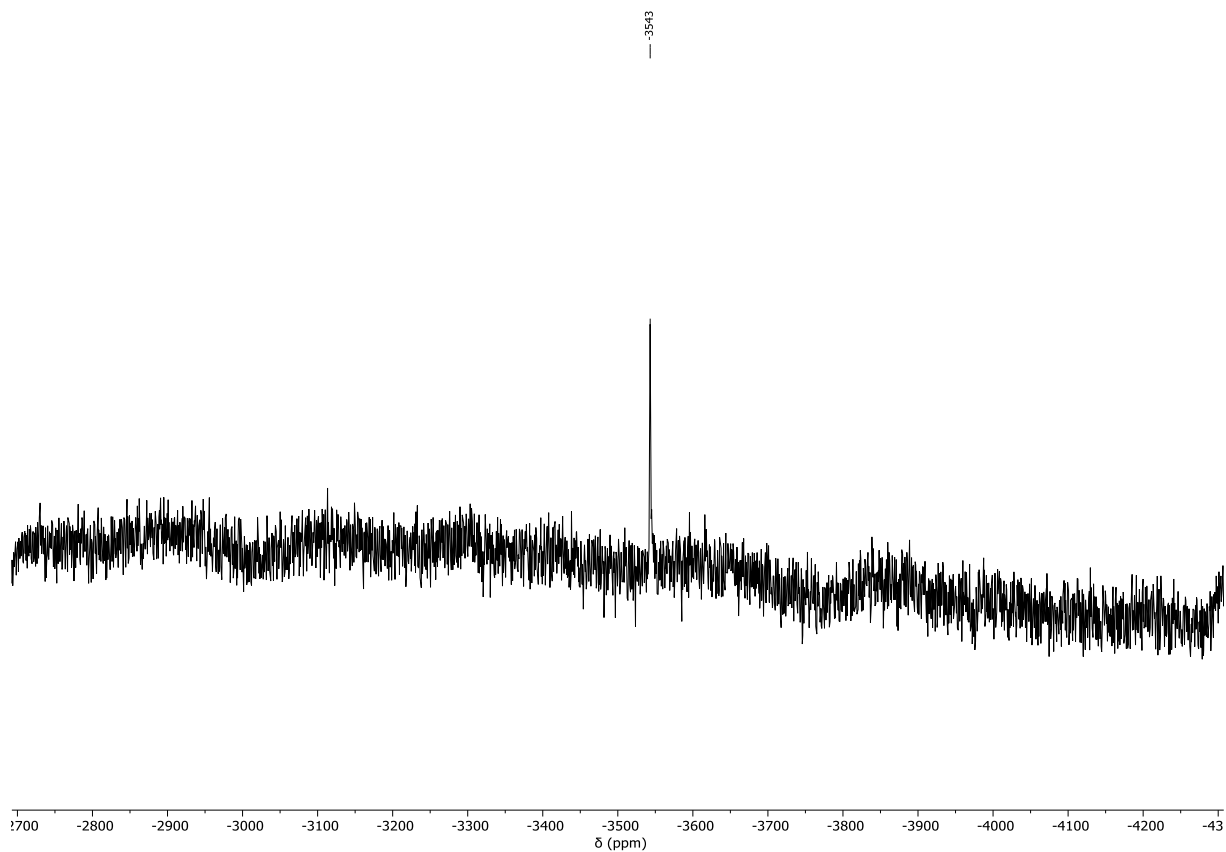


Figure S103: ^{195}Pt -NMR spectrum (86 MHz, DCM-d_2) of $[\text{PtL}_6]$.

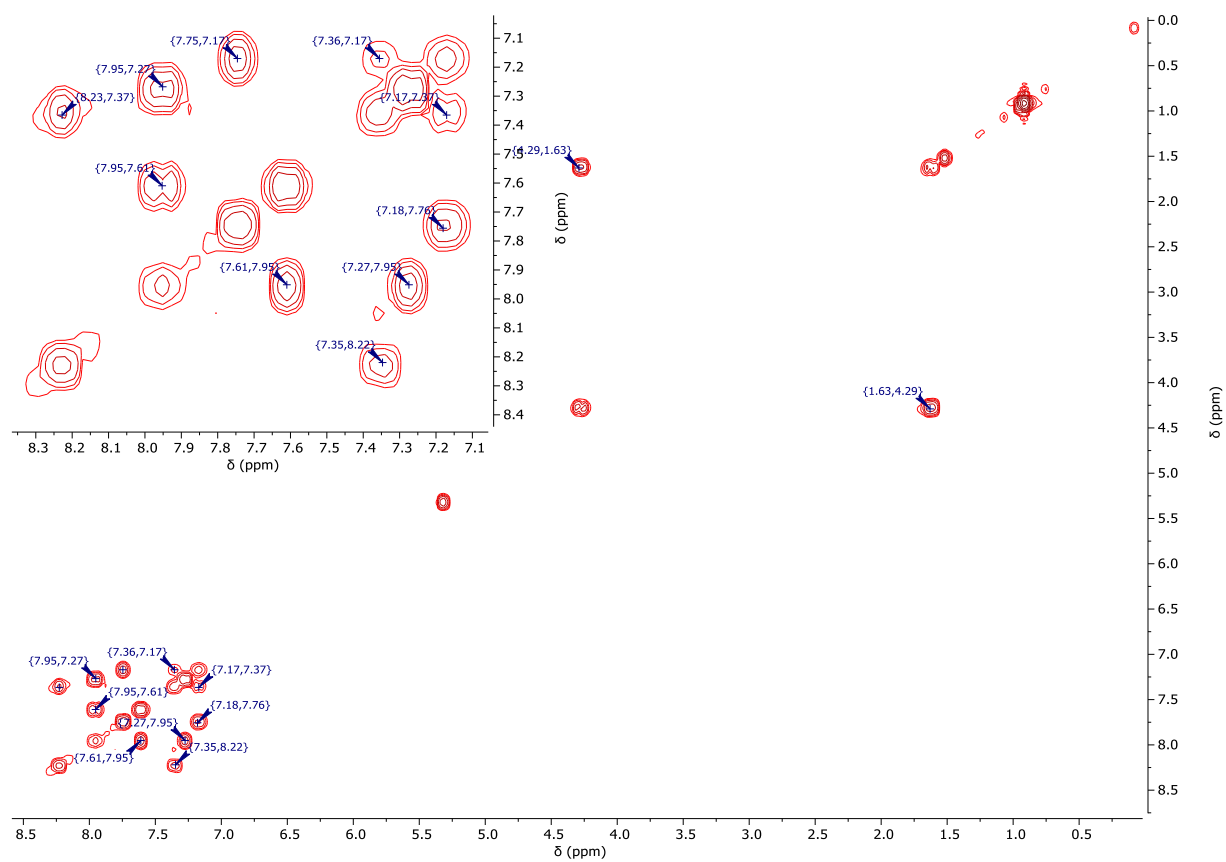


Figure S104: $^1\text{H}/^1\text{H}$ -COSY-NMR spectrum (400 MHz/400 MHz, DCM-d_2) of $[\text{PtL}_6]$.

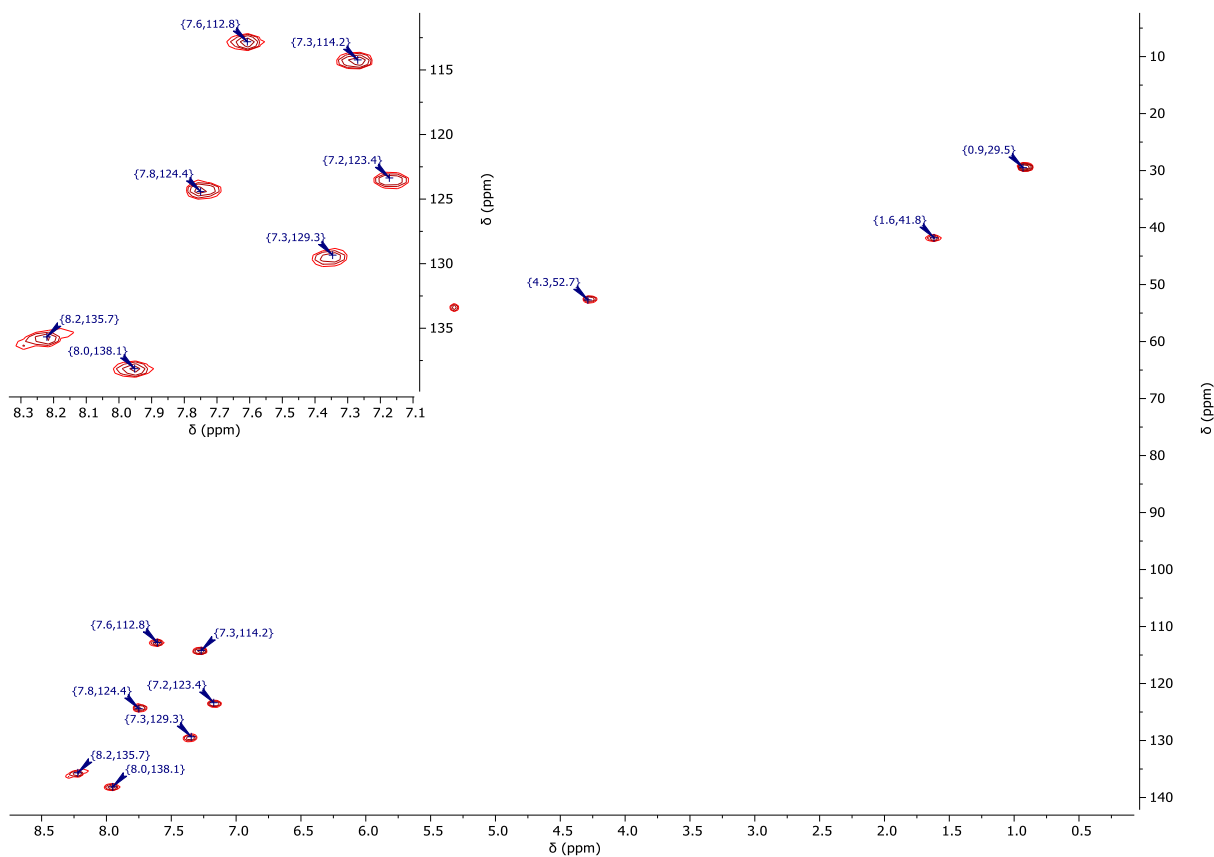


Figure S105: $^1\text{H}/^{13}\text{C}$ -gHSQC-NMR spectrum (400 MHz/101 MHz, $\text{DCM-}d_2$) of $[\text{PtL}_6]$.

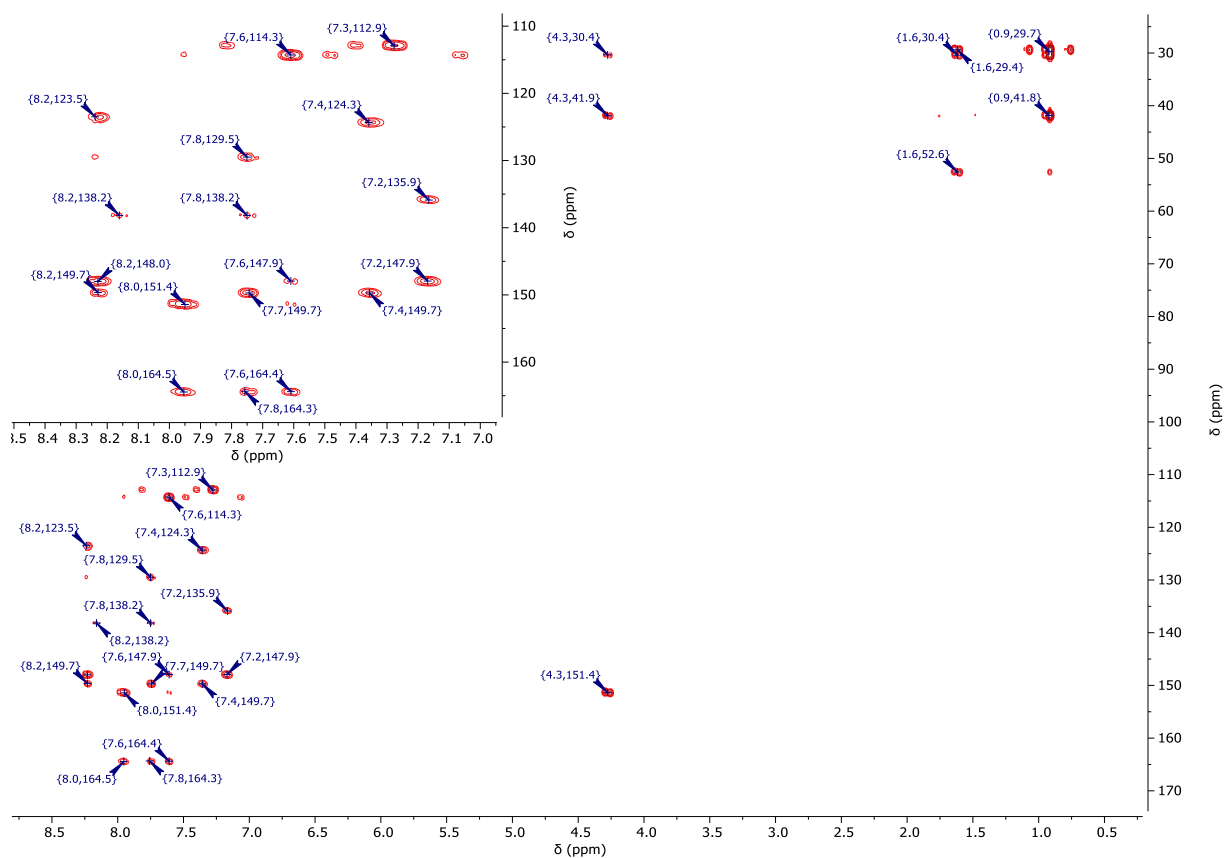


Figure S106: $^1\text{H}/^{13}\text{C}$ -gHMBC-NMR spectrum (400 MHz/101 MHz, $\text{DCM-}d_2$) of $[\text{PtL}_6]$.

III. Single-crystal X-ray diffractometry

Data sets for the compounds were collected with Bruker D8 Venture CMOS diffractometer. Software package used to prepare material for publication: Mercury.

Table S1: Parameters and data from the single crystal measurements.

Complex	I ₁	A ₃	A ₄	[PtCl(L ₂)]	[PtCl(L ₄)]	[PtL ₆]
Formula	C ₉ H ₈ N ₃ SBr	C ₁₉ H ₂₀ N ₃ SBr	C ₁₃ H ₁₄ N ₃ SOBr	C ₂₀ H ₂₂ N ₃ SPtCl	C ₁₉ H ₁₈ N ₃ SOPtCl	C ₂₈ H ₂₇ N ₃ Pt
Fw	270.15	402.35	340.23	567.00	566.96	600.61
CCDC No.	2252944	2252953	2252945	2252967	2252954	2252950
Crystal color	Block, colourless	Block, colourless	Plate, colourless	Plate, yellow	Plate, yellow	Block, yellow
a/Å	7.5374 (4)	13.1301 (7)	16.1143 (6)	14.5638 (19)	9.5422 (3)	14.0249 (8)
b/Å	11.5452 (7)	11.5938 (6)	9.5694 (4)	10.5045 (14)	17.5621 (5)	9.1333 (5)
c/Å	11.477	23.7910 (13)	9.1527 (4)	12.9701 (17)	18.7821 (5)	17.9006 (10)
α/°	90	90	90	90	114.892 (1)	90
β/°	97.305 (2)	90	100.169 (1)	105.206 (4)	100.541 (1)	109.321 (2)
γ/°	90	90	90	90	93.195 (1)	90
V/Å³	990.65 (10)	3621.7 (3)	1389.21 (10)	1914.8 (4)	2775.68 (14)	2163.8 (2)
Space group	P2 ₁ /n	Pbca	P2 ₁ /c	P2 ₁ /c	P $\bar{1}$	P2 ₁ /c
Crystal system	monoclinic	orthorhombic	monoclinic	monoclinic	triclinic	monoclinic
Z value	4	8	4	4	6	4
μ(MoKα)/mm⁻¹	4.32	2.390	3.104	7.59	7.85	6.507
F000	536	1648	688.0	1096	1632.0	1176
F000'	535.51	1647.14	681.57	1090.86	1624.35	1169.78
h,k,l_{max}	10, 16, 16	13, 17, 35	22, 13, 12	19, 13, 17	13, 24, 26	19, 12, 25
N_{ref}	2914	6049	4092	4553	16105	6347
T_{min}, T_{max}	0.169, 0.397	0.566, 0.733	0.416, 0.624	0.265, 0.611	0.632, 0.746	0.174, 0.452
T_{min}'	0.142	0.438	0.360	0.211	0.191	0.132

X-ray diffractometric analysis of I₁ (sad_ve9_p21n_a; CCDC-Nr.: 2252944):

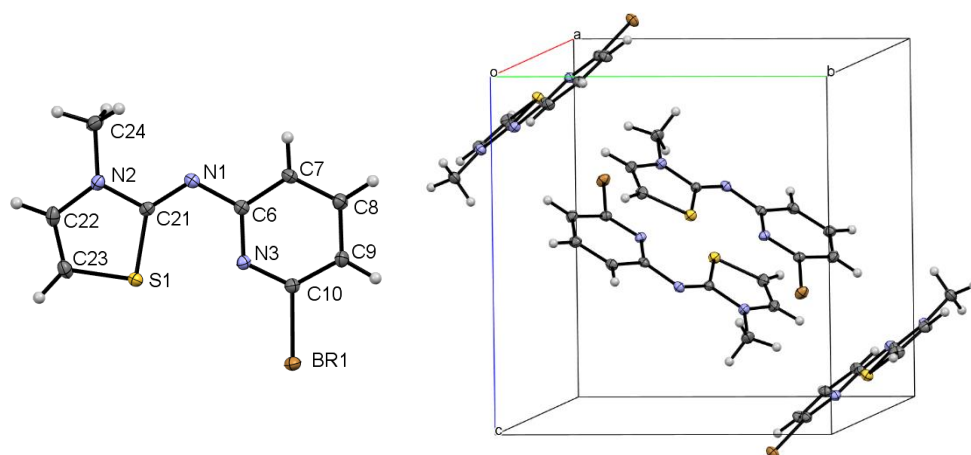


Figure S107: Molecular structure of compound I₁ in a single crystal (left) and display of the packing (right). Displacement ellipsoids shown at 50 % probability.

X-ray diffractometric analysis of A₃ (VeS5_pbca_a; CCDC-Nr.: 2252953):

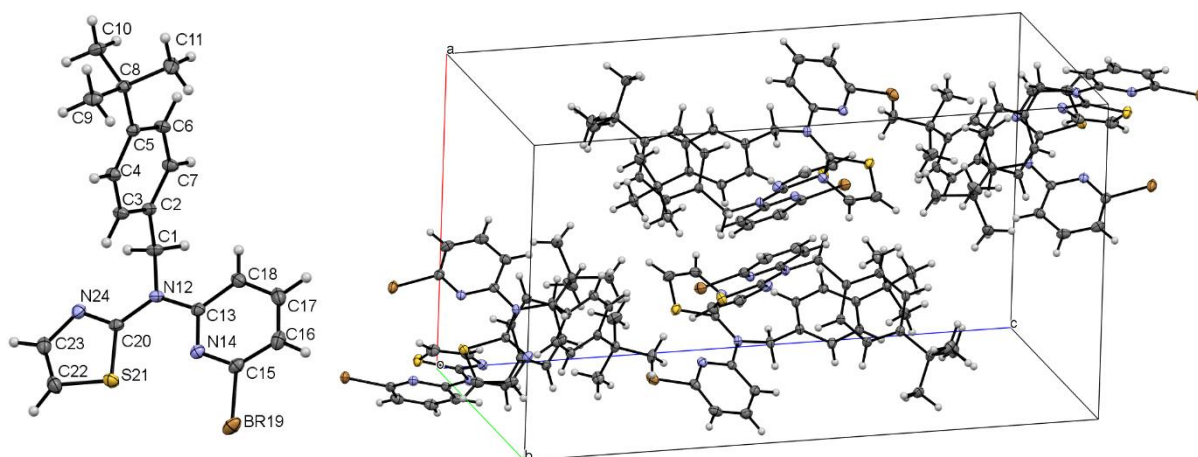


Figure S108: Molecular structure of compound A₃ in a single crystal (left) and display of the packing (right). Displacement ellipsoids shown at 50 % probability.

X-ray diffractometric analysis of A₄ (sad_ve10_p21c_a; CCDC-Nr.: 2252945):

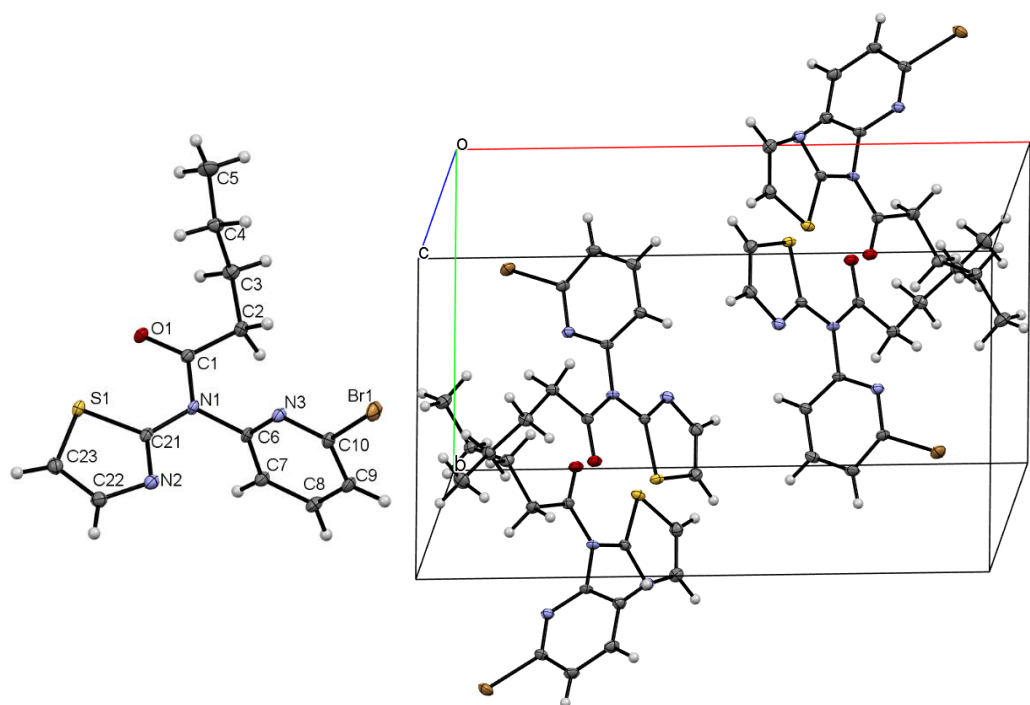


Figure S109: Molecular structure of compound A₄ in a single crystal (left) and display of the packing (right). Displacement ellipsoids shown at 50 % probability.

X-ray diffractometric analysis of [PtCl(L₂)] (VdS4_p21c_a ; CCDC-Nr.: 2252967):

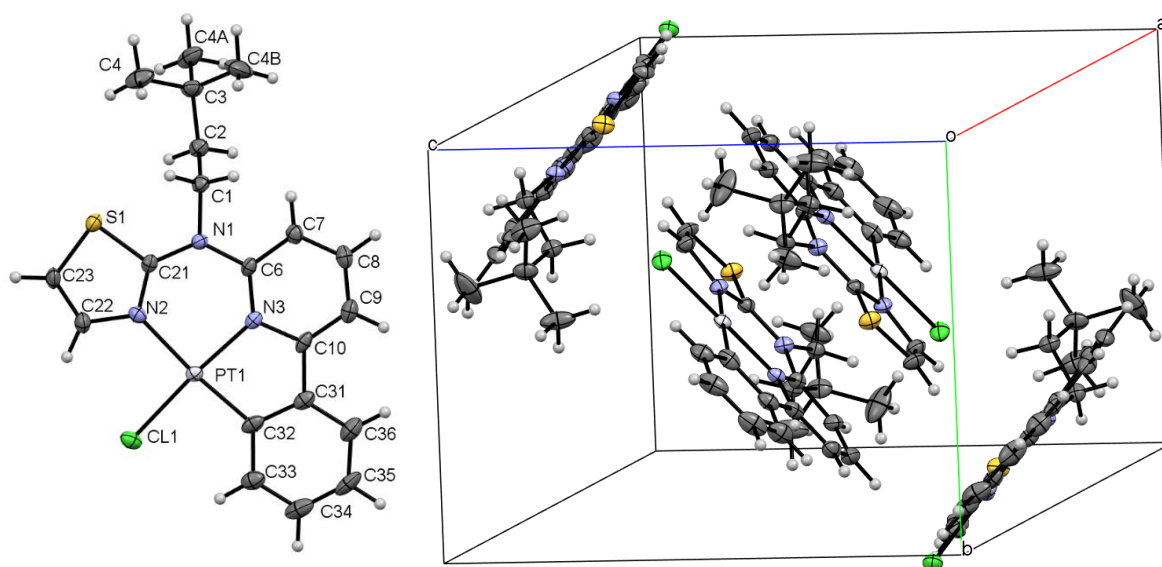
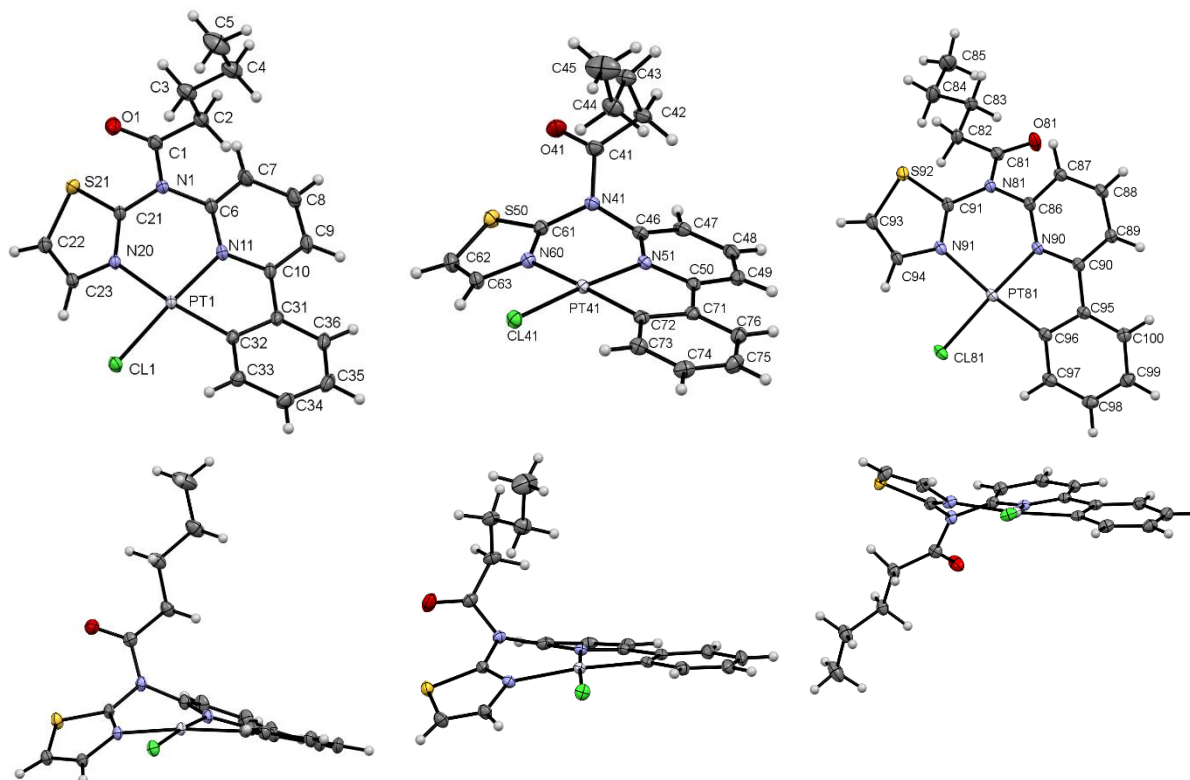


Figure S110: Molecular structure of compound [PtCl(L₂)] in a single crystal (left) and display of the packing (right). Displacement ellipsoids shown at 50 % probability.

Table S2: Selected bond lengths and angles for [PtCl(L₂)].

X-Y	<i>d</i> (X-Y) in Å	X-Y-Z	θ (XYZ) in °
Pt1-N2	2.071 (5)	N2-Pt1-N3	91.64 (17)
Pt1-N3	2.005 (4)	N3-Pt1-C32	83.2 (2)
Pt1-C32	1.962 (6)	C32-Pt1-Cl1	92.64 (17)
Pt1-Cl1	2.3075 (13)	Cl1-Pt1-N2	92.58 (13)
		N2-Pt1-C32	175.97 (13)
		N3-Pt1-Cl1	175.68 (12)

X-ray diffractometric analysis of [PtCl(L₄)] (Vis2_p-1_b; CCDC-Nr.: 225254):**Figure S111:** Molecular structures of compound [PtCl(L₄)] in a single crystal (top) and the display of the distortion of the coordination plane (bottom) for all three different molecules. Displacement ellipsoids shown at 50 % probability.

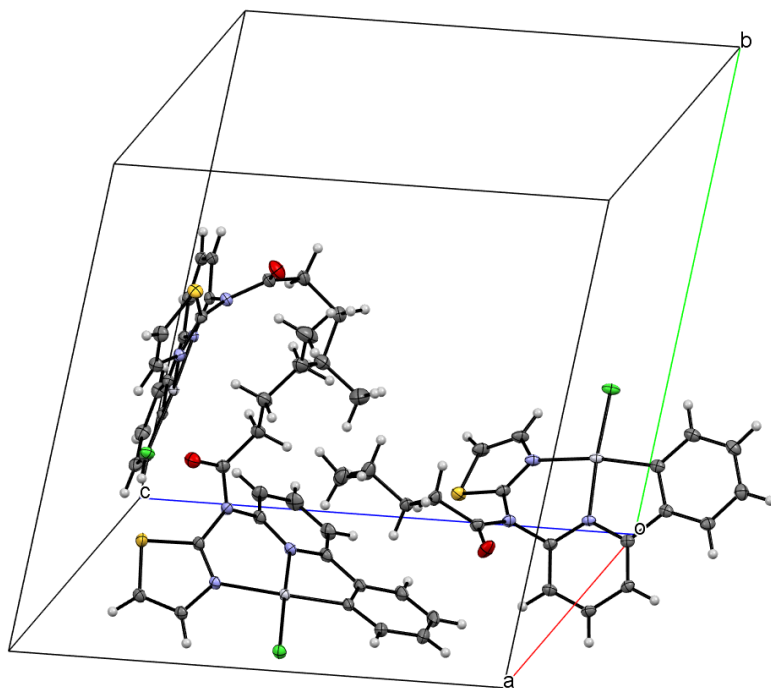


Figure S112: Asymmetric cell of the crystal structure of [PtCl(L₄)]. Displacement ellipsoids shown at 50 % probability.

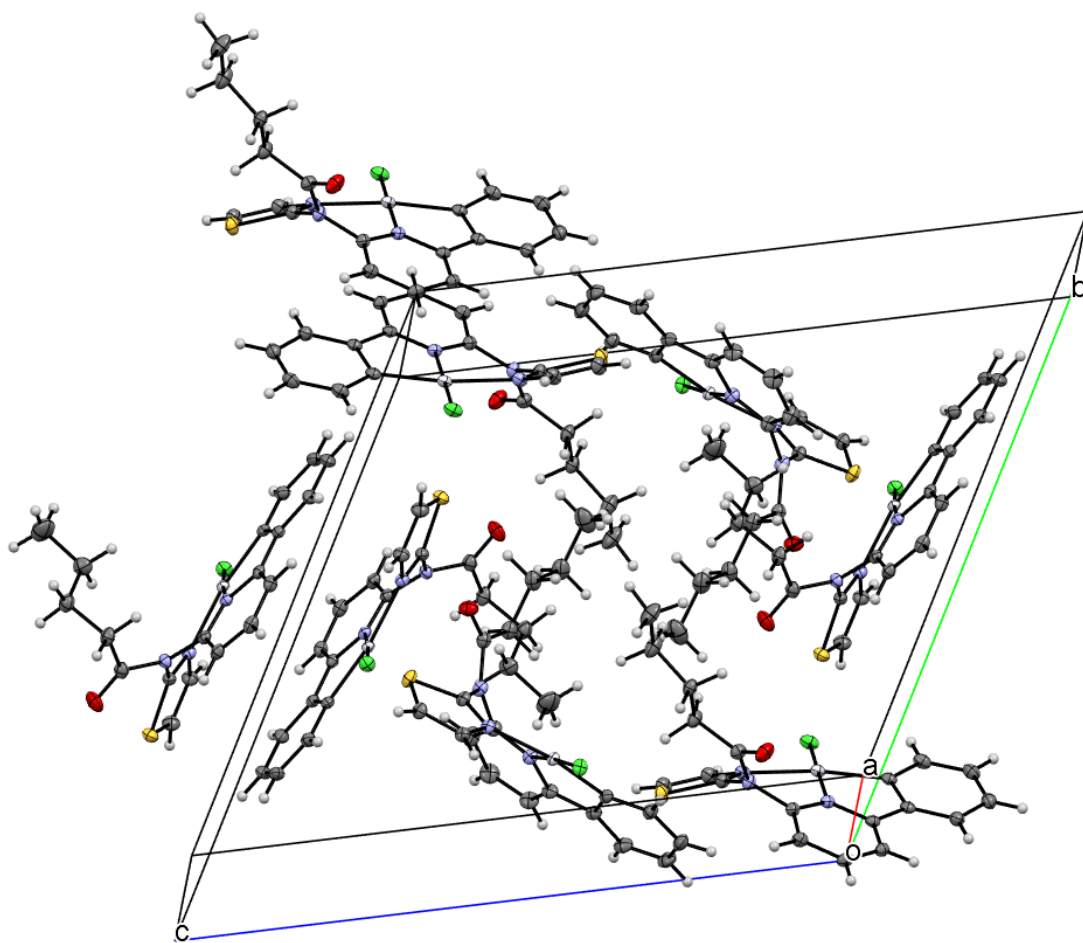
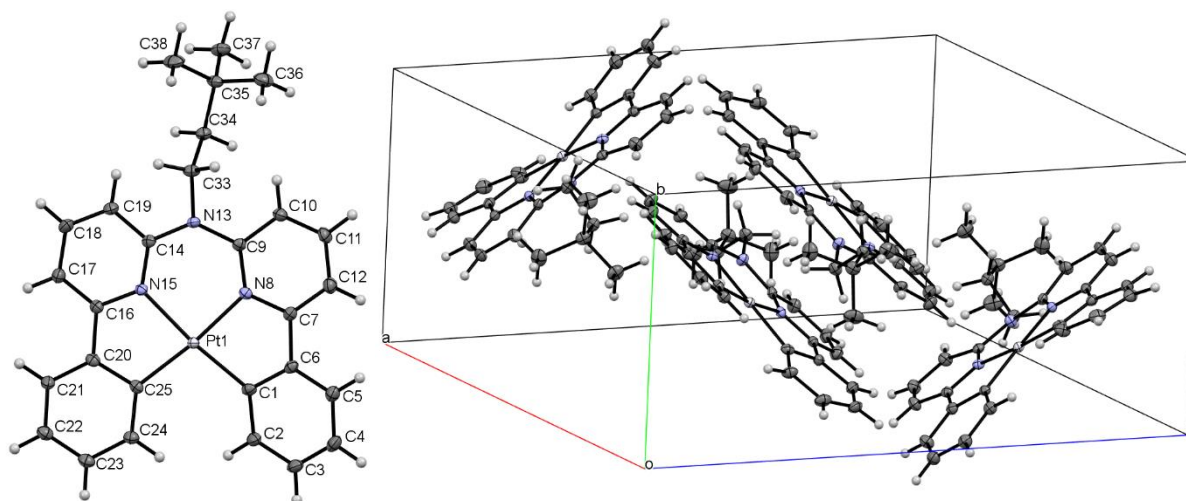


Figure S113: Display of the crystal packing of [PtCl(L₄)]. Displacement ellipsoids shown at 50 % probability.

Table S3: Selected bond lengths and angles for [PtCl(L₄)].

X-Y	<i>d</i> (X-Y) in Å	X-Y-Z	θ (XYZ) in °
Pt1-N11	1.9876 (14)	N11-Pt1-N20	89.44 (6)
Pt41-N51	1.9956 (14)	N51-Pt41-N60	90.80 (6)
Pt81-N90	2.0021 (13)	N90-Pt81-N91	90.84 (6)
Pt1-N20	2.1040 (14)	N20-Pt1-C32	168.36 (6)
Pt41-N60	2.0884 (14)	N60-Pt41-C72	169.68 (6)
Pt81-N91	2.0946 (15)	N91-Pt81-C96	171.19 (6)
Pt1-C32	1.9796 (17)	C32-Pt1-Cl1	96.37 (5)
Pt41-C72	1.9765 (17)	C72-Pt41-Cl41	95.03 (5)
Pt81-C96	1.9797 (17)	C96-Pt81-Cl81	95.43 (5)
Pt1-Cl1	2.2996 (4)	Cl1-Pt1-N11	175.86 (4)
Pt41-Cl41	2.3046 (4)	Cl41-Pt41-N51	176.42 (4)
Pt81-Cl81	2.3097 (4)	Cl81-Pt81-N90	174.36 (4)
		N11-Pt1-C32	81.48 (7)
		N51-Pt41-C72	82.18 (6)
		N90-Pt81-C96	82.02 (6)
		N20-Pt1-Cl1	92.22 (4)
		N60-Pt41-Cl41	91.66 (4)
		N91-Pt81-Cl81	91.23 (4)

X-ray diffractometric analysis of [Pt(L₆)] (Ve12sadb21c_a; CCDC-Nr.: 2252950):**Figure S114:** Molecular structure of compound [Pt(L₆)] in a single crystal (left) and display of the packing (right). Displacement ellipsoids shown at 50 % probability.**Table S4:** Selected bond lengths and angles for [Pt(L₆)].

X-Y	<i>d</i> (X-Y) in Å	X-Y-Z	θ (XYZ) in °
Pt1-N8	2.0478 (19)	N8-Pt1-N15	91.83 (8)
Pt1-N15	2.0514 (19)	N15-Pt1-C1	174.05 (8)
Pt1-C1	1.997 (2)	C1-Pt1-C25	103.24 (10)
Pt1-C25	2.010 (2)	C25-Pt1-N8	173.38 (8)
		N8-Pt1-C1	82.45 (9)
		N15-Pt1-C25	82.56 (9)

IV. Steady-state and time resolved photoluminescence spectroscopy:

Absorption spectra were measured with a Shimadzu UV-1900i UV-VIS-NIR spectrophotometer.

Steady-state excitation and emission spectra were recorded on a FluoTime 300 spectrometer from PicoQuant equipped with a 300 W ozone-free Xe lamp (250-900 nm), a 10 W Xe flash-lamp (250-900 nm, pulse width *ca.* 1 μ s) with repetition rates of 0.1 – 300 Hz, double excitation monochromators (Czerny-Turner type, grating with 1200 lines/mm, blaze wavelength: 300 nm), diode lasers (pulse width < 80 ps) operated by a computer-controlled laser driver PDL-828 “Sepia II” (repetition rate up to 80 MHz, burst mode for slow and weak decays), two double-grating emission monochromators (Czerny-Turner, selectable gratings blazed at 500 nm with 2.7 nm/mm dispersion and 1200 lines/mm, or blazed at 1200 nm with 5.4 nm/mm dispersion and 600 lines/mm) with adjustable slit width between 25 μ m and 7 mm, Glan-Thompson polarizers for excitation (after the Xe-lamps) and emission (after the sample). Different sample holders (Peltier-cooled mounting unit ranging from -15 to 110 °C or an adjustable front-face sample holder), along with two detectors (namely a PMA Hybrid-07 from PicoQuant with transit time spread FWHM < 50 ps, 200 – 850 nm, or a H10330C-45-C3 NIR detector with transit time spread FWHM 0.4 ns, 950-1700 nm from Hamamatsu) were used. Steady-state spectra and photoluminescence lifetimes were recorded in TCSPC mode by a PicoHarp 300 (minimum base resolution 4 ps) or in MCS mode by a TimeHarp 260 (where up to several ms can be traced). Emission and excitation spectra were corrected for source intensity (lamp and grating) by standard correction curves. For samples with lifetimes in the ns order, an instrument response function calibration (IRF) was performed using a diluted Ludox[®] dispersion. Lifetime analysis was performed using the commercial EasyTau 2 software (PicoQuant). The quality of the fit was assessed by minimizing the reduced chi squared function (χ^2) and visual inspection of the weighted residuals and their autocorrelation. All solvents used were of spectrometric grade (Uvasol[®], Merck).

Photoluminescence quantum yields were measured with a Hamamatsu Photonics absolute PL quantum yield measurement system (C9920-02) equipped with a L9799-01 CW Xe light source (150 W), a monochromator, a C7473 photonic multi-channel analyser, an integrating sphere and employing U6039-05 software (Hamamatsu Photonics, Ltd., Shizuoka, Japan).

Table S5: Complete emission data and Φ_L , as well as excited state lifetime data for each complex in DCM at 298 K and in frozen glassy matrix of DCM/MeOH (V:V = 1:1) at 77 K. For multiexponential decays, the amplitude-weighted average lifetimes are given as well as the different components in square brackets with relative amplitudes as percentages in parentheses.

Complex	Medium (T/K)	λ_{em}	λ_{exc}	τ_{av}	$\Phi_L \pm 0.02/\pm 0.05$
[PtCl(L ₁)]	DCM, air (298)	495, 530, 566sh	370sh, 348, 317, 281	14.98 ± 0.06 [16.48 ± 0.05 (88); 3.87 ± 0.19 (12)] (ns)	< 0.02
	DCM, Ar (298)			14.58 ± 0.03 [14.95 ± 0.04 (82); 2.0 ± 0.2 (18)] (ns)	< 0.02
	Glassy matrix (77)	483, 519, 560, 600sh	365, 346, 310	23.52 ± 0.08 [29.9 ± 1.2 (39); 19.4 ± 1.1 (61)] (μs)	> 0.98
[PtCl(L ₂)]	DCM, air (298)	495, 530, 560sh	370, 350	21.72 ± 0.04 (ns)	< 0.02
	DCM, Ar (298)			15.94 ± 0.05 [20.53 ± 0.05 (73); 5.8 ± 0.5 (13); 0.9 ± 0.1 (14)] (ns)	< 0.02
	Glassy matrix (77)	487, 520, 564	366	32.86 ± 0.05 [36.2 ± 0.2 (77); 21 ± 1 (23)] (μs)	> 0.98
[PtCl(L ₃)]	DCM, air (298)	496, 528, 560sh	408sh, 368, 352	18.2 ± 0.4 [28.01 ± 0.05 (59); 4.24 ± 0.20 (41)] (ns)	< 0.02
	DCM, Ar (298)			25.7 ± 0.5 [27.2 ± 0.2 (91); 10 ± 3 (9)] (ns)	< 0.02
	Glassy matrix (77)	484, 518, 551	368, 350, 310	24.88 ± 0.02 [30.9 ± 0.4 (35); 21.7 ± 0.3 (65)] (μs)	> 0.98
[PtCl(L ₄)]	DCM, air (298)	504, 533, 569sh	n.d.	n.d.	n.d.
	DCM, Ar (298)			n.d.	n.d.
	Glassy matrix (77)	487, 522, 560, 600sh	413sh, 395sh, 366, 343,	12.42 ± 0.04 [29 ± 8 (2); 12.1 ± 0.1 (98)] (μs)	> 0.98
[PtCl(L ₅)]	DCM, air (298)	493, 529, 567sh	413sh, 367, 348, 319sh	0.2323 ± 0.0006 (μs)	< 0.02
	DCM, Ar (298)			0.2695 ± 0.0006 (μs)	< 0.02
	Glassy matrix (77)	488, 526, 558, 609sh	397sh, 368, 312	45.72 ± 0.06 [50.5 ± 0.5 (74); 32 ± 2 (26)] (μs)	> 0.98
[Pt(L ₆)]	DCM, air (298)	510, 546, 585sh	405, 366, 346sh	0.2354 ± 0.0003 (μs)	< 0.02
	DCM, Ar (298)			4.203 ± 0.002 (μs)	0.54
	Glassy matrix (77)	500, 537, 575sh	391sh, 373, 335	11.436 ± 0.009 [10.5 ± 0.1 (82); 15.5 ± 0.6 (18)] (μs)	0.97

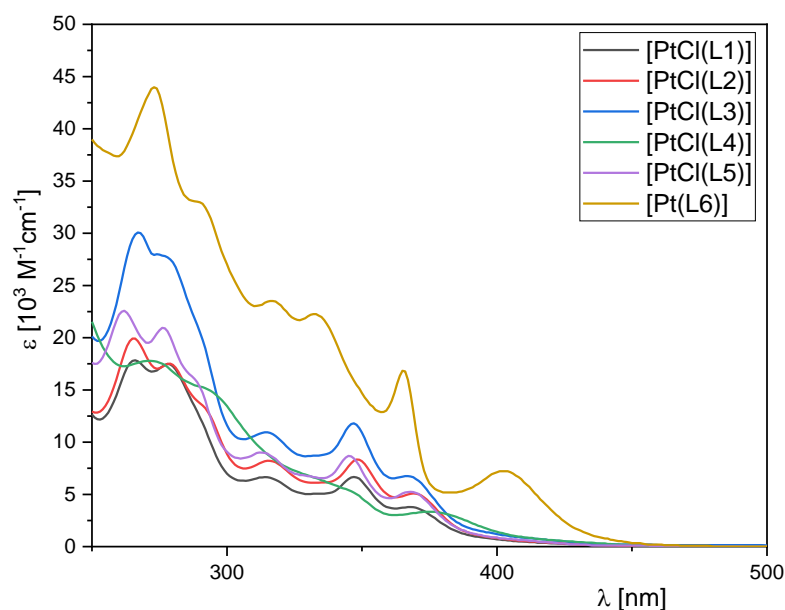


Figure S115: Molar absorption coefficient of **[PtCl(L₁)]** (black), **[PtCl(L₂)]** (red), **[PtCl(L₃)]** (blue), **[PtCl(L₄)]** (green), **[PtCl(L₅)]** (pink) and **[Pt(L₆)]** (yellow) (validity range: $c = 5 \times 10^{-5} - 1 \times 10^{-6}$ M in DCM at 298 K).

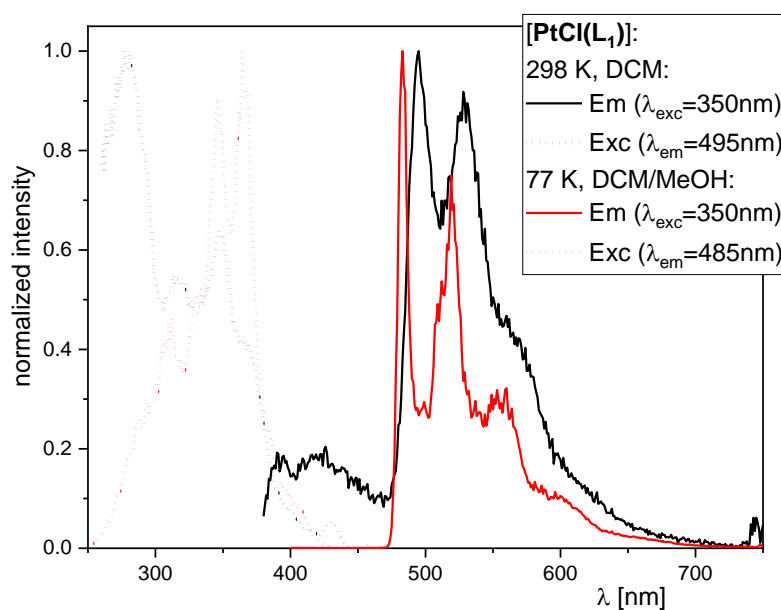


Figure S116: Excitation (dotted line) and emission spectra (solid line) of **[PtCl(L₁)]** ($\lambda_{exc} = 350$ nm; $\lambda_{em} = 495$ nm at 298 K, $\lambda_{em} = 485$ nm at 77 K) at 298 K in fluid DCM (black) and at 77 K (red) in a frozen glassy DCM/MeOH matrix (V:V = 1:1). All solutions were optically diluted ($A < 0.1$). Spectra normalized to the highest intensity. Signals between 350-450 nm can be attributed the background noise in combination to low signal from the initial compound.

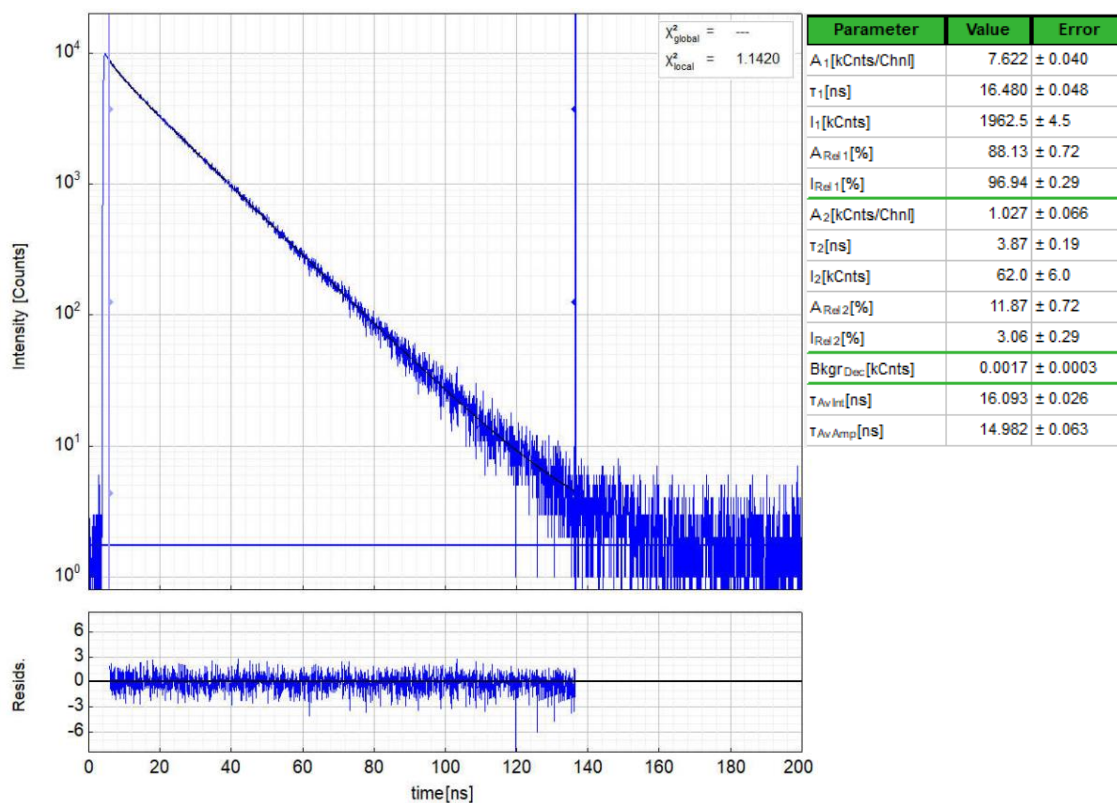


Figure S117: Left: Raw (experimental) time-resolved photoluminescence decay of [PtCl(L₁)] in fluid DCM at 298 K (air-equilibrated), including the residuals ($\lambda_{\text{exc}} = 376.7$ nm, $\lambda_{\text{em}} = 495$ nm). Right: Fitting parameters including pre-exponential factors and confidence limits.

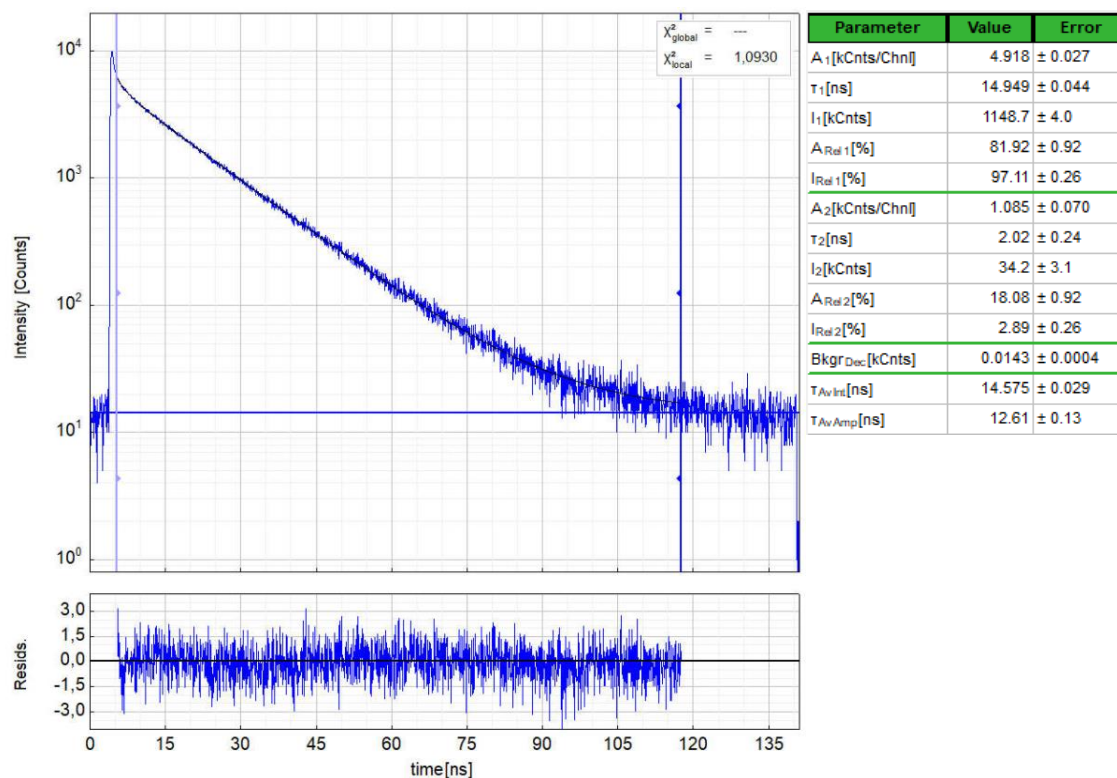


Figure S118: Left: Raw (experimental) time-resolved photoluminescence decay of [PtCl(L₁)] in fluid DCM at 298 K (Ar-purged), including the residuals ($\lambda_{\text{exc}} = 376.7$ nm, $\lambda_{\text{em}} = 495$ nm). Right: Fitting parameters including pre-exponential factors and confidence limits.

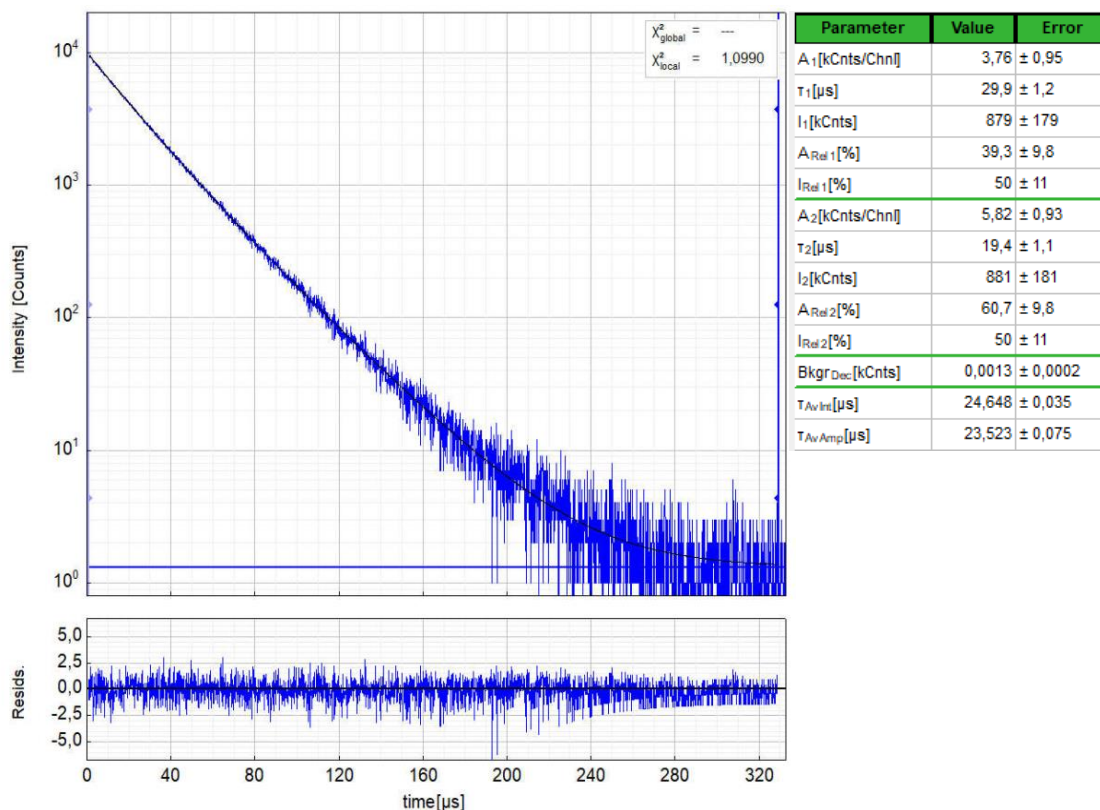


Figure S119: Left: Raw (experimental) time-resolved photoluminescence decay of **[PtCl(L₁)]** in a frozen glassy DCM/MeOH matrix (V:V = 1:1) at 77 K, including the residuals ($\lambda_{exc} = 376.7$ nm, $\lambda_{em} = 485$ nm). Right: Fitting parameters including pre-exponential factors and confidence limits.

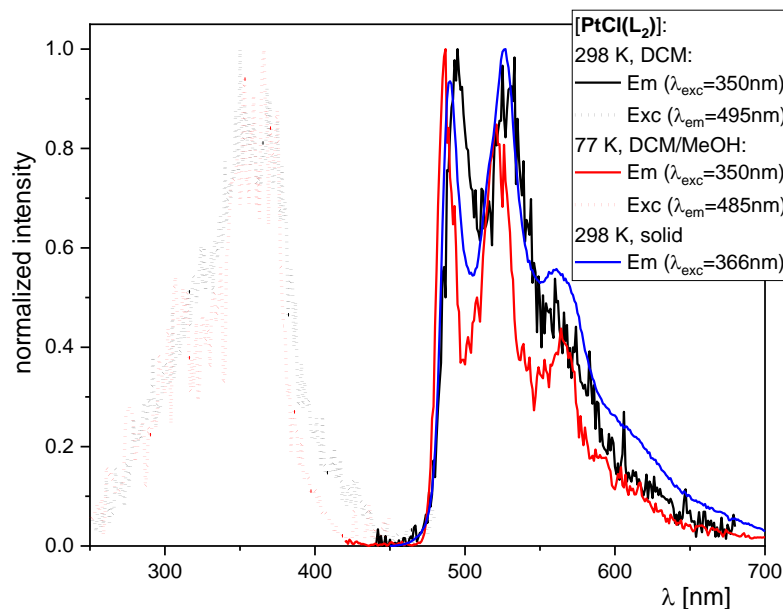


Figure S120: Excitation (dotted line) and emission spectra (solid line) of **[PtCl(L₂)]** ($\lambda_{exc} = 350$ nm, $\lambda_{em} = 495$ nm at 298 K, $\lambda_{exc} = 350$ nm, $\lambda_{em} = 485$ nm at 77 K, $\lambda_{exc} = 366$ nm as solid) at 298 K in fluid DCM (black) as a solid (blue) and at 77 K (red) in a frozen glassy DCM/MeOH matrix (V:V = 1:1). All solutions were optically diluted ($A < 0.1$). Spectra normalized to the highest intensity.

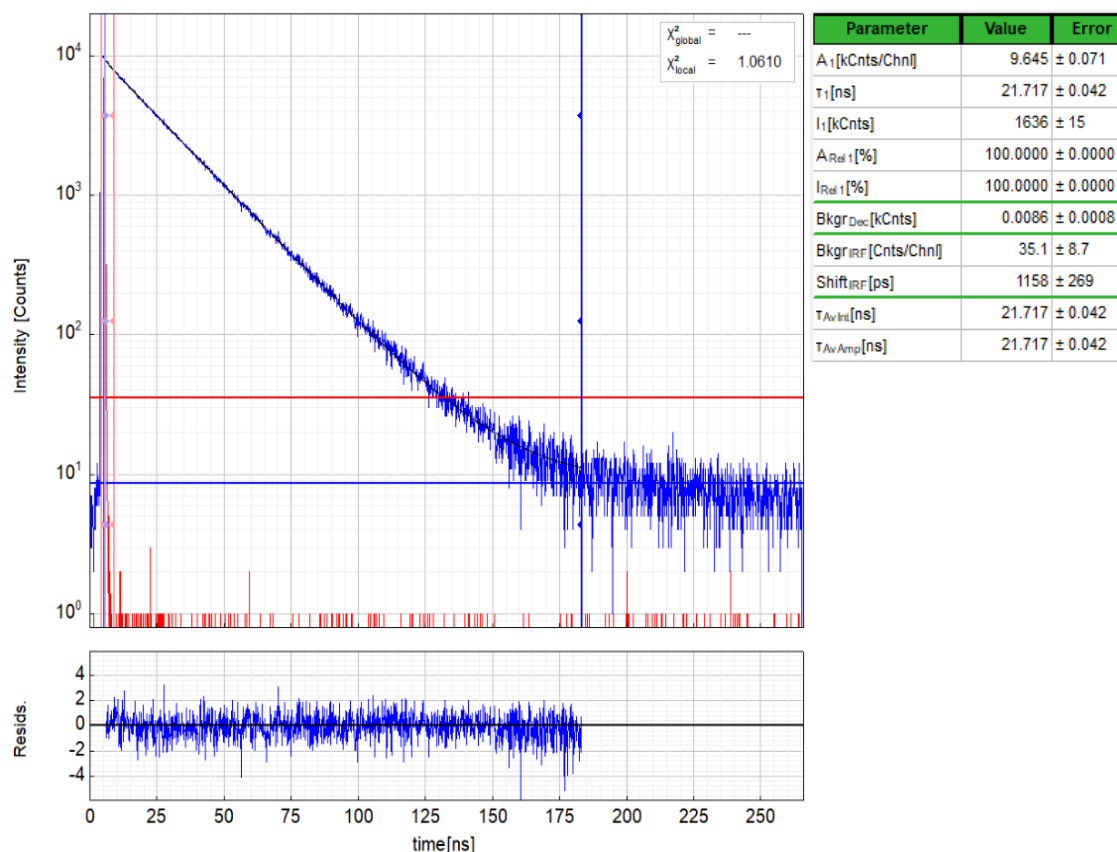


Figure S121: Left: Raw (experimental) time-resolved photoluminescence decay of [PtCl(L₂)] in fluid DCM at 298 K (air-equilibrated), including the residuals ($\lambda_{exc} = 376.7$ nm, $\lambda_{em} = 495$ nm). Right: Fitting parameters including pre-exponential factors and confidence limits.

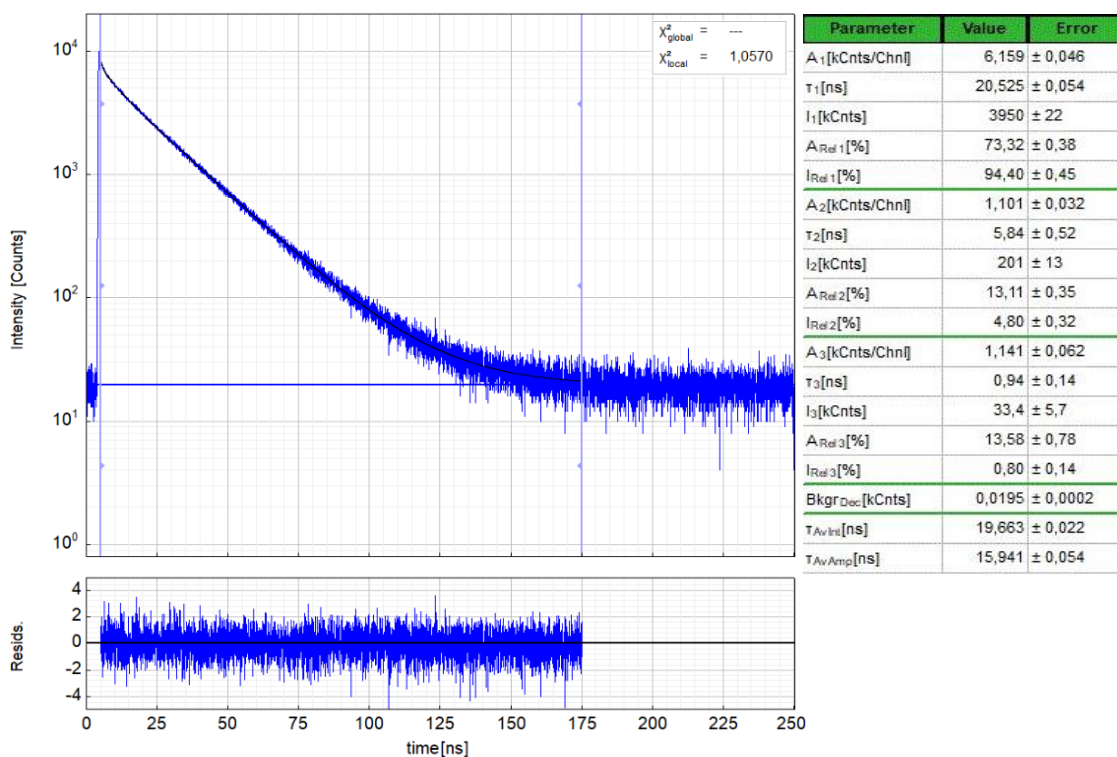


Figure S122: Left: Raw (experimental) time-resolved photoluminescence decay of [PtCl(L₂)] in fluid DCM at 298 K (Ar-purged), including the residuals ($\lambda_{exc} = 376.7$ nm, $\lambda_{em} = 495$ nm). Right: Fitting parameters including pre-exponential factors and confidence limits.

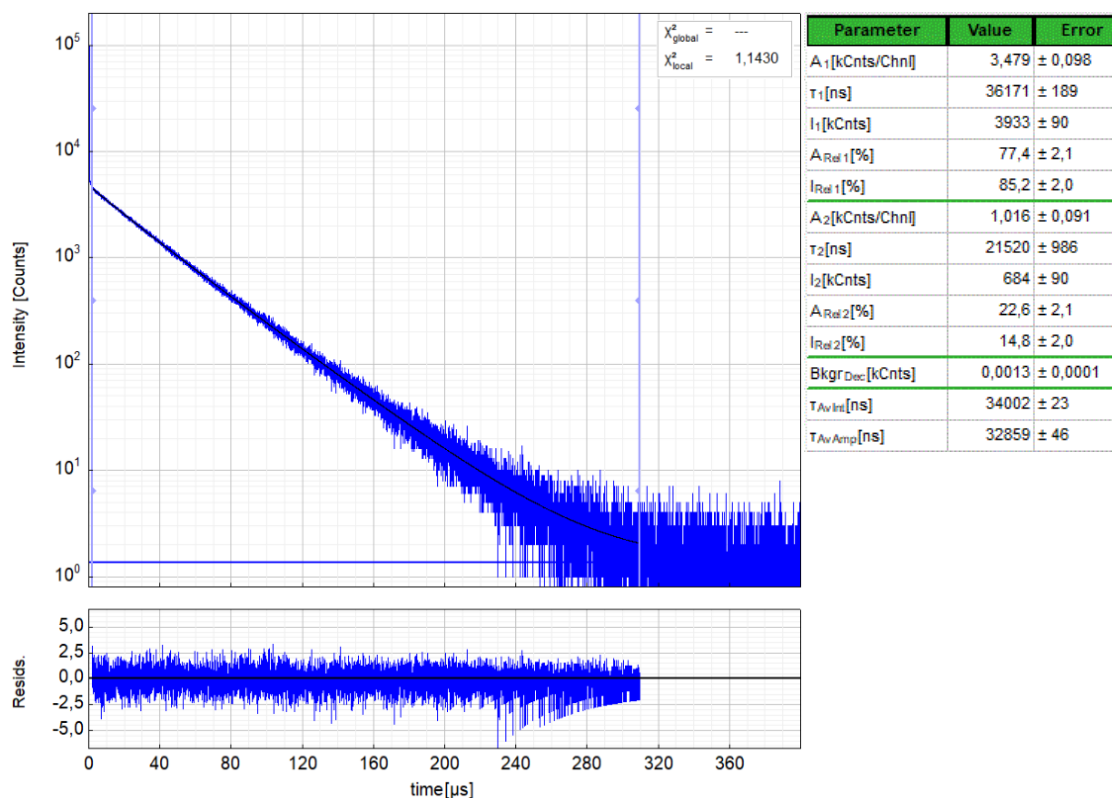


Figure S123: Left: Raw (experimental) time-resolved photoluminescence decay of $[\text{PtCl}(\text{L}_2)]$ in a frozen glassy DCM/MeOH matrix (V:V = 1:1) at 77 K, including the residuals ($\lambda_{\text{exc}} = 376.7$ nm, $\lambda_{\text{em}} = 485$ nm). Right: Fitting parameters including pre-exponential factors and confidence limits.

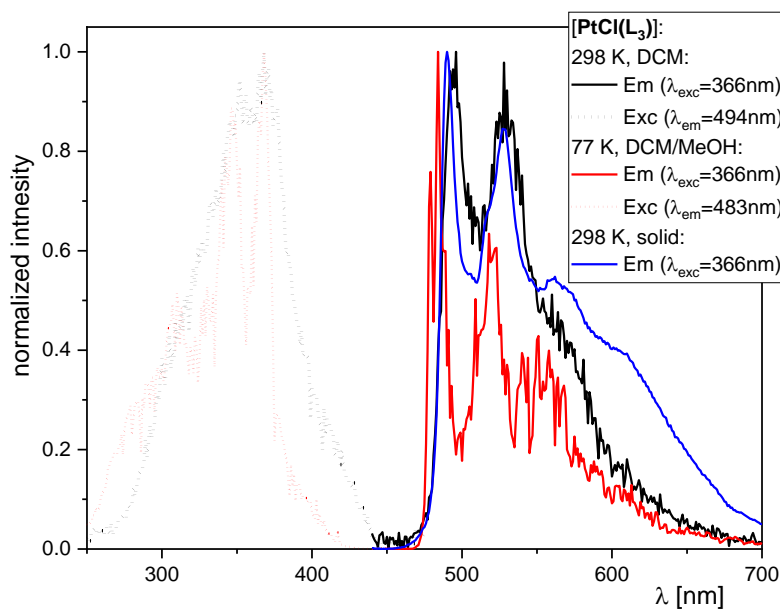


Figure S124: Excitation (dotted line) and emission spectra (solid line) of $[\text{PtCl}(\text{L}_3)]$ ($\lambda_{\text{exc}} = 366$ nm; $\lambda_{\text{em}} = 494$ nm at 298 K, $\lambda_{\text{em}} = 483$ nm at 77 K) at 298 K (black) in fluid DCM, at 77 K (red) in a frozen glassy DCM/MeOH matrix (V:V = 1:1) and as a solid (blue). All solutions were optically diluted ($A < 0.1$). Spectra normalized to the highest intensity.

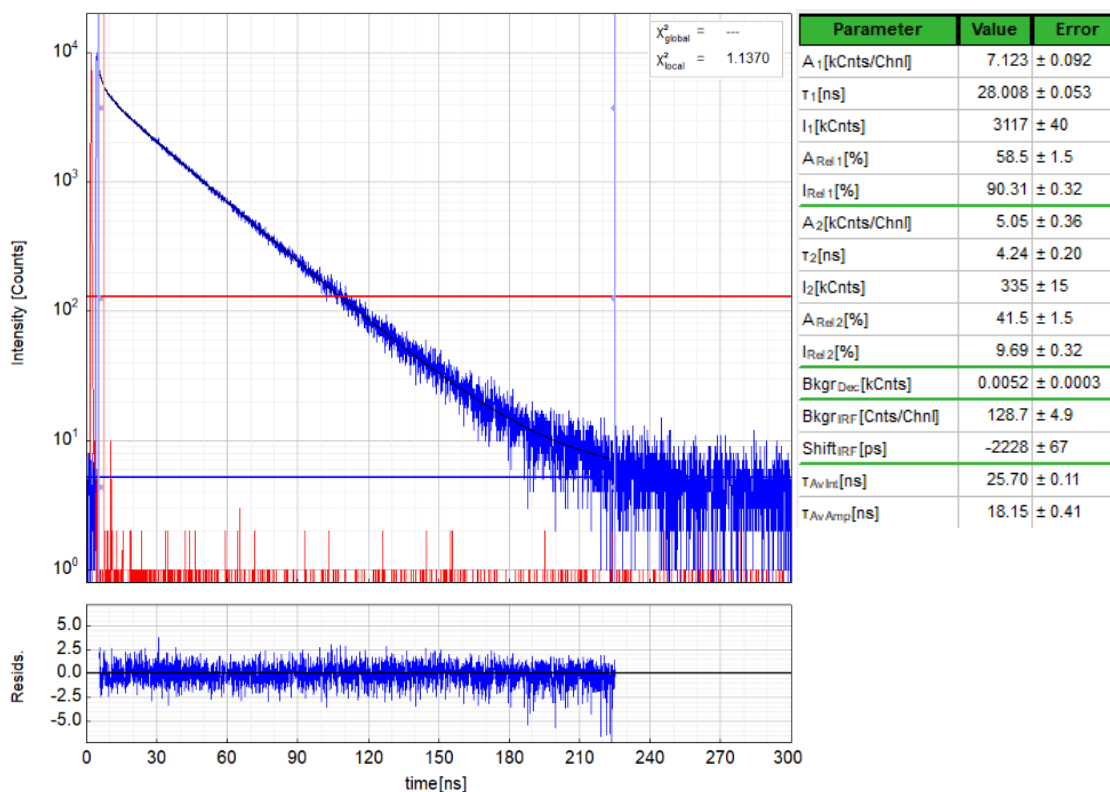


Figure S125: Left: Raw (experimental) time-resolved photoluminescence decay of [PtCl(L₃)] in fluid DCM at 298 K (air-equilibrated), including the residuals ($\lambda_{exc} = 376.7$ nm, $\lambda_{em} = 494$ nm) and IRF (red, $\lambda_{exc} = 376.7$ nm, $\lambda_{em} = 376.7$ nm). Right: Fitting parameters including pre-exponential factors and confidence limits.

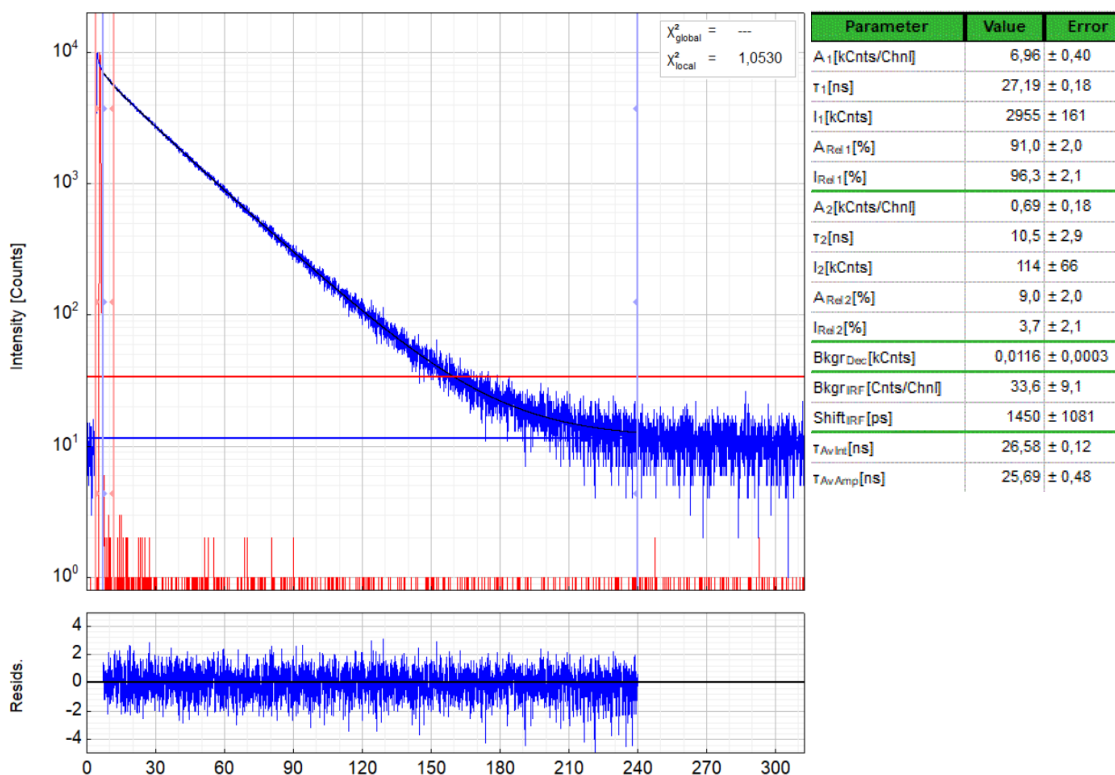


Figure S126: Left: Raw (experimental) time-resolved photoluminescence decay of [PtCl(L₃)] in fluid DCM at 298 K (Ar-purged), including the residuals (blue, $\lambda_{exc} = 376.7$ nm, $\lambda_{em} = 494$ nm) and IRF (red, $\lambda_{exc} = 376.7$ nm, $\lambda_{em} = 376.7$ nm). Right: Fitting parameters including pre-exponential factors and confidence limits.

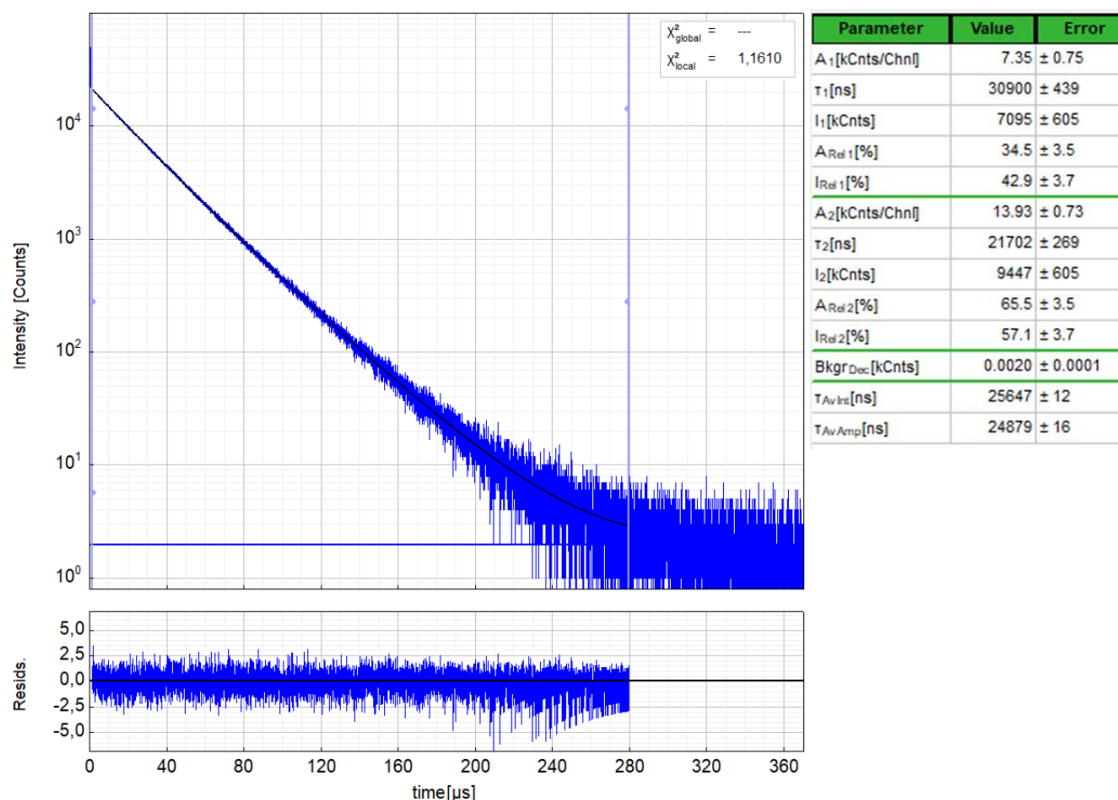


Figure S127: Left: Raw (experimental) time-resolved photoluminescence decay of **[PtCl(L₃)]** in a frozen glassy DCM/MeOH matrix (V:V = 1:1) at 77 K, including the residuals ($\lambda_{exc} = 376.7$ nm, $\lambda_{em} = 483$ nm). Right: Fitting parameters including pre-exponential factors and confidence limits.

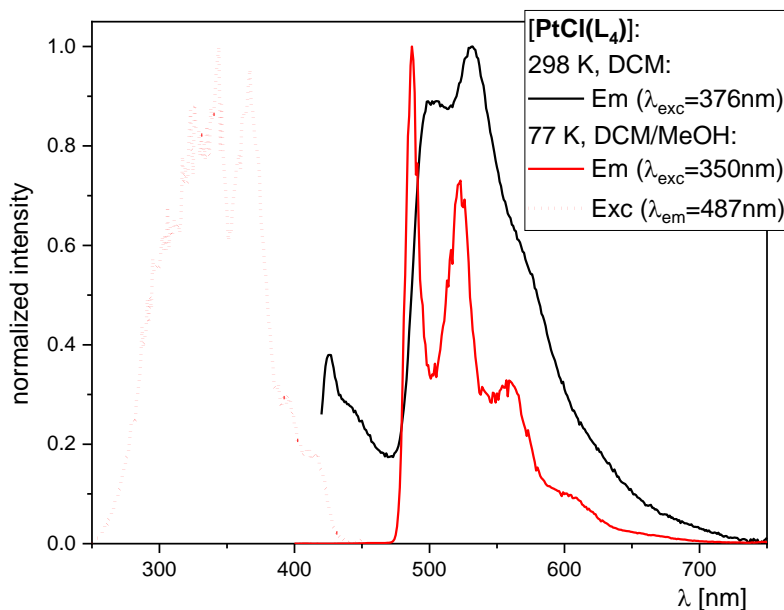


Figure S128: Excitation (dotted line) and emission spectra (solid line) of **[PtCl(L₄)]** ($\lambda_{exc} = 376$ nm (laser) at 298 K, $\lambda_{exc} = 350$ nm and $\lambda_{em} = 487$ nm at 77 K) at 298 K in fluid DCM (black) and at 77 K (red) in a frozen glassy DCM/MeOH matrix (V:V = 1:1). All solutions were optically diluted ($A < 0.1$). Spectra normalized to the highest intensity. Signals between 400-450 nm can be attributed the background noise in combination to low signal from the initial compound.

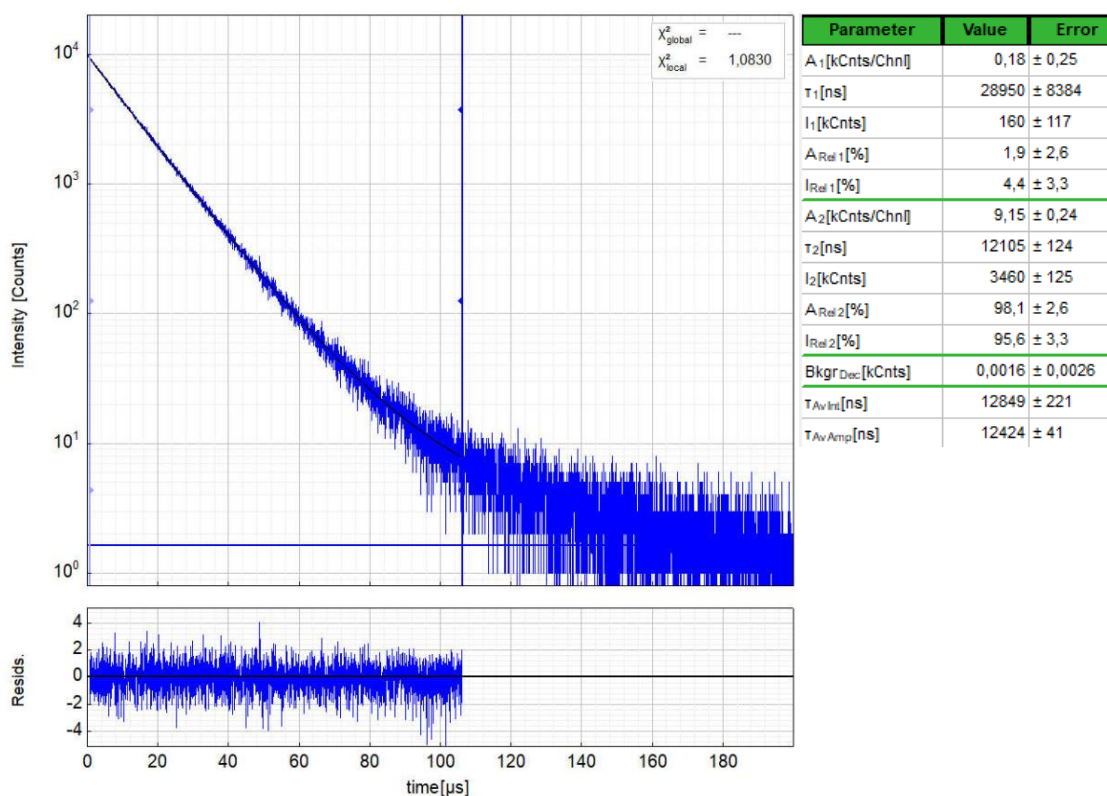


Figure S129: Left: Raw (experimental) time-resolved photoluminescence decay of **[PtCl(L₄)]** in a frozen glassy DCM/MeOH matrix (V:V = 1:1) at 77 K, including the residuals ($\lambda_{exc} = 376.7$ nm, $\lambda_{em} = 487$ nm). Right: Fitting parameters including pre-exponential factors and confidence limits.

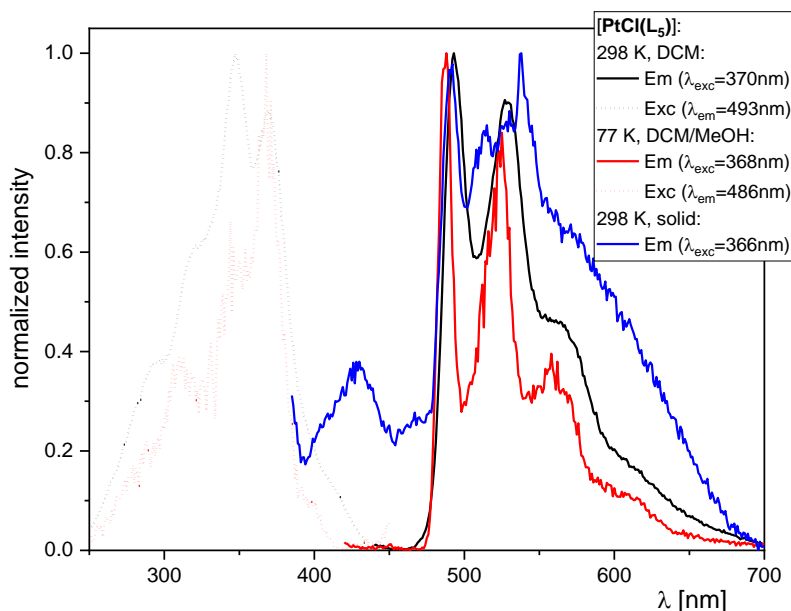


Figure S130: Excitation (dotted line) and emission spectra (solid line) of **[PtCl(L₅)]** ($\lambda_{exc} = 370$ nm and $\lambda_{em} = 493$ nm at 298 K, $\lambda_{exc} = 368$ nm and $\lambda_{em} = 486$ nm at 77 K, $\lambda_{exc} = 366$ nm as solid) at 298 K (black) in fluid DCM, at 77 K (red) in a frozen glassy DCM/MeOH matrix (V:V = 1:1) and as a solid (blue). All solutions were optically diluted ($A < 0.1$). Spectra normalized to the highest intensity.

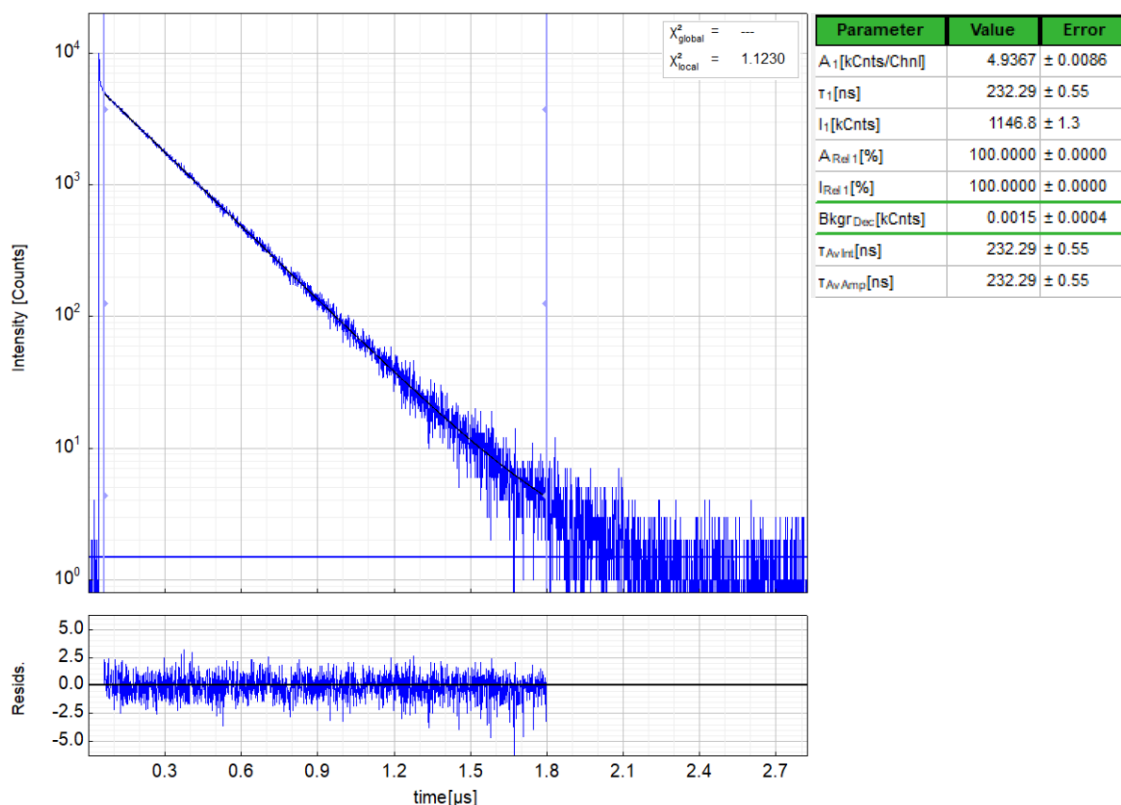


Figure S131: Left: Raw (experimental) time-resolved photoluminescence decay of [PtCl(L₅)] in fluid DCM at 298 K (air-equilibrated), including the residuals ($\lambda_{exc} = 376.7$ nm, $\lambda_{em} = 493$ nm). Right: Fitting parameters including pre-exponential factors and confidence limits.

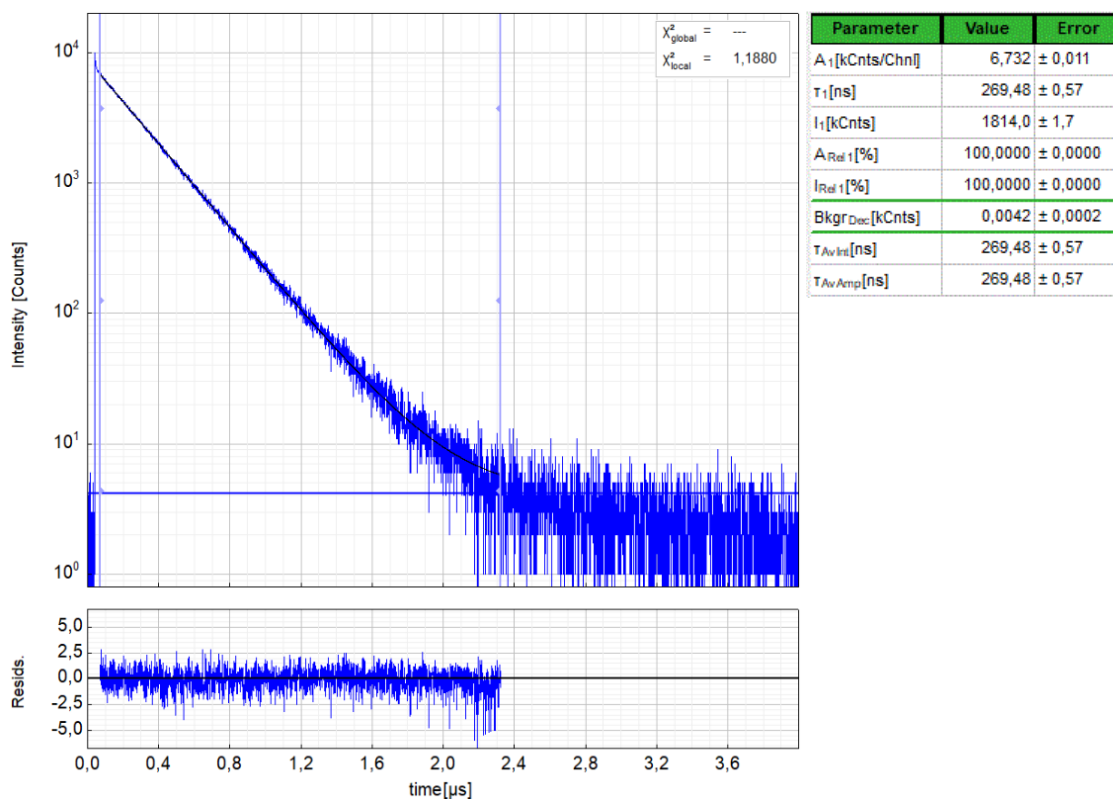


Figure S132: Left: Raw (experimental) time-resolved photoluminescence decay of [PtCl(L₅)] in fluid DCM at 298 K (Ar-purged), including the residuals ($\lambda_{exc} = 376.7$ nm, $\lambda_{em} = 493$ nm). Right: Fitting parameters including pre-exponential factors and confidence limits.

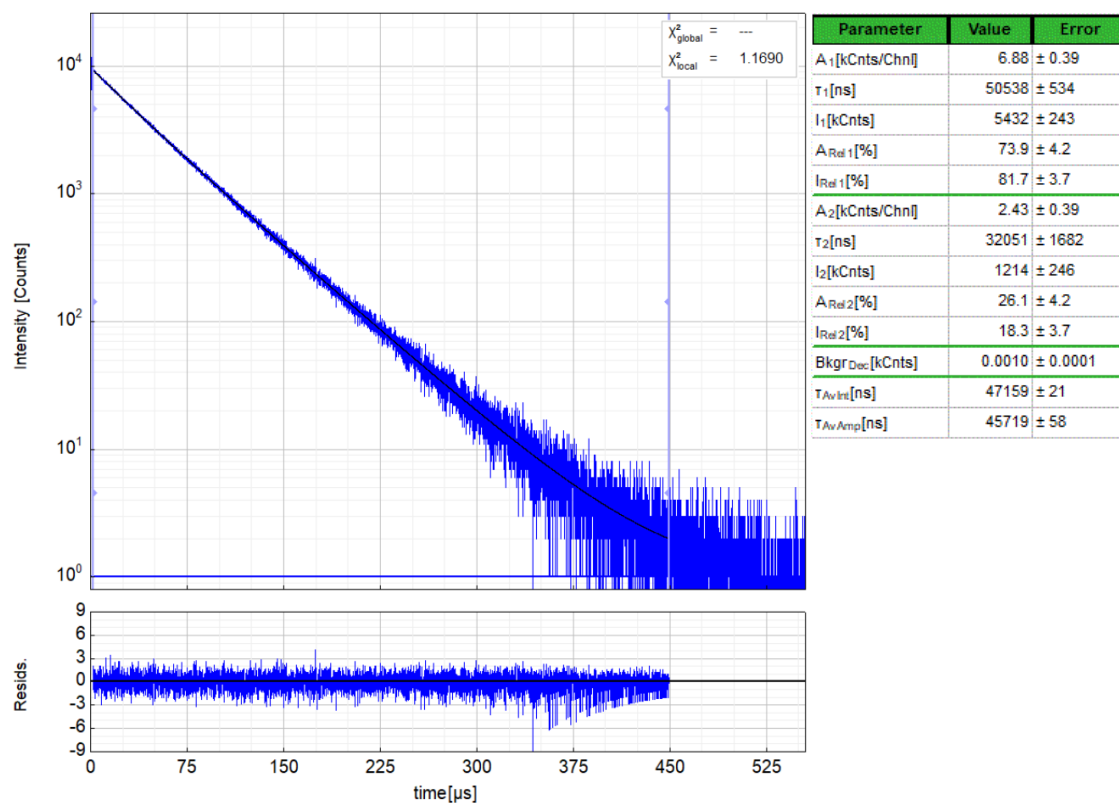


Figure S133: Left: Raw (experimental) time-resolved photoluminescence decay of **[PtCl(L₅)]** in a frozen glassy DCM/MeOH matrix (V:V = 1:1) at 77 K, including the residuals ($\lambda_{exc} = 376.7$ nm, $\lambda_{em} = 485$ nm). Right: Fitting parameters including pre-exponential factors and confidence limits.

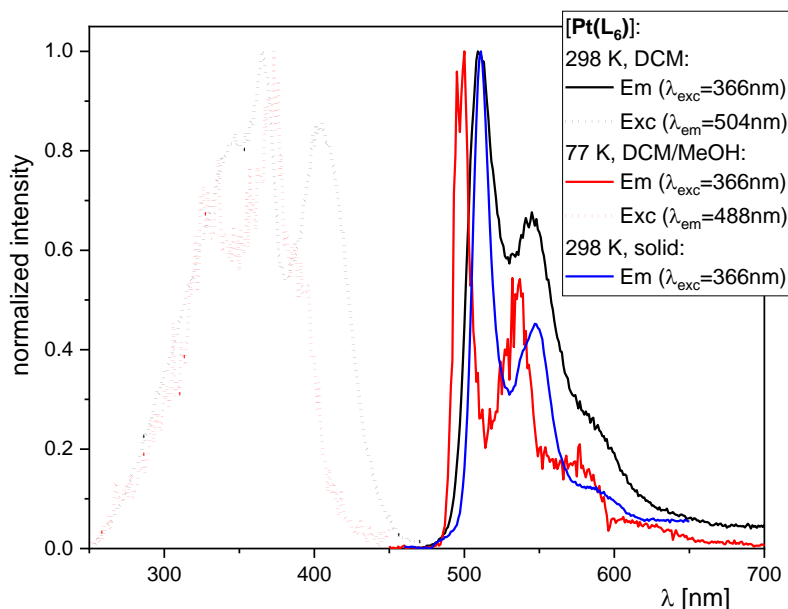


Figure S134: Excitation (dotted line) and emission spectra (solid line) of **[Pt(L₆)]** ($\lambda_{exc} = 366$ nm; $\lambda_{em} = 504$ nm at 298 K, $\lambda_{em} = 488$ nm at 77 K) at 298 K (black) in fluid DCM, at 77 K (red) in a frozen glassy DCM/MeOH matrix (V:V = 1:1) and as a solid (blue). All solutions were optically diluted ($A < 0.1$). Spectra normalized to the highest intensity.

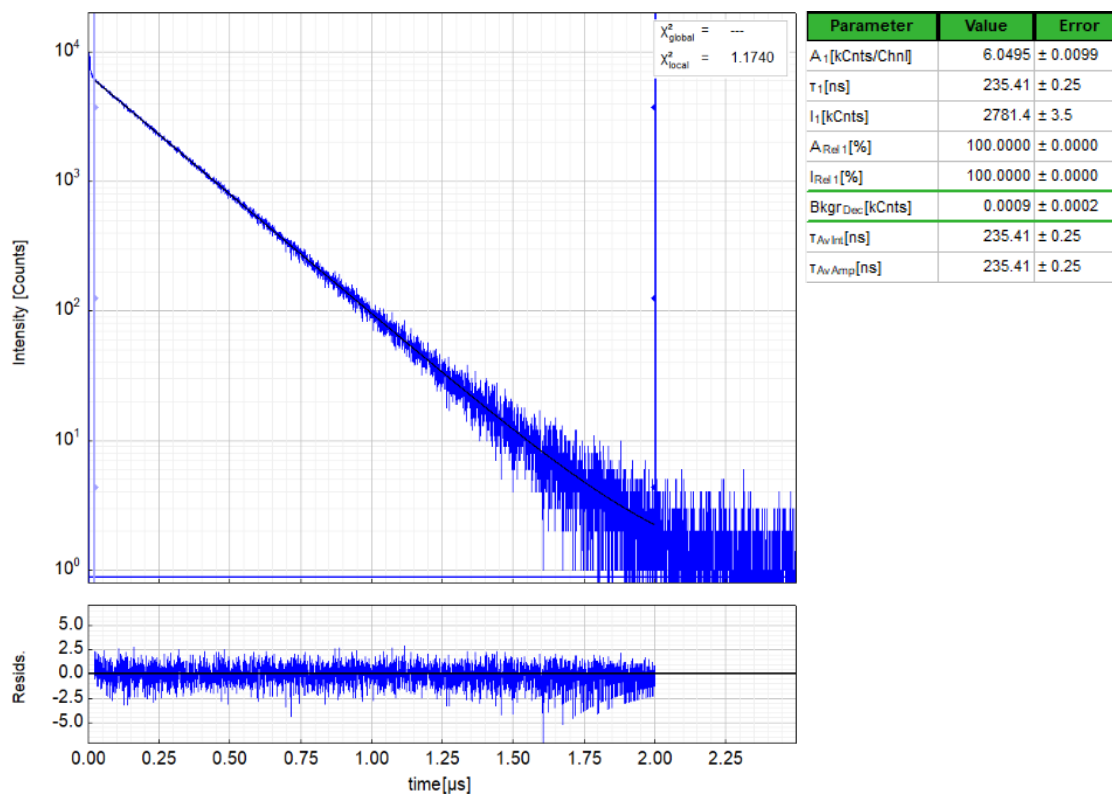


Figure S135: Left: Raw (experimental) time-resolved photoluminescence decay of [Pt(L₆)] in fluid DCM at 298 K (air-equilibrated), including the residuals ($\lambda_{exc} = 376.7$ nm, $\lambda_{em} = 504$ nm). Right: Fitting parameters including pre-exponential factors and confidence limits.

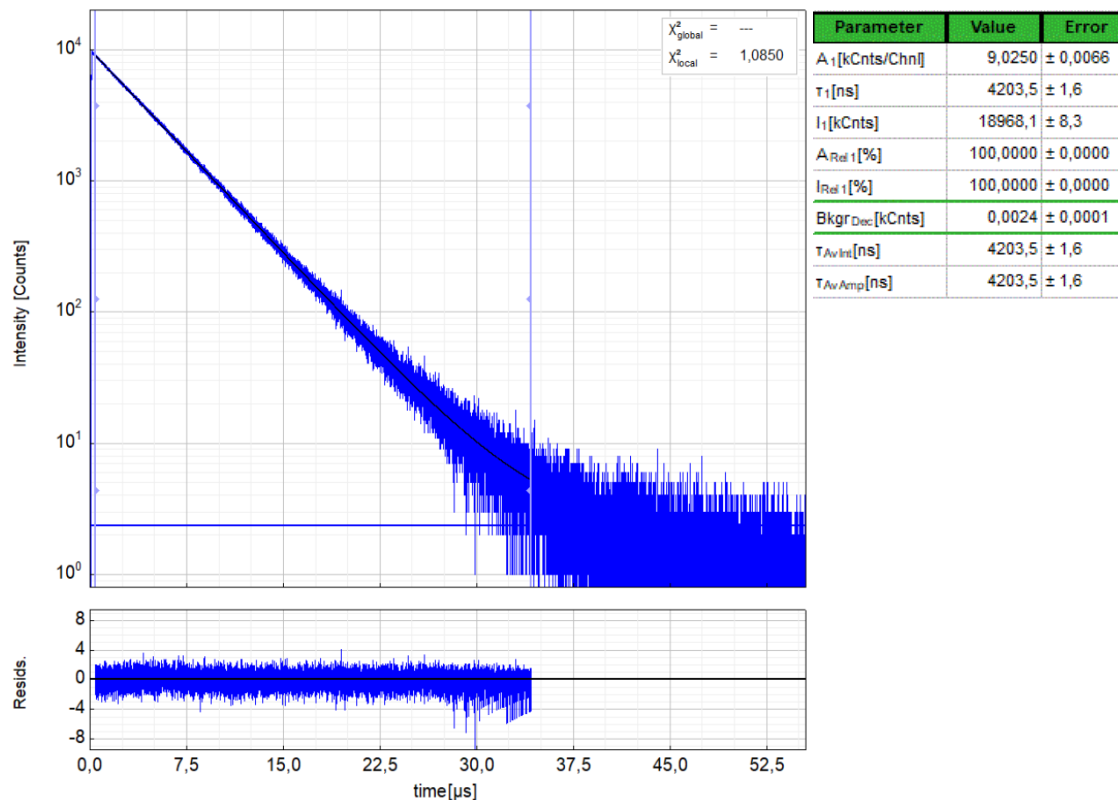


Figure S136: Left: Raw (experimental) time-resolved photoluminescence decay of [Pt(L₆)] in fluid DCM at 298 K (Ar-purged), including the residuals ($\lambda_{exc} = 376.7$ nm, $\lambda_{em} = 504$ nm). Right: Fitting parameters including pre-exponential factors and confidence limits.

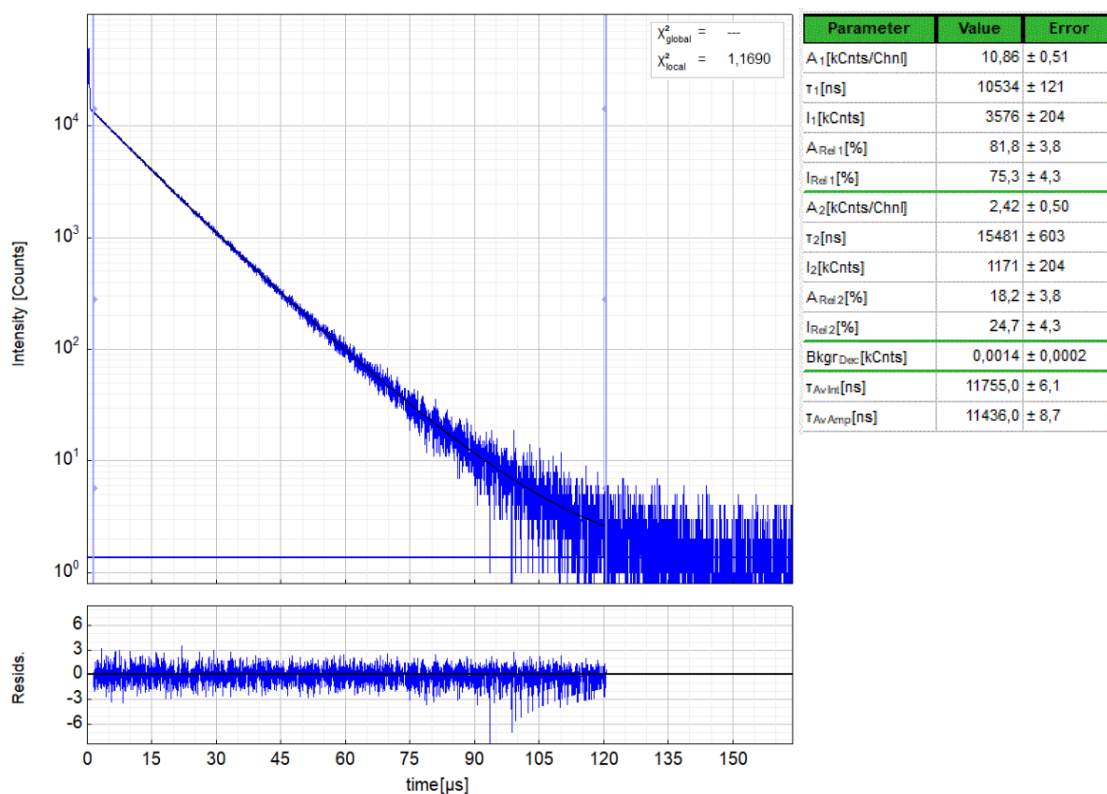


Figure S137: Left: Raw (experimental) time-resolved photoluminescence decay of [Pt(L₆)] in a frozen glassy DCM/MeOH matrix (V:V = 1:1) at 77 K, including the residuals ($\lambda_{\text{exc}} = 376.7$ nm, $\lambda_{\text{em}} = 488$ nm). Right: Fitting parameters including pre-exponential factors and confidence limits.

V. References

- [1] Knedel, T.-O.; Buss, S.; Maisuls, I.; Daniliuc, C. G.; Schlüsener, C.; Brandt, P.; Weingart, O.; Vollrath, A.; Janiak, C.; Strassert, C. A. Encapsulation of Phosphorescent Pt(II) Complexes in Zn-Based Metal–Organic Frameworks toward Oxygen-Sensing Porous Materials. *Inorg. Chem.*, **2020**, *59*, 10, 7252–7264. DOI: 10.1021/acs.inorgchem.0c00678.
- [2] Zhang, E.-X.; Wang, D.-X.; Huang, Z.-T.; Wang, M.-X. Synthesis of (NH)_m(NMe)_{4-m}-Bridged Calix[4]pyridines and the Effect of NH Bridge on Structure and Properties. *J. Org. Chem.* **2009**, *74*, 22, 8595-8603. DOI: 10.1021/jo901609u.